THÈSE

présentée à

L'UNIVERSITÉ DES SCIENCES et TECHNOLOGIES DE LILLE

pour obtenir

le grade de Docteur ès Sciences Physiques

par

Michel LE BRAS
Docteur de Troisième Cycle

*ETUDE DU PROCESSUS RETARDATEUR DE FLAMME INDUIT PAR LA
CARBONISATION ABLATIVE DE MATERIAUX POLYMERES
APPLICATION AUX MATÉRIAUX INTUMESCENTS*

oOo

TOME 2 - *ETUDE PROSPECTIVE et PERSPECTIVES*

Soutenue le 08 Octobre 1997 devant la Commission d'Examen

Président	J.-M. LEROY	Professeur
Rapporteurs	J.-C. BROSSE	Professeur
	G. CAMINO	Professeur
Examinateurs	J. VERDU	Professeur
	H. BAUSSART	Professeur
	G. ANTONINI	Professeur

SOMMAIRE

TOME II

GLOSSAIRE

Termes génériques

CA	adjuvant agent de carbonisation
CP	adjuvant précurseur d'espèces catalytiques
FR	retardateur de la flamme
FRS	systèmes d'adjuvants retardateurs de la flamme
SA	adjuvant agent de synergie

Termes généraux

at.	mole d'atome
HTT, T_{tr}	plus haute température du traitement thermique (°C)
F	indice statistique de Fisher
mol.	mole de molécule
P	pression (Pa)
PI	indice de plasticité
r	coefficient de régression
R	constante de Boltzmann
W	masse (kg, g)
t	temps (s, min., h)
T	température (°C ou K)
T_g	température de la transition vitreuse (°C, K)
X	teneur en additif (% pondéral)
λ	conductibilité thermique

Produits et matériaux

APB	pentaborate d'ammonium
APP, PPA	polyphosphate d'ammonium
BCOH, βcD	β-cyclodextrine
BZN	borate de zinc
DDA	dicyandiamine
DDS	diamino 4, 4' diphényle sulfone
EVA28	éthylène (72%) - acétate de vinyle (28%)
EVAx	copolymère éthylène (100-x%) - acétate de vinyle (x %)
FEABu5	copolymère éthylène (95 %) - acrylate de butyle (5%)
FEABu13	copolymère éthylène (87%) - acrylate de butyle (13%)
HDPE	polyéthylène haute densité
LDPE	polyéthylène basse densité
LN	polyéthylène
LQVA5	copolymère éthylène (95%) - acétate de vinyle (5%)
LQVA15	copolymère éthylène (85%) - acétate de vinyle (15%)
LRAM2,8	copolymère éthylène (92,2%) - acrylate de butyle (5%) - anhydride maléique (2,8%),
LRAM 3.5	copolymère éthylène (91,5%) - acrylate de butyle (5%) - anhydride maléique (3,5%)
LYABu30	copolymère éthylène (70%)- acrylate de butyle (30%)
LYAMe30	copolymère éthylène (70%) - acrylate de méthyle (30%)
MOH	mannitol
NK	argile naturelle de structure kaolinite
PA	polyamide

PA-6	polyamide-6
PE	polyéthylène (lactène Elf Atochem, melt index : 20 g/10 min à 190°C)
PER	pentaérythritol
PP	polypropylène isotactique
PY	pyrophosphate (diphosphate) diammonique
PS	polystyrène
SK	kaolinite de synthèse
SOH	d-sorbitol
TGMDA (TGDDM)	tétraglycidyle-méthylène-dianiline
TMS	tétraméthyle silane
TXXXX	argile réfractaire du lot XXXX
XOH	xylitol
YZSM-5	zéolithe de type ZSM-5
Y	zéolithe de type Y
3A	zéolithe de type KA (3A)
4A	zéolithe de type 4A (cocation Na)
5A	zéolithe de type CaA (5A)
10X	zéolithe de type CaX (10X)
13X	zéolithe de type NaX (13X)

Abréviations techniques

LOI	indice (index) limite d'oxygène (% volumique)
UL-94	test ANSI/ASTM D635-77 (classement V0, V1 ou V2)

calorimètre à cône

ehc	chaleur effective de combustion (kJ/kg)
m, m'	flux de matière (massique) (kg/m^2)
P	puissance calorifique volumique
q, q'	flux de chaleur, irradiance (kW/m^2)
rhr	flux calorimétrique (rate of heat release) (kW/m^2)
t.h.e.	chaleur émise (kJ)
t_i	temps pour atteindre l'ignition (s)

modèle du front de dégradation

T_d	température du front de dégradation
$T_{tc}, T_s, T_{éch}$	température au sein de l'échantillon
$x(\alpha,t)$	distance du front de dégradation au support

Analyses thermiques

ATG	analyse thermogravimétrique
DTG	thermogravimétrie différentielle
TG	thermogravimétrie
DSC	calorimétrie différentielle
W, M	masse résiduelle (kg %)
ΔH	enthalpie de la réaction, de la transformation
$\Delta W, \Delta M, \Delta T$	différence de masse calculée
α	degré (taux) de conversion (kg/kg ou kg %)
ΔG	différence de masse calculée ou masse résiduelle

<u>IKP</u>   <u>paramètres cinétiques invariants</u>

A_{jv}, A_{inv} facteurs pré-exponentiel apparent, invariant (s^{-1})

B_v, I_v paramètres déduits de l'effet de compensation

E_{jv}, E_{inv} énergie d'activation apparente et invariante (kJ/mole)

dW/dt   vitesse de la perte de masse (kg/s)

$(d\alpha/dT)_{iv}$ valeur de la courbe dérivée au point α_{iv}

$f_j(\alpha)$, Sj $j^{ème}$ fonction de dégradation

k_v constante de vitesse invariante (s^{-1})

n   ordre de réaction

P_j probabilité associée à la fonction $f_j(\alpha)$

$q(F_j)$ distribution F

T_v température déduite de l'effet de compensation (K)

β_v vitesse de chauffe (K/min)

Γ fonction Gamma

Spectroscopies

<u>IR, FT-IR</u>   absorption dans l'infra-rouge, id. à transformées de Fourrier

v   nombre d'onde (cm^{-1})

<u>RMN (NMR)</u>   résonance magnétique nucléaire

CP   en polarisation croisée

DD   avec découplage dipolaire

J   constante du couplage

MAS   avec rotation à l'angle magique

T_1 ET T_2 temps de relaxation

δ glissement chimique (ppm)

FWHM   largeur à demi hauteur (ppm)

<u>RPE (ESR ou EPR)</u>   résonance paramagnétique électronique

C^* concentration en complexes radicalaires

g   facteur spectroscopique (de Landé)

K = B/A   facteur de forme

H   valeur du champ magnétique (T)

n, nsp, N_{sp} nombre de spins (spin/kg)

bande X (X band)   à une fréquence d'environ $9,5 \times 10^9$ Hz

<u>XPS (ESCA)</u>   spectroscopie de photoélectrons X

E   énergie de la liaison (eV)

FWHM   largeur du signal à la demi-intensité (eV)

<u>XRD</u>   diffraction des rayons X

d   distance interréticulaire ($\overset{.}{A}$ ou nm)

$\beta_{½}$ largeur à mi-hauteur (radians)

θ angle de diffraction (de Bragg)(°)

λ longueur d'onde des rayons X incidents (nm)

La décision attendue est tombée comme un couperet : à partir du 1er janvier 1997, l'amiante est banni de pratiquement toute l'industrie française. Cette fibre cancérigène, responsable de près de 2000 décès en France en 1996, était déjà interdite dans de nombreux pays d'Europe [136]. Chômage technique et arrêt de production sont le lot de filiales de nombreuses entreprises. Pourtant les solutions de remplacement existent : composite ciment - fibre de verre pour les revêtements ondulés et les ardoises, mélange polyalcool vinylique- cellulose pour le flocage des bâtiments, polyester renforcé de fibre de verre pour les canalisations, mélange de fibres de verre et de céramiques avec une poly-aramide et la mousse d'acier pour les garnitures de frein, fibres aramide, para-aramide (kevlar), twaron, fibres de verre ou de céramiques pour les textiles isolants, fibres kevlar, fibres de roche, téflon (PTFE) pour les joints plats et les tresses. Ces solutions de remplacement, plus chères et souvent moins performantes, sont aujourd'hui mises en oeuvre. **Charge reste à l'utilisateur de définir ses exigences et de payer le coût, fonction de ces exigences**. Les seules entreprises en difficulté sont celles qui ont été inaptes à anticiper et donc n'ont pas développé la recherche des produits de remplacement.

Les applications des polymères de consommation sont limitées par leur mauvaise tenue au feu, en particulier quand elles nécessitent de bonnes propriétés mécaniques qui interdisent l'ajout d'adjuvants FR (hydroxydes ou hydrates [137, 138, 139]) à des taux de charges élevés.

Depuis les années 60 [140-142], les polymères de consommation FR sont obtenus par l'ajout (5 à 30 % pondéral) d'adjuvants organo-halogénés développant les « synergies » P-Cl, P-Br, Sb_2O_3-Cl ou Sb_2O_3-Br [143, 144]. Dès leur première application, leur inconvénient « majeur », à savoir l'émission de gaz corrosifs (acides chlorhydrique ou bromhydrique) et de fumées opaques, est connu et accepté comme « un mal nécessaire ». De nombreux travaux traitent de la réduction de leur pouvoir corrosif (addition de produits phosphorés ou de dérivés de la mélamine) et de l'action d'agents « suppresseurs de fumées ». Une compilation des formulations

commerciales des organo-halogénés et leurs applications est présentée par Pal et Macskasy (1991) [10].

A la fin des années 80, la présence de produits toxiques et cancérigènes dans les produits de combustion des polymères FR est rapportée. A titre d'exemples, différentes études caractérisent le tétrabromodibenzyle dioxine dans les produits de la pyrolyse du décabromodiphényle éther (adjuvant dont l'utilisation est généralisée) [145], le pentabromodibenzofurane dans les suies et les goudrons résultant de la combustion de PS « haut impact » FR [146], des dibenzofuranes polybromés dans les gaz de combustion du polybuthylène-téréphtalate FR [147], des dibenzofuranes polybromés et des dibenzodioxines dans ceux de polyesters FR et de résines polyépoxydes FR [148]. Le Brominated Flame Retardant Industry Panel a coordonné à cette époque un programme de recherche par expérimentation animale (ingestion ou contact dermique sur rats et lapins puis observations 4 semaines avant autopsie) [146]. La conclusion de l'étude est l'absence de toxicité à court terme des produits de la combustion des polymères contenant des adjuvants halogénés. Actuellement, le résultat de l'étude est sévèrement critiqué car les effets à long terme des produits suspects n'étaient pas considérés. Finalement, les Grands Organismes (Nations Unies, Communauté Européenne) préconisent la limitation de l'emploi des adjuvants halogénés et la recherche d'agents de remplacement [14-15].

Les adjuvants intumescents sont susceptibles de substituer les systèmes contenant des halogènes. Des formulations intumescentes des polyoléfines FR sans halogène sont d'ailleurs commercialisées avec le système adjuvant APP/polyurée depuis le début des années 80 [149, 150]. Leur application dans l'industrie est cependant limitée par le coût de revient comparativement élevé des formulations intumescentes qui provient du prix des matières premières (à titre d'exemple : 1 kg d'APP vaut environ 30 FF) et de leur mise en œuvre qui demande, selon les propriétés requises, un nombre plus ou moins important d'opérations unitaires [42, 45]. **L'homme de l'art** (producteur de résines ou transformateur) **doit néanmoins anticiper une décision politique brutale,** rechercher et développer des matériaux de rechange en conservant en mémoire l'exemple de l'amiante.

CHAPITRE III

FORMULATION DE NOUVEAUX MATERIAUX THERMOPLASTIQUES
RETARDATEURS DE FLAMME INTUMESCENTS
-
ETUDE PROSPECTIVE

La recherche d'une formulation intumescente performante peut être conduite selon deux voies différentes, à savoir, la recherche d'une formulation originale qui conduit à associer de nouveaux précurseurs des catalyseurs de carbonisation (CP) et agents carbonisants (CA) ou à optimiser une formulation connue par ajout d'agents de synergie (SA) qui peuvent augmenter l'activité du système catalytique ou le rendement en carbone de la réaction.

Notre Groupe a évalué plusieurs CP associés à différents polyols dans le PP. Ce sont des sels d'ammonium d'acides minéraux [39, 109, 112, 151-155] dont la décomposition thermique et/ou la réaction avec les CA libère de l'ammoniac et de l'eau qui servent d'agents du gonflement initial du matériau expansé.

Des polyols produits par l'industrie agro-alimentaire, des dérivés de l'amidon [39] ainsi que le polyamide-6 (PA-6) [47-48,156-160] sont les CA présentés. Les difficultés résultant de leurs utilisations ainsi que leurs intérêts respectifs seront discutés dans la première partie de ce chapitre. La protection par le matériau intumescent sera précisée en considérant les réactions radicalaires qui interviennent dans le processus [161].

Des effets de synergie ont été observés lors de l'ajout d'un adjuvant en faible teneur au système FR. Les synergies argiles/APP, zéolithes/APP [46, 162-167] et BCOH/polyols [39, 161] sont présentées en illustration dans cette partie du Chapitre.

Un effet de synergie est observé lorsque l'EVA est mélangé au système PA-6/APP et aux mélanges (« blends ») PP/PA-6/APP [47-48, 156-157]. L'influence des co-monoméres fonctionnalisés, contenant éventuellement une zéolithe, sera présentée dans le deuxième paragraphe du Chapitre qui présentent différents

systèmes FR copolymère de l'éthylène/APP/PER et copolymère de l'éthylène/APP/PER/4A.

Une discussion des mécanismes qui prennent place dans l'ensemble des systèmes en synergie présentés permet, dans cette dernière partie, la sélection des paramètres physiques et chimiques qui permettent les propriétés FR optimales, et conduit à proposer des lois pour la formulation de polymères de consommation FR.

III-1. *évaluation de nouveaux adjuvants*

Vandersall A.L. [32] proposent 6 règles arbitraires pour la formulation d'un matériau intumescent :

1- le matériau doit être (contenir) la source d'un acide minéral qui se forme entre 150 et 215°C,

2- le matériau doit contenir un polyol qui réagit avec l'acide, à une température égale ou légèrement supérieure à celle de la formation de l'acide, pour former des esters,

3- le matériau doit fondre avant ou pendant l'estérification,

4- un résidu phospho-carboné doit se former lors de la dégradation thermique des esters,

5- la libération de l'eau et des autres produits de dégradation des esters doit permettre le bouillonnement et la production d'écumes,

6- finalement, le produit de dégradation des esters doit se solidifier en conservant un caractère expansé (alvéolé).

Une septième doit être ajoutée lorsque le matériau est constitué de polymère : la réaction d'estérification et, a fortiori, la carbonisation des esters ne doit pas se produire dans les conditions de la transformation ou de la mise en forme des polymères (à titre d'exemples, les températures d'extrusion du PE, du PP, du PS et du PA-6 sont classiquement respectivement : 160, 150 (ou 170), 200 et 200°C [168] et celle de l'injection-moulage du mélange PP - talc : 225 à 250°C [44]). Les adjuvants doivent donc être choisis en fonction de leur réactivité dans ces conditions. Notre expérience montre en effet qu'une estérification amorcée dans un

extrusiomètre est dommageable au polymère et, plus particulièrement, à l'état de la surface de l'ensemble fourreau - vis.

Cette partie de l'étude concerne des formulations du PP isotactique. Elle compare trois CP : APP, PY (pyrophosphate diammonique, $(NH_4)_2H_2P_2O_7$) et APB (pentaborate d'ammonium, $(NH_4)_2B_{10}O_{16},8H_2O$) en association avec le PER. Le PY est utilisé car des espèces pyrophosphates acides sont toujours caractérisées dans les matériaux intumescents obtenus avec APP. L'APB est un adjuvant FR efficace du polychlorure de vinyle et du polyuréthanne dans lesquels il permet la formation d'un matériau carbonisé intumescent et qui, en addition, se décompose à basse température pour former *in situ* un matériau vitreux superficiel [169] qui, par référence aux travaux de Kroenke [25], peut induire seul la performance FR. Ces formulations conduisent à la formation d'un matériau intumescent abondant lors du traitement thermique des mélanges entre 300 et 350°C.

Vandersall A.L. [32] affirme aussi que l'efficacité d'un CA est fonction de sa teneur en carbone et en sites susceptibles de participer au processus de déshydratation (groupements hydroxyle). Les travaux de Schmidt Y. [39] montrent que ces relations observées dans les peintures intumescentes, ne sont pas retrouvées dans le PP ou le PE. En effet, à titre d'exemples, l'association du PY avec deux stéréoisomères : le mannitol (MOH) et le d-sorbitol (SOH) dans le PE conduit à des performances au feu très différentes, respectivement LOI = 26 ± 0.5 % volumique et absence de classement UL-94 et LOI = 23± 0.5 % volumique et classement UL-94 V0.

L'étude présente les performances de différents polyols (PER, xylitol (XOH), MOH, SOH) et d'un dérivé de l'amidon (BCOH) en association avec PY. Cette partie de l'étude permet de discuter l'existence de relations entre ces performances et le rendement pour la carbonisation du système adjuvant et/ou le caractère radicalaire des matériaux carbonés formés.

Les travaux de notre groupe concernant les associations intumescentes PA-6/APP et PA-6/EVA/APP [157-160] et ceux de Levchik S.V. et al. sur la carbonisation des polyamides induite par l'APP [27, 170-171], ont conduit à utiliser comme adjuvant un mélange maître PA-6/EVA/APP dont les performances seront comparées à celles des autres systèmes adjuvants CP/polyols présentés.

Thermal Behaviours of Ammonium Polyphosphate-Pentaerythritol and Ammonium Pyrophosphate-Pentaerythritol Intumescent Additives in Polypropylene Formulations

RENÉ DELOBEL, MICHEL LE BRAS, NAJIB OUASSOU
AND FATIA ALISTIQSA

> Laboratoire de Physico-Chimie des Solides
> E.N.S.C.L., U.S.T.L.F.A.,·-
> BP 108
> 59652 Villeneuve d'Ascq Cedex, France

ABSTRACT: The comparative study of the intumescent formulations (polypropylene-ammonium polyphosphate-pentaerythritol) and (polypropylene-ammonium pyrophosphate-pentaerythritol) shows that the highest fire retardance property of the second system may be related to the existence of a protective carbonaceous coating stable in the temperature range 300–550°C. Comparatively, the stability of the carbonaceous coating on the first system is only observed between 300 and 420°C. A ^{31}P N.M.R. study shows the presence (in the carbon-based layers) of acidic phosphate species (Lewis acids) which result from the thermal degradation of the additive mixtures. In the particular case of (PP-PPA-PER), these species degrade at 420°C to give phosphorus oxide. The study reveals that, with (PP-PY-PER), an additional protective char (stable in the temperature range 420–550°C) is formed by a reaction between the Lewis acids and the oxidized products of the thermo-oxidative degradation of the polymer.

INTRODUCTION

POLYPHOSPHATE-POLYOLS MIXTURES are potentially useful fire retarder additives in polyethylenic formulations because, contrary to the commercial antimony oxide-halogenated hydrocarbons mixtures, they don't evolve any toxic or corrosive agent in the conditions of fire. It has been previously proposed that the protection of the polymeric materials containing these additives is provided by shields which result from an intumescence phenomenon [1–2].

In a previous paper [3] dealing with fire-retardant polypropylene (PP)-based formulations, we have reported that the intumescent mixture diammonium pyrophosphate-pentaerythritol (PY-PER) leads to higher performances than the ammonium polyphosphate-pentaerythritol (PPA-PER) systems. It has been shown that thermal treatment of a (PP-PY-PER) formulation develops at a temperature lower than 350°C an intumescent coating (result of a three steps process: reaction between the additives, hydrolysis of the P-O-P chains and eventual condensation and degradation of the resulting esters) and then, at higher temperature ($T < 600°C$), a carbonaceous shield. The intumescent coating and the carbonaceous shield have been proposed as frameworks of carbon [6] which contain less than 6% of hydrocarbon species and which support acidic phosphate species [7]. The study of (PP-PY-PER) has precised the role played by these phosphate species through, in particular, their reaction with products resulting from the thermo-oxidative degradation of the polymer.

The aim of the present work was the characterization of the materials resulting from the mixtures (PY-PER) and (PPA-PER) and of the protective coatings which were formed on the formulations (PP-PY-PER) and (PP-PPA-PER) (PPA: Exolit 422, Hoechst) during thermal treatments or in the conditions of fire. The formation of these materials was first put forward by thermogravimetric (TG) analysis under air or inert gas (N_2) flows. Their spectroscopic characterizations were then carried out by ^{31}P N.M.R. and E.S.R., this last technique allowing us to follow the carbonization process. This comparative study permits a phenomenologic explanation of the observed different fire-retardance performances of the two formulations via the knowledge of the chemical processes which lead to the formation of the protective coatings.

EXPERIMENTAL

Materials

Raw materials were PP (powder supplied by Atochem), PER (Prolabo

R.P. grade), PPA [$(NH_4PO_3)_n$, $n = 700$, Hoechst Exolit 422, soluble fraction in H_2O: < 1 wt %]. Diammonium pyrophosphate $(NH_4)_2H_2P_2O_7$ was synthesized in this Laboratory using the previously published procedure proposed by Swanson et al. [8]: bubbling of ammonia into a solution (temperature lower than 10°C) obtained by dissolution of solid pyrophosphoric acid in cold 95% ethanol (end of the ammoniation when the apparent "pH" reaches about 3) and direct filtration. The cake was then dried under air flow and/or vacuum at room temperature. The solid was then characterized by a X-ray diffraction study [spectrum obtained using a Guinier-de Wolff chamber with $Cu_{K\alpha}$ (filter Ni, $\lambda = 1.54178 \times 10^{-10}$ m)] which reveals the presence of the orthorhombic phase of diammonium pyrophosphate [9].

Initial mixtures were first prepared after a mechanical grinding and a sifting (200×10^{-6} m) of the raw materials. Sheets [$(3 \times 10^{-3}) \times 0.2 \times 0.2$ m] were then obtained using a Darragon pressing machine at $T = 190$°C with a pressure of 10 MPa.

The present study was restricted to two series of formulations with a PP/additives ratio: 80/20 (wt/wt), the compositions of the additives being expressed by PER $= X$ ($0 < X < 20$ weight %) and PY (or PPA) $= 20 - X$ (weight %).

Limiting Oxygen Index Test

Limiting oxygen index (L.O.I.) was measured using a Stanton Redcroft instrument on sheets [$(6.5 \times 10^{-3}) \times (6.5 \times 10^{-2}) \times 0.2$ m] according to the standard "oxygen index" test (ASTM D2863/77).

Thermal Degradation

Thermal degradation studies were carried out either with temperature programming (heating rate: 300°C $\times$ h^{-1}) or at constant temperature under synthetic air (Air Liquide grade) or under inert gas (N_2, Air Liquide U grade) flows (5×10^{-7} $Nm^3 \times s^{-1}$), using a Setaram MTB 10-8 thermobalance. Powdered materials [PY, PPA, PER, (PY-PER) and (PPA-PER)] or compression moulded sheet materials [PP, (PP-PY-PER) and (PP-PPA-PER)] were studied. In each case, samples were 20×10^{-6} Kg. The experimental TG curves of the mixtures or of the moulded samples were compared with the curves calculated using the relations:

$$(\Delta M(PY\text{-}PER)_T)_C = ((100 - 5X) \times ((\Delta M(PY)_T)_E)) + (5X \times ((\Delta M(PER)_T)_E))/100$$

$$(1)$$

$$(\Delta M(\text{PPA-PER})_T)_c = ((100 - 5\text{X}) \times ((\Delta M(\text{PPA})_T)_\varepsilon)) + (5\text{X} \times ((\Delta M(\text{PER})_T)_\varepsilon))/100$$

$$(2)$$

$$(\Delta M(\text{PP-PY-PER})_T)_c - ((80 \times ((\Delta M(\text{PP})_T)_\varepsilon) + (20 \times ((\Delta M(\text{PY-PER})_T)_\varepsilon))/100$$

$$(3)$$

$$(\Delta M(\text{PP-PPA-PER})_T)_c = ((80 \times ((\Delta M(\text{PP})_T)_\varepsilon) + (20 \times ((\Delta M(\text{PPA-PER})_T)_\varepsilon))/100$$

$$(4)$$

where $[\Delta M(A)_T]_c$ and $[\Delta M(A)_T]_\varepsilon$ were respectively the losses of weight calculated and experimental of a compound or a mixture A at the temperature T. The difference between the experimental and calculated curves was then obtained by a simple subtraction point by point.

Profiles of the temperature "in the surface" of the polymeric formulations (in the conditions of a fire) were measured in moulded materials using a thermocouple crimpled in the samples (2×10^{-3} m below the initial surface). Burning was insured using a butane flame (3×10^{-2} m above the initial surface, incidence angle: 45°).

The comparative differential scanning calorimeter analysis (DSC) of PY and PPA was carried out under synthetic air flow (5×10^{-7} $\text{Nm}^3 \times \text{s}^{-1}$), using the Netzsch DSC 444 in the temperature range 25–420°C (heating rate: 300°C × h^{-1}).

Spectroscopic Analyses

The study was restricted to solid samples resulting from isothermal treatments (12 h under air) or from the flaming up of the sheets. In those conditions, it may be assumed that an eventual hydrolysis process in air may be neglected if the analysis was carried out in a short time (<8 h) after the end of the treatments.

[31]P N.M.R. spectra were recorded using a Brucker 400 spectrophotometer operating at 162 MHz (no spinning, external reference: 85% H_3PO_4). When broad or unresolved signals were observed, the study was carried out after a dissolution of the samples in dimethyl sulfoxide (DMSO-D_6, C.E.A. grade) or in D_2O ("Uvasol" Merck grade). In that last case, the detected species were only considered as probes of the initial composition of the samples because dissolving may lead to hydrolysis processes which induce eventual breakings of the P-O-P and C-O-P bonds. The assignments of the signals were proposed from comparisons with signals of commercial high purity phosphates (or phosphorus oxides) or from data in the literature [10].

E.S.R. spectra were recorded at 25°C using a Varian "E line" spec-

214

trophotometer (ν = 9.5 × 10^9 Hz (X-band), modulation: 10^3 Hz, standard: "Strong Pitch" Varian). Every observed signal presenting Gaussian shapes [6], the concentrations of the paramagnetic species were computed using a simple method of integrating of the signals.

RESULTS AND DISCUSSION

Fire Retardant Performances

The variations of the L.O.I. values versus the PY and the PPA contents, respectively in (PP-PY-PER) and (PP-PPA-PER) (Figure 1), confirm the existence of synergistic effects with (PP-PY-PER) (highest L.O.I. value: 27.1 belonging to PY/PER = 1.558 (wt/wt), i.e., a ratio P/PER = 2 atoms × Mol.$^{-1}$) [3] and with (PP-PPA-PER) [highest L.O.I.
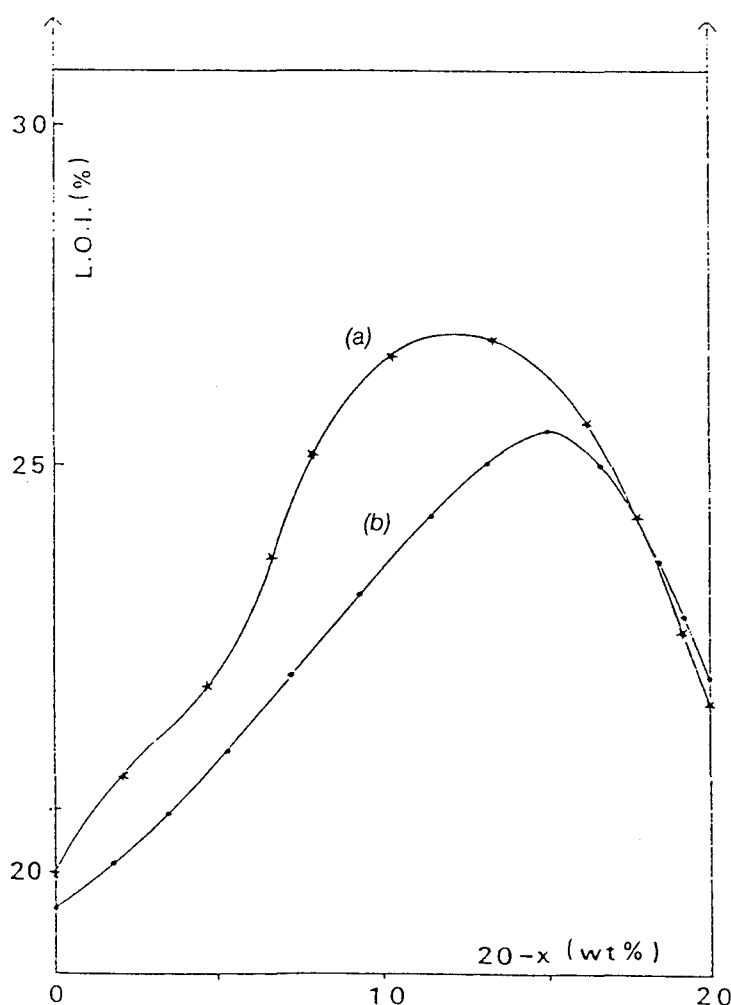
Figure 1. Plots of limiting O$_2$ index of (PP-PY-PER) (a) and (PP-PPA-PER) (b) versus the amounts of ammonium phosphates.
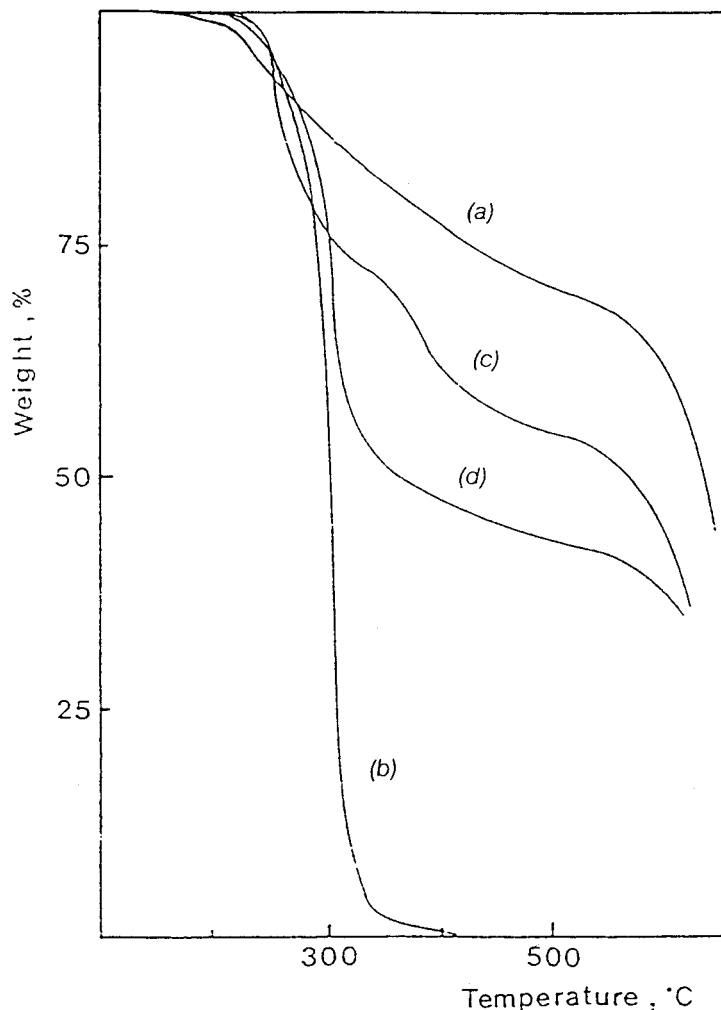
Figure 2. TG curves of PY (a), PER (b) and (PY-PER) experimental (c) and calculated (d) (from R. Delobel et al. [3]).

value: 25 belonging to PPA/PER = 3 (wt/wt), i.e., P/PER = 2.4 atoms × Mol.$^{-1}$]. These results confirm our previous studies viz. the best fire-retardance is obtained with (PP-PY-PER).

Further studies were restricted to (PY-PER) and (PPA-PER) mixtures and (PP-PY–PER) and (PP-PPA-PER) formulations with PY/PER and PPA/PER ratios for which the best fire-retardant properties were observed.

Thermal Behaviours of (PY-PER) and (PPA-PER)

The TG analysis of the two mixtures in air (Figures 2, 3 and 4) characterizes 3 domains previously discussed [7]:

• For temperatures lower than 290°C, a reaction between the two additives (esterification with loss of ammonia and water) occurs.
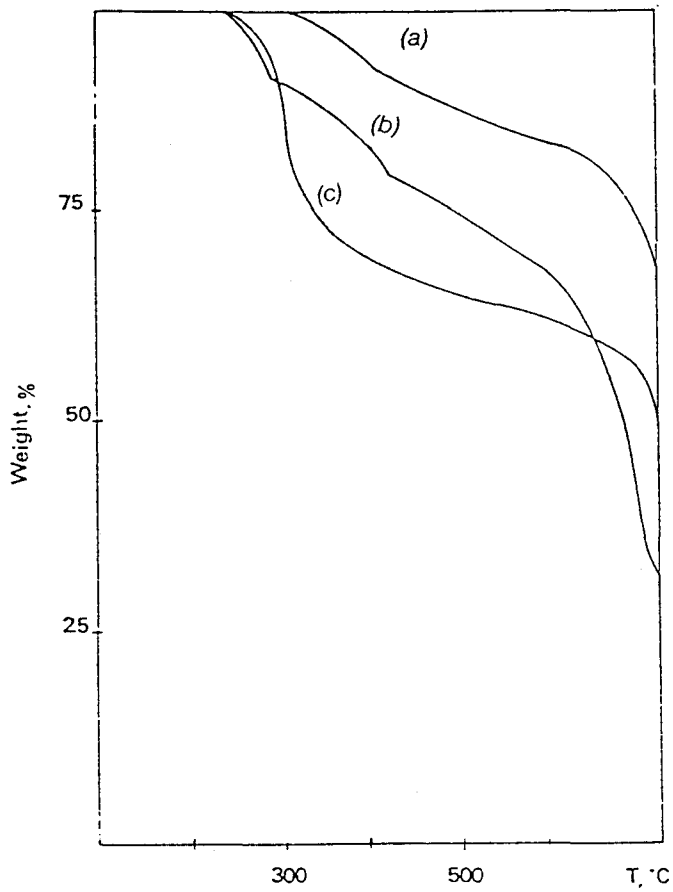
Figure 3. TG curves of PPA (a), (PPA-PER) experimental (b) and calculated (c).
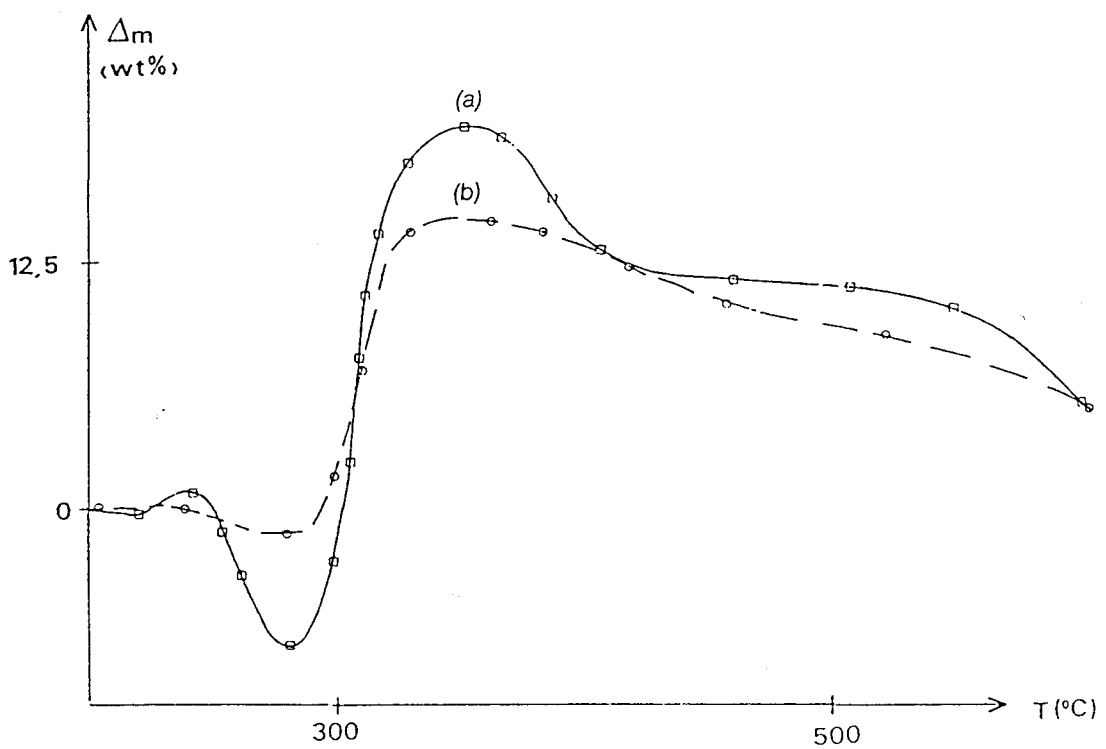
Figure 4. Differences between the experimental TG curves of (PY-PER) (a) and (PPA-PER) (b) and the curves calculated according (1) and (2) vs. the temperature.

91

- In the temperature range: $290 < T < 350\,°C$, the intumescence process takes place (the corresponding material will be so-called INTUMESCENT COATING in this text).
- At higher temperature, the formation of a carbonaceous residue (so-called "HIGH TEMPERATURE" RESIDUE in this text), relatively stable between 450 and 650°C, is put forwards.

It is remarkable that the amounts of intumescent coating and of "high temperature" residue obtained with (PPA-PER) are slightly lower than the amounts obtained with (PY-PER).

A study under an inert gas flow confirms the existence of three domains and shows that the amounts of intumescent coatings obtained are comparable to the amounts obtained in air [11]. It may thus be assumed that oxygen does not play any part in the intumescence pro-
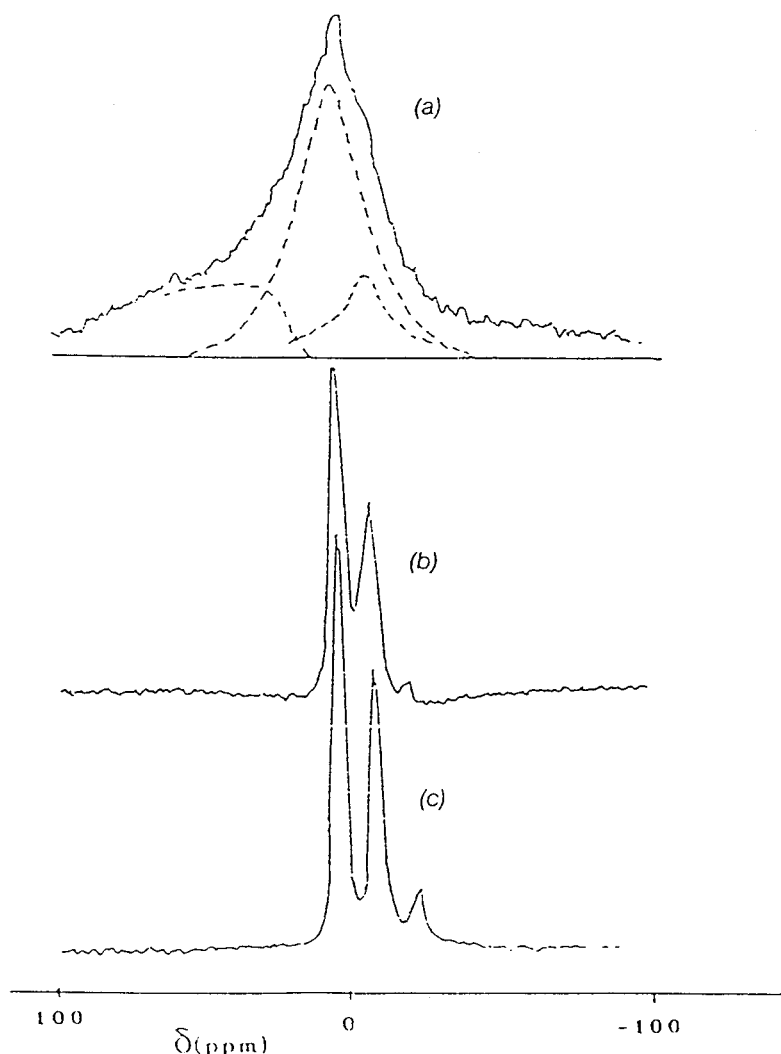
Figure 5. ^{31}P NMR spectra of (PY-PER) [after thermal treatments at 190°C (a) and at 420°C (b)] and of (PP-PY-PER) after flaming up (c).
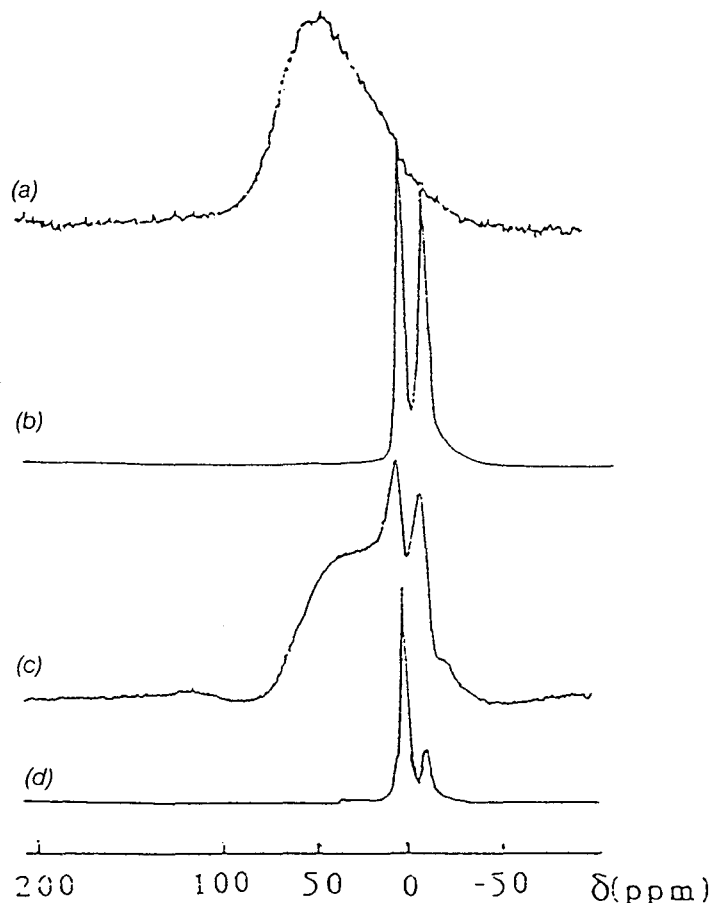
Figure 6. ^{31}*P NMR spectra of (PPA-PER) (after thermal treatments at 280°C (a), 350°C (b) and 420°C (c)) and of (PP-PPA-PER) after flaming up (d).*

cess and so further spectroscopic study was restricted to the materials resulting from the treatments of the additive mixtures in air.

Typical examples of ^{31}P NMR spectra obtained with samples treated at temperatures belonging to each of the three domains are reported in Figures 5 and 6.

Signals obtained with (PY-PER) have been previously ascribed or discussed [7]. It may be reported that, at temperatures lower than 280°C, the signal (center of mass between 0.97 and 2.18 ppm, linewidth at half height higher than 1900 Hz) is assigned to a mixture of orthophosphate esters and pyrophosphate esters (deduced of a treatment of the spectrum in the hypothesis of signals with Lorentzian shapes) which results from a reaction between the two additives and from an additional hydrolysis or (and) a condensation process. At higher temperatures, signals are assigned to acidic orthophosphates ($2.7 < \delta < 2.9$ ppm) or pyrophosphates species ($-8.5 < \delta < -8$ ppm), relatively low amounts of polyphosphates (δ about -20 ppm) are only observed in the "high temperature" residue ($T > 350°C$).

Table 1. Solid ^{31}P N.M.R. spectra of (PPA-PER) function of the thermal treatment (12h under air flow) and of the coating formed on (PP-PPA-PER) in the conditions of a fire.

Temperature °C	Condensed or Unsymmetric Species			Orthophosphates			Polyphosphates (End Groups)			Polyphosphates (Middle Groups)		
	c.m. ppm	FWHM Hz	Cp %	δ ppm	FWHM Hz	Cp %	δ ppm	FWHM Hz	Cp %	δ ppm	FWHM Hz	Cp %
280	38(a)	9,660	100									
350				2.17	600	44.4	−10.31	813	49.4	−23*	1500	6.1
430	33(a)	9,800	76.6*	5.00	1300	15.5*	−6.7	1370	7*	−22*	1330	0.8*
PP-PPA-PER (after flaming up)				1.66	670	75	−9.63	830	18	−22	1420	<7

δ: chemical shift, c.m.: center of mass, F.W.H.M.: linewidth at half height, *: deduced from spectrum treatment, (a): anisotropic shift, Cp: relative amount of ^{31}P (at %).

(PPA-PER) presents very different spectra, at least in the lowest and in the highest temperature ranges. The assignments of the signals are reported in Table 1.

In the temperature range 200–290°C, the broad band may be assigned to esters which form without breaking of the initial polyphosphate chain, any phosphate species with short P-O-P chains being never observed. The study in solution of the samples proves unambiguously the esterification process. Indeed, if the resulting ester(s) is not solubilized in DMSO-D$_6$ [contrary to esters formed with (PY-PER)], the spectra obtained with samples solubilized in D$_2$O reveal the presence of at least one orthophosphate ester (quintuplet: $\delta = -1.84$ ppm, $J_{P-H} = 11.3$ Hz) which results from the breaking of the polyphosphate P-O-P chain during the solubilization process.

The observed different behaviours of (PY-PER) and (PPA-PER) in this temperature range may be explained by the different thermochemical and physical properties of the two ammonium phosphates. TG [Figures 2(a) and 3(a)] and D.S.C. (Figure 7) characterize these differences.

1. PY melts at about 166°C [strong endothermic phenomenon at 166°C, apparent melting temperature: 169°C (measurement using a Kofler bank)]. Contrary to previously reported data [9], no significant decomposition of PY is observed at temperatures lower than the melting point. At temperatures higher than 170°C, the decomposition occurs (losses of H$_2$O and traces of NH$_3$ when $T < 200$°C, weight loss: $< 1.5\%$ at 200°C).
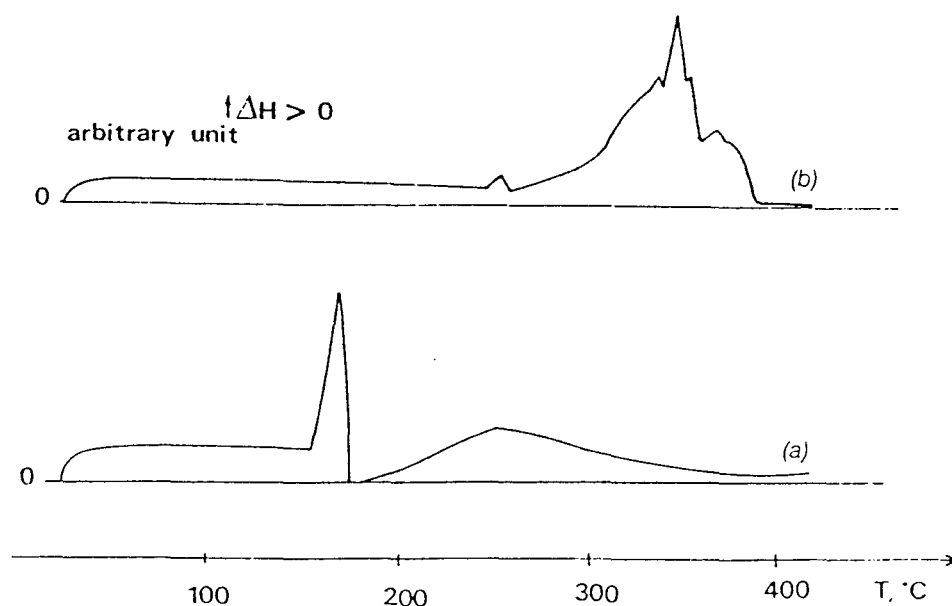

Figure 7. D.S.C. analysis of PY (a) and PPA (b).

2. PPA shows a first decomposition at 250°C (first endothermic phenomenon); its melting is not observed till the decomposition occurs. The main decomposition occurs at a highest temperature: about 300°C.

In the temperature range corresponding to the development of the intumescent coating, the observed species are mainly orthophosphates and pyrophosphates. The amounts of condensed phosphates (pyro- or polyphosphates) are higher than the corresponding amounts formed with (PY-PER) [3,7]. The study in solution of (PPA-PER) shows one acidic orthophosphate species (δ = 1.13 ppm, 58.7 at. %), two neutral pyrophosphate species (δ = -4.32 and -5.07 ppm, traces), three acidic end groups belonging to pyro- or polyphosphates (δ = -10.73, -10.84 and -11.23 ppm, 47.1 at. %) and one middle group belonging to long chain (or ring) polyphosphates (δ = -24.66 ppm, 4.7 at. %). In that case, the absence of P-H coupling does not allow the characterization of any ester. The spectrum in solution (Figure 8) presents nevertheless two signals at δ = -14.54 and δ = -15.01 ppm (4% of the ^{31}P) which may be assigned to $PO_4(R\phi_2)$ and $PO_4\phi_3$ (R: alkyl and ϕ: phenyl groups) respectively. Their presence in (PPA-PER) corroborates the previously proposed mechanism for the formation of intumescent carbonaceous coatings through the formation of aromatic intermediates [6].

When the intumescent coating decomposes ($T > 350$°C), ortho- and pyrophosphates species are detected in low amounts, comparatively with (PY-PER) in the same conditions, moreover, only traces of polyphosphate(s) are characterized. These three species disappear when the time of the isothermal treatment is long or when the temperature increases. The main observed "phosphate" specie(s) gives rise to a broad anisotropic signal [never observed with (PY-PER)] of which assignment is critical. The i-r spectrum of this material being closely related to the spectrum of P_4O_{10}, a comparative N.M.R. study with phosphorus oxide (under several controlled conditions of hydrolysis) shows that the main phosphorus-based component possesses a structure similar to the cage-like structure of P_4O_{10}. The study in solution does not characterize any organophosphorus compound, the only observed phosphate species are an acidic orthophosphate (δ = 0.54 ppm) and polyphosphate(s) characterized by several acidic end groups ($-10.7 < \delta < -12.4$ ppm) and middle groups ($-23.6 < \delta < -25.8$ ppm). These last observed species may arise either from the solubilization of products which compose the "high temperature" residue or from the hydrolysis of the phosphorus oxide.

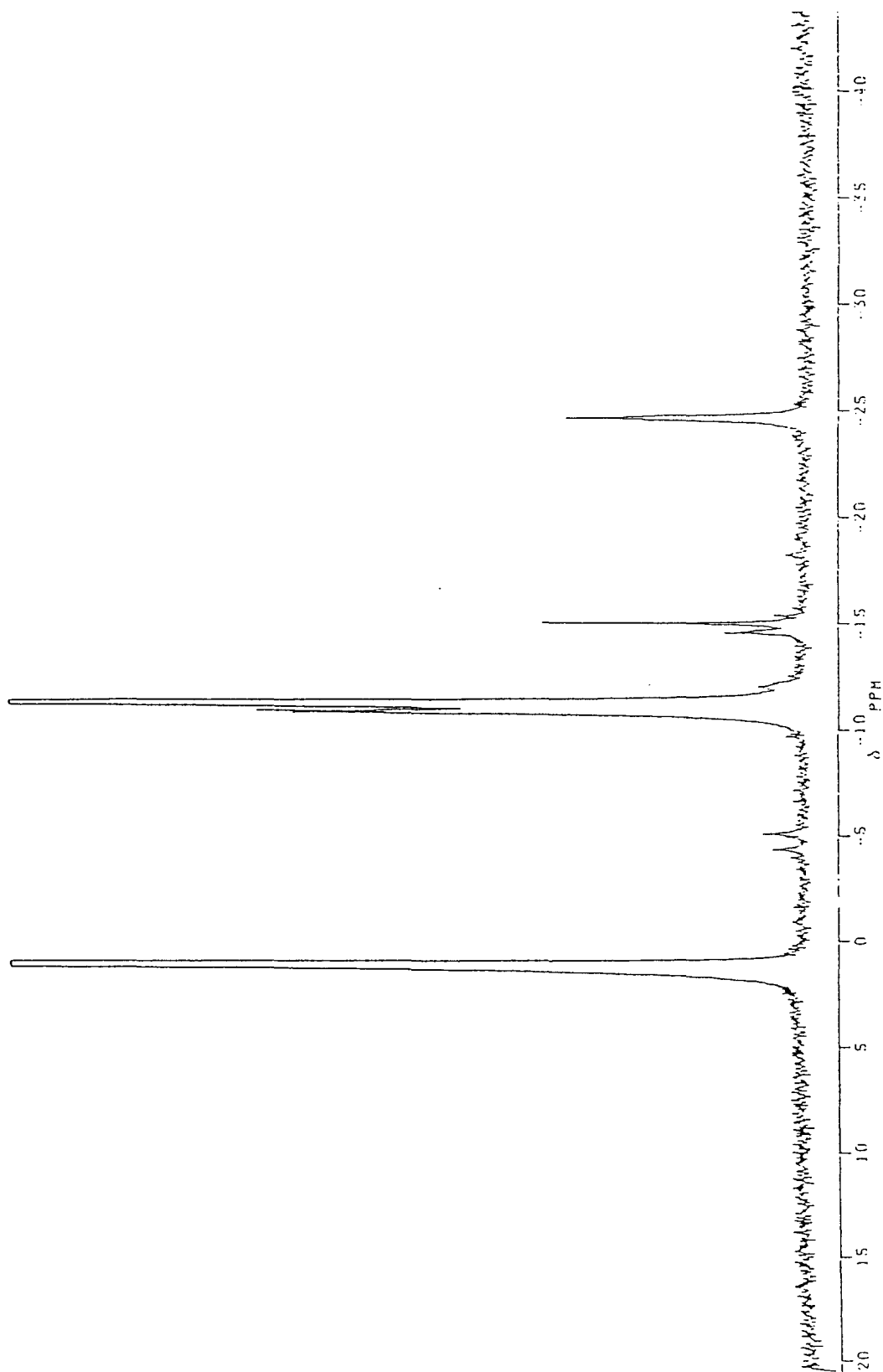The results of the [31]P N.M.R. study of (PPA-PER) prove that the ther-

Figure 8. ^{31}P N.M.R. spectrum of (PPA-PER) after the thermal treatment at 350°C (sample solubilized in DMSO-D6).

97

mal degradation of the phosphate species in the intumescent coating leads to the formation of phosphorus oxide. On the contrary, such a degradation process is never observed in (PY-PER), acidic phosphates species remaining observed in the "high temperature" residue. These two behaviours may be explained by the different compositions of the two intumescent materials (different values of δ and D.W.H.M. of the phosphate species and different amounts of condensed species).

The E.S.R. spectroscopic results of (PY-PER) and (PPA-PER) show the formation of carbon. The observed signals possess the same characteristics in the two mixtures (spectroscopic splitting factor $g = 2.00$, linewidth between points of maximum slope: 15×10^{-4} T). They may be assigned to free radicals trapped in the carbon-based materials [12–13], probes of the existence of carbon which results from the thermal degradation of the additive mixtures [6]. A comparison between the paramagnetic species concentrations versus the temperature (Figure 9) shows that these concentrations are in a same order of magnitude when $T > 280°C$. Nevertheless, the curves show that the carboniza-
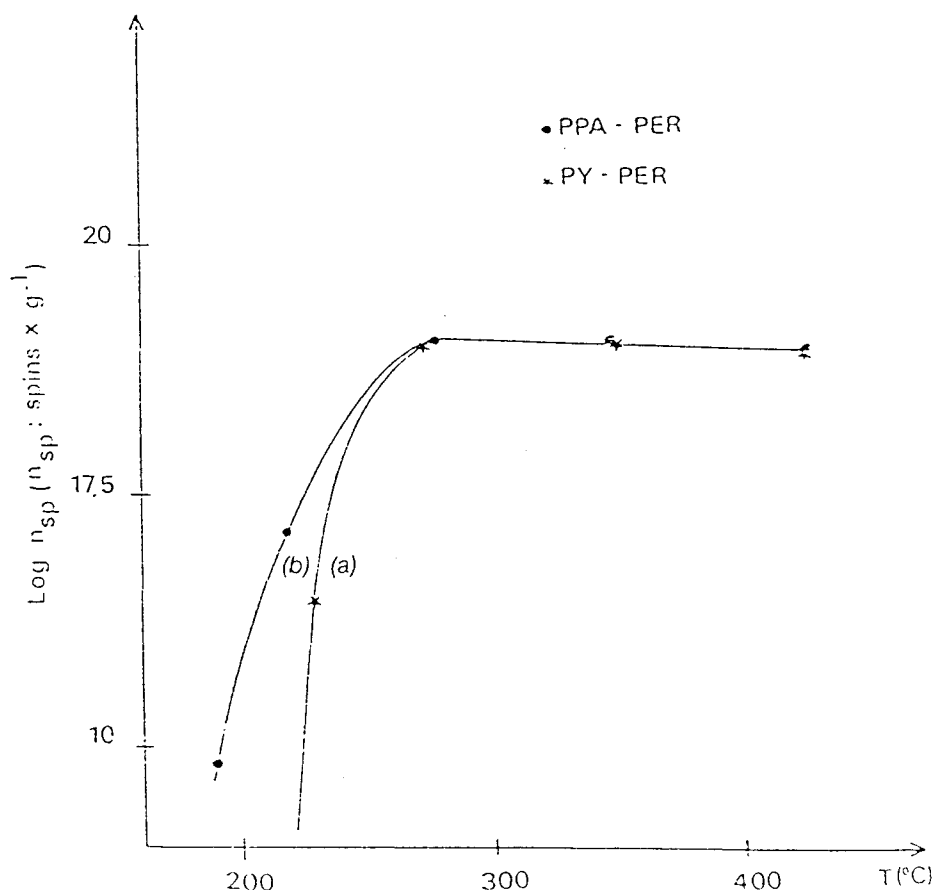

Figure 9. Concentrations of the paramagnetic species in (PY-PER) (a) and in (PPA-PER) (b) vs. the temperature.

tion process of (PPA-PER) begins at a lower temperature than the carbonization of (PY-PER).

As a result, the comparative spectroscopic study of (PY-PER) and (PPA-PER) versus the temperature confirms that the intumescent coatings are frameworks of carbon which support phosphate species, mainly ortho- and pyrophosphates acidic species. In the particular case of (PPA-PER), the study suggests that phenyl phosphates may be proposed as intermediates for the formation of carbon. When the intumescent coatings decompose, the observed phosphorus-based species are very different. With (PY-PER) a weak condensation process leads mainly to acidic pyrophosphates and, with (PPA-PER), a degradation of the phosphates species belonging to the intumescent coating leads to the formation of species that are very likely partially hydrated forms of the phosphorus oxide.

Thermal Behaviours of (PP-PY-PER) and (PP-PPA-PER)

Figures 10–12 characterize three different domains versus the temperature:

1. In the temperature ranges 200–315°C (PP-PY-PER) and 200–295°C (PP-PPA-PER), a degradation of the polyolefinic materials is observed (dashed areas in Figures 10 and 11). This process may be related to the presence of the additives in the matrix which lowers its thermal stability by formation of defects: peroxides or free radicals (during the compounding of the material or the oxidative thermal treatment [3]) or by change of the crystallinity of PP "in the interface polymer-additive [14]."
2. In the temperature ranges 315–400°C and 295–400°C, a protection of the polyethylenic systems is observed. It begins in the temperature range where the rate of the thermal degradation of PP in air is high. In our experimental conditions, the amounts of protected materials are quite the same. Expanded carbonaceous foaming materials are observed on the surface of the treated samples.
3. At higher temperatures, the protective effect decreases. It fully disappears at about 500°C with (PP-PPA-PER). On the other hand, an additional carbonaceous residue (stable in the temperature range 480–600°C) is formed with (PP-PY-PER) (this residue will be so-called CHAR in this text).

It is obvious that TG analysis doesn't give a true image of the behaviour of the formulations in the conditions of the fire because the experimental conditions (temperature programming, no flame) are very
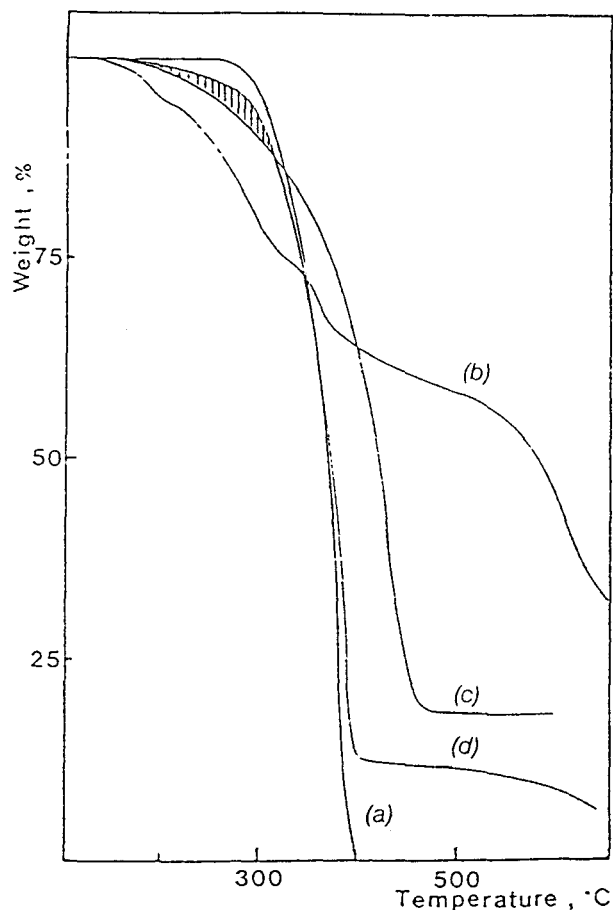
Figure 10. TG curves of PP (a), (PY-PER) (b) and (PP-PY-PER) experimental (c) and calculated (d) under air flow (from R. Delobel et al. [3]).

different. They allow nevertheless the postulation of the chemical changes of the different systems and the characterization of the stable materials which form during the thermal treatments.

The profiles of temperature observed "in the surface" of (PP-PY-PER) and (PP-PPA-PER) under forced burning conditions (Figure 13) allow us to specify the temperatures in the polyolefinic matrixes and in their protective shields during the process. The experimental curves verify that the expanded carbonaceous layers prevent heat transfer towards the undecomposed bulks (maximum temperatures at the "interface polymer-carbonaceous coating": about 220°C). The observed profiles of temperature in the two carbonaceous materials are very different. With (PP-PY-PER), the temperature increases gently from 225°C in the interface to about 550°C in the outer surface of the carbon layer. With (PP-PPA-PER), the temperature increases sharply to about 310°C and then nearly linearly up to 420°C, the temperature which corresponds, in that case, to the complete disappearing of the protective coating.
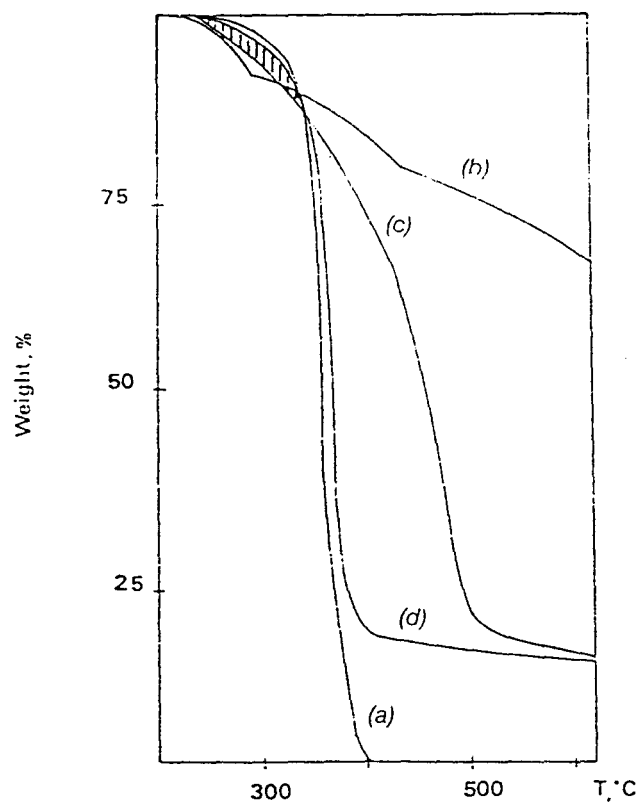
Figure 11. TG curves of PP (a), (PPA-PER) (b) and (PP-PPA-PER) experimental (c) and calculated (d) under air flow.
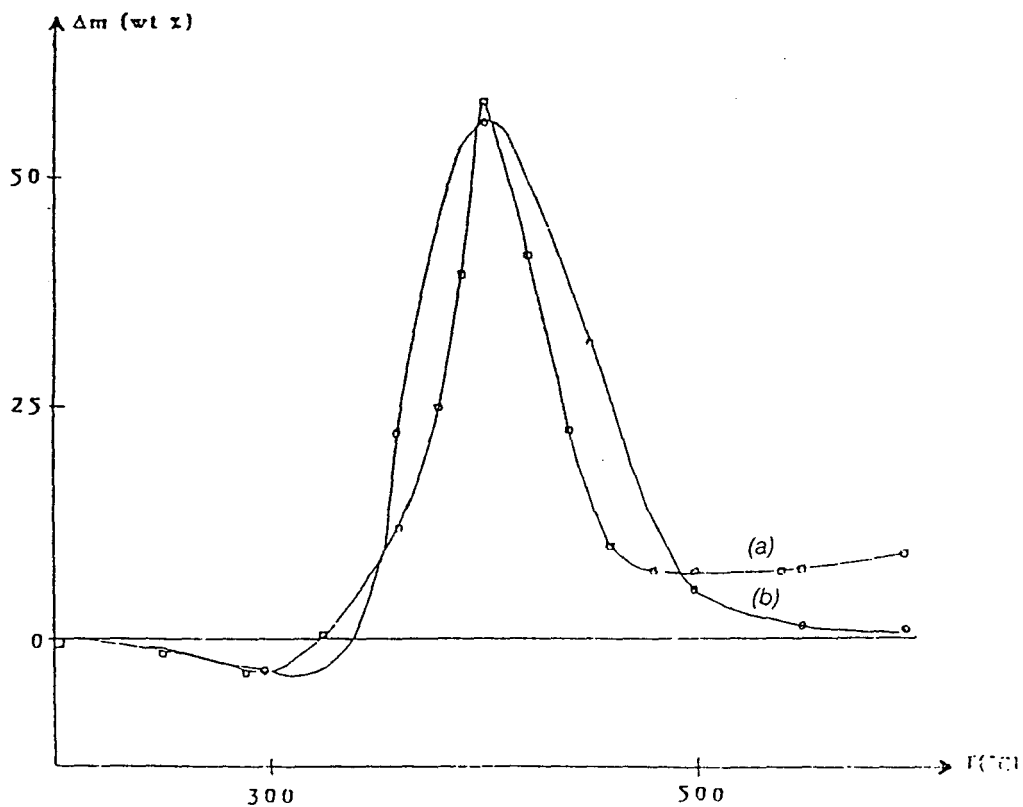

Figure 12. Calculated differences between experimental and calculated TG curves [according to (3) and (4)] of (PP-PY-PER) (a) and (PP-PPA-PER) (b) in air.
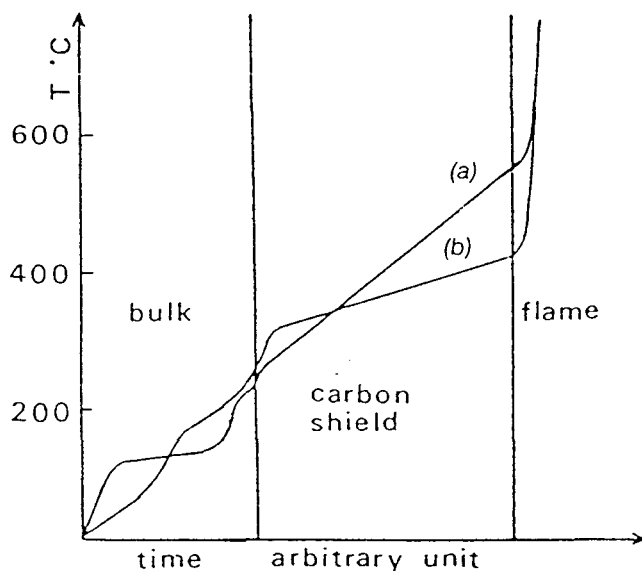
101

Figure 13. Profiles of the temperatures in the "surface" of (PP-PY-PER) (a) and (PP-PPA-PER) (b) in the conditions of a fire.

These last results have to be discussed with regards to the studies of the thermal degradations of the additive mixtures and of the formulations. In the "interfaces polymer-carbon layer," the measured temperatures correspond to the temperature of the end of the reaction between the additives (esterification) and to the beginning of the carbonization processes. In the particular case of (PP-PPA-PER), the temperatures in the protective coating ($310 < T < 420°C$) belong to the stability range of the corresponding intumescent coating. It is shown that, at least with (PP-PPA-PER), the "high temperature" residue resulting from the degradation of the intumescent coating does not play a significant part in the protection of the polymeric material at high temperature. With (PP-PY-PER), it may be proposed that the insulative coating ($220°C < T < 550°C$) is a mixture of carbon-based materials which consist of the intumescent coating, of the "high temperature" residue and of the "high temperature" char.

These facts are corroborated by the N.M.R. study of the carbonaceous coatings obtained with (PP-PY-PER) and (PP-PPA-PER) under forced burning conditions (Figures 5 and 6). The phosphate species in the protective materials are the same as the species observed after the isothermal treatments of (PY-PER) and (PPA-PER), respectively in the temperature ranges: 350–600°C and 290–350°C. The greater part of these species (respectively 88 and 93% of the ^{31}P) are acidic phosphates. The presence of Lewis acids in each protective coating seems to be significant, nevertheless the part that they play in the formation of these coatings has to be elucidated.

In a recent paper dealing with the (PP-PY-PER) system [7], it has been proposed that, in a first step, these acidic species (Lewis acids) play a main part in the formation of the intumescent coating according to the mechanism:

- breaking of the P-O-C and of C-C bonds of the esters (results of the reaction between the additives) and then dehydration which leads to olefins
- formation of precursors resulting from the interaction of these olefins with the Lewis acids (reactants or more probably catalysts) [15]
- crosslinkings which lead to polyaromatic structures
- dehydrogenation of these last structures which leads to a framework of carbon (intumescent coating and "high temperature" residue) supporting the acidic phosphate species.

The observed protection of (PP-PY-PER) in the "high temperature" range ($T > 420°C$) may be explained by the formation, in an additional step, of a char. Its formation may be explained by a reaction of the products resulting from the thermo-oxidative degradation of PP with the acidic phosphate species which are formed during the thermal treatment [6,7]. Similar mechanisms have been previously reported by Kishore [16] (work dealing with the action of ammonium phosphate in polystyrene fire retardancy) and by Khalturinsky who proposes a catalytic part played by Lewis acids (formed from phosphorus-based systems) in the fire retardance of cellulose [17].

TG analysis (Figures 14, 15 and 16) shows that the two formulations present the same behaviour in inert gas. It verifies that a protection of (PP-PY-PER) and (PP-PPA-PER) is provided by intumescent coatings formed from the additive mixtures [(PY-PER) and (PPA-PER)]. In these conditions, a stable char formed from PP or its pyrolysis products is never observed. This last result agrees well with the hypothesis of an additional carbon layer which develops [on the surface of (PP-PY-PER)] only from oxidized products resulting from the degradation of PP in air.

The study of the formulation (PP-PPA–PER) under air shows that its protection is only carried out by an intumescent coating. It may be considered that this coating forms according to the same mechanism as that of the intumescent coating on (PP-PY-PER). Furthermore the formation of a char (arising from the polymer) is not observed with this formulation. Moreover, the study of (PP-PPA-PER) shows that the presence of the "high temperature" residue doesn't lead to a marked protection of the polymeric bulk. It may be proposed that the "high temperature" residues play only a part as a "catalytic" support of the Lewis acid
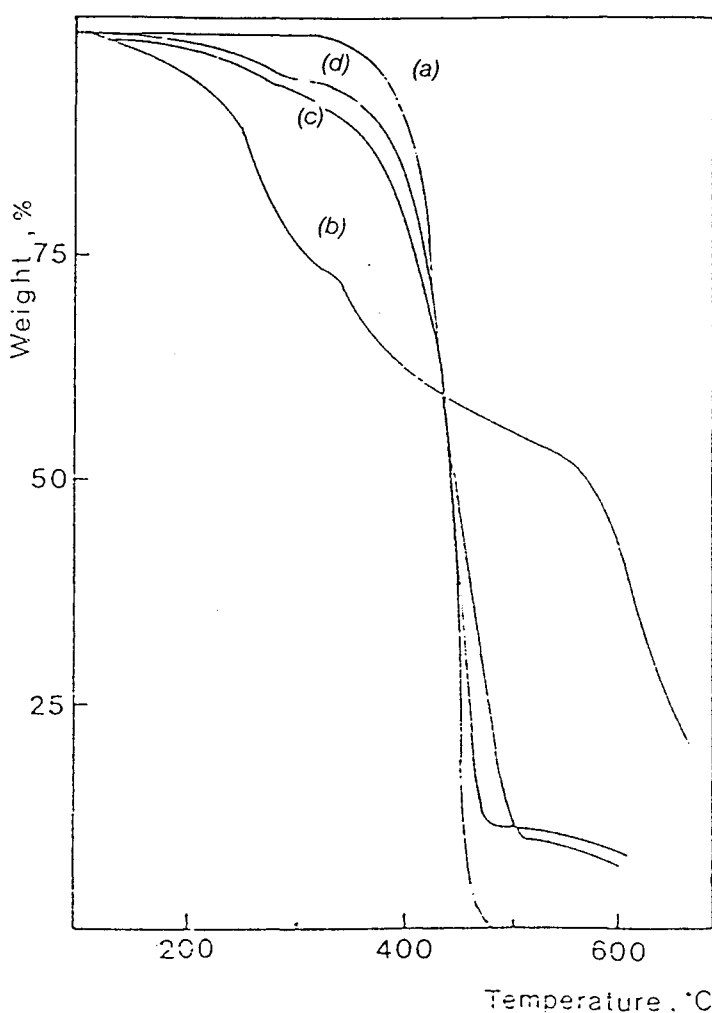
Figure 14. TG curves of PP (a), (PY-PER) (b) and (PP-PY-PER) experimental (c) and calculated (d) under N_2 flow (from R. Delobel et al. [3]).

species on (PP-PY-PER) or as a support of phosphorus oxide on (PP-PPA-PER).

The present comparative study shows unambiguously that char develops on the surface of (PP-PY-PER) via a reaction of the oxidized products (resulting from the degradation of PP in air) with the acidic phosphates supported by a carbon framework. The resulting esters (previously characterized by an i-r study [4]) may decompose according to the same mechanism as the esters which are formed by reaction between the additives. This decomposition leads to the formation of new structures of carbon stable at relatively high temperature. With (PP-PPA-PER), it may be assumed that such a char cannot form because there is no acidic phosphate species in the "high temperature" residue resulting from the degradation of the intumescent coating.

To conclude, these results allow us to propose that the protection of

the polymeric material may be provided, in the low temperature range (*T* < 420°C), by the carbonaceous shields which result from the thermal degradation of the additive mixtures. The protective effects are clearly improved in the particular case of (PP-PY-PER) by the existence of stable structural form(s) of carbon in the highest temperature range. This last carbon-based structure results from the reaction between the products of the thermo-oxidative degradation of PP and the Lewis acids which are stable in this temperature range. This last statement agrees well with Montaudo's works [flame retardance of intumescent (PP-PPA-polyureas) systems] which put forwards a direct relation between the increase of the L.O.I. values and the increase of the amounts of a "char residue" obtained during the thermal treatment of the formulations in air [17].
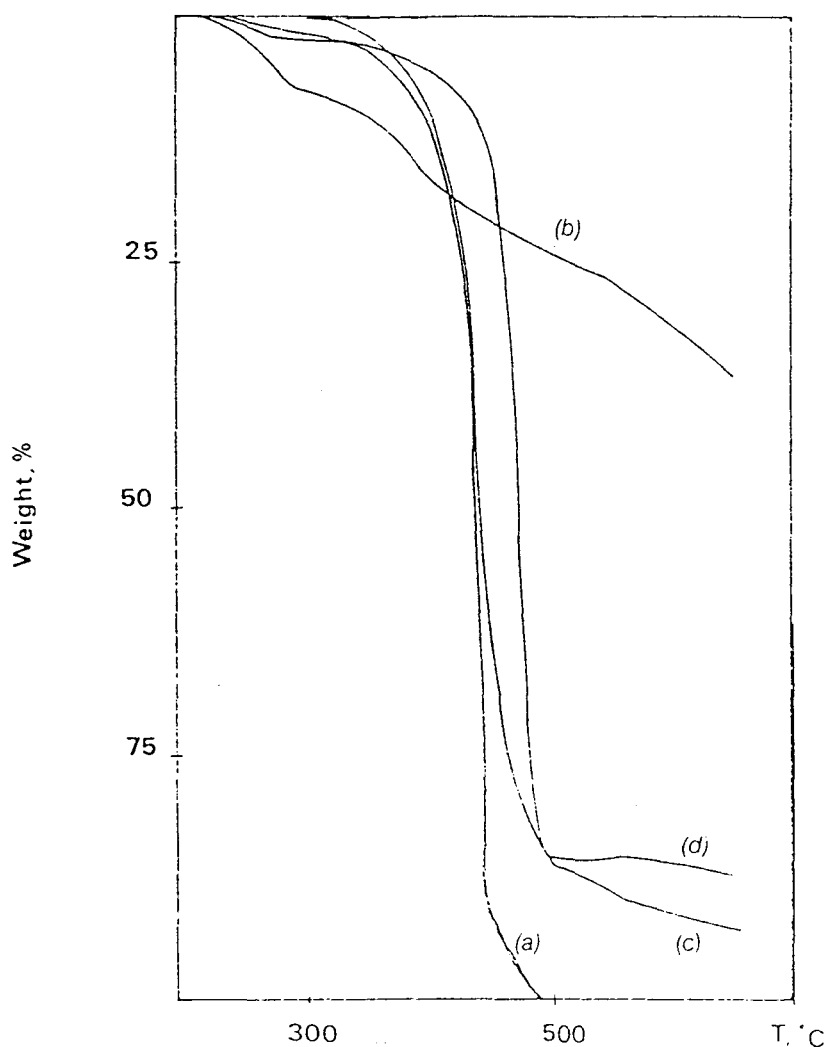

Figure 15. TG curves of PP (a), (PPA-PER) (b) and (PP-PPA-PER) experimental (c) and calculated (d) under N₂ flow.
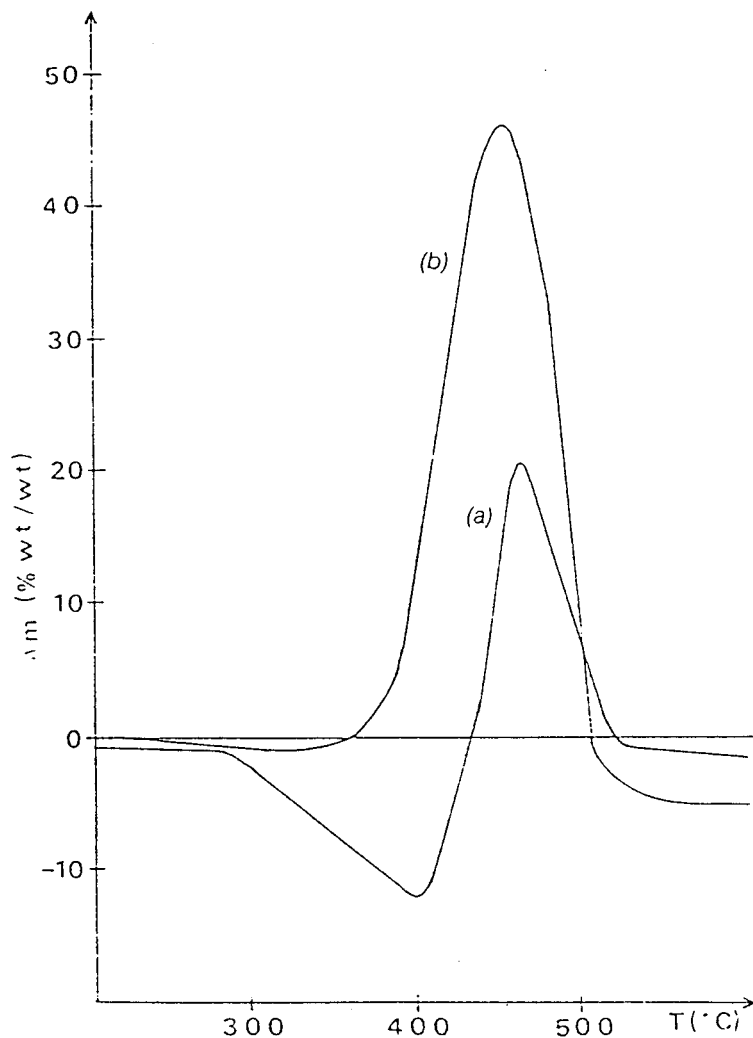
Figure 16. TG in nitrogen of (PP-PY-PER) (a) and (PP-PPA-PER) (b): differences between the experimental curves and the curve calculated according (3) and (4).

CONCLUSION

The comparative study of the two polyolefinic formulations shows that the protections of the polymeric matrixes may be provided by two different carbon-based coatings on the undecomposed bulks. These two coatings result respectively from the intumescence process arising from phosphate-polyol mixtures and from the reaction of oxidized products of the thermo-oxidative degradation of PP with acidic species supported in the carbonaceous shield. The study shows that the best fire retardance is provided when the two kinds of carbon-based coatings are formed from a same system. The presence of stable acidic phosphate species is required for the existence of char in the "high temperature"

range ($420\,°C < T < 550\,°C$). So, it may be assumed that these Lewis acids play a main part in the protective process.

From these statements, it may be proposed that a performance intumescent fire-retardant polyethylenic-based formulation has to produce Lewis acids and to give rise to a foamed carbon-based structure (support for these Lewis acids), at a temperature lower than temperature where the oxidative degradation of the polymer becomes significant. The precursor of these acids has to be selected in such a way to obtain species stable over a large temperature range.

REFERENCES

1. Vandersall, H. L. *J. Fire Flammability*, 2:97 (1971).
2. Camino, G., L. Costa and L. Trossarelli. *Polym. Deg. & Stab.*, 6:243 (1984); Camino, G., L. Costa and L. Trossarelli. *Polym. Deg. & Stab.*, 7:25 (1984).
3. Delobel, R., N. Ouassou, M. Le Bras and J.-M. Leroy. *Polym. Deg. & Stab.*, 23:349 (1989).
4. Delobel, R. *Proceed. of the Third Meeting on Fire Retardant Polymers*, Turin (1989), G. Camino, ed., A.I.M. pub., Turin, p. 28 (1989).
5. Camino, G., L. Costa, L. Trossarelli, F. Costanzi and G. Landoni. *Polym. Deg. & Stab.*, 8:3 (1984).
6. Le Bras, M., R. Delobel, R. Descressain and J.-M. Leroy. *Bull. Soc. Chim. Belg.*, 98(9–10):735 (1989).
7. Delobel, R., M. Le Bras, N. Ouassou and R. Descressain. *Polym. Deg. & Stab.*, in press.
8. Swanson, C. and F. McCollough. *Inorg. Synthesis*, J. Kleinberg, ed. New York: McGraw-Hill, 7:65 (1963).
9. Frazier, A. W., J. P. Smith and J. R. Lehr. *J. Agr. Food Chem.*, 13(4):316 (1965); A.S.T.M. 20–86.
10. Crutchfield, M. M., C. H. Duncan, L. H. Lechter, V. Mark and J. R. Van Wazer. *P31 Nuclear Magnetic Resonance—Topics in Phosphorus Chemistry*, M. Grayson and E. J. Griffith, eds. New York:Wiley Interscience (1967); Van Wazer J. R., C. F. Callis, J. N. Shoolery and R. C. Jones. *J. Am. Chem. Soc.*, 78:5115 (1956).
11. Ouassou, N. Thèse, Lille (1990).
12. Singer, L. S. and I. C. Lewis. *Appl. Spectrosc.*, 36(1):52 (1982).
13. Alger, R. S. *Electron Paramagnetic Resonance: Techniques and Applications*, New York:Wiley Interscience, p. 416 (1974).
14. Chabert, B. and J. M. Haudin. Colloque "Matrices et Fibres Polymères— Nouveaux Aspects Chimiques et Physiques," G.F.P.–A.M.A.C., *Sophia-Antipolis* (November 23, 1989).
15. Tauster, S. J. *J. Catal.*, 27:307 (1972).
16. Kishore, K. and K. Mohandas. *Combustion and Flame*, 43:145 (1981).
17. Khalturisnky, N. A. and Ai. Ai. Berlin. "Degradation and Stabilization of Polymers," (Volume 2), H. H. G. Jellinek and H. Kachi, eds., New York: Elsevier Pub., pp. 253–259 (1989).
18. Montaudo, G., E. Scamporrino and D. Vitalini. *J. Polym. Sci.*, 21:3361 (1983); Montaudo, G. and C. Puglisi. "Third Meeting on Fire Retardant Polymers," *Turin* (September 21, 1989).

New Intumescent Formulations of Fire-retardant Polypropylene—Discussion of the Free Radical Mechanism of the Formation of Carbonaceous Protective Material During the Thermo-oxidative Treatment of the Additives

Michel Le Bras, Serge Bourbigot, Christelle Delporte

Laboratoire de Physico-chimie des Solides, ENSCL, Université des Sciences et Technologies de Lille BP 108, F-59652 Villeneuve d'Ascq Cedex, France

Catherine Siat, Yannick Le Tallec

Centre de Recherches et d'Etude sur Les Procédés d'Ignifugation des Matériaux (CREPIM), Zone Initia, F-62 Bruay la Bussière, France

The study compares five new intumescent additive mixtures and a carbonizing additive system with the ammonium polyphosphate–pentaerythritol system and additive formulations previously developed in laboratory in terms of fire retardancy of polypropylene-based formulations. The mixture of diammonium pyrophosphate and polyols produced by agrochemical industry xylitol and d-sorbitol (carbonization agent) are FR additive mixtures of interest for polyolefins. Moreover, the FR performance of the mixture of ammonium polyphosphate and polyamide-6 is reported. It is proposed that boric acid salts have to be developed as precursors for carbonization catalytic species. A thermal analysis study shows that FR performances and amounts of carbonaceous materials resulting from the thermal degradation of the additive mixtures are not related. An additional compilation of previous spectroscopic studies by the laboratory confirms that the intumescent process results from the formation of polyaromatic species and that FR systems maintain acidic species in a relatively high temperature range. An ESR study discusses the presence of π radicals in the protective coating formed using the additive systems. It provides information on the size of the carbonaceous structures in the materials and the presence of crystalline phases in the coating. Finally, the participation of free radicals in the formation of chemical bonds between the materials produced from the additives and the products of the degradation of the polymer is discussed.

INTRODUCTION

The use of polyolefins and particularly of polypropylene in electrical, building or transport applications is often limited because of their poor fire resistance. Thermal and thermo-oxidative decomposition (via a radical chain mechanism with both direct and indirect branching) and combustion of these polymers has been extensively studied.[1] Their burning mechanism is similar to that of the gaseous hydrocarbons arising from their degradation (fuels).[2]

The authors' laboratory has developed several fire retardant (FR) polyolefin-based formulations where protection is carried out by the formation in the conditions of a fire of a surface glassy[3] or intumescent[4] material, i.e. the formation of an expanded carbonaceous structure on the flame front.[5,6] On particular, it has formulated intumescent isotactic polypropylene (PP)-based FR materials for batteries, flooring and carpet fibre applications.

Formulations containing intumescent additives are generally mixtures of carbonization agents and carbonization catalysts (products which form stable acidic species when heated)[7] and eventually, a spumific agent.[8] Previous studies from the authors' laboratory have

shown that the intumescent structure consists of carbonaceous and polyaromatic species which structure (carbon organization characteristic of a pregraphitization stage[9]) grows when the temperature increases[7,10] and that synergistic agents (clays[11] or zeolites[12,13]) enhance the thermal stability of the intumescent shields.

The first intumescent additive system tested in PP was a mixture of pentaerythritol (PER, carbonization agent) and ammonium polyphosphate (APP, carbonization catalyst).[4,6] Most recently, the authors' laboratory has developed new additive mixtures using pyrophosphoric acid and boric acid salts as acidic species precursors, several polyols produced by the agrochemical industry (d-sorbitol (d-glucitol), i-sorbitol, d-mannitol (mannite), dextrose (d-glucose) and xylitol (xylite)) and polymers (polyamides, poly(vinyl alcohol), ethylene–vinyl alcohol copolymers) as carbonization agents and several synergistic agents (refractory clays, zeolites, silicilic acid, siloxanes, dextrins such as β-cyclodextrin (cycloheptaamylose) and polymers such as ethylene–vinyl acetate copolymers).

Previous studies show that PP plays a part in the formation of the protective char: chains of the polymer are linked to the polyaromatic structures and thus may

provide the mechanical properties of interest in the shield.[5,10] This stabilization of the polymer links in the coating limits the depolymerization process and evolution of the resulting small flammable molecules and then contributes to the FR performance of the formulation.

The chemical reaction(s) which allow the formation of thermally stable bonds between the PP links and the polyaromatic structure of the intumescent materials are not known. We have previously proposed that the oxidized products arising from the thermo-oxidative degradation of the PP matrix react with acidic phosphate species which form during thermal treatment to give, in a first step, esters which eventually transform in the second step into olefinic or aromatic species.[6] Then we propose that the 'carbon' structure forms from these species via a chemical free radical polymerization process (additional crosslinkings and dehydrogenation).[14]

A recent experiment in the authors' laboratory has shown that the temperature of the carbonaceous shield formed from an FR intumescent formulation lies between 280°C and 550°C (Fig. 1). We reported recently on the strong paramagnetic character of the materials resulting from the thermal treatment of several intumescent additives mixtures in this temperature range.[6,12,15,16] This observation is very interesting because it suggests that the shield becomes paramagnetic on exposure to a flame. The free radicals formed may react with the degradation gases and/or the radical species arising from the scission of the polymer chains and so, may, via direct radical reactions, trap polymer links in the carbonaceous structure.

The paramagnetic species in intumescent materials create an electron spin resonance (ESR) signal. Its interpretation may be based on the existence of stable carbenes,[17] the formation of aromatic free radicals involving a thermal bond dissociation at the most reactive sites of the polyaromatic structure during the carbonization process[18] or the formation of free radical intermediates during the reaction of polynuclear aromatic hydrocarbons with oxygen (in this case the spectroscopic factor g is high).[19] The free radicals 'trapped' in the polyaromatic structure of the intumescent material may be considered as probes enabling the proposal that the formation of this material involves a free radical reaction scheme.

This paper compares seven new original formulations of PP with two previously published ones. It concerns mixtures of two or three of the additives:

- Ammonium polyphosphate (APP),[6] diammonium pyrophosphate (PY)[20] or diammonium pentaborate (APB)[16] as carbonization catalysts
- Pentaerythritol (PER), xylitol (XOH), mannitol (MOH), d-sorbitol (SOH), β-cyclodextrin (BCOH)[15] or polyamide-6 (PA-6)[21] as carbonization agents
- Zeolite 4A (4A)[22] and an ethylene-vinyl acetate (8%) (EVA-8) as synergistic agents. EVA-8 plays two roles in the formulation: it increases the Limiting Oxygen Index (LOI) and the 'compatibility' of APP in PA-6 (it maximizes the interfacial bonding and so prevents rejection of the mineral additive throughout the polymer matrix.[23])

First, this paper reports on the FR performance of these additive mixtures in PP using Limiting Oxygen Index[24] and UL-94[25] tests. Second, a thermogravimetric (TG) study of the thermal stability of the carbonaceous materials resulting from a thermooxidative treatment of the additives mixtures is presented. This study allows the measurement of the highest temperature of treatment (HTT) which corresponds to a particular stable material. Then it deals with the ESR spectroscopic study of the stable materials. Finally, the FR classification will be related to the 'trapped' free radical concentrations in the intumescent materials and in residues resulting from their thermal degradation.

EXPERIMENTAL

Materials

The polymer was isotactic PP (supplied as powder by Solvay). The catalyst precursors (CP) were APP $((NH_4PO_3)_n$, $n = 700$, Hoechst Exolit 422, soluble fraction in H_2O: < 1 wt%), PY (synthesized in the laboratory[15] using the procedure of Swanson et al.:[26] reaction of NH_3 with $H_4P_2O_7$ in ethanol at a temperature lower than 10°C. In fact, it is a mixture of ammonium ortho-, pyro- and polyphosphate with more than 50 wt% of diammonium pyrophosphate) and APB $((NH_4)_2B_{10}O_{16}$, $8H_2O$, supplied by Aldrich-Chemie).

The carbonization agents (CA) were PER (Aldrich R.P. grade), XOH (supplied by Aldrich, 98 wt%), MOH (Aldrich 'ACS reagent' grade), SOH (supplied by Aldrich, 97 wt%), BCOH (supplied by Roquette Frères (Lestrem—France)) and PA-6 (supplied as pellets by Rhône-Poulenc).

The synergistic agents (SA) were 4A (Si/Al = 1, compensation cation: Na, powder supplied by Ceca) and EVA-8 (ethylene-vinyl acetate (8%) copolymer (Lactene); powder supplied by Elf Atochem).
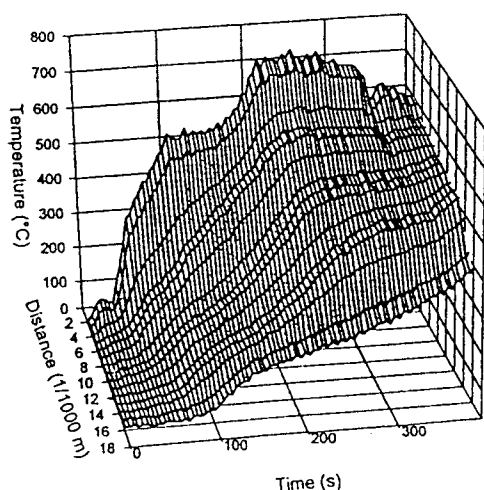

Figure 1. Experimental temperature profile in the surface of the intumescent PP-APP-PER formulation in the conditions of a fire (oxygen percent in air = LOI + 4, air flow: 28.3×10^{-5} m^3 s^{-1}) (after S. Bourbigot and L. Morice, 1996, unpublished results).

Table 1. Composition of the additive mixtures					
Mixture label	CP	CA	SA	CA/(CA+CP) (wt%)	SA/(CP+CA+SA) (wt%)
I	APP	PER	—	25	—
II	APP	PER	4A	25	5
III	APP	PA-6	EVA-8	68.8	10.3
IV	PY	PER	—	39.1	—
V	PY	XOH	—	33.33	—
VI	PY	MOH	—	33.33	—
VII	PY	SOH	—	33.33	—
VIII	APB	PER	—	33.33	—
IX	PY	BCOH	—	66.66	—

This study was carried out using the PP/(PP + additives) ratio: 70 wt%. Table 1 details the components of the additive mixtures. (CP/CA) and SA/(SA + CP + CA) ratios are deduced from the LOI curves (higher synergistic effect) and are discussed as results.

Two different preparation modes of the additive mixtures were used. Mixtures without PA-6 were first prepared by ball-milling after mechanical grinding and sieving $(200 \times 10^{-6} \, \text{m})$ of the raw materials. Mixtures with PA-6 were mixed at 215°C during the time required to reach a stationary state (constant values of the measured torque and of the temperature after the loading peak) using a Brabender Laboratory Mixer measuring head (type 350/EH, roller blades, 50 RPM). Control of the mixing conditions were performed using a data-processing torque rheometer system (Brabender Plasti-Corder PL2000).

The additives were then incorporated at 30 wt% in PP using different procedures. Sheets $(100 \times 100 \times 3 \, \text{mm}^3)$ of each powdered formulation were first obtained after ball-milling, using a Darragon compression press at 200°C with a pressure of 3 MPa.

Mixtures of formulations I, II, III and IX were mixed at 200°C using a Brabender Laboratory Mixer measuring head using the procedure previously described. Sheets were then obtained using the compression press at 200°C and at a pressure of 3 MPa.

Finally, formulations I, II and III were processed as extrudate using the Brabander DSK 42/7 a twin-screw compounder (temperature of intermeshing and mixing zones respectively 215°C and 235°C, temperature of the rod dies 215°C, 50 rpm) controlled using the data-processing torque rheometer system (Brabender Plasti-Corder PL2000). Pelletizing was performed using the Darragon conveyor belt and pelletizer. Sheets were then obtained using the compression press at 200°C and at a pressure of 3 MPa.

Before each ESR analysis, isothermal treatments of the additive mixtures were carried out under air flow $(10^{-5} \, \text{m}^3/\text{s})$ at characteristic HTT during the time required to reach a steady state, i.e. weight loss rates versus time became null. The conditions of additional spectroscopic studies (NMR, XRD) have been reported in references 12 and 16.

Fire testing

LOI (Minimum Oxygen Concentration to Support Candle-like Combustion of Plastics) was measured using a Stanton Redcroft instrument on strips $(120 \times 60 \times 3)$ mm^3 according to the standard 'oxygen index' test.[24] For comparison unmodified PP gave a LOI value of 17%.

UL-94 classification was obtained on strips $(8 \times 60 \times 3)$ mm^3 according the conditions of the standard test[25] which provides only a qualitative classification of the samples (V0, V1, V2 and not classed (NC) labelled samples).

The results of the tests of an identical formulation processed using the three different preparation procedures are the same (variation of the LOI < 1% and the same UL classification). They confirm a previous proposal: FR performance of one formulation depends on the processing procedure when the conditions of the procedure are closely related.[13]

Thermogravimetric analyses

TG analyses were carried out as reported in reference 12. The curves of weight difference between the experimental and theoretical TG curves were computed as follows:

- $M_{add1}(T)$: values of weight given by TG curve of the catalyst precursor
- $M_{add2}(T)$: values of weight given by TG curve of the carbonization agent
- $M_{add3}(T)$: values of weight given by TG curve of the synergy agent
- $M_{exp}(T)$: values of weight given by TG curve of the mixture of the additives
- $M_{th}(T)$: theoretical TG curve computed by linear combination between the values of weight given by TG curves of each of the additives
- $D(T)$: curve of weight difference: $D(T) = M_{exp}(T) - M_{th}(T)$

Electron spin resonance

All ESR spectra were recorded at 25°C using the dual-sample cavity 'E190' of the spectrometer Varian 'E line' (klystron frequency about 9.5 GHz (X band), modulation frequency: 10^5 Hz) with a sweep width of $0.04T$ about a centre frequency of $0.34T$. Constant experimental acquisition parameters in common were a modulation amplitude of 4×10^{-6} T, a conversion time of 10 ms and a RC filter time constant of 64 ms. The incident adequate microwave power was kept weak to avoid signal saturation and linewidth broadening.

The splitting spectroscopic factor (g) and free radical concentrations were calculated referring to a standard ('strong pitch' supplied by Brucker, $g = 2.0023$ and spin concentration: $3 \cdot 10^{15}$ sp. $\times$ cm^{-1}).

Spectroscopic functions fitting with the signal are generally Lorentzian, Gaussian, Voigt functions or a combination of these functions. The concentrations of the paramagnetic species were computed using a method of integrating the signals. Some high HTT samples present signals with more complicated lineshapes. The concentrations were then computed using a method of double integration of the area of the spectra.[27]

RESULTS

Fire retardant performances

Typical examples of the variation of LOI values of the new PP-based formulations versus their CP, CA and SA weight concentrations are illustrated respectively in Figs 2, 3 and 4. They show that the FR performance results from a synergistic effect. Such curves are obtained using additive mixtures I to VIII. The compositions of these mixtures which correspond to the maximum synergistic effect are shown in Table 1.

The LOI of the PP-P7-BCOH system is comparatively poor, so BCOH is not a good CA (Fig. 5). Study of

Figure 5. Normalized fire testing values (LOI) versus β-cyclodextrine concentration in PP-P7-BCOH formulations.
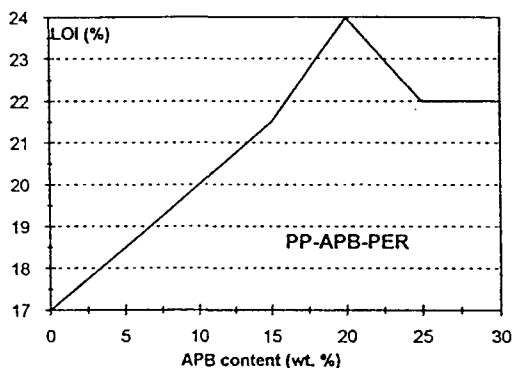
Figure 2. Normalized fire testing values (LOI) versus APB concentration in PP-APB-PER formulations.
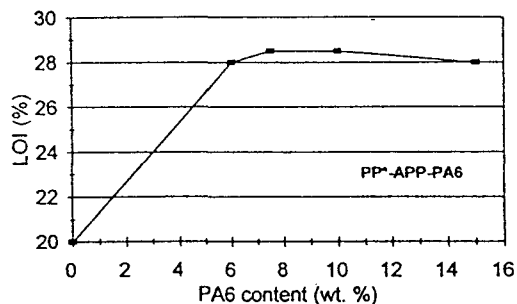
Figure 3. Normalized fire testing values (LOI) versus PA-6 concentration in PP-APP-PA-6 formulations.
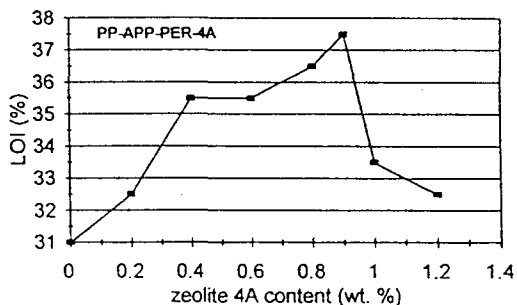
Figure 4. Normalized fire testing values (LOI) versus 4A concentration in PP-APP-PER-4A formulations.
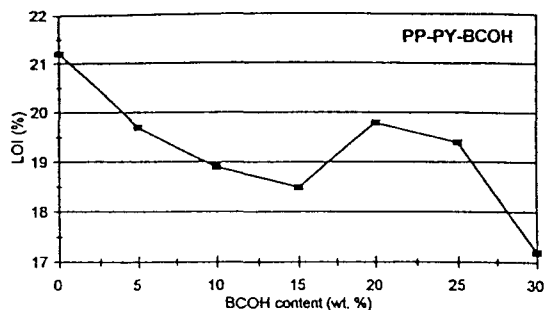
Table 2. Results of the fire retardancy tests of the PP-based formulations

Mixture	I	II	III	IV	V
LOI (%)	32	42	28.5	35	24
UL-94	V0	V0	V0	V0	V0

Mixture	VI	VII	VIII	IX	
LOI(%)	23.8	24	24	19.8	
UL-94	NC	V0	NC	NC	

NC: not classed by the test.

formulation IX is nevertheless presented in this work because this system yields a carbonization process during its thermooxidative treatment and, furthermore, is found to be a synergistic component when used in some polyolefin–phosphate–polyol systems (M. Le Bras and Y. Le Tallec, unpublished results).

Table 2 presents FR performances of the PP–additive formulations corresponding to the additive mixtures studied. It shows that formulations I to VIII give a FR character but that formulations VI, VIII and IX do not yield an UL-94 classification (because of dripping with cumulative combustion time higher than 70 s).

Thermogravimetric analysis

A previous study of the APP–PER system[13] has shown that reaction between the additives begins at about 250°C to give a carbonaceous material with a comparatively enhanced stability up to 600°C. It points out the temperature ranges of the steps of the carbonization process: reaction between the additives (ester formation) begins at about 175°C, development of an intumescent material (280–350°C), formation of a 'high-temperature' carbonaceous material (relatively stable in the temperature range 430–560°C) and, finally, degradation of this material with subsequent evolution of phosphorus oxide.[6]

The present study shows that mixtures II, IV, V, VI and VII present the same reaction steps during their carbonization processes. First, a reaction between the additives begins at about 150°C to give a carbonaceous material at 260°C with a comparatively enhanced stability up to 570°C. Then the development of the

intumescent material (260–350°C) occurs followed by the formation of a carbonaceous material (430°C) relatively stable in the temperature range 430–480°C and finally, the degradation of this material occurs successively.

Figure 6 compares the TG curves of the APP–PA-6 mixture with those of its components in isolation. It shows that a reaction between the additives takes place at about 200°C with formation of an expanded carbonaceous material (visual observation) and that this material degrades at about 390°C to form a non-expanded carbonaceous material which is relatively stable in the temperature range 400–550°C.

The weight-difference curve of the mixture III (Fig. 7) is very different from those of the APP–polyol mixtures (I, II and IV to VII). It shows that a reaction between the two additives occurs at a relatively low rate from 200°C up to about 275°C and then at a higher rate in the range 275–390°C. In this latter temperature range, evolution of gases resulting from the reaction may be assumed to be responsible for the foamed character of the residual material. At 390°C, these 'encapsulated' gases evolve and the expanded property of the material is lost. In the 390–550°C range, the residual weight of the relatively stable material is about the same as the one computed in the hypothesis that no reaction occurs between the additives. The additional severe weight loss observed between
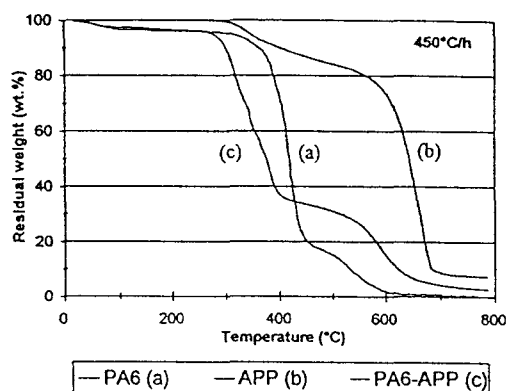
550°C and 660°C may be assigned to the degradation of phospho-carbonaceous species and to the subsequent sublimation of phosphorus oxide. This last degradation step finally leads to the formation of a low amount of residue with a good thermal stability up to 800°C.

Figure 8 presents the weight loss curve of mixture VIII. It shows the first thermal degradation of APB which degrades from 80°C with evolution of H_2O and NH_3.[16] Then a reaction between APB and PER takes place which leads to the successive formation of two carbonaceous products with comparatively enhanced stabilities respectively in the temperature ranges 270–375°C and 430–600°C. The reaction between the additives (formation of esters of the boric acid) begins from 80°C and the carbonization process occurs between 205°C and 330°C. This last reaction leads to the formation of an intumescent material (visual observation). Its degradation results in the loss its in expanded character at 400°C and to the 'high-temperature' residue stable in the 400–560°C range.

A comparison between the thermal degradation of the APP–PER (I) and the APB–PER (VIII) mixtures shows similar behaviour. But the thermal stability of the intumescent material obtained from VIII is lower than that of I.

The weight-difference curve computed from the mixture IX TG data (Figure 9) shows that reaction between the additives begins at 170°C. The carbonization process of IX takes place at 270°C and leads to a glassy, unexpanded (visual observation) carbonaceous material which decomposes at about 360°C[15] to give

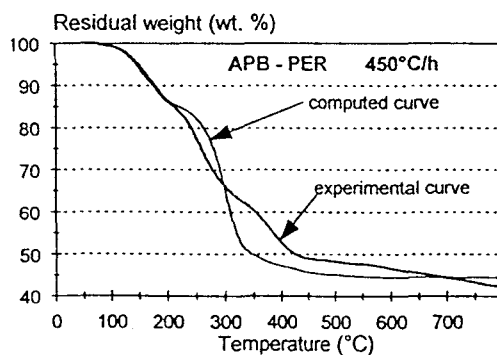Figure 6. Experimental TG curves of (a) PA-6, (b) APP and the APP–PA-6 mixture under air flow.

Figure 7. Weight-difference curve of the APP-PA-6 mixture computed from curves of Fig. 6.

Figure 8. Experimental and computed TG curves of the APB–PER mixture under air flow.
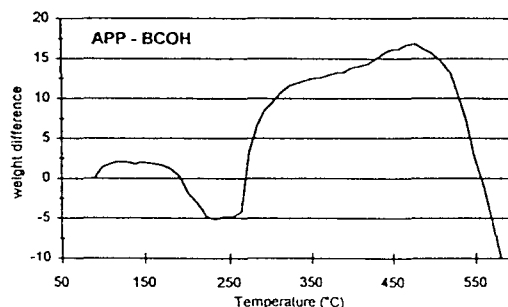

Figure 9. Weight-difference curve of the APP–BCOH mixture.

Table 3. Characteristics of chars resulting from the thermal treatment of the additive mixtures

Additive mixtures	HTT (°C)	Treatment time (h)	Residual weight (wt%)	Materials
I	225	12	91	Brown paste
	280	12	82	Intumescent material
	350	12	72	Intumescent material
	430	12	45*	Non-expanded 'carbon' residue
	560	12	6*	Non-expanded 'carbon' residue
II	280	12	85	Intumescent material
	350	12	75	Intumescent material
	430	12	52*	Non-expanded 'carbon' residue
	560	12	15*	Non-expanded 'carbon' residue
III	240	12	72	Paste and intumescent material
	390	12	36*	Partially intumescent material
	440	12	11*	Non-expanded 'carbon' residue
	530	12	7*	Non-expanded 'carbon' residue
IV	240	24	87	Brown paste
	280	24	75	Intumescent material
	350	24	64	Intumescent material
	420	24	52*	Non-expanded 'carbon' residue
V, VI and VII	190	24	78	Black or brown pastes
	230	24	59	Carbonaceous materials
	320	24	52	Intumescent material
	430	24	22*	Non-expanded 'carbon' residue
	530	24	7*	Non-expanded 'carbon' residue
VIII	200	10	83	Carbonaceous paste
	300	10	58	Intumescent material
	320	10	47*	Non-expanded 'carbon' residue
	400	10	45*	Non-expanded carbon-like residue
	450	10	42*	Non-expanded grey residue
IX	190	24	78	Brown paste
	230	24	73	Black paste
	320	24	61	Carbonaceous glassy material
	430	24	27*	Non-expanded 'carbon' residue
	530	24	16*	Non-expanded 'carbon' residue

* Deduced from TG curves, the hydrophilic character of the material does not allow to obtain the residual weight in standard conditions in air.

a 'high-temperature residue' comparatively stable in the range 360–515°C.

This TG study allows the selection of HTT of the additive mixtures which allows representative characteristic materials to be obtained resulting from isothermal treatments of the mixtures. Table 3 reports the values of the HTT and describes the resulting materials. Four different forms of carbonization behaviour are shown by the residual weight compilation:

(1) Formation of a large amount of intumescent material (residual weight > 70 wt%) and of non-expanded material (residual weight > 50 wt%) using formulations II and IV

(2) Formation of a large amount of intumescent material and of a low amount of non-expanded material using formulations I and III

(3) Formation of a small amount of intumescent material and of non-expanded material using formulations V, VI, VII and VIII

(4) Formation of a small amount of glassy 'carbon' and a large amount of 'high-temperature' non-expanded material using formulations IX.

Analysis of the free radicals 'trapped' in the carbonization products

Every sample studied gives rise to an ESR signal and so presents a paramagnetic character. Typical examples on the newly observed signals are presented in Fig. 10 and the corresponding fit analyses of the integrated signal are given in Figs. 11–13.

Characteristic data (obtained from this work and from previous results from the authors' laboratory) of the ESR spectra of the additives mixtures heat treated at a temperature belonging to the range used for the processing procedure (175–240°C, function of the additives) and at characteristic HTT are reported in Table 4.

The observed signals (line shapes and spectroscopic factors closed to 2) may be assigned according to Alger[29] and Singer and Lewis[30] to free radicals 'trapped' in carbonaceous structures, i.e. π-radicals in which the unpaired electron is delocalized over polynuclear aromatic ring systems. It is generally proposed that these stable radicals are odd-alternate aromatics produced by a thermally induced molecular rearrangement and polymerization processes in pitches.
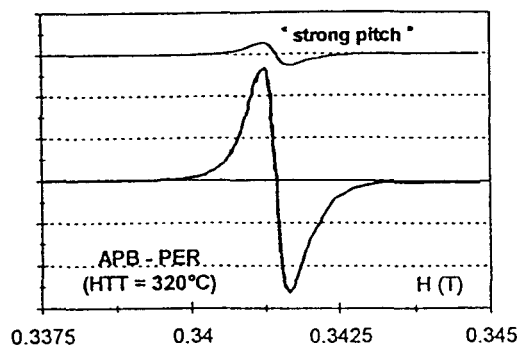
Figure 10. X-band ESR spectrum of the APB–PER mixture heat treated at 320°C under air.
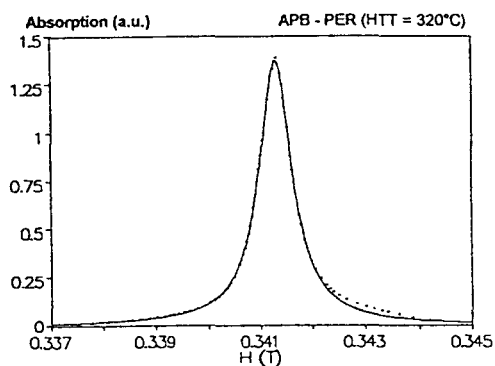

Figure 11. Integrated ESR spectrum (one Lorentzian function) of the APB–PER mixture heat treated at 320°C.
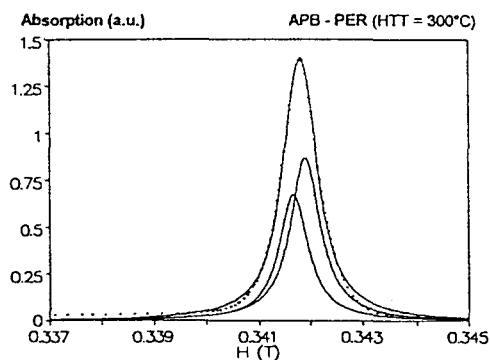

Figure 12. Integrated ESR spectrum (two Lorentzian functions) of the APB–PER mixture heat treated at 300°C under air.

Figure 13. Integrated ESR spectrum (one Voigt and one Gaussian function) of the APP–PA-6 mixture heat treated at 390°C under air.

Figure 14. Integrated ESR spectrum (one Lorentzian and one Gaussian function) of the APP–PA-6 mixture heat treated at 440°C under air.

Line shape analysis is relatively easy in most of the recorded signals. ESR lines with a homogeneous Lorentzian shape are explained by individual 'spin packets' in which all the free-radical spins behave cooperatively like a single-spin system. It may be assigned to radical species that are large and that consequently have few protons. Lines with inhomogeneous almost Gaussian line shape correspond to the envelope of several distributed 'spin packets'. They may be assigned to the existence of several small radical species and, consequently, a comparatively high concentration of protons and/or the presence of
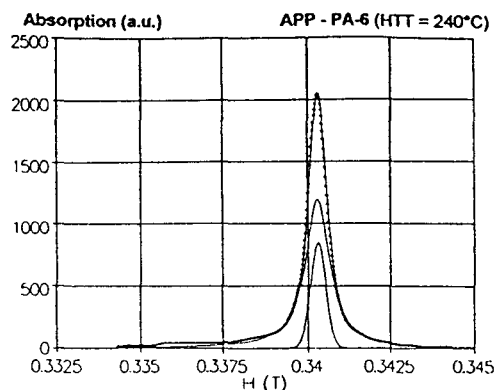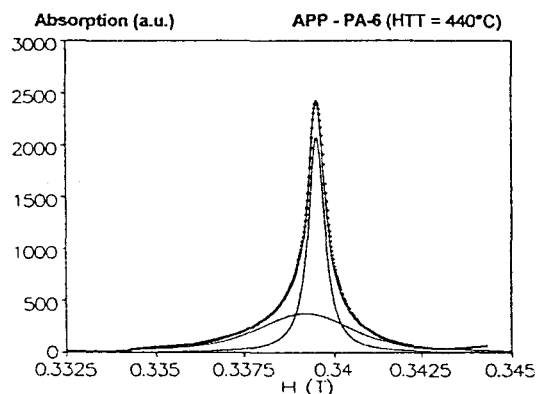
chemical functions (such as alkyl or aryl groups and oxidized species) bound to the carbon structure.[31] The profile of the Voigt spectral function is the theoretical line shape for a convolution of a Gaussian and a Lorentzian. Therefore corresponding lines may be assigned either to the co-existence of the two types of carbon species in the material giving rise to lines with a same spectroscopic factor or to species corresponding to an intermediate step of the carbonization process (the presence of both small and large particles of 'carbon' species similar in a chemical sense).

Lines for which no fit may be proposed from the slope-normalization method may be explained in three different ways. First, the signal may be composed of two Lorentzian lines with very different values of the spectroscopic factor (formulations V, VI and VII in which the presence of at least two different well-structured radical species may be assumed). Second, homogeneous broadening whose sources may be spin–lattice interaction, interactions with the radiation field, diffusion of excitation through the sample and fluctuation in the local field or inhomogeneous broadening which may be assigned to hyperfine interactions or hyperfine anisotropy broadening, may give (in formulation IX) a very broad

Table 4. Characteristics of the ESR spectra of chars resulting from the thermal treatment of the additive mixtures

Additive mixtures	HTT (°C)	Functions	Width (T)	g	log (ns) (log(spin/kg))	References
I	190	G[a]	3.0[b]	2.0030[b]	≈ 17	6, 12
	280	G[a]	3.8[b]	2.0037[b]	20.4	
	350	G + L[a]	1.4[b]	2.0030[b]	21.4	
	430	G + L[a]	2.8[b]	2.0052[b]	21.1	
	560	G + L[a]	0.5[b]	2.0019[b]	21.6	
II	350	nd	1.6	2.0027[b]	21	12
	430	nd	1.1	2.0009[b]	21.1	
	560	nd	1.7	2.0018[b]	21	
III	240	V (28)	16.3	2.0015	22.1	This paper
		L (72)	3.4	2.0137		
	390	V (62)	3	2.0033	22.2	
		G (38)	32	1.991		
	440	G (60)	16.1	2.0031	21.0	
		L (40)	3.0	2.0018		
	530	G (8)	13.0	2.031	19.4	
		L (37)	3.8	2.0025		
		G (54)	8.6	1.9972		
IV	190	G[a]	6[b]	2.00	≈ 14	14, 28
	240	V[a]	8[b]	2.00	19.8	
	280	G[a]	9[b]	2.00	21.8	
	350	V[a]	4.4[b]	2.00	21.7	
	420	L + G[a]	4.1[b]	2.00	21.5	
V	190	V[a]	8[b]	2.0033[b]	20.2	This paper
	230	L[a]	6.5[b]	2.0030[b]	19.4	
	320	nd	3[b]	2.003[b]	20.4	
	430	L[a]	10[b]	2.0031[b]	19.4	
	530	L[a]	3[b]	2.0015[b]	20	
VI	190	V[a]	7[b]	2.0028[b]	19	This paper
	230	L[a]	6[b]	2.0029[b]	20.5	
	320	nd	3[b]	2.003[b]	21.5	
	430	L[a]	3[b]	2.0032[b]	20.8	
	530	nd	3[b]	2.003[b]	20.9	
VII	190	nd	28[b]	1.999[b]	16	This paper
	230	G[a]	7[b]	2.0029[b]	18.9	
	320	nd	3[b]	2.003[b]	22.3	
	430	V[a]	3[b]	2.0035[b]	20.5	
	530	L[a]	3.5[b]	2.0028[b]	20.8	
VIII	200	L (62)	3.4	1.997	20.7	This paper
		L (38)	3.5	1.995		
	300	L (65)	3.7	1.992	20.4	
		L (35)	1.8	1.990		
	320	L	3.7	1.995	20.5	
	400	L	4.1	1.997	20.4	
	450	L	5.0	1.998	19.8	
IX	190	V[a]	6.5[b]	2.0033[b]	19.9	This paper
	230	L[a]	6.6[b]	2.0030[b]	20	
	320	L[a]	4.5[b]	2.0037[b]	20.9	
	430	nd	4.2[b]	2.005[b]	19.5	
	530	nd	3[b]	2.003[b]	18.7	

G( ), L( ) and V( ): line shape respectively described by a Gaussian, a Lorentzian and a Voigt function (numbers in brackets: relative percent of free electrons of the line in the signal), nd: fit not determined by the method, g: spectroscopic splitting factor (absolute error on the last digit).
[a] Shape fits determined using the slope normalization method[29].
[b] Characteristic of the whole of the signal.

line which does not allow computation of the baseline. Finally, there are more complex line shapes such as Dysonian[32] which may be assigned to the presence of conductive components in the material.[33]

Observed lines of the carbonaceous matrials are generally narrow (peak-to-peak line width $< 10T$). They characterize large radicals which result in small electron–proton interactions mainly responsible for the line width.

Lines with the highest widths are shown by formulation III in which the presence of small polyaromatic structures is proposed.

Carbonaceous materials resulting from the degradation of the APP–polyol and APP–PA-6 systems show lines with classical values of the spectroscopic splitting factor ($g \geqslant 2.00$). Variations of g versus HTT show that the highest values are obtained when $420°C \geqslant HTT \geqslant 440°C$. High values of g between 2.0029 and 2.0041 are generally assigned to free-radical intermediates with chemically bound oxygen in the structure (stable aryloxy radicals[19]) formed during the reaction of polynuclear aromatic hydrocarbons with oxygen.

Values of g (lower than 2.00) shown by lines recorded using the products of degradation of the APP –PA-6 and the APB–PER mixtures, are unexpected. Such g values have been previous observed in commercial carbon blacks.[34] The effect on the g value of the addition of boron as impurity in single crystal and polycrystalline graphite has been mentioned previously.[35] It is well known that the spin magnetic moment of an electron may be influenced by various interactions with the electron environment. These interactions result in a shift of the ESR line with respect to the free electron position.

The presence of more or less hydrated phosphorus oxides is expected in the products of the degradation of formulation III and whatever are HTT, the products of the degradation of the formulation VIII always contain a solid crystalline phase (mixture of boron oxide and boric acid characterized using X-ray diffraction.[16]) Upon interaction of the π-radical (lone electron in a π orbital) onto the surface of the oxide, the surface crystal field may split the π electron energy level, thus removing its degeneracy to give two new separated orbitals. The resulting new energy levels may correspond to the excitation of the electron and consequently, the observed g value is less than $g_e = 2.0023$.

DISCUSSION

The study presents original additive mixtures developed in the authors' laboratory which allow good FR properties (at least convenient LOI and UL-94 classifications) to be obtained. Two of them are mixtures of the diammonium pyrophosphate (CP) and a polyol (CA) produced by the agrochemical industry (xylitol or d-sorbitol) and the third is composed of ammonium polyphosphate (CP) and polyamide-6 (CA).

The FR properties obtained using PA-6 as the carbonizing agent are very interesting because in recent years there has been much interest in the development of alloys based on engineering polymers such as polyamides. For example, blends of polyamides with polyolefins offer good chemical resistance, low water sorption and mechanical properties of interest.[36] In particular, toughened versions of both PA-6 and PP[37] have become important industrial products which, for example, find applications in packaging because of their good oxygen barrier properties of the blend.[38]

Moreover, the study shows that the borate may be used in a catalytic system for the formation of intumescent materials. Nevertheless, use mixture VIII in PP formulations has two main disadvantages: the reaction between the additives takes place during the processing procedure with evolution of gaseous products and the intumescent material formed from VIII shows a comparatively poor thermal stability (it decomposes at a temperature 30°C lower than the intumescent material obtained using mixture I).

Mixture IX does not allow the formulation of FR polypropylene. In fact, our study shows that the use of mixture IX in PP formulations has two main disadvantages: the carbonaceous material formed in the temperature range where PP decomposes does not present an expanded character and its thermal stability is comparatively low (degradation at a temperature 35°C lower than the intumescent coating formed from I).

The thermo-oxidative degradation of PP in a low-temperature range ($T < 280°C$) is a process which leads to the slow evolution of propene, γ-lactone, aldehydes and ketones.[39,40] In general, this process does not contribute to the production of fuels and does not cause self-ignition. At about 300°C the rate of evolution of the fuels (aldehydes, ketones and small oxidized chains of the polymer[41]) is high enough for a significant participation of the polymer in a fire. The protective material formed from the FR additives may then be the intumescent material (formed in the range 280–350°C), the unexpanded residue (stable in the range 400–450°C) or the 'high-temperature' residue. The direct relation between the LOI values and the carbonization process[42] and more, with the amount of the carbonaceous material formed from the formulations, previously proposed by Montaudo[43] may be studied.

Figure 15 shows that such a direct relation is not observed. In particular, formulation III which gives comparatively low amounts of the three different carbonaceous materials presents a relatively high value of LOI. Furthermore, formulations I and II which transform in low amounts of 'high-temperature residue' may show high LOI values.

We previously proposed that the protective character of a carbonaceous material depends on its dynamic properties,[12,44] its physical composition, most particularly the presence of both amorphous and crystalline phases[44]
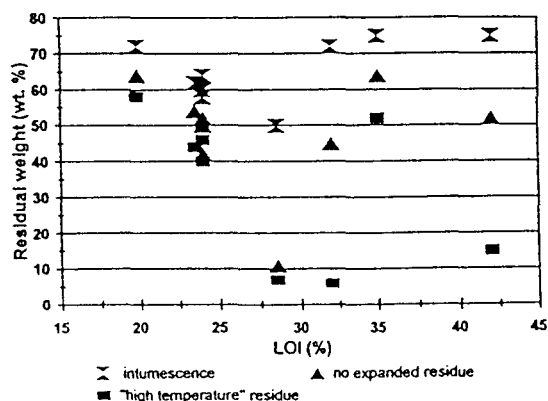

Figure 15. Average amounts of residual carbonaceous materials resulting from the thermo-oxidative degradation of formulations I to IX versus the corresponding Limiting Oxygen Index.
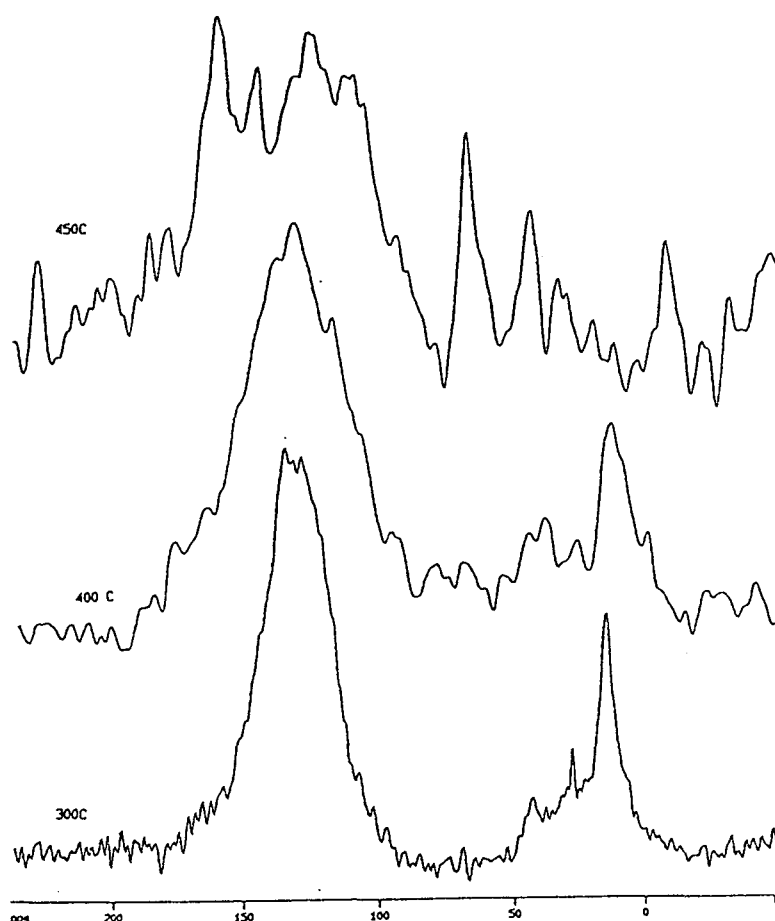
Figure 16. MAS–DD NMR spectra of the APB–PER system versus HTT (C. Delporte, unpublished results).

and/or its chemical composition and properties.[7,10] This discussion will be restricted considering only the chemical properties of the carbonaceous materials.

The carbonaceous materials resulting from intumescence are generally formed by polyaromatic stacks. Materials formed from formulations I, II, IV, V, VI and VII which contain APP or PY are also composed of phosphocarbonaceous species the acidic character of which in the high-temperature range plays a part in the FR properties[6] because it allows a reaction with the products of degradation of the polymer and thus the formation of polyethylenic links.[10] Materials formed from formulation III have the same composition (SIAT *et al.*, unpublished results).

From the literature[6,20,45,46] we may assume that the first step in char formation consists in the formation of esters of the phosphoric acid formed by NH_3 elimination from the phosphates and hydrolysis of the phosphate chains. The following steps leading to carbon–carbon unsaturations and the formation of the aromatic species from the esters is also well known.[7,47]

Mixture VIII presents a similar carbonization process. As an illustration, the ^{13}C DD-MAS NMR spectra (using magic-angle spinning (MAS) and high-power 1H dipolar

decoupling (DD)) of the heat treated system are presented in Fig. 16 and their assignments are shown in Table 5.

Table 5. Assignments of CP and DD-MAS NMR ^{13}C spectra of the APB–PER system versus HTT

HTT	δ (ppm)	Assignments	References
200	18.5	C_{CH_2}	7, 48, 49
	48	C_{CH_2-O}	50
	137 (100–160)	$C_{ar-H}, C_{ar\,C}, C_{ar-N}, C_{ar\,O}$	7, 48, 51, 52
300	17.5	C_{CH_2}	7, 48, 49
	30	C_{CH_2}	7, 48, 49
	46	C_{CH_2-O}	50
	138 (110–150)	$C_{ar-H}, C_{ar\,C}, C_{ar\,N}, C_{ar\,O}$	7, 48, 51, 52
400	13	C_{CH_2}	7, 48, 49
	39	C_{CH_2}	7, 48, 49
	131 (100–200)	$C_{ar\,H}, C_{ar\,C}, C_{ar\,N}, C_{ar\,O}$	7, 48, 51, 52
450	161 (80–170)	$C_{ar\,H}, C_{ar\,C}, C_{ar\,N}, C_{ar\,O}$	7, 48, 51, 52

C_{CH_2}, branched alkyl carbon; $C_{ar\,H}$, protonated aromatic carbon; $C_{ar\,C}$, non-protonated aromatic carbon; $C_{ar\,O}$, oxygenated aromatic carbon; $C_{ar\,N}$, nitrogenated aromatic carbons and/or nitrogenated carbons with conjugated bonding in heterocycles; $C_{CH_2\,O}$, oxygenated branched alkyl carbon.
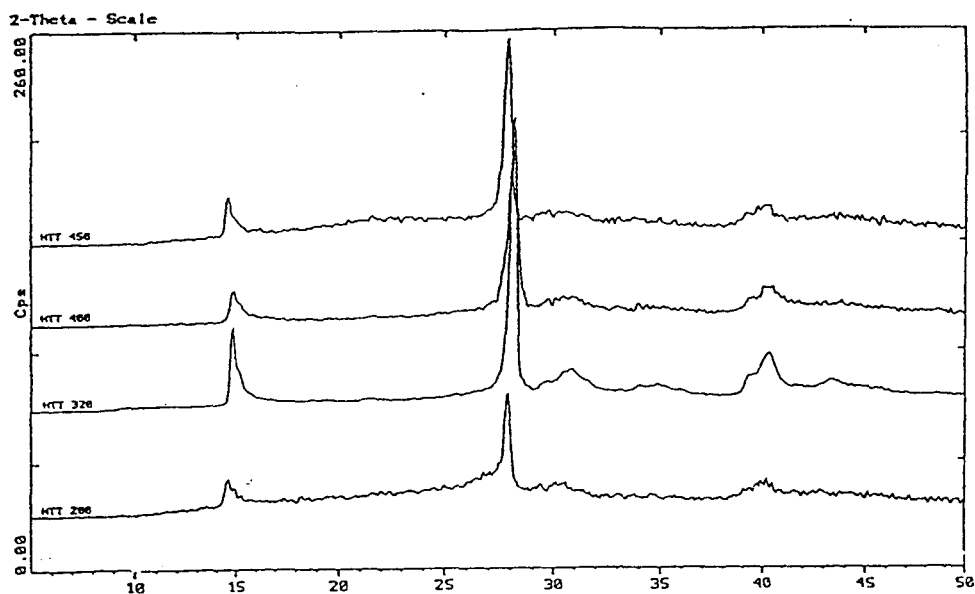
Figure 17. X-ray diffraction spectra of the APB–PER system versus HTT (C. Delporte, unpublished results).

Each spectrum presents a broad band between 110 and 160 ppm assigned to the presence of several aromatic and polyaromatic species which proves that the cyclization process occurs at a low temperature. Broadening of the signal at 400°C and 450°C results from the oxidation of the polyaromatic species. The presence of nitrogenated carbons in the material is generally observed in the products resulting from the degradation of ammonium 'phosphates'–CA mixtures and the reaction of ammonia with the hydrocarbonaceous products of the degradation.[53] The presence of groups C_{CH_2-O} and C_{ar-O} is explained at least partially by the formation of borocarbonaceous species in the material. This last observation leads to the assumption that the first steps for the formation of the carbonaceous materials are the same as those proposed for the formation of carbon from phosphate–polyol mixtures (formation of ester dehydrogenation and then formation of the polycyclic structures).

X-ray diffraction spectra of the APB–PER systems versus HTT are presented in Fig. 17. The observed diffraction patterns can be assigned to a crystalline phase of either H_3BO_3[54] or B_2O_3.[55] They show that the whole of the boron species are not bound on the carbonaceous structure and proves for each HTT the presence of boric acid able to react with oxygenated hydrocarbons and, finally, the presence of the crystalline boron-based phase which may be responsible for the particular values of the g factor of the corresponding ESR lines.

Mixture IX shows a particular thermal behaviour. Materials arising from carbonization are formed from hydrocarbons presenting conjugated dienes and oxidized functions resulting from the degradation of the dextrine in isolation (Y. Schmidt-Le Tallec, unpublished result). The thermal behaviour of the mixture may then be related to that of the cellulose[56] and the phosphate–cellulose systems.[57]

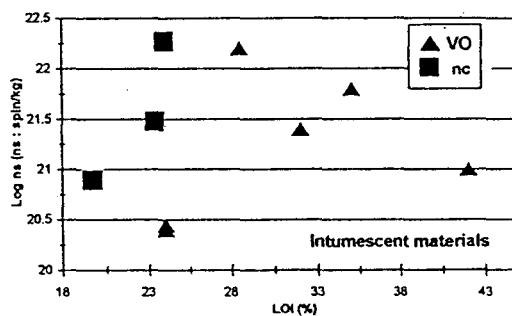The final steps of the formation of the carbonaceous materials may involve free radical reactions (dehy-

Figure 18. Free radical concentrations in intumescent materials (resulting from the thermal degradations of mixtures I to IX) versus the related limiting index values.
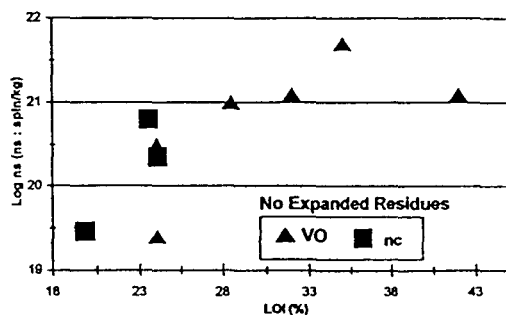

Figure 19. Free radical concentrations in the unexpanded residues (resulting from the thermal degradations of mixtures I to IX) versus the related limiting index values.

drogenation, cyclization and polymerization). It is assumed that the formation of the observed π radical species takes place during these steps. The concentrations of the stable free radicals measured by ESR are a probe of
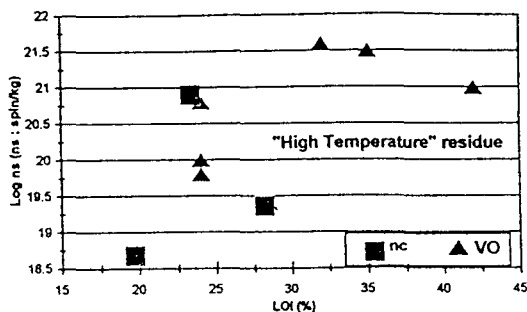
Figure 20. Free radical concentrations in the 'high-temperature' residues (resulting from the thermal degradations of mixtures I to IX) versus the related limiting index values.
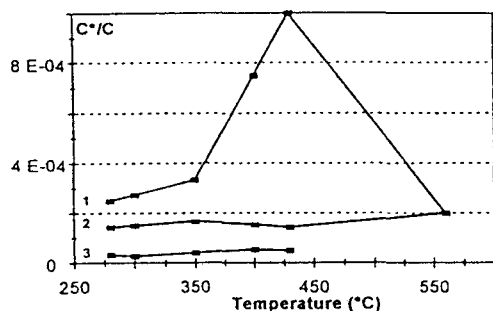

Figure 21. Relative free radical concentrations C* in the APP–PER-4A (curve 1; after reference 12), the APP–PER (curve 2; after reference 12) and APB–PER (curve 3) systems versus HTT. C*: concentration in paramagnetic species; C: respective concentration in atomic carbon.

the processes and allow comparison of the paramagnetic character of the materials resulting from the additive treatment. Figures 18–20 show the measured concentration as compared with the FR characters of these additives in PP. They indicate that no relation exists between the two variables in the intumescent materials. However, a spin concentration at least equal to 10^{21} spins kg^{-1} in the intumescent and in the non-expanded residue is always required to obtain LOI $\geqslant 28\%$. Moreover, a spin concentration at least equal to 10^{21} spins kg^{-1} in the 'high-temperature' residue is always required to obtain LOI $\geqslant 30\%$. In addition, this study shows that systems which do not allow a UL-94 classification, always present a low concentration ($< 10^{21}$ spins kg^{-1}) of the free radical species.

Previous studies[7,10,12] and the reported study of APB–PER thermal behaviour have shown that the residues are not only composed of carbonaceous species but may also be 'composite' material containing free acid species and oxide phases. Therefore, the evaluated paramagnetic character of intumescent materials and of residues is not that of the 'carbon' phase. Figure 21 shows the amounts of paramagnetic species related to the whole of the 'carbons' in three of the considered systems versus HTT. It indicates that a relation exists between the LOI sequence ($LOI_{APB-PER} < LOI_{APP-PER} < LOI_{APP-PER-4A}$) and the C*/C sequence. In addition, it shows that materials presenting a somewhat similar paramagnetic character do not necessarily contain the same amount of potentially reactive species.

The relation between free radical in the carbonaceous materials resulting from a thermal treatment of the additives and the FR behaviour of these additives is easy to explain by a reaction between gaseous free radical products arising from the thermal degradation of the polymer (scission of the polymer chain or oxidative process) and the 'activated' carbon species in the intumescent coating and/or the non-expanded residue. Such reactions explain the presence of polymer links in the protective coating which forms in fire conditions and thus leads to a decrease in the evolution of the flammable gaseous mixture from the system to the flame. Moreover, the reaction is, in fact, a termination–recombination process which may decrease the rate of pyrolytic degradation of the carbon-based material.

CONCLUSION

This study compares seven new intumescent FR additive mixtures and a carbonizing additive system with the classical APP–PER system and two additive formulations previously developed in the authors' laboratory in term of fire retardancy of polypropylene-based formulations.

It shows that the mixture of diammonium pyrophosphate (precursor for a carbonization catalytic species) and polyols produced by agrochemical industry (Xylitol and d-sorbitol; carbonization agent) are FR additive mixtures of interest in polyolefins. Moreover, it reports the good FR performance of the mixture of ammonium polyphosphate and polyamide-6. Finally, it proposes that boric acid salts have to be developed as precursors for carbonization catalytic species.

A thermal analysis study proposed steps for the formation of the intumescent, the non-expanded and eventually the 'high-temperature' residue. It shows that the FR performances and the amounts of carbonaceous materials resulting from the thermal degradation of the additives mixtures are not related.

A reported additional compilation of some previous spectroscopic studies in the authors' laboratory confirms that the intumescent process results from the formation of polyaromatic species and that FR systems maintain acidic species in a relatively-high temperature range.

Finally, an ESR study shows the presence of free radicals in the protective coating formed using the additive systems. It indicates that a line shape analysis of the ESR signal provides information on the size of the carbonaceous structures in the materials. Moreover, the values of the spectroscopic factor are proposed as probes for the presence of crystalline phases in the coating. The study proposes that at least two components of the protective shield must possess a high paramagnetic character to obtain the protective property. Finally, the participation of free radicals in the formation of chemical bonds between the materials produced from the additives and the products of the degradation of the polymer is discussed. This participation is proposed as responsible in the FR process via two different steps: it decreases the evolution of fuels and is a termination step in the free radical reaction scheme of the pyrolysis of the protective material.

REFERENCES

1. C. Vasile and R. B. Seymour (eds), *Handbook of Poly-olefins—Synthesis and Properties*, Marcel Dekker, New York (1993).
2. V. N. Kondariev, Chain reactions. In *Comprehensive Chemical Kinetics*, ed. by C. H. Bamford and C. F. H. Tipper, Elsevier, Amsterdam (1969).
3. W. J. Kroenke, *J. Mater. Sci.* 21, 1123–73 (1986).
4. G. Camino, L. Costa and L. Trossarelli, *Polym. Deg. & Stab.* 7, 25 (1984).
5. R. Delobel, M. Le Bras and N. Ouassou, *Polym. Deg. & Stab.* 30(1), 41 (1989).
6. R. Delobel, M. Le Bras, N. Ouassou and F. Alistiqsa, *J. Fire Sci.* 8(2), 85 (1990).
7. S. Bourbigot, M. Le Bras and R. Delobel, *Carbon* 31(8), 1219–30 (1993).
8. H. L. Vandersall, *J. Fire & Flammability* 2, 97–140 (1971).
9. J. D. Brooks and G. H. Taylor, *Carbon* 3, 185 (1965).
10. S. Bourbigot, M. Le Bras, R. Delobel, P. Breant and J.-M. Tremillon, *Carbon* 33(3), 283–94 (1995).
11. M. Le Bras and S. Bourbigot, *Fire and Materials* 20, 39–49 (1996).
12. S. Bourbigot, M. Le Bras, R. Delobel, R. Descressain and J. P. Amoureux, *J. Chem. Soc., Faraday Trans.* 92(1) 149–58 (1996).
13. S. Bourbigot, M. Le Bras, P. Breant, J.-M. Tremillon and R. Delobel, *Fire and Materials* (1996), in press.
14. M. Le Bras, R. Delobel, R. Descressain and J.-M. Leroy, *Bull. Soc. Chim. Belg.* 98(9-10), 735–40 (1989).
15. Y. Schmidt-Le Tallec, *Valorisation de différents polyols dans des systèmes retardants de flamme: application au poly-éthylène*, Doctoral Dissertation, Lille (1992).
16. C. Delporte, *Etude du nouveau système intumescent retardateur de flamme pentaborate d'ammonium/pentaéryth-ritol—Application au polypropylène*, Diplôme d'Etudes Approfondies 'Spectroscopies', Dissertation, Lille (1995).
17. J. Rychly, L. Matisova-Richla and J. Placek, *Collection Czechoslov., Chem. Comm.* 44, 3665–75 (1979).
18. I. C. Lewis and L. S. Singer, *Carbon* 5, 373–81 (1967).
19. I. C. Lewis and L. S. Singer, *J. Phys. Chem.* 85, 354–60 (1981).
20. R. Delobel, M. Le Bras and N. Ouassou, *Polym. Deg. & Stab.* 30, 41–56 (1990).
21. S. Siat and M. Le Bras, *Matériaux Polymères et Procédés—Colloque Annuel du GFP*, Nancy, 21–23 November 1995, p. 29.
22. S. Bourbigot, *Les zéolithes, Nouveaux Agents de Synergie dans les Systèmes Intumescents—Compréhension des Mécanismes de Protection du Polyéthylène et de ses Dérivés*, Doctoral Dissertation, Lille (1993); S. Bourbigot, M. Le Bras, R. Delobel, P. Breant and J.-M. Tremillon, *Fire Retardant Polymers 5th European Conference—Sci. Fire Chemistry Discussion Group*, Salford, 4–7 September 1995.
23. F. Pouille, *Etude Spectroscopique de Formulations 'Retard au Feu' à base de Polyamide*, Diplôme d'Etudes Approfondies *Spectroscopies*, Dissertation, Lille (1995); E. Felix, *Etude structurale par RMN du Solide de Formulations ignifugeantes à base de PA6*, Diplôme d'Etudes Approfondies *Spectroscopies*, Dissertation, Lille (1995).
24. Standard Test Method for Measuring the Minimum Oxygen Concentration to Support Candle-like Combustion of Plastics, ASTM D2863/77, Philadelphia.
25. Tests for Flammability of Plastic Materials for Part in Devices and Appliances, Underwriters Laboratories, Northbrook, ANSI/ASTM D635-77.
26. C. Swanson and F. McCollough, *Inorg. Snyth.* 7, 65 (1963).
27. S. A. Raymond, *Electron Paramagnetic Resonance*, p. 200, Wiley Interscience, New York (1968).
28. N. Ouassou, *Etude d'un Nouveau Système Intumescent 'Retard au Feu': Pyrophosphate Diammonique—Pentaeryth-ritol; Application au Polypropylène*, Doctoral Dissertation, Lille (1991).
29. R. S. Alger, *Electron Paramagnetic Resonance: Techniques and Applications*, pp. 42–60, Interscience, New York (1968); J. S. Hyde, *Experimental Techniques in EPR*, 6th Annual NMR—EPR Varian Workshop, Varian Associates Instrument Division, Palo Alto (1961).
30. L. S. Singer and I. C. Lewis, *Appl. Spectrosc.* 36(1), 52–7 (1982).
31. L. S. Singer, I. C. Lewis, D. M. Riffle and D. C. Doetschman, *J. Phys. Chem.* 91, 2408–15 (1987).
32. F. J. Dyson, *Phys. Review* 98(2), 349–59 (1955); G. Feher and A. F. Kip, *Phys. Review* 98(2), 337–48 (1955).
33. R. H. Lewis and G. E. Maciel, *J. Mater. Sci.* 30, 5020–30 (1995).
34. R. L. Collins, M. D. Bell and G. Kraus, *J. Appl. Phys.* 30, 56 (1959).
35. L. S. Singer and G. Wagoner, *J. Chem. Phys.* 37(8), 1812–17 (1962); G. Wagoner, *Phys. Rev.* 70, 647 (1960).
36. A. Gonzalez-Montiel, H. Keskkula and D. R. Paul, *Polymer* 36(24), 4587–637 (1995).
37. M. J. Modic and L. A. Pottick, *Polym. Eng. Sci.* 33, 819 (1993).
38. R. M. Holsti-Miettinen, K. P. Pertilä, J. V. Seppälä and M. T. Heino, *J. Appl. Polym. Sci.* 58, 1551–60 (1995).
39. J. H. Adams, *J. Polym. Sci.* A1 8, 1269–77 (1970).
40. A. Hoff and S. Jacobsson, *J. Appl. Polym. Sci.* 29, 465–80 (1984).
41. K. Barabas, M. Iring, S. Laszla-Hedrig, T. Lelen and F. Tudos, *Eur. Polym. J.* 14, 405–7 (1978).
42. D. W. Van Krevelen, *Polymer* 16(8), 615–20 (1975); D. W. Van Krevelen, *Comprehensive Chemical Kinetics*, Volume 14, pp. 344–57, ed. by C. H. Brandford and C. F. H. Tipper, Elsevier Science, New York (1975).
43. G. Montaudo, E. Scamporino and D. Vitalini, *J. Polym. Sci., Polym. Chem.* 21, 3361 (1983).
44. R. Delobel, M. Le Bras, Y. Schmidt and S. Bourbigot, *Proceedings of the Int. Symp. Moffis 91—Mineral and Organic Functional Fillers in Polymers*, ed. by G. F. P. Le Mans (1991) pp. 79–85; R. Delobel, S. Bourbigot, M. Le Bras, J.-M. Leroy and B. Kanovnik, *Polimerni Materijali Smanjene Gorivosti*, Drustvo Plasticara i Gumaraca, Zagreb (1990), pp. 08/01-04.
45. K. Kishore and K. Mohandas, *Combust. & Flame* 43, 145–53 (1981).
46. S. V. Levchik, L. Costa and G. Camino, *Polym. Deg. & Stab.* 36, 229–37 (1992).
47. S. V. Levchik, L. Costa and G. Camino, *Polym. Deg. & Stab.* 36, 31 (1992).
48. A. Grint, G. P. Proud, I. J. F. Poplett, K. D. Bartle, S. Wallace and R. S. Mathews, *Fuel* 68, 1490 (1989).
49. S. Supaluknari, I. Burgar and F. P. Larkins, *Org. Geochim.* 15, 509 (1990).
50. T. M. Duncan and D. C. Douglass, *J. Chem. Phys.* 87, 87 (1984).
51. G. E. Maciel, V. J. Bartuska and F. P. Miknis, *Fuel* 58, 391 (1979).
52. W. L. Earl and D. L. Vanderhart, *J. Magn. Reson.* 48, 35 (1982).
53. S. Bourbigot, M. Le Bras, L. Gengembre and R. Delobel, *Appl. Surface Sci.* 81, 299–307 (1994).
54. Bradley *et al.*, JCPDS, Powder Diffraction File 23-1034.
55. Senkovits and Hawley JCPDS, Powder Diffraction File 6-297.
56. T. P. Nevell and S. Haig Zeronian, *Cellulose Chemistry and its Applications*, Ellis Horwood, Chichester (1985).
57. W. E. Franklin, *J. Fire Sci.* 1(5-6), 165–76 (1983).

III-1-b. Discussion synthétique

L'adjuvant PY/PER présente une sélectivité plus importante que celle de APP/PER pour la synthèse du « carbone » intumescent. Il assure, d'une part, une stabilité thermique des espèces phosphates acides peu condensées qui ne permet pas la formation d'un oxyde de phosphore dans le résidu obtenu aux hautes températures (T ≥430°C) et, d'autre part, la formation, lors du processus d'estérification, d'une quantité comparativement faible d'espèces radicalaires susceptibles de modifier la matrice polymère. Ces caractéristiques permettent une stabilité thermique de PP/PY/PER sous air, supérieure à celle de PP/APP/PER. En effet, la protection du matériau commence dès 300°C (320°C pour PP/APP/PER), température à laquelle la vitesse apparente de la décomposition thermo-oxydante de PP est faible.

Par ailleurs, les espèces acides dans le matériau carboné non expansé « maintiennent » des fragments des chaînes du PP dans ce résidu « haute température » qui est alors un bouclier thermique pour le matériau résiduel. En conséquence, la quantité de matériau carboné ex-PP/PY/PER, présent dans un domaine de température étendu (300 - 550°C), est plus importante que celle du matériau ex-PP/APP/PER (stable dans le domaine 315 - 430°C).

Finalement, l'étude confirme que la stabilisation des chaînes du PP dans le matériau protecteur s'effectue par deux réactions différentes :

• réaction des produits oxydés, résultats de la dégradation thermo-oxydante du PP, avec les espèces phosphates acides

• et terminaison des réactions en chaînes radicalaires par réaction entre les radicaux libres formés lors de la pyrolyse de la matrice polymère et les espèces radicalaires du matériau carboné formé par la réaction des adjuvants seuls.

La comparaison des dégradations des deux formulations sous inerte montre que la protection de PP/PY/PER provient principalement de la réaction entre espèces oxydées et phosphates acides.

Le pyrophosphate diammonique en association avec le PER permet d'obtenir des formulations du PP aux performances FR supérieures à celles obtenues avec APP/PER : LOI > 25 % volumique, classements V0 et M2, pour des taux en adjuvants inférieurs à 20 % pondéral.

L'adjuvant APB/PER ne donne pas un classement FR satisfaisant au PP. L'absence de performance peut s'expliquer par la faible stabilité du matériau intumescent qui perd son caractère expansé dès 320°C. Une étude IR complémentaire prouve que la totalité du ABP ne réagit pas avec le polyol (Figure III-1). En effet, lorsque HTT $\geq$ 200°C, le spectre de l'adjuvant montre que l'acide borique H_3BO_3 se forme (Figure III-2) parallèlement aux esters (les groupements B - O - C sont caractérisés par les absorptions caractéristiques $\nu_{sym\ (B-O)}$ et $\nu_{asym\ (B-O)}$ respectivement à 1454 et 1192 cm^{-1} [172-174]). Les phases cristallines H_3BO_3 [175] et B_2O_3 [176] sont observées sur les spectres XRD quelle que soit HTT < 200°C.
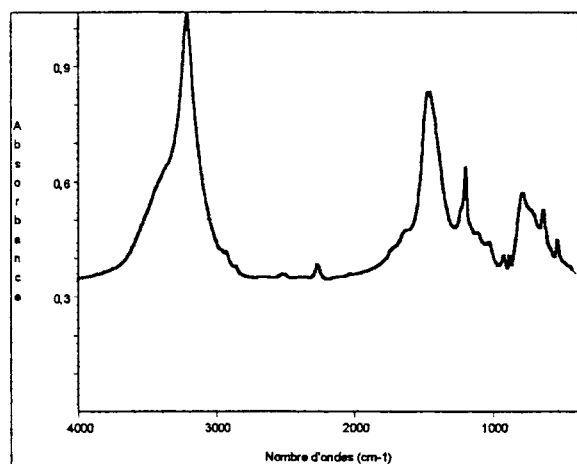

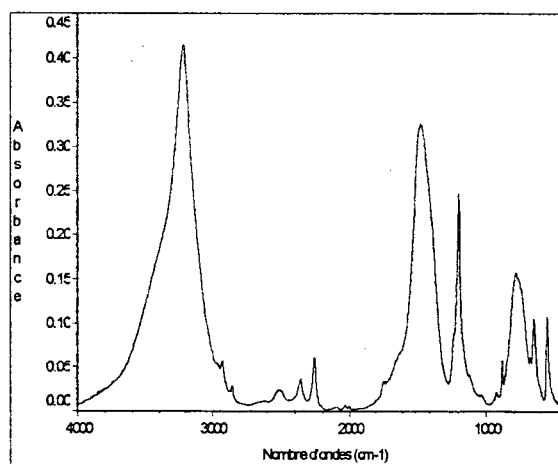Figure III-1. : Spectre I.R. de APB/PER à HTT 200°C   Figure III-2. : Spectre I.R. de H_3BO_3

Comme discutée dans le chapitre II, la présence d'une phase cristalline dans le « carbone » intumescent conduit à la perte du caractère expansé et de l'imperméabilité aux gaz et, donc, à l'absence de caractère protecteur. Un produit vitreux superficiel cohérent ne se forme pas à partir de ABP/PER, vraisemblablement à cause de la coexistence d'une phase solide (carbone) avec la phase fondue.

Les critères de sélection (taux de charge < ou = 0,30 % pondéral, LOI > 25 % volumique, classement V0) excluent l'utilisation des sucres et des dérivés de l'amidon (homologues de la cellulose) comme adjuvants CA dans les formulations du PP. Les valeurs des LOI > 21 % volumique montrent cependant que les matériaux intumescents issus des systèmes APP/sucre possèdent un caractère protecteur,

faible dans le PP, qui mérite néanmoins d'être testé dans les formulations des autres polyoléfines.

Le mélange maître PA-6/PER est un adjuvant FR prometteur pour la formulation des polyoléfines. Son intérêt sera illustré plus précisément à la fin de ce Mémoire.

La relation entre la quantité de carbone formée lors du traitement de l'adjuvant et la propriété FR, préalablement proposée par Montaudo G. et al. [149], n'est pas vérifiée. L'absence de relation montre que tous les matériaux carbonés formés ne possèdent pas des réactivités et/ou des propriétés dynamiques équivalentes.

La réactivité des matériaux carbonés a été évaluée en considérant leur teneur en radicaux libres. En effet, l'association d'un CA et d'un CP développe lors du traitement thermique des réactions en chaînes radicalaires. L'importance des processus radicalaires est évaluée en mesurant par ESR la teneur en complexes π dans les résidus, après trempe [177]. La technique spectroscopique est intéressante car elle permet de comparer les dimensions des structures polyaromatiques et de mettre en évidence la présence de phases cristallines (oxydes) du matériau. Une teneur en espèces radicalaires au moins égale à 10^{21} spins/kg dans le matériau intumescent est nécessaire pour obtenir des valeurs du LOI élevées.

La participation des radicaux libres dans la formation de liaisons stables entre le matériau carboné (formé lors du traitement thermique des adjuvants) et les produits formés lors de la dégradation du polymère est discutée. Ces réactions participent aux processus de protection au feu en diminuant le flux de gaz combustibles vers la flamme et en permettant des réactions de terminaison dans la chaîne de réactions de la pyrolyse du polymère.

III-2   Evaluation de *nouveaux agents de synergie*

Les formulations commerciales des polymères de consommation contiennent généralement plusieurs adjuvants, produits organiques ou minéraux, mélangés aux polymères pour modifier leurs propriétés physiques (par exemples, les plastifiants

ou les charges de renfort) ou chimiques (par exemples, les stabilisants ou les oxydants).

Parmi les charges utilisées, un certain nombre de charges de renforts (dioxyde de titane [178], talc [179] , zéolithes [180] et argiles [45]), de plastifiants (résines [181]) et d'oxydants (oxydes de vanadium et vanadates [182] et dioxyde de manganèse [27]), utilisés seuls ou en association avec des adjuvants FR, conduisent à l'augmentation des performances FR des formulations.

Les aluminosilicates (argiles et zéolithes) sont utilisés en tant que catalyseurs dans de nombreuses synthèses chimiques industrielles [183]. Les études antérieures de notre Groupe ont montré que l'ajout d'argiles dans des formulations PP/APP/PER, aptes au filage pour l'application moquette en aiguilleté, conduit à des effets antagonistes ou synergiques selon la structure de l'argile utilisée [42, 45].

Les argiles sont des matériaux naturels complexes, généralement un mélange de minéraux dont le composant principal est un aluminosilicate. Les caractéristiques des minéraux capables de tenir un rôle dans le processus de l'intumescence sont nombreuses (composition chimique, structure cristalline de la phase aluminosilicate, distribution de la taille des particules, teneur en eau absorbée ou en eau de composition, propriétés dynamiques et stabilité thermique). Nous présentons dans ce paragraphe une étude (utilisant l'analyse en composantes principales [184]) qui propose des règles générales pour la formulation des systèmes intumescents FR PP/APP/PER/argile.

Les caractéristiques des zéolithes susceptibles d'avoir une action sur une formulation intumescente polymère/APP/PER/zéolithe sont, elles aussi, nombreuses. Nous présentons une étude parallèle considérant la composition chimique, la topologie de la charpente, son potentiel d'adsorption et sa teneur en eau. Elle précise le mode d'action des minéraux, agents de synergie (SA), et le type structural du minéral qui permet d'obtenir l'effet optimal.

Les effets de l'ajout du SA : zéolithe de type NaA (4A), sur la décomposition thermo-oxydante des systèmes APP/PER/4A et LRAM3,5/APP/PER/4A sont étudiés par les techniques de caractérisation utilisées dans les Chapitres précédents.

Une étude complémentaire par RMN du ^{1}H en basse résolution dans les solides considère les temps de relaxation spin - réseau T_1 et spin - spin T_2 qui

permettent de préciser l'homogénéité des matériaux. Les matériaux étant hétérogènes [23, 185], la diffusion de spin peut être étudiée en utilisant la séquence de Goldman-Shen [186], elle permet l'estimation de la taille des domaines présentant la relaxation lente [187] et la discussion de la formation des domaines amorphes dans les matériaux carbonés protecteurs. Le LRAM3,5 est le terpolymère retenu pour l'étude; en effet, il permet d'obtenir l'effet de synergie optimal parmi la série de formulations de copolymères de l'éthylène développées au Laboratoire [106]. Cet effet des matrices polymères sera présenté dans le paragraphe suivant.

La cellulose et de nombreuses dextrines (dérivés de l'amidon) carbonisent naturellement lors de leur dégradation thermo-oxydante. Nous avons choisi la BCOH comme molécule modèle. Il faut rappeler que son utilisation dans les formulations PP/APP/BCOH n'a pas permis d'obtenir une performance FR.

Nous présentons, en dernière partie, une évaluation comparative de plusieurs formulations PE/APP/sucre, PE/APP/BCOH et PE/APP/PER. Un effet de synergie provenant de l'association de BCOH et des adjuvants APP/sucre et APP/PER est recherché en utilisant des plans d'expérience pour les mélanges selon la procédure de Scheffé [188]. Cette procédure a été préalablement utilisée par Hirschler et al. pour déterminer les compositions optimales de mélanges Sb_2O_3 - oxydes métalliques (en association avec des adjuvants halogénés) pour des formulations FR [189] ou de mélanges d'oxydes pour réduire la formation de fumées lors de l'inflammation de différents polymères [190].

Les effets de synergie éventuels seront ensuite discutés en considérant les caractéristiques structurales des matériaux carbonés produits par la dégradation thermo-oxydante des adjuvants, et la réactivité de ces matériaux pour les produits de la dégradation du polymère.

III-2-a. Résultats

Mineral Fillers in Intumescent Fire Retardant Formulations — Criteria for the Choice of a Natural Clay Filler for the Ammonium Polyphosphate/Pentaerythritol/Polypropylene System

Michel Le Bras and Serge Bourbigot

Laboratoire de Chimie Analytique et de Physico-Chimie des Solides, ENSCL, USTL, BP 108, F59 652 Villeneuve d'Ascq, Cedex, France

Addition of natural clay materials in intumescent polypropylene-based formulations (additive: ammonium polyphosphate and pentaerythritol) leads either to a decrease or to an increase of their fire retardant performances versus the chemical or the physical characteristics of the clay materials. A study of the factors affecting these performances has been carried out using linear and principal components analysis. This analysis shows that the results of the evaluation tests (LOI and UL 94) are affected in different ways by the adduct of the different clay material and that an increase in the LOI is not necessarily related to an increase in the UL 94 classification. LOI values are improved by the presence of the montmorillonite and of illite clay minerals which may react with acidic phosphate to form active carbonization catelysts. in addition, the results of the LOI test are improved by the presence of quartz and other foreign minerals in the clay materials. This study discusses the part played by the different constitutive minerals in the formation of defects in the polymer chain during the mixing process. It is proposed that the presence of these defects leads to a change in fire retardant performance.

INTRODUCTION

Intumescent additives in paints[1] or thermoplastics[2,3] are halogen-free systems which give fire retardancy by developing under heat flux a carbonaceous expanded shield which provides protection to the material or its support. The shield limits the heat transfer to the substrate and fuel transport from the material to the flame.[4] This work studies an intumescent formulation which associates ammonium polyphosphate (APP, carbonization catalyst), pentaerythritol (PER, carbonization agent) and polypropylene (PP, polymer matrix). This system (additives' level equalling 30%) leads to a V-0 classification by the UL-94 test[5]

Mineral fillers for use in reinforced plastics or resins offer several advantages such as: an aid in producing a smooth surface finish, reductions in cracking and shrinkage, contributions to high dielectric strength and resistance to chemical action and weathering.[6] In particular, China clay (kaolin) filler is widely used in compounds because it gives improved flow in the moulding process and hence ensures uniform distribution of reinforcement.[7] The authors' laboratory has used clays as fillers in intumescent polypropylene-based formulations because low amounts of these materials (1–5wt%) increase the 'mixing' of the formulations during the extrusion process and then allow spinning for fibre manufacture for unwoven fabrics.

Clay minerals are essentially hydrous aluminium silicates, with magnesium or iron exchanging wholly or in part the aluminium in some minerals, and with alkalis or alkaline earths also present as constitutents of some of them. Some clays are composed of a single clay mineral, but in many there is a mixture. In addition to the clay minerals some clay materials contain varying amounts of so-called non-clay minerals such as quartz, calcite, titanium dioxide or other metal oxides (called minerals in this text).

Previous studies in the author's laboratory have shown that addition of natural clay materials in our formulations leads to a severe loss of its fire retardant property. As an illustration, Figure 1 compares the results of a fire test (Limiting Oxygen Index (LOI[8] of the formulations (APP/PER/PP) and (APP/PER/Kaolin/PP), the latter formulations having a constant additives (APP + PER + Kaolin) 30%(wt) level and 0 < Kaolin/APP + PER + Kaolin < 1/3 ratios. The 'kaolin' used is a natural material (supplied by Silice et Kaolin, Barbières, France) and it may be assumed that it is a mixture of clay minerals. The figure shows that, in this case, a loss of the property becomes significant for amounts of filler higher than 1.5%(wt).

Several causes for the loss in fire retardancy may be proposed: initial thermal degradation caused by the presence of induced cracks in the polymeric material, reaction of the acidic phosphate species (which play leading part in the formation and the stability of the carbonaceous shield[9]) with the filler, and/or the presence of induced cracks in the intumescent material.[10]

A direct explanation of the loss in fire retardancy by one property of the filler is quite difficult. Indeed, the part played by each of the several characteristic factors of the mineral fillers requires discussion, i.e. their chemical composition (amount of Al, Si, Fe, alkalis, alkaline earths, etc.), the crystalline phases in the clay material, their particle size distribution, their moisture or constituent H_2O content, their dynamic properties (plasticity index and dry bending strength) and their thermal behaviour (loss on ignition, dry shrinkage and water absorption after firing). In fact the number of these variable factors is too high to allow a direct explanation from one sample.
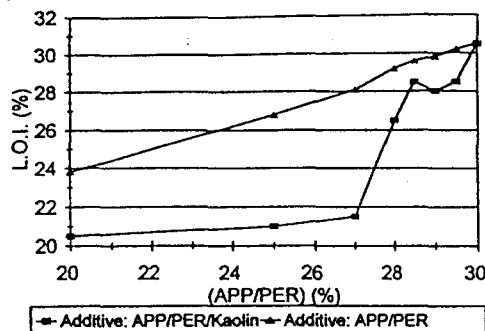
Figure 1. LOI versus the (APP/PER) content in the formulations (APP/PER/PP) and (APP/PER/Kaolin/PP).

Table 1. Mineral analysis of the ceramic and refractory clays

Grade	Kaolinite (%)	Illite (%)	Montmorillonite (%)	Fe–Ti minerals (%)	Quartz (%)
T2847	21	12	1	1	65
T2086	20	18	3	2	57
T2293	28	25	5	2	40
T2371	34	19	4	2	41
T2891	45	12	1	2	40
T2815	30	26	4	1	39
T2873	20	25	13	10	32
T2898	56	9	1	2	32
T2779	22	28	9	12	29
T2316	38	27	7	1	27
T2858	40	31	5	2	22
T2315	42	32	7	2	17
T2325	72	10	2	2	14
T2777	63	16	5	4	12

The solution may consist of collecting several values of the LOI (quantitative variable) and of the UL-94 (qualitative variable) tests obtained from several (APP/PER/Clay/PP) formulations using different natural clay materials, and looking for correlations between these 'property' variables and the chemical and physical characteristics (as quantitative variables) of the clay materials. These eventual correlations in the set of experimental or collected variables may then be studied using an ordinary linear regression method and, more precisely, a principal components analysis using a procedure developed by Heermann.[11]

This paper presents the fire retardancy properties of formulations which contain a synthetic kaolin (kaolinite structure), a natural 'kaolin' or fourteen different natural clay materials (ceramic and refractory clays composed of mixtures of kaolinite, illite, montmorillonite, quartz and Fe, Ti-based crystalline minerals). It presents the calculated correlations between the different characteristics of the clay minerals and the fire retardant properties of the formulations and finally proposes criteria for the choice of a clay material filler in intumescent PP-based fire retardant formulations.

EXPERIMENTAL

Material

The materials were PP (supplied by Elf-Atochem), PER (Aldrich RP grade), APP ($(NH_4PO_3)_n$, $n = 700$, Hoechst Exolit 422, soluble fraction in H_2O: < 1 wt%), a synthetic kaolin ($Al_2Si_2(OH)_4$, Merck grade), a natural China clay (P300 supplied by Silice et Kaolin) and several ceramic and refractory clays (T grades supplied by Martin & Pagenstecher GmbH) with crystalline compositions (measured by X-ray diffraction) reported in Table 1. The clay materials used allow us to obtain a set of quantitative variables which may be described by the elementary statistics data reported in Table 2.

The study has been carried out using the APP/PER mixture for the ratio APP/PER = 3(wt/wt). Indeed, in the particular case of polyolefins, the fire retardant properties are maximum for this ratio.[12,13] The additives were incorporated at 28% (wt) in the polymer. Initial mixtures

were first prepared by ballmilling after mechanical grinding and sieving (2×10^{-4} m). The content of clay materials 2% (wt), corresponds to the previously presented significant loss of the fire retardancy property of the (APP/PER/Kaolin/PP) formulation.

Samples were mixed at 190°C during the time required to reach a stationary state (constant values of the measured torque and of the temperature after the loading peak) using the Brabender Laboratory Mixer measuring head (type 350/EH, roller blades, 50 rpm). Control of the mixing conditions was performed using a data-processing torque rheometer system (Brabender Plasti-Corder PL2000). Sheets ($100 \times 100 \times 3$ mm³) were then obtained using a Darragon compression press at 190°C and at a pressure of 3 MPa.

Combustion tests

The limiting oxygen index was measured using a Stanton Redcroft instrument on sheets according to the standard 'oxygen index' test.[8] It is based on the determination of the percentage of oxygen in a gas mixture which will just sustain the candle-like burning of a sample. This test is not directly relevant to a natural fire situation but provides numerical values for research and quality control. Absolute precision on the LOI value was estimated as 0.2%.

UL-94 classification was obtained according the conditions of the standard test[5] which provides only a qualitative classification of the samples. Such a classification does not show evidence of any direct correlation with quantitative variables. Data obtained were nevertheless included as 'guest' variables in the procedure of the principal components analysis. For this, notations 10, 6, 3 and 0 were respectively assigned to the V0, V1, V2 and unclassified labelled samples.

Statistic relations between variable characteristics of the clay materials and the fire retardant properties of the clay-containing formulations

The computation of the values of correlation coefficients of eventual linear relations was first carried out using the spreadsheet Quattro Pro 5 (Borland). The principal

Table 2. Chemical, structural, dynamic and thermal characteristics of the ceramic and refractory clays

Chemical variable	Arithmetic mean	Standard deviation	'Physical' variable	Arithmetic mean	Standard deviation
SiO_2 (wt %)	66.2	8.82	Loss on ignition (%)	8.14	2.63
Al_2O_3 (wt %)	25.47	7.03	DB strength ($N\,mm^{-2}$)	7.37	2.98
TiO_2 (wt %)	1.43	0.50	FS at 1000°C (%)	2.54	1.78
Fe_2O_3 (wt %)	2.88	3.46	WA (%)	10.68	3.87
CaO (wt %)	0.21	0.08	Plast. (PI)	103	13.1
MgO (wt %)	0.41	0.18	Dry S (%)	5.15	1.10
K_2O (wt %)	1.91	0.88	% > 125 μm	1.06	1.16
Na_2O (wt %)	0.18	0.07	% > 63 μm	3.61	3.77
Al/Si (% at/at)	40.74	16.66	% < 20 μm	92.57	6.32
Kaolinite (%)	41.93	21.47	% < 2 μm	67.93	15.33
Illite (%)	19.35	9.00			
Montmorillonite (%)	4.47	3.38			
Fe–Ti–minerals (%)	3.00	3.26			
Quartz (%)	31.13	16.46			

DB strength: dry bending strength; FS: firing shrinkage; WA: water absorption after firing at 1000°C; Plast.: plasticity index according to Instron; Dry S: dry shrinkage; % > : particle size distribution (wt %)

components analysis was then carried out using the STAT-ITCF computational method (Institut Technique des Céréales et des Fourrages, Paris) (see reference 14 and references therein). The method of analysis by principal components is a descriptive one which may be briefly outlined by the following steps:[15]

- Acquisition of variables or variates
- Elementary description of these data (average, mean and standard deviation)
- Change of the variables and variates in centred variables
- Elaboration of a matrix of the correlations among the variables
- Reproduction of the matrix of correlations with unity in the diagonal (matrix of the eigenvector) which allows the edition of principal vectors of principal axes
- Edition of the principal components described mathematically as linear combination of the variables (five principal component axes)
- Computation of the 'aids' for analysis, in particular of the correlations
- Drawing of the correlations' circles (in our case ten) in the plane corresponding to two principal axes and study of the representation of each 'individual' entity in the corresponding graphic plane.

Interpretation of the results consists first of checking the representation of the variables in the circles and distinguishing the poorly represented, moderately represented and highly represented variables. Second, eventual rotation of the principal axes allows the definition of distinct groups of correlated variables. It may be recalled that neighbours may be explained by the existence of a relation between two variables (or between a variable and a principal axis) and that orthogonal positions may

be explained by the corresponding absence of relations.

In the present study, the correlations' circles were drawn using only centered variables obtained from the variable characteristics of the clay material. Fire retardancy data were then introduced in the calculation as 'supplementary' or 'guest' variables which were not used in the computation of the principal axes. Each search for eventual relations was carried out using five computed principal axes which allowed the study of the variables in ten different correlation circles.

RESULTS AND DISCUSSION

Evaluation of fire retardant performances

Table 3 presents the results of the fire retardancy tests depending on the clay material used. The introduction of different clay materials in the intumescent formulations leads to different values of the LOI (arithmetic mean: 27.2%, standard deviation: 1.7%) and very different UL rankings. LOI values imply that the introduction of clay materials in the intumescent formulation may lead to an apparently synergistic effect (synthetic kaolinite and T2847), to a negligible effect (T2891 and T2779) or to an antagonistic effect.

We have to comment on the behaviour of the 'UL 94 samples' when they were ignited. The V0 classifications are obtained from a cumulative combustion time for five tested samples lower than 50 s when V2 classifications result from dripping with a cumulative combustion time lower than 70 s. The formulation undefined by the test (T2086) shows both dripping and a combustion time of the sample higher than 50 s.

Table 3. Results of the fire retardancy tests of the formulations

Clay	SK	NK	T2847	T2086	T2293	T2371	T2891	T2815
LOI (%)	30	26.5	30.5	26.4	25.6	26	28.5	26.4
UL-94	V0	V0	V0	NC	V0	V2	V0	V0
Clay	T2873	T2898	T2779	T2316	T2858	T2315	T2325	T2777
LOI (%)	27	26	29	25	27.4	27	24.6	27.5
UL-94	V2	V2	V2	V0	V0	V2	V0	V0

SK: synthetic kaolinite, NK: natural 'Kaolin', NC: not classed by the test.

Furthermore, the study shows that no relation exists between the LOI and the UL tests results. As an example, addition of the T2779 filler leads to a relatively high LOI value (29%) and a poor UL classification (V2) where addition of the T2325 filler leads to a low LOI value (24.6%) and the V0 classification.

Relations between the characteristics of the clays' materials and the fire retardant properties

For the first time, the existence of eventual relations between the LOI values and the chemical or physical characteristics of the clay material are studied using linear regressions (LOI% = $a \times$ variate + b). Table 4 presents the calculated data corresponding to the apparently significant relations observed (level (probability of the null hypothesis): $\alpha < 0.05$[16]) and Figs 2 and 3 illustrate the distribution of the LOI values versus, respectively, the content of Kaolinite (no significant relation: correlation factor $R = 0.224$; $\alpha > 0.05$) and the amount of grains (agglomerate of particles) with diameters greater than 2×10^{-5} m ($R = 0.743$, $\alpha < 0.001$).

Eight significant linear relations may be proposed from the computation. One of these relations implies that an increase of the SiO_2/Al_2O_3 ratio leads to the increase of the LOI values. A previous study in the authors' laboratory using other alumino-silicate minerals has shown that LOI values decrease when the SiO_2/Al_2O_3 ratio increases.[17] The different behaviour of the minerals
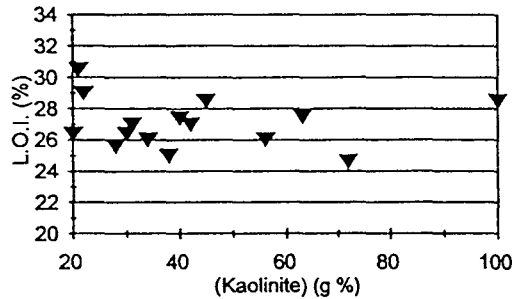

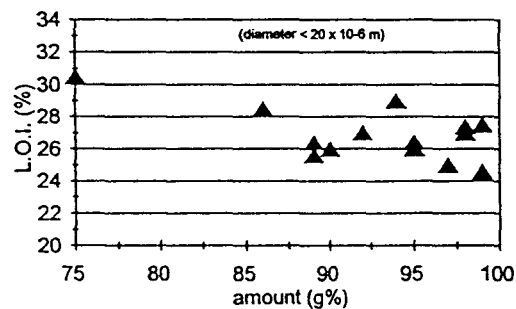Figure 2. LOI versus the amount of kaolinite in the clay material.

Figure 3. LOI versus the amount of grains smaller than 20×10^{-6} m.

Table 4. Computed linear correlations between the LOI values and the clays variables

Variate	a	a standard deviation	b	b standard deviation	R^2	Level α
SiO_2/Al_2O_3 (g g^{-1})	0.605	0.334	25.37	1.68	0.318	< 0.05
Montmorillonite (g%)	− 0.479	0.240	28.70	1.63	0.36	0.02
Dry bending strength (N mm^{-2})	− 0.65	0.44	30.9	1.8	0.263	< 0.05
Plasticity index (PI)	− 0.110	0.063	38.05	1.72	0.341	0.03
> 125 × 10^{-6} m	1.108	0.314	25.8	1.2	0.671	< 0.001
> 63 × 10^{-6} m	0.306	0.103	25.7	1.3	0.590	< 0.001
< 20 × 10^{-6} m	− 0.170	0.063	42.82	1.41	0.558	< 0.001
< 2 × 10^{-6} m	− 0.06	0.035	31.04	1.73	0.33	0.03
Kaolinite* (g%)	− 0.0045	0.031	27.28	2.19	0.004	≫ 0.05

*Not significant correlation, see Fig. 2.

used in the two studies will be explained in the general discussion.

A second significant relation leads to the assumption that an increase in the montmorillonite content decreases the LOI. This relation will be discussed below taking into account the chemical composition of this clay. A third relationship shows that increase in the dry bending strength and in plasticity lead to decreases in the LOI. It is proposed that an increase in the shear stress arising from the addition of the filler depends on the dynamic properties of this compound. The resulting change in the polymer chain may then explain the change in fire behaviour, Finally, a last significant relation suggests that filling with clays with low-diameter grains leads to low LOI values when clays with relatively high diameters result in high LOI.

The significance of these computed relations has, nevertheless, to be discussed. The relation between LOI and the amount of grains with diameters less than 20×10^{-6} m may lead us to suppose that the LOI value in the absence of these is about 43%. The experimental value of the LOI measured using a formulation without any clay is about 31%. The computed linear relation is incorrect even though the computed correlation coefficient is high.

Fallacies in interpreting calculated correlation coefficients require discussion. It is well known that 'false positives' may be found between variates that happen to be changing together, for possibly related reasons but certainly not a mutual cause and effect.[18] Spurious relationships may also appear if correlating a part with the whole; in particular, ratios (such as SiO_2/Al_2O_3) need careful scrutiny before applying correlation analyses to them. Finally, a rather subtle fallacy is to combine data from two or more separate groups as though they were a single homogeneous population.

It may be proposed that the incorrect relation obtained testing morphological data results from a linear component of the curve of the LOI values corresponding to an antagonistic system. Furthermore, correlation is a measure of linear relation only between two variables; a third variable, to which both these variables may be related, may play a misleading part.

DISCUSSION ON THE EXISTENCE OF RELATIONS BETWEEN THE VARIABLES' CHARACTERISTICS OF THE FILLERS

Figures 4 and 5 show circles of the correlations of the chemical variables in which highly represented variables are heavy straight lines and moderately represented variables by thin lines. The main component axes 1, 2 and 4 used in these representations are computed, respectively, using mainly all the chemical data except those related to the kaolinite, data related to kaolinite, mineral and quartz and finally data related to alkalis and alkaline earth constituents of the clay materials.

The figures show that SiO_2, Al_2O_3 and the Al/Si ratio are closely related to the quartz content. In addition, the respective amounts of quartz, kaolinite, and montmorillonite are not related, the contents of illite
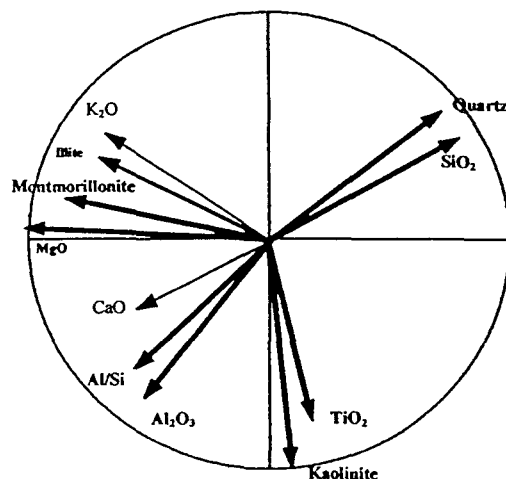

Figure 4. Correlations circle for chemical data on the clay materials (horizontal axis 1: vertical axis 2).
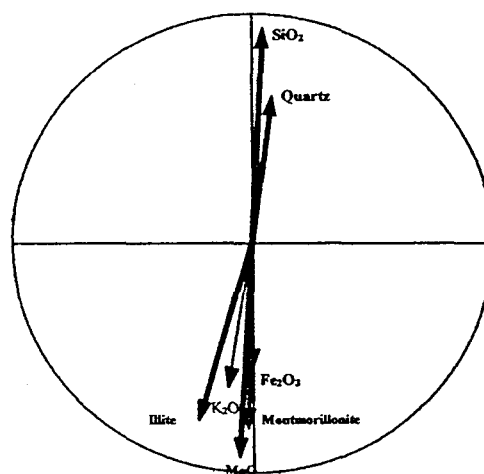

Figure 5. Correlations circle for chemical data on the clay materials (horizontal axis 4: vertical axis 1).

and montmorillonite may be related and those of K_2O, MgO and Fe_2O_3 (and Na_2O as deduced from other less significant correlations circles) are related to the former and, finally, no relation exists between CaO and the other constituents of the clay minerals. It may be expected that CaO is present in calcite, as a contaminant of the minerals.

The study of eventual relations between 'physical variables' is comparatively poor (Fig. 6 presents the more interesting correlations circle). Nevertheless, the study puts forward a relation between water absorption of the clay materials and their losses during ignition. Furthermore, rheological data seem both to be related and to decrease when the clay content of grains less than 20×10^{-6} m increases.

Then relationships which exists between all the variable data of the clay materials were tested. Three significant correlation circles (Fig. 7, 8 and 9) are computed using three principal axes, 1, 2 and 3, which correspond, respectively, to the quart content related to the rheological
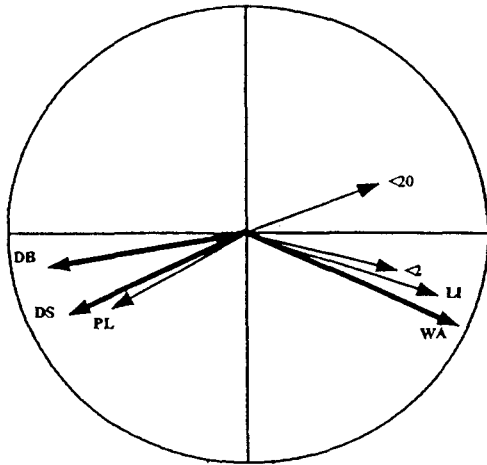
Figure 6. Correlations circle for the 'physical data' on the clay materials. DB—dry bending strength; DS—dry shrinkage; PL—plasticity index; LI—loss on ignition; WA—water absorption deduced from thermal behaviour.
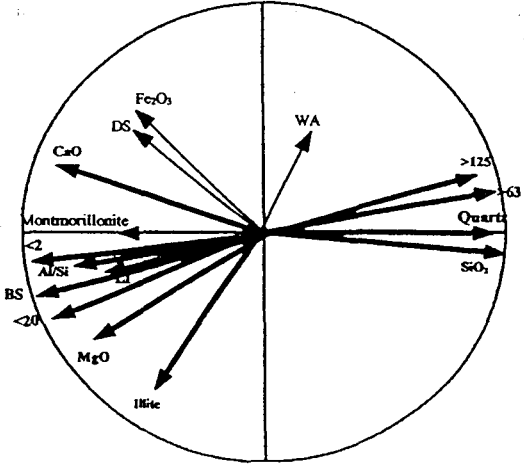

Figure 9. Correlations circle for data on the clay materials (horizontal axis 1: vertical axis 3).
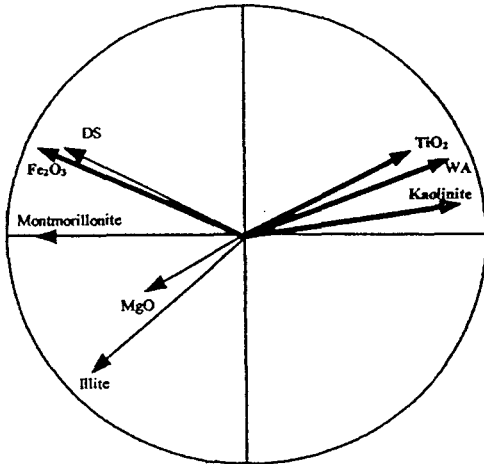

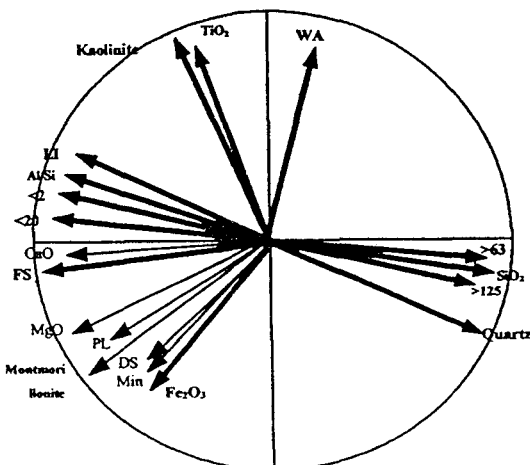Figure 7. Correlations circle for data on the clay materials (horizontal axis 2: vertical axis 3).

Figure 10. Structure of kaolinite layer (after Gruner[6,19] and Brindley[20]).

Figure 8. Correlations circle for data on the clay materials (horizontal axis 1: vertical axis 2). FS—firing (1000°C) shrinkage.

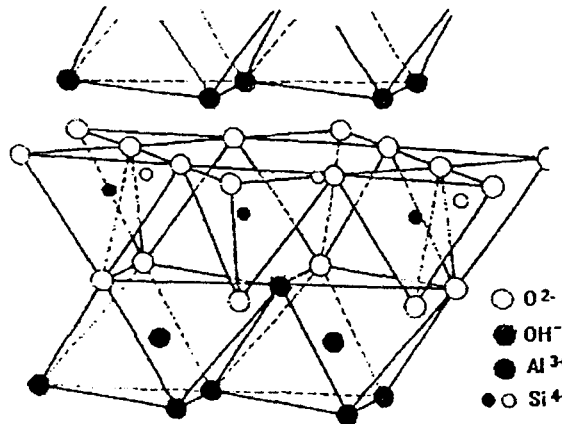and morphological data, to the structural data related to their thermal behaviour and to the chemical composition related to the morphological data.

Correlation circles allow us to propose that dry shrinkage and the plasticity index (which may be assumed to be two independent variables) increase when the Fe_2O_3, the minerals or the montmorillonite contents increase. Moreover, they show that water absorption after firing at 1000°C is related to the kaolinite and the TiO_2 content, fire (1000°C) shrinkage increases when the calcite (CaO) content increases, the content of grains larger than 63 or 125×10^{-6} m increases when the quartz content (SiO_2 content) increases, the content of grains more than 20 or 2×10^{-6} m increases when the clay minerals content (Al/Si ratio) increases and, finally, that loss on ignition and dry bending strength increase when the contents of clay minerals and of small grains increase.

The structures and the chemical compositions of the clay structural phases have to be discussed to explain the observed relations. Figure 10 shows diagrammatically the structure of the kaolinite layer and that the charges within the structure are balanced, i.e. there are no charges
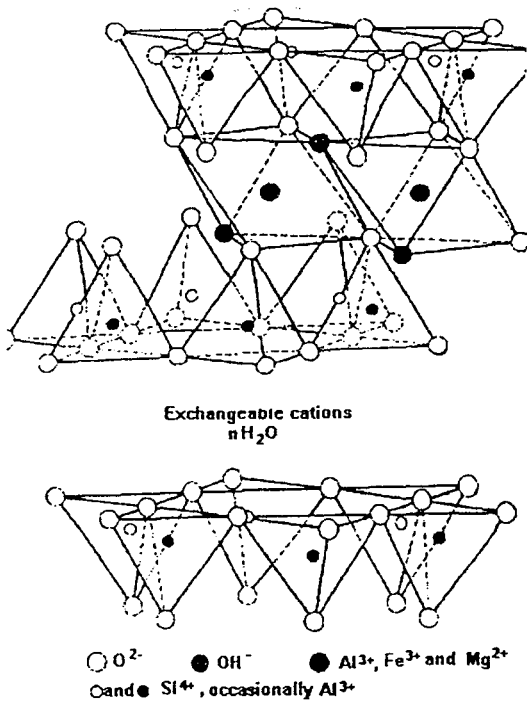
Exchangeable cations
$n H_2O$

$\bigcirc$ O^{2-} $\bullet$ OH^- $\bullet$ Al^{3+}, Fe^{3+} and Mg^{2+}
$\bigcirc$ and $\bullet$ Si^{4+}, occasionally Al^{3+}

Figure 11. Structure of montmorillonite (according to Hendricks[6,22]).

on the lattice due to substitution within the lattice. In a few instances very small amounts of substitution of Fe and/or Ti for Al is observed in a relatively poor crystalline variety. Because of the superposition of O^{2-} and OH in adjacent units, the units are held together tightly by hydrogen bonding between the layers. As a consequence, the mineral forms six-sided flake-shaped units in sizes from about 3×10^{-7} to 4×10^{-6} m.[21]

Figure 11 shows diagrammatically the structure of montmorillonite. It illustrates that in the stacking of the silica–alumina–silica unit, O^{2-} layers of each unit are adjacent to O^{2-} of the neighbouring units with the result that there is a very weak bond and an excellent cleavage between them. The outstanding feature of the montomorillonite structure is that water and exchangeable cations can enter between the unit layers. Furthermore, montmorillonite always differs from its theoretical formula, $Al_4Si_8O_{20}(OH)_4$, n (interlayer) H_2O, because of substitutions within the lattice of Al and possibly P for Si in tetrahedral coordination and/or Mg, Fe and other minerals from Al in the octahedral sheet. Finally, montmorillonite tends to occur in equidimensional, extremely thin flake-shaped units, relatively readily dispersible to extremely small particle sizes; this seems particularly true when Na is the exchangeable cation.

The illite clays, similar in their general structural characteristics to the micas,[23] form a mineral group rather than a mineral species. The unit is the same as that for montmorillonite except that some of the Si is always replaced by Al, and the resultant charge deficiency is balanced by K ions. Also, a small amount of water may be present between the silicate layers. Illite has generally small, poorly defined hexagonal flakes[24] having a diameter less than 3×10^{-7} m.

Clay minerals have the property of absorbing certain anions and cations and retaining them in an exchangeable state. The common exchangeable cations are Ca, Mg, H, Na, K and ammonium ions. In the use of clay mineralogy, ion exchange is important because the nature of the ion may influence substantially the physical properties and, in particular, the plastic property of the material.

Water which can be held by clay materials studied may be into two categories: water in pores and/or around the particles of the material (its removal requires generally very little energy and a temperature only a little above room temperature is adequate for it complete elimination) and in the case of montmorillonite and, to a user extent, illite, underlayer water which causes swelling and expansion characteristics (its complete elimination requires temperatures approaching at least 100°C; this elimination is not easily reversible.)

Between 400°C and 700°C the hydroxyl structural water is lost. Within this same temperature range the structure of the clay minerals and, subsequently, the physical properties may be altered.[6]

These considerations allow an explanation of the relation deduced from principal component analysis. Relations of Fe (substitute of Al) amounts with the montmorillonite content and of K, Mg and Na (interlayer exchangeable ions) with the montmorillonite and the illite contents become obvious. The absence of relations between Ca and the amounts of clay materials confirms that this element is mainly present in calcite.

Furthermore, the relation between water absorption of the clay materials and loss during ignition proves that the absorbed water amount is low compared to the content of hydroxyl groups. The relation between dry shrinkage and the plasticity index and the Fe_2O_3, the minerals or the montmorillonite contents (which are related data) is easily explained.

Loss on ignition related to the clay minerals content may be explained by removal of hydroxyl groups and water evolution at temperatures higher than 400°C. Firing (1000°C) shrinkage increase is related to an increase in the calcite content; It may be assumed that the thermal degradation of calcite (contaminant material of the clay) which provides CaO leads to the shrinkage and that the part of the structural changes of the clay materials during the thermal treatment may be neglected.

Finally, the relationships between the amount of small particles and the clay materials content and between the amount of large particles and the quartz content is explained by the very different granulometry of these materials.

To conclude this part of the study, a comparison of conclusions from mathematical analysis and literature data proves the validity of the statistical model.

RELATIONS BETWEEN FIRE RETARDANT PERFORMANCES AND THE VARIABLES' CHARACTERISTICS OF THE FILLERS

Figures 12 to 17 present correlation circles for chemical or physical variables of the clay minerals in which LOI and UL 94 data are introduced as supplementary
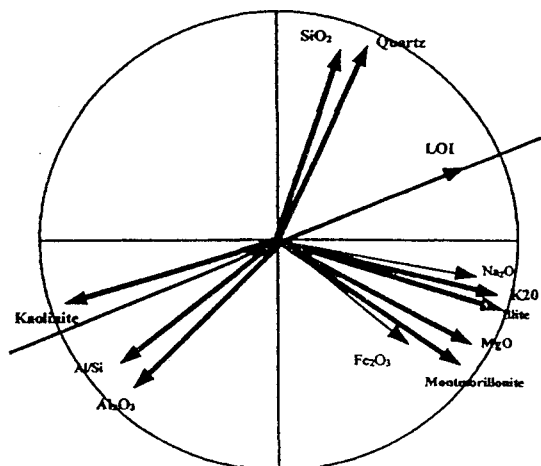
46

Figure 12. Correlations circle for LOI and chemical data on the clay materials (horizontal axis 1: vertical axis 2).
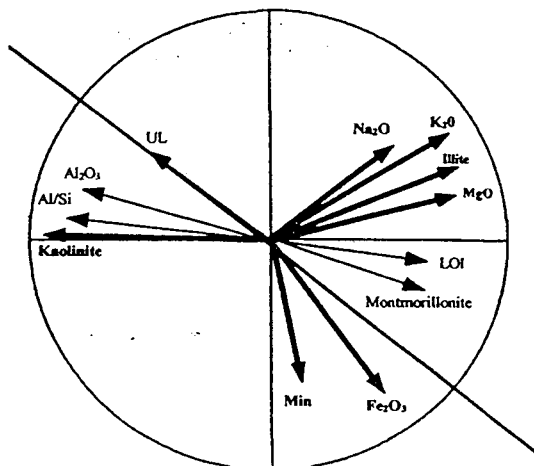

Figure 15. Correlations circle for UL 94, LOI and chemical data on the clay materials (horizontal axis 1: vertical axis 3).
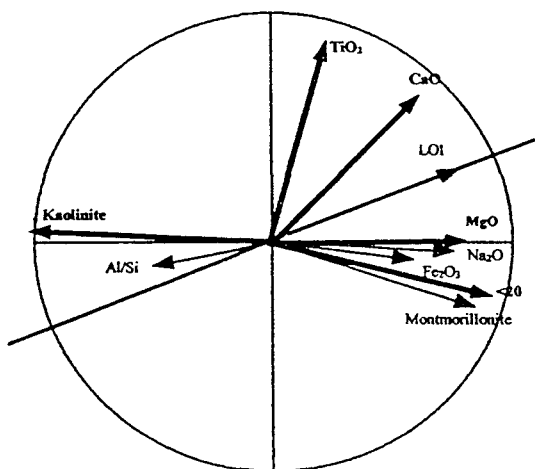

Figure 13. Correlations circle for LOI and chemical data on the clay materials (horizontal axis 1: vertical axis 4).
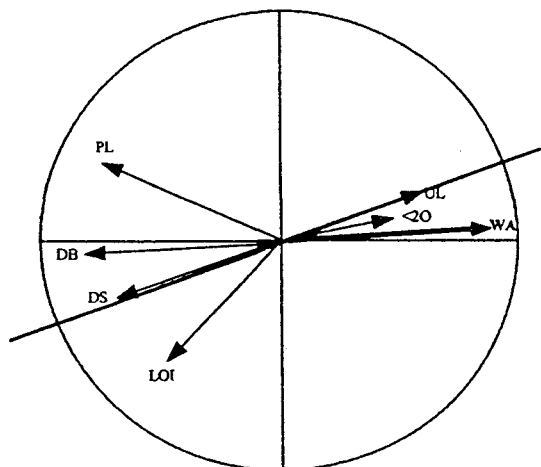

Figure 16. Correlations circle for UL 94, LOI and 'physical' data on the clay materials (horizontal axis 2': vertical axis 5').
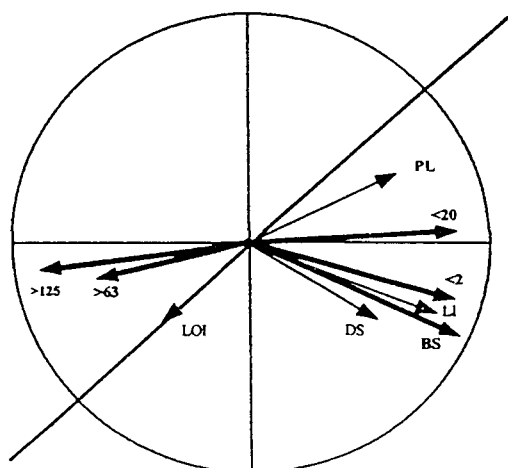

Figure 14. Correlations circle for LOI and 'physical' data on the clay materials (horizontal axis 1': vertical axis 5').

variables. With the reported principal axes' systems, LOI is a highly represented variable (Fig. 12) or a moderately represented one (Figs 13 to 17) when the UL 94 result is a variable not represented (Figs 12 to 14) or moderately represented (Figs 15 to 17).

LOI data are present in the circles plotted using the principal axes corresponding to both the structure of the clay materials and the amount of calcite (axis 1) with the respective amounts of Al and Si in the materials (axis 2), of exchangeable cations (axis 3) and of non-clay materials: calcite and titanium dioxide (axis 4), in the circles plotted using the principal axes corresponding to both the size of particles and the thermal textural change of the materials (axis 1') with rheological data (axis 2') and with plasticity (axis 5') and finally, in the circles plotted using the principal axes corresponding to plasticity (axis 5') with other rheological data (axis 2'). UL 94 classification data are only represented in circles corresponding to both the structure of the clay materials (axis 1) with the amount of exchangeable cations (axis 3) and in circles corresponding to the axes' systems computed using 'physical' data (axes 1' with 2' and 2' with 5').
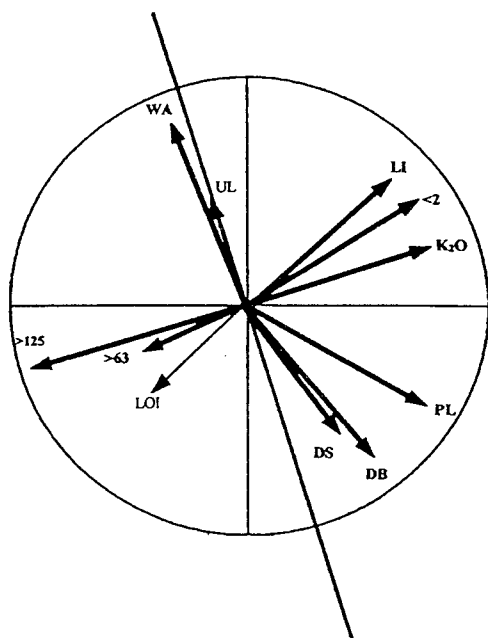
Figure 17. Correlations circle for UL 94, LOI and 'physical' data on the clay materials (horizontal axis 1': vertical axis 2').

Correlation circles in which both LOI and UL 94 results are represented allows to propose that a direct relationship between their two sets of data does not exist and, in addition, that characteristics of the clay materials which increase the LOI values may decrease the UL 94 classification of the formulations.

Figures 12 to 17 show that increases in the amount of the kaolinite clay mineral, of the Al_2O_3 content and of the Al/Si ratio lead to decrease in the LOI values and that these do not depend on the contents of quartz, TiO_2, Fe_2O_3, montmorillonite and illite clay minerals. In addition, the LOI values nevertheless increase when the content of Na_2O, K_2O and MgO increase. The figures show also that increases in the amounts of clay particles larger than 63 and 125×10^{-6} m and the related decrease in the plasticity of the clay material lead to an increase in the LOI values and that the other 'physical' characteristics and, in particular, thermal changes in the clay materials do not have any influence on the LOI.

In addition, figures 15 to 17 show that the increase in the Al_2O_3 content of the clay materials (and consequently in the amount of Kaolinite mineral leads to an increase in the UL 94 classification. They show also that the UL 94 classification is improved by the decrease in the amounts of montmorillonite (and thus in the Fe_2O_3 content) in the clay materials. Finally, they indicate that the UL 94 classification increases when the relative amounts of particles smaller than 20×10^{-6} m increase, when the water absorption deduced from firing increases and when dry shrinkage and dry bending strength decrease.

GENERAL DISCUSSION

The study shows that addition of fillers in the polymer matrix of a fire retardant intumescent formulation may change the fire behaviour of the material. In particular, clays materials in the intumescent (PP–APP–PER) formulation may lead to an improvement or to a relative loss of the property, depending on the chemical or 'physical' characteristics of the clay materials.

A comparison of the changes in the fire retardant performance of the formulations versus the nature of their filler was carried out using two different evaluation tests. This work shows that a direct relation does not exist between the change in the LOI values and the change of the UL 94 classification. The observation that oxygen index and UL 94 are not linked is well known to all FR chemists and technologists.

The LOI test considers the necessary conditions for the existence and the extinction of the upper flame. These conditions depend on the diffusion nature of the flame and therefore on the change in the internal structures of the corresponding deflagrations, their rate of energy release and the respective rate of transport of fuel and oxidizer into the flame.[25] The rate of fuel transport seems to be the variable that is the factor affecting the flame structure. It depends on both the heat transfer from the flame to the material and the kinetics data of the degradation of this material.

UL 94 test were carried out with an oxygen concentration (about 20% in air) corresponding to the extinction of the flame related to the formation of the protective carbonaceous expanded coating on the surface of the polymer formulations. The measured performances were, functions of the dynamic rheological properties of the carbonaceous material. In particular, its viscosity must be high enough to avoid the formation and the fall of the molten polymer via an 'encapsulation' process. The dynamic properties of the coating material depend on its chemical nature[26] and also on the eventual presence of defects which may be initiators for the formation of cracks in the coating, which subsequently loses its insulating character[10] and then allows the free diffusion of heat and gases.

Moreover, the present study shows that computed linear relations between the variable characteristics of the clay materials studied and the corresponding LOI values are not significant. Fallacies in interpreting their correlation coefficients (linear components of curves corresponding to synergistic or antagonist effects and linkage of the tested variables with untested variables) have been discussed. The results of the principal components analysis must now be considered.

The LOI test gives a quantitative evaluation of the behaviour of a material in a fire; this supplementary variable is consequently always represented in the correlation circles. UL 94 classification gives qualitative variables, and our resulting quantitative evaluation is therefore poor and the representation of this variable in correlation circles is also comparatively poor.

The main result of this study consists of showing inverse relationships between the LOI and the UL 94 data when the chemical composition (amounts of calcite and of exchangeable cations) plasticity and rheological variables of the clay materials are considered. In addition, no relationship between the results of the two tests is observed when the size of the filler particles or the thermal textural change of the clay materials are variables studied.

48

The decrease in the LOI values when the Al/Si ratio increases shows that the computed linear relation is significant. LOI values also decrease when the kaolinite clay mineral content increases (and, subsequently, the Al_2O_3 content increases because the Al/Si ratios of kaolinite, montmorillonite and illite clay minerals are, respectively, 1, 1/2 and approximately 1/3).

A previous study in the authors' laboratory using another class of alumino:silicate minerals has shown that phosphate species may react with silica species to give a new active carbonization catalyst.[17] However, this study proposes that the LOI values increase when the Al/Si ratio increases. The difference in fire behavior between the two classes of minerals may be explained by the nature of this last class of alumino-silicate minerals, which contain easily exchangeable ions and cause removal of the Al ions from their lattices in the presence of an acid.

The present principal component analysis does not show any relation between the LOI values and the montmorillonite or the illite (two minerals containing exchangeable ions) content of the clay materials. The observed relationship between the increase in the LOI values and the increase in the Na_2O, K_2O and MgO contents (Na, K, and Mg are exchangeable cations of the montmorillonite and the illite minerals) allows us to propose that increases in contents of each of these minerals leads to an increase in the LOI values. The absence of a direct relation with the LOI may then be explained by the influence of other structural composition variables, particularly the kaolinite mineral content which is not related to the other minerals' contents (Fig. 4). It is worth noting that in our formulation the antagonistic effect of alkalis or alkaline earths with phosphate FR species, previously observed in cellulose-based materials,[27] does not appear. It may be proposed that the related formation of inactive phosphate species does not take a main part in the chemical processes which occur in fire conditions.

The previously proposed formulation of P–O–Si catalytic species (active for the carbonization process leading to the formation of the protective shield) may be checked because substitution within the lattice of montmorillonite or illite minerals of phosphorus for silicon in tetrahedral coordination is possible.[6] Discussion on the chemical nature of these species is, of course, not the object of this paper. It has been shown previously that the formation of these species changes the kinetics of the thermal behaviour of the PP-based intumescent formulations and, in particular, affects their invariant kinetic parameters and their modes of degradation.[13,17] The linear relation between their values of the LOI evaluation test and the invariant activation energies[28] which has been proposed[6] explains the observed change in LOI.

This study shows that particles larger than 63×10^{-6} m are composed of quartz and other minerals because clay minerals form readily dispersible units smaller than 4×10^{-6} m. Therefore increase in the LOI values of the formulations with an increase in the amounts of large clay particles and the related decrease in the plasticity of the filler may be explained by resulting high shear stresses during the mixing process. The formation of mechano-radicals enhanced by high shear stress results from the main chain scission of the PP (see

reference 29 and references therein). It is obvious that scission of the polymer chain leads to a decrease in the molecular weight of the polymer. In addition, the mechanical process may lead to severe modifications of the PP (defects in the molecular chain of the polymer, eventual chain branching, presence of ketone groups) which may result in a modified (or disordered) crystal structure of the isotactive PP[30] and/or to change in the molecular morphology of the semicrystalline polymer.[31,32]

A previous study of the relation between the LOI and the invariant activation energy of intumescent systems suggests that decomposition rates higher than that of the sole polymer and an early decomposition of the systems are necessary to increase their LOI. It is proposed that there is a relation between the rate of development of the protective coating (resulting from a condensed phase mechanism) and the rate of the initial matrix decomposition.[33] All the modifications of the polymer matrix during the mixing process may result in a material with a comparatively low thermal stability which needs a low temperature for the beginning of its thermal degradation and then the early development of the intumescent process.

The study does not prove the existence of relations between chemical activities of the fillers and the UL 94 classification. Relations between the classification and the kaolinite mineral amount, the water absorption and the amount of particles smaller than 20×10^{-6} m may be discussed. High values of these characteristics of the clay materials are related to low amounts of quartz and minerals in them. Addition of the fillers leads to comparatively low shear stress during the mixing process and so the molecular chain of the polymer and its dynamic properties are not modified. Consequently, the V0 classification of the formulation without fillers is preserved. As previously discussed, if high shear stress results from the mixing process the molecular weight of PP decreases and the related dynamic properties are affected. In particular changes in the viscosity and the melt index lead to a easy melting of the polymer matrix and so to dripping.

Observed decrease in the UL 94 classification when the amount of montmorillonite mineral increases shows that performance is not directly related to the formation of catalytic species active for the carbonization process and/or to the synthesis of particular 'carbon' species in the coating. This relation may be better explained by the related high fire shrinkage of clay particles in the intumescent coating, these particles being initiators for the development of cracks for the loss of the insulative character of the shield.

Finally, relations with the dry shrinkage may be easily explained. It may be proposed that the formation of defects (holes and/or cracks) in the solid formulations which form in the low-temperature range increase the rate of their thermal degradation in fire conditions.

CONCLUSION AND SUMMARY

In this work we have studied the part played by clay material fillers in the fire behavior of the intumescent PP/APP/PER system using the LOI and UL 94 tests.

According to their chemical or 'physical' characteristics, added clays increase or decrease the measured fire retardant performances of the formulations. A study of the factors affecting the performances has been carried out using linear regression and the principal components analyses. This shows that linear regression is not, in that particular case, a good procedure to for showing eventual relations. Principal components analysis shows that the results of the two evaluation tests are affected in different ways by the addition of different clay materials and that an increase in the LOI value does not lead necessarily to the best UL 94 classification.

Discussion of the increase in LOI values has taken into account the reactivity of the montmorillonite and the illite minerals with acidic phosphate and the resulting formation of catalytic species active in the carbonization process. In addition, the study allows us to propose that the results of this test are improved when the filler materials contain quartz mineral and other foreign minerals. The resulting increase in the viscosity of the material leads to a mechano-radical degradation of the polymer matrix during the mixing process which allows easy formation of the protective coating.

The study does not put forward any relation between the UL 94 classification and the chemical characteristics of the clay materials. It is proposed that this classification is affected by changes in the molecular chain of the polymer which occur during the mixing process and lead to the easy melting of the matrix. Therefore the classification is good when the amount of clay mineral and, in particular, of kaolinite mineral is high. Finally, its is proposed that the presence of minerals with high fire shrinkage leads to the formation of cracks in the intumescent coating and to the loss of its protective character.

Acknowledgements

REFERENCES

1. H. L. Vandersall, *J. Fire & Flammability* 2 (1971) 97–140.
2. G. Bertelli, G. Camino, E. Marchetti, L. Costa, E. Casorati and R. Locatelli *Polym. Deg. & Stab.* 25, 277–92 (1989).
3. A. Marchal, R. Delobel, M. Le Bras, J.-M. Leroy and D. Price, *Polym. Deg. & Stab.* 44, 263–72 (1994).
4. S. Bourbigot, M. Le Bras and R. Delobel, *J. Fire Sci.* 13 (1-2), 3 (1995).
5. Tests for Flammability o Plastic Materials for Part in Devices and Appliances, Underwriters Laboratories, Northbrook, ANSI/ASTM D635-77.
6. R. E. Grim, International Series in the Earth Sciences, *Applied Clay Mineralogy*, McGraw-Hill, New York (1962).
7. N. L. Hancox, and R. M. Mayer, *Design Data for Reinforced Plastics*, Chapman & Hall, London (1994).
8. Standard Test Method for Measuring the Minimum Oxygen Concentration to Support Candle-like Combustion of Plastics. ASTM D2863/77, Philadelphia.
9. R. Delobel, M. Le Bras, N. Ouassou, and F. Alistiqsa, *J. Fire Sci.* 8(2), 85 (1990).
10. R. Delobel, M. Le Bras, Y. Schmidt and S. Bourbigot, in *Actes Int. Symp. on Minerals and Organic Fillers in Polymers*, GFEAP, Le Mans (1991).
11. E. F. Heeermann, *Psych.* 28, 161–72 (1963).
12. F. Alistiqsa, Doctoral dissertation, University of Lille (1993).
13. S. Bourbigot, R. Delobel, M. Le Bras and D. Normand, *J. Chim. Phys.* 90, 1909–28 (1993).
14. G. Philippeau, Comment interpréter les résultats d'une analyse en composantes principales. ITCF Paris (1986).
15. H. H. Harman, *Modern Factor Analysis*, The University of Chicago Press, Chicago (1976).
16. R. A. Fisher and F. Yates, *Statistical Tables for Biological Agricultural and Medical Research*, Oliver and Boyd, Edinburgh (1957).
17. S. Bourbigot, Doctoral dissertation, University of Lille (1993).
18. G. M. Clarke, and D. Cooke, *A Basic Course in Statistics*, Edward Arnold, London (1992).
19. J. W. Gruner, Z. Krist. 83, 75–88 (1932).
20. G. W. Brindley, *X-ray Identification and Crystal Structures of Clay Minerals*, Mineralogical Society of Great Britain monograph, London (1951).
21. P. F. Kerr, P. K. Hamilton, D. W. Davis, T. G. Rochow and M. L. Fuller, *Am. Petrol Inst. Project 49 Prelim.*, Rept. 6 New York (1950).
22. S. B. Hendricks, *J. Geol.* 50, 276–90 (1942).
23. R. E. Grim W. F. Bradley and G. Brown, *The Mica Clay Minerals — X-ray Identification and Crystal Structures of Clay Minerals*, Mineralogical Society of Great Britain monograph, London (1951).
24. C. E. Weaver, *Am. Mineralogist* 38, 279–89 (1953).
25. L. Amable and A. W. Forman, *Fundamental Aspects of Combustion*, Oxford University Press New York (1993).
26. R. Delobel, S. Bourbigot, M. Le Bras and J. M. Leroy, *Savjetovanje Polimerni Materijali Smanjene Gorivosti*, Opatija, Yugoslavia, (1990): R. Delobel, S. Bouribigot, M. Le Bras, J. M. Leroy and B. Kanovnik, *Flame Retardancy of Polymeric Materials* ed-by Z Janovic, Society of Plastics and Rubber Engineers, Zagreb (1990).
27. J.-M. Leroy, P. Walrave, R. Delobel, M. Le Bras, J.-F. Hennette and D. Le Maguer, *Actes du Ier Coll. Francophone sur l'ignifugatin des Polymères*, Saint Denis (France), 87–88 (1985).
28. A. I. Lesnikovich and S. V. Levchik, *J. Thermal Anal.* 30, 677 (1985).
29. J. Sohma, *Colloid Polym. Sci.* 270, 1060–65 (1992).
30. D. T. Quillin, D. F. Caulfield and J. A. Koutsky, *J. Appl. Polym. Sci.* 50, 1187–94 (1993).
31. C. Dupoisson, *Diplome d'Études Approfondies* Dissertation, University of Lille (1993).
32. J. O. Iroh and J. P. Berry, *Polymer* 34(22), 4747–51 (1993).
33. S. Bourbigot, R. Delobel, M. Le Bras and Y. Schmidt, *J. Chim. Phys.* 89, 1835–52 (1992).

Zeolites: New Synergistic Agents for Intumescent Fire Retardant Thermoplastic Formulations— Criteria for the Choice of the Zeolite

Serge Bourbigot,* Michel Le Bras

Laboratoire de Physico-Chimie des Solides, E.N.S.C.L., Université des Sciences et Technologies de Lille, BP 108, F-59652 Villeneuve d'Ascq Cedex, France

Patrice Bréant

CERDATO (Elf-Atochem), F-27470 Serquigny, France

Jean-Michel Trémillon

GRL (Elf-Atochem), BP 34, F-64170 Lacq, France

René Delobel

CREPIM, Parc de la Porte Nord, F-62700 Bruay la Bussière, France

The adduct of zeolites in intumescent formulations of thermoplastic polymers (additives: ammonium polyphosphate and pentaerythritol) leads to a great improvement in their fire retardant performance. A classification of different groups (A, X, Y, Mordenite and ZSM-5) is presented. The influence of the physicochemical properties of the zeolites is discussed. TG analyses reveal that the zeolite may act as a catalyst for the development of the intumescent carbonaceous material and stabilize the carbonaceous residue resulting in the degradation of the intumescent shield. Characterized by MAS-NMR ^{27}Al and ^{29}Si, it is proposed that alumino- and silicophosphate species formed are catalysts active for the synthesis of a protective carbon-based material.

INTRODUCTION

Intumescence technology has recently found a place in polymer science as a method of providing flame retardance (FR) to polymeric materials.[1] On heating fire retardant intumescent materials form foamed cellular charred layers on the surface, which protects the underlying material from the action of heat flux or flame (a physical barrier which slows down heat and mass transfer between the gas and condensed phases).

Generally, intumescent formulations contain three active ingredients: an acid source, a carbonific (or polyhydric) compound, and a spumific agent.[2] First, the acid source breaks down to yield a mineral acid, then it takes part in the dehydration of the carbonific to yield the carbon char and finally, the spumific decomposes to yield gaseous products. These last cause the char to swell and hence provide the insulating material which then decomposes under the action of the outer heat flux (Fig. 1).

The association of an ammonium polyphosphate (APP) (acid source and the spumific due to evolution of ammonia from the APP on heating) and the pentaerythritol (PER) (carbonific) has been shown as an FR intumescent system.[3] A previous study has shown that the resulting carbonaceous coating protects a polymeric matrix at temperatures lower than 375°C.[4] The loss of the protective character is related to a change in the dynamic properties of the char and to its thermal degradation.

FR intumescent additives' systems allow the formation of a carbonaceous shield composed of polyaromatic stacks[5] in the temperature range where the polymer degrades. The resulting shield has an intrinsic insulating character. In addition, the carbonaceous material may act as a support for catalytic phosphate species[3] which react with the evolved products arising from the thermal degradation of the polymer to form new polyaromatic molecules which take part in insulation and in the dynamic properties of the upper shield.[6]

The APP/PER system provides good FR properties in thermoplastics,[7] particularly in polyethylenic matrices. Commercially available intumescent formulations could also contain fillers:[8-10] titanium dioxide, resin binder plasticizers and alumino-silicate (clay) materials. These fillers may act as synergistic agents in intumescent FR formulations. Among the possible alumino-silicate fillers, Beyer et al.[11] proposed that zeolites present a potential application as FR material: the combination of zeolites and conventional heat-insulating materials ensures an enhancement of the protective effect.

Zeolites are tectosilicates characterized by a three-dimensional framework of AlO_4 and SiO_4 tetrahedra.[12] The framework contains channels and interconnected voids which are occupied by the cation and water molecules. The negative charges due to AlO_4 are balanced by cations. The size of the voids or the channels is approximately that of the usual organic molecules. The ideal chemical formula is $M_{x/n}[(AlO_2)_x, (SiO_2)_y]zH_2O$. The part in the formula in brackets is the framework of the zeolite with a ratio $y/x \geqslant 1$ (Lowenstein rule[13]) and M^{n+} is the balance cation.

The only item of a zeolite structure which can be precisely specified is the topology of the aluminosilicate framework. All the others, such as the distribution of atoms in the crystallographic equivalent sites, are complex and uncertain.[14] It is considered[15] that the link modes of the primary polyhedra (truncated octahedra, Fig. 2) by defined geometric units called SBU (Secondary Building Units) [16] are the basis of the zeolites' classification. With this classification seven groups are obtained (Table 1).

In the laboratory we have associated the FR APP/PER system with zeolites in polyolefinic matrices (PE, ethylene copolymers, PP and their blends).[17,18] A recent study[19] has shown that the synergistic FR effect arising from the zeolite adduct depends strongly on the polymeric matrix. In particular, using a 4A zeolite, this effect is greatest when the thermal degradation of the polymer leads to the formation of carboxylic acidic species which may play a part in a condensed phase process.[7] A typical matrix leading to this important FR effect is the ethylene-butyl acrylate-maleic anhydride terpolymer.

This work deals with a classification of the FR property of new intumescent systems containing several zeolites belonging to different structural groups (see

Table 1). The results presented concern the terpolymer ethylene-butyl acrylate-maleic anhydride (LRAM3.5). In a first step the synergistic effects caused by the minerals are studied. Relations between the chemical properties of the fillers and the FR performance are then sought. The part played by the aluminosilicate in the thermal degradation of the insulating material will be put forward using thermogravimetric (TG) analyses. Then the formation of species able to play a part as catalysts for the 'synthesis' of the carbon-based material of interest is studied using MAS-NMR ^{29}Si and ^{27}Al.
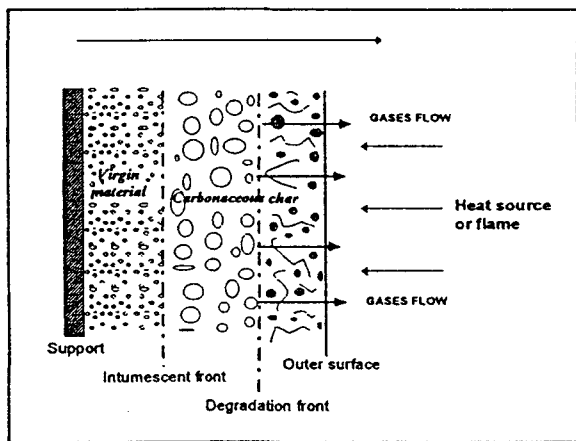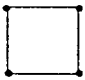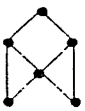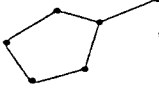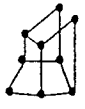

Figure 1. Intumescent model.

Table 1. Groups of zeolites.

| Group		Secondary building units
1		S4R (zeolites: analcime, phillipsite, etc.)
2		S6R (zeolites: erionite, offretite, T, etc.)
3		D4R (zeolites: A, λ, ZK-4, etc.)
4		D6R (zeolites: faujasite, x, λ, chabazite, etc.)
5		Complex 4-1, Unit T_5O_{10} (zeolites: natrolite, thomsonite, etc.)
6		Complex 5-1, Unit T_6O_{16} (zeolites: mordenite, ferrierite, etc.)
7		Complex 4-4-1, Unit $T_{10}O_{20}$ (zeolites: clinoptilolite, etc.)

α   β   D4R

D6R   γ   ε
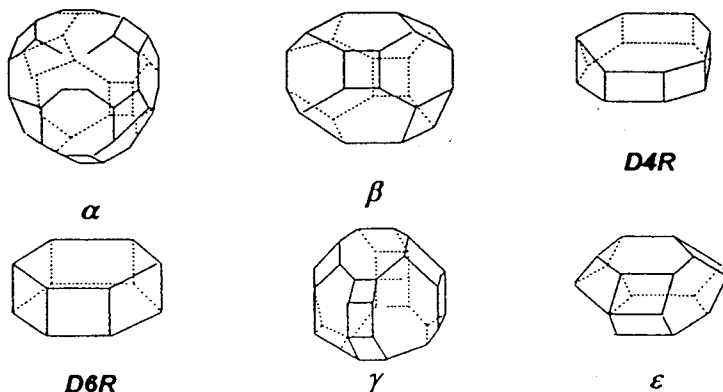
Figure 2. Primary polyhedra (Si or Al atoms lie at the edges and oxygen atoms occupy the middle of the lines).

EXPERIMENTAL

Materials

The raw materials were a LRAM 3.5 terpolymer supplied by Elf-Atochem, synthetic zeolites supplied by Ceca (Table 2), PER (Aldrich R.P. grade) and APP ($(NH_4PO_3)_n$, $n = 700$, Hoechst Exolit 422). The study was carried out using the APP/PER for the ratio APP/PER = 3 (wt/wt). In the case of polyethylenic materials, the fire-retardant properties are indeed maximum for this ratio.[1-3] Initial mixtures (additives + filler were 30 wt% in the formulation) were first prepared by ball-milling after mechanical grinding and sifting (200 μm) of the raw materials. Sheets were then obtained using a Darragon press at 160°C with a pressure of 30 bars. The procedure used was not conventional. Samples obtained present an additive dispersion close to that of samples obtained by an extrusion using a contra-rotative twin screw extrudor (samples processed by Elf Atochem—Serquigny).

Fire testing

Limiting Oxygen Index (LOI: a standard test method for measuring the minimum oxygen concentration to support candle-like combustion of plastics) was measured using a Stanton Redcroft instrument on $120 \times 60 \times 3$ mm³ sheets according to the standard 'oxygen index' test (ASTM D2863/77, American Society for Testing and Materials, Philadelphia). As an example, the LRAM 3.5 gives a LOI value of 20%.

It may be noticed that the LOI values of samples processed according to our procedures are equal to (or 1% higher than) the LOI values of samples resulting from an extrusion process and are thus representative data.

TG analyses

TG analyses were carried out at 3°C min⁻¹ under synthetic air or nitrogen (flow rate = 5.10^{-7} m³ s⁻¹; Air Liquide grade) using a Setaram MTB 10-8 microbalance. In each case the mass of sample used was fixed at 15 mg and the samples (powder mixtures) were positioned in open vitreous silica pans. The precision of the temperature measurement was 1.5°C over the whole of the range.

The curves of weight difference between the experimental and theoretical TG curves were computed as follows:

- $M_{poly}(T)$: values of weight given by TG curve of the polymer
- $M_{add}(T)$: values of weight given by TG curve of the additives
- $M_{exp}(T)$: values of weight given by TG curve of the polymer + the additives
- $M_{th}(T)$: theoretical TG curve computed by linear combination between the values of weight given by TG curves of the polymer and the additives: $M_{th}(T) = 0.7\, M_{poly}(T) + 0.3\, M_{charge}(T)$.
- $\Delta(T)$: curve of weight difference: $\Delta(T) = M_{exp}(T) - M_{th}(T)$.

The $\Delta(T)$ curves allow us to show an eventual increase or decrease in the thermal stability of the polymeric matrix and the additives system related to the presence of one or every additive.[3]

NMR spectroscopy of additives systems

High-resolution NMR spectra of the solids were performed on a Brucker MSL 300 spectrometer (7.05 T) and were recorded in a 4 mm Brucker probe spinning at 10 kHz. The spectrometer frequencies were 59.595 MHz for ²⁹Si and 78.172 MHz for ²⁷Al. The pulse lengths were typically 2 μs for silicon and 1 μs for aluminium. Typically, 20 000 scans for ²⁹Si and 4000 scans for ²⁷Al were needed to obtain spectra with a convenient signal/noise ratio. The references used were the tetramethylsilane (TMS) for silicon and $Al(H_2O)_6^{3+}$ for aluminium.

RESULTS AND DISCUSSION

Fire behavior of the formulations LRAM3.5-APP/PER-zeolites

Study of the fire behavior of the materials requires consideration of the physical and chemical characteristics of the zeolites. In particular structure, adsorption and acid properties may be taken into account.

In order to understand adsorption phenomena in zeolites, one has to remember that the rigid aluminosilicate framework has voids which are occupied by cations and also by water molecules.[20] The latter are eliminated by heating, creating voids in the network. The void

Table 2. Chemical characteristics of the zeolites

Building units	Formula	Units	Structure type	Si/Al (at/at)	Aperture size (nm)
D4R	$K_9Na_3[(AlO_2)_{12}(SiO_2)_{12}]$, 27H₂O	α, β	KA (3A)	1	0.32
D4R	$Na_{12}[(AlO_2)_{12}(SiO_2)_{12}]$, 27H₂O	α, β	NaA (4A)	1	0.35
D4R	$Ca_{4.5}Na_3[(AlO_2)_{12}(SiO_2)_{12}]$, 27H₂O	α, β	CaA (5A)	1	0.42
D6R	$Ca_{21.5}Na_{43}[(AlO_2)_{86}(SiO_2)_{106}]_2$, 76H₂O	β	CaX (10X)	1.23	0.8
D6R	$Na_{86}[(AlO_2)_{86}(SiO_2)_{106}]$, 276H₂O	β	NaX (13X)	1.23	0.9–1
D6R	$Na_{56}[(AlO_2)_{56}(SiO_2)_{136}]_2$, 250H₂O	β	Y	2.4	1
T_6O_{16}	$Na_8[(AlO_2)_8(SiO_2)_{40}]$, 24H₂O	–	Mordenite	5	0.67–0.7
	$Na_{0.7}[(AlO_2)_{0.7}(SiO_2)_{95.3}]$, 16H₂O	–	ZSM-5	140	0.52–0.58

spaces are composed of a set of cavities connected by windows. The adsorption influence in the zeolites will thus depend on the size of the apertures and the dipolar moment of the fixed molecule.

The size of the apertures depends on the zeolite structure and on the number and the size of the cations. The molecules may diffuse into the network only if they can pass through the aperture.[21]

It is admitted that the acid properties of the zeolites are the basis of their catalytic activities.[22] By definition, an acid solid is a solid able to adsorb a base chemically. An acid site may either provide a proton (Brönsted site) or accept electron pairs (Lewis site).[21]

The structure and, in particular, the Si/Al ratio influence the acid properties of the zeolite[23] and an increase in the strength of the acid sites is observed when the Si/Al ratio increases and at the same time the number of these sites decreases.[24,25] Formation of the acidic sites also depends on the thermal treatment of the zeolite. The maximum Brönsted acidity is observed at about 400–450°C whereas the Lewis acidity is significant from 600°C.[26]

In this study, three characteristics of the zeolites, used namely, the structure of the zeolite (aperture size and cation influence, cavity diameter), total water loss and the Si/Al ratio are considered.

Zeolites A and X belong respectively to the D4R and D6R crystallographic groups (Table 2) and may be exchanged by cations. It seems therefore interesting to compare the FR synergistic effect in intumescent formulations of different A and X zeolites in order to study the structure and the cation (K^+, Na^+, Ca^{2+}) influence and the effect of the aperture size. The curves of the LOI values versus the zeolite level (Figs 3 and 4) show that a synergistic effect is observed for all zeolites and that the LOI maxima are at about 1.5 wt% of zeolite. For a type of zeolite the maxima of the LOI values are very close and there is, therefore, no significant influence by the alkali cation on maximum performance. Nevertheless, the fire behavior versus the zeolite level is quite different, in particular for zeolite levels greater than 3 wt% where a decrease in performance depends on the zeolite type. In the case of an X-type zeolite, a calcium compensation cation seems favorable whereas in an A-type zeolite the

contrary is observed. There is therefore no relation between the compensation cation or the aperture size of the zeolites and the FR performance.

In order to study the influence of the Si/Al ratio, the sodium zeolites Y (Si/Al = 2.43), mordenite (Si/Al = 5) and ZSM-5 (Si/Al = 140) were used to measure the FR performances of the LRAM3.5-APP/PER-Zeolites formulations (Fig. 5). The trends observed are similar with maxima of the LOI values reached at 1.5 (Y) or 2 wt% (mordenite and ZSM-5) of zeolite. These values demonstrate significant differences (LOI = 40% with the Y zeolite and LOI = 36% with the ZSM-5 zeolite). If no direct relation between the Si/Al ratio and the LOI values is observed (LOI of 13X close to LOI of ZSM-5 and lower than LOI of 4A), we may nevertheless propose that a low Si/Al ratio is favorable to obtain better performance. Further, this result is confirmed by the LOI values obtained using the sodium 4A (Fig. 3). It is therefore of interest to discuss the fire behavior of the materials versus the other physical and chemical properties of the zeolites.

A molecule may diffuse into the framework of a zeolite if its diameter is smaller than the aperture of the zeolite.

Figure 4. LOI values versus X zeolites' level of formulations LRAM3.5-APP/PER-Zeolites (additives' level remaining constant, equaling 30 wt%)

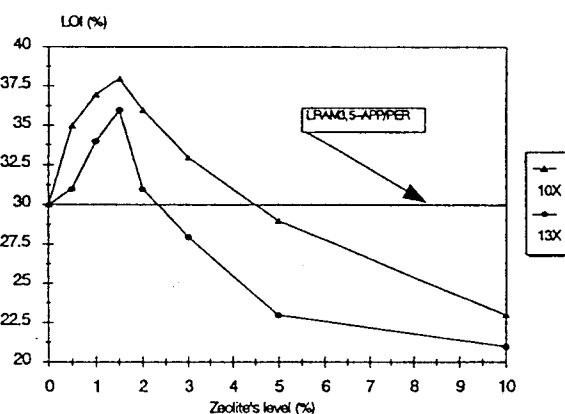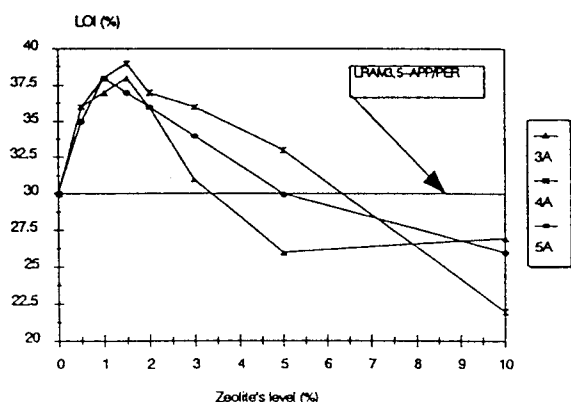Figure 3. LOI values versus A zeolites' level of formulations LRAM3.5-APP/PER-Zeolites (additives' level remaining constant, equaling 30 wt%)
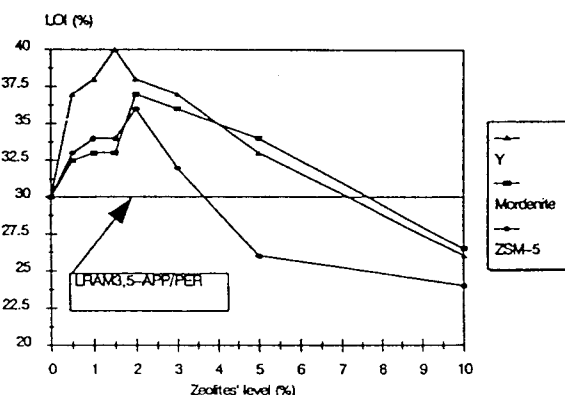

Figure 5. LOI values versus Y, mordenite and ZSM-5 zeolites' level of formulations LRAM3.5-APP/PER-Zeolites (additives' level remaining constant, equaling 30 wt%)
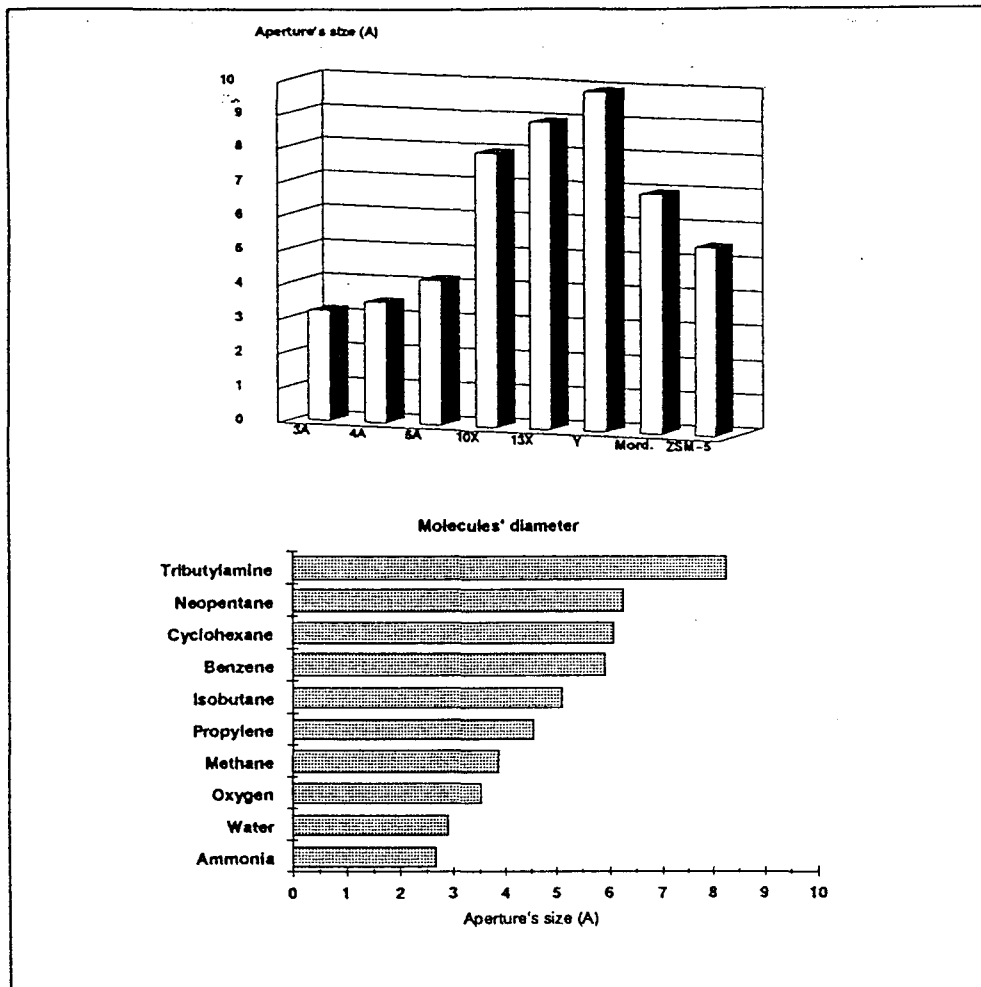
Figure 6. Molecules being able to be adsorbed versus the aperture size of the zeolites used.

Figure 6 compares zeolite aperture size with the equivalent diameter (computed according to the Lennard-Jones method) of some molecules.[14] The figure shows that only three molecules may be adsorbed by each zeolite: oxygen, ammonia and water. That a selective adsorption influences the FR performance is therefore not considered likely. Furthermore, it has been shown that oxygen adsorption does not occur at room temperature. There is therefore no possibility of oxygen adsorption during combustion of the material.

According to Camino et al.[27] the reaction between APP and PER leads to the formation of ammonia and water when the temperature increases and which may evolve to 'blow' the coating, resulting in the intumescence phenomenon. A zeolite adsorbs ammonia from about 250-300°C which corresponds to the desorption of the last water molecule.[14] Therefore an assumption concerning the influence of the ammonia adsorption may be proposed.

The zeolites are hydrated from 27 (A zeolites) to 280 (Faujasite) water molecules which may be desorbed between 100°C and 300°C. Nevertheless, whatever the water content is able to desorb, no influence is observed

on the FR performances (for example, identical LOI curves between 4A and Y). The water desorption of the zeolite during the combustion of the material does not play a part in the fire behavior of the formulations.

The FR performance seems to be enhanced by a low Si/Al ratio. The strength of the acidic site increases when the Si/Al ratio increases but, at the same time, the number of sites decreases. This suggests therefore that high quantity of acidic sites is preferred to an increase in their strength in order to improve the fire behavior of the materials.

Zeolites are aluminosilicates and thus it seems interesting to compare formulations containing an amorphous aluminosilicate (China clay with kaolinite composition) with zeolites (Fig. 7). It is seen that the curves have the same behavior and that the better performances are always obtained at 1.5 wt% in aluminosilicate. Nevertheless, it should be noted that the FR performances achieved with the kaolin are always lower than these obtained with the 4A and Y zeolites. This suggests therefore that an aluminosilicate with a zeolite structure has to be used in order to obtain the best FR performances.

150

In a recent paper dealing with FR performances of intumescent clay mineral containing formulations[10] we proposed that the resulting LOI classification depended on the content of exchangeable cations of the clay (LOI values increase when the number of exchangeable cations per unit cell increases). Kaolinite-type minerals do not have such cations whereas zeolites do. It may therefore be proposed that the FR performance depends on the exchange properties of the aluminosilicates.

Thermal behavior of the formulation LRAM3.5-APP/PER-4A

TG analyses of the LRAM3.5-based formulations containing 1.5 w% of the zeolite 4A (Fig. 8) show that the intumescent process leads to the protection of the polymeric matrix in the temperature range
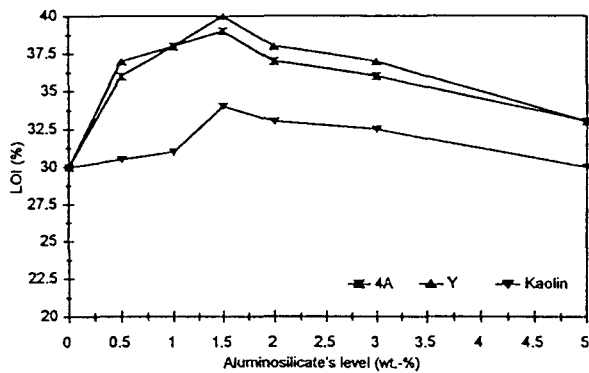

Figure 7. LOI values versus 4A, Y and Kaolin zeolites' level of formulations LRAM3.5-APP/PER-Aluminosilicates (additives' level remaining constant equaling, 30 wt%)

$250°C < T < 450°C$ and that the presence of the zeolite provides a residue stable at $T > 550°C$. Previous studies[1,3,7] identify the different processes which occur in the material versus the temperature. In the 250–450°C range an intumescent material is formed which degrades in the 450–550°C range to provide a carbonaceous residue without an expanded character. This residue degrades at temperatures higher than 550°C. In the case of formulation with zeolite the residue forms in the 450–500°C. Its comparatively high thermal stability at temperatures higher than 550°C may be related to the formation of a stable carbonaceous material and to oxides arising from the degradation of 4A (the residue amounts are, respectively, 15 and 5 wt% in the systems with and without 4A).

A comparison between the experimental TG curves of the LRAM3.5-APP/PER and LRAM3.5-APP/PER-4A systems (under air and N_2) and the computed curve deduced from the linear combination of the TG curves of the sole components is presented in Fig. 9. This shows clearly that oxygen occurs in the formation of the intumescent shield.

Under conditions of thermooxidative degradation it is observed that protection by the intumescent phenomenon is a two-step process. Nevertheless, it is noted that the difference of weight loss in the system containing zeolite is always higher than that of the system without zeolite, in particular in the range 370–450°C. This suggests that the zeolite activates the development of the intumescent process.

Observed ΔT at temperatures higher than 550°C does not support the comparatively high amount of stable residue obtained with the LRAM3.5-APP/PER-4A system. Indeed, the difference between the system with and without zeolite is only 4 wt% at 650°C (compared with 10 wt% deduced from the TG curves). This value is nevertheless proof of the part the polymer played in the
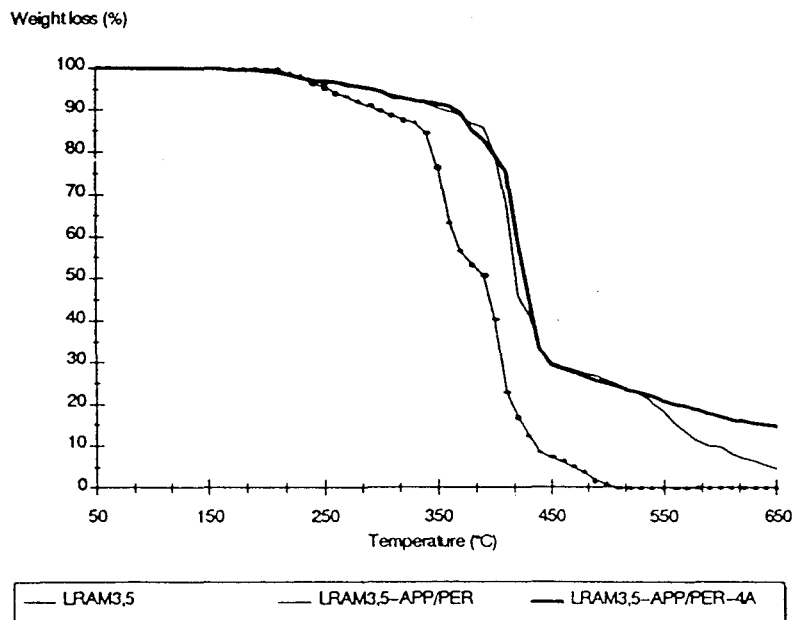

Figure 8. TG curves of the LRAM3.5-based formulations (under air).

formation of the stable carbonaceous material. The 6 wt% difference in the high-temperature residue is mainly due to the reaction between the additives as shown in Fig. 10.

Figure 9 shows that under pyrolytic conditions the rate of degradation of the polymeric matrix is increased in the temperature range 370–450°C in the case of formulation without zeolite whereas the contrary is observed in formulation with zeolite. This means therefore that the zeolite delays the pyrolysis of the system and may develop a protective material in the temperature range 420–460°C. This may explain the fire behavior differences between both formulations. Indeed, the presence of 4A leads to a decrease in the fuel (products of the pyrolytic degradation of the polymer) release rate and then affects the regime of the upper flame.

MAS NMR [27]Al and [29]Si spectroscopic study of the heat treated APP/PER-4A system

In order to understand the part played by the zeolite in the protective material, the solid state NMR [27]Al and [29]Si are powerful analytical tools. A spectrochemical study was undertaken using the heat treated APP/PER-4A system at four characteristic temperatures[7] which
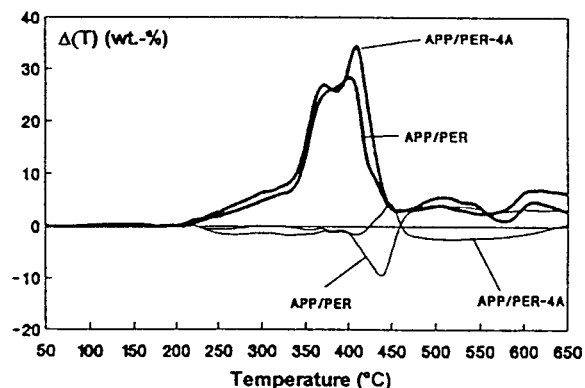
Figure 9. Weight loss differences deduced from TG curves under air (heavy line) and nitrogen (light line) of the LRAM3.5-APP/PER and LRAM3.5-APP/PER-4A systems
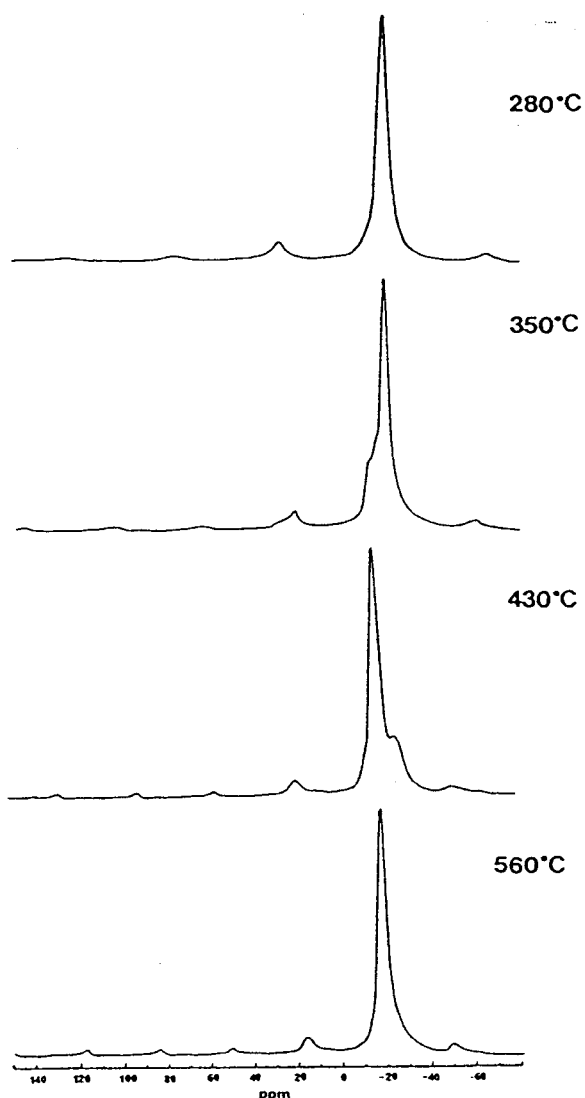
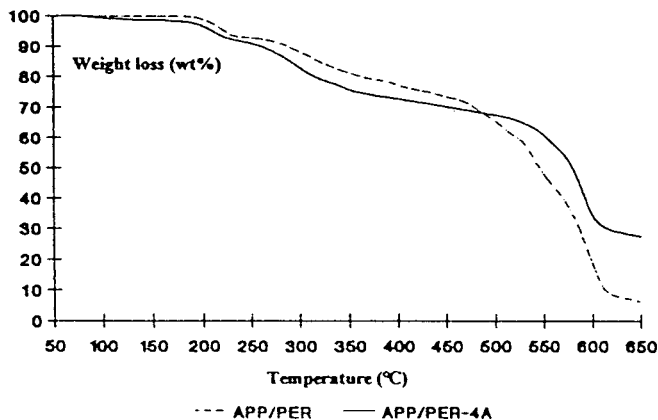Figure 11. MAS-NMR [27]Al spectra of the heat-treated APP/PER-4A system.

Figure 10. TG curves under air of the APP/PER and APP/PER-4A systems.

correspond to the beginning of the formation of the intumescent material (280°C), the maximum of intumescence (350°C), the carbonaceous residue (430°C) and the high-temperature residue (560°C).

Figure 11 presents the MAS-NMR ^{27}Al spectra of the heat treated APP/PER-4A system. This shows that the thermal treatment leads to the complete disappearance of the tetrahedral [AlO$_4$] unit of the zeolite ($\delta = 58$ ppm) [28,29] and, in fact, the complete destruction of the zeolite framework.

At every temperature, bands at about $- 18$ ppm are observed which may be assigned to octahedral [AlO$_6$] units.[30] The overlapping in the bands observed at 350°C and 430°C may be assigned to [AlO$_6$] units having different binding angles.[30] It is interesting to note that the isotropic chemical shift is moved to the strong fields. This may be because of the presence of phosphorus, in particular, within the second sphere of coordination. This P has a marked effect upon the peak position of an AlO$_x$ units which shifts from $+ 10$ to $- 20$ ppm for Al [OAl]$_6$ to Al [OP]$_6^{30-33}$. This shows therefore that the zeolite is destroyed to form aluminophosphates from 280°C. The dissymetry of the peaks observed from 350°C may be assigned to different Al–O–P binding angles due probably to heterogeneities in the material.

In order to confirm the reactivity in the solid state between the APP and the zeolite, a APP/4A mixture (1:1 wt/wt) has been heat treated at 280°C. The MAS-NMR ^{27}Al spectrum (Fig. 12) shows two peaks at 58 and $- 17$ ppm which can be assigned to [AlO$_4$] units in a zeolitic framework and to [AlO$_6$] units in aluminophosphates, respectively. This proves that a reaction between APP and 4A takes place with subsequent formation of [AlO$_6$] and/or Al [OP]$_6$ species.

MAS-NMR ^{29}Si spectra of the heat-treated APP/PER-4A system (Fig. 13) show bands at about -120 ppm at each temperature and from 350°C an additional band at about $- 215$ ppm. They may be assigned respectively to [SiO$_4$] units and to [SiO$_6$] units.[34] As above, the chemical shifts are moved to the strong fields which may be due, according to Weeding et al.,[34] to the presence of

phosphorus atoms in the second coordination sphere of Si providing greater shielding of the silicon nuclei. MAS-NMR ^{29}Si thus confirms the preceding results (destruction of the zeolite framework) and shows that APP reacts with the zeolite to form silicophosphate species. Moreover, a few silicophosphate species exist which have a silicon in the octahedral position. These compounds have been studies in the case of P$_2$O$_5$-SiO$_2$ systems.[35-37] It has been shown by Tillmans et al.[36] that they may be only silicon pyrophosphate [SiP$_2$O$_7$] and [Si$_5$O(PO$_4$)$_6$] constituted of isolated [SiO$_6$] octahedra and [SiP$_2$O$_7$] groups having a tetracoordinated silicon linked to PO$_4$ tetrahedra.

Finally, the MAS-NMR ^{27}Al and ^{29}Si study shows that the zeolite is completely destroyed from 280°C by reaction with the APP. This complete destruction involves the formation of a highly reactive phosphate species (aluminophosphate and silicophosphate species).

It has been previously shown that the reaction between APP and PER (ester formation[27] and hydrolysis of the phosphate chain[3]) leads to the formation of an active catalyst for the carbonization process. It is proposed that new active species formed in situ in the heat treated material containing 4A are also catalysts for the synthesis of 'carbon' (stable and protective at high temperatures) from the polymer pyrolysis products.

CONCLUSION

In this work we have proposed new intumescent formulations for polyethylenic materials. The use of zeolites as synergistic agents in an APP/PER system improves the performances significantly (up to 35% compared with the APP/PER system). Comparison of several zeolites used in intumescent formulations has shown that there is no relation between the type of exchangeable cation or the aperture size of the zeolites and the FR performance, and that the use of an aluminosilicate with a zeolitic structure leads to the best FR performance.
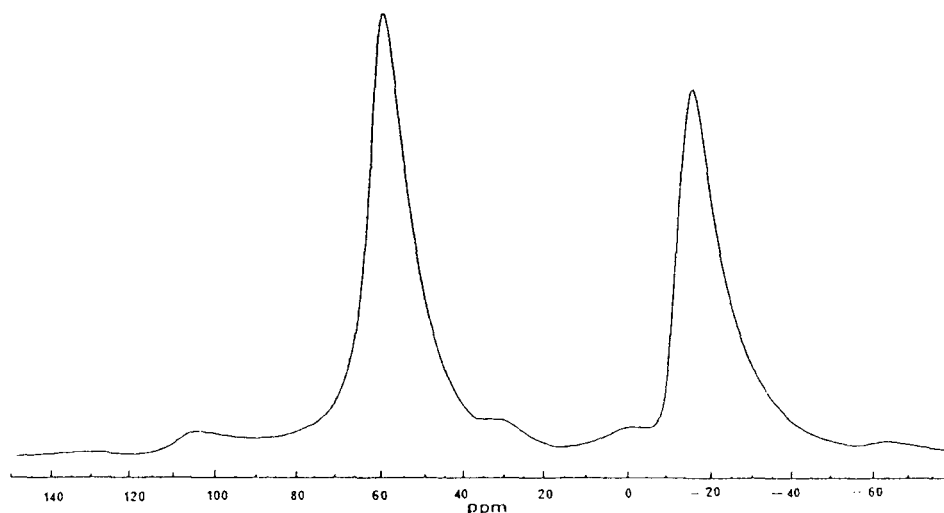
Figure 12. MAS-NMR ^{27}Al spectra of the heat-treated APP-4A mixture at 280°C.
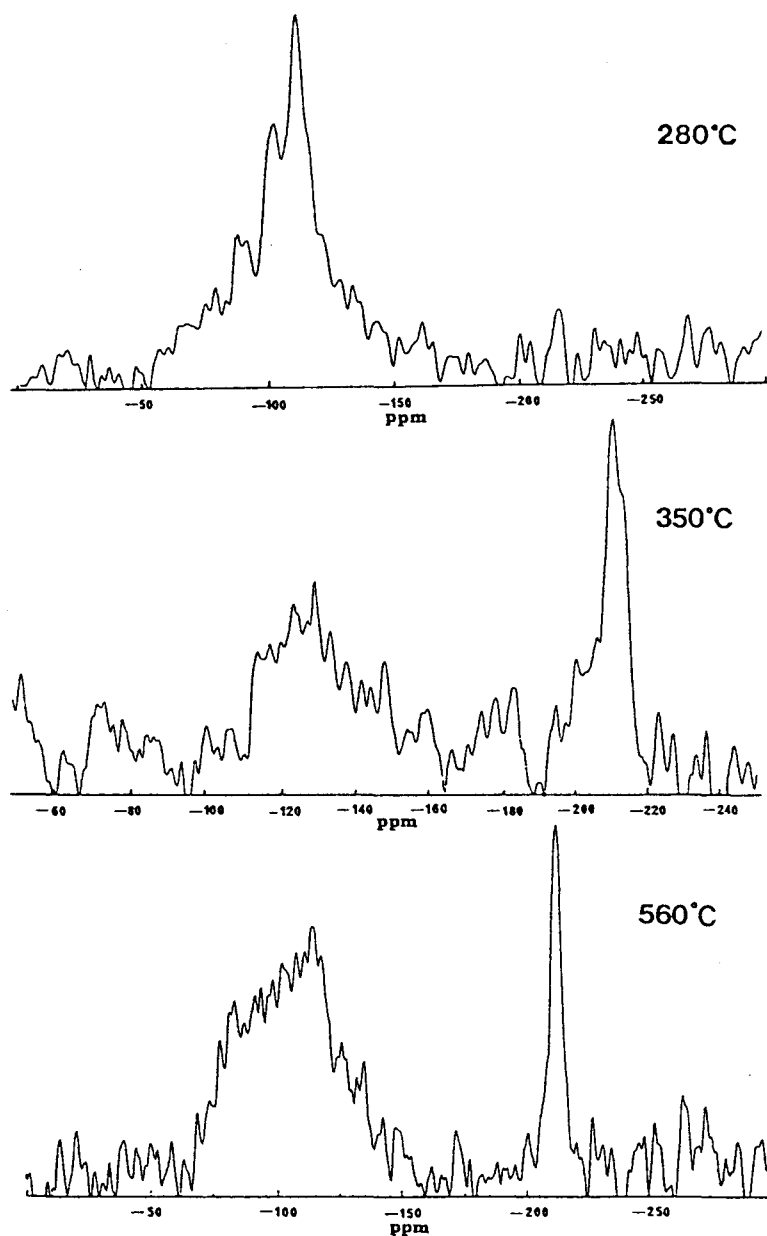
Figure 13. MAS-NMR ^{29}Si spectra of the heat-treated APP/PER-4A system.

Moreover, the study seems to show that a very high Si/Al ratio leads to a decrease in FR performance. It may be assumed that an increase in the additive level leads to a reduction in FR performance rather than the Si/Al ratio because ZSM-5 and 13X give similar LOI values but at slightly different concentrations despite a different Si/Al ratio (140 versus 1.23).

The zeolite acts to improve the development of the intumescent process and to stabilize the carbonaceous residue resulting in the degradation of the intumescent shield. The formation of aluminosilicophosphate species is proposed, which may be catalysts active for the synthesis of a protective 'carbon'.

154

REFERENCES

1. G. Camino, *Actes du 1er Colloque francophone sur l'Ignifu-gation des Polymères*, ed. by J. Martel, Saint-Denis (France) (1985) p. 36.
2. H. L. Vandersall, *J. Fire & Flamm.* **2**, 97 (1971).
3. R. Delobel, M. Le Bras, N. Ouassou and F. Alistiqsa, *J. Fire Sci.* **8**(2), 85 (1991).
4. S. Bourbigot, M. Le Bras and R. Delobel, *J. Fire Sci.* **13**(1-2), 3 (1995).
5. S. Bourbigot, M. Le Bras and R. Delobel, *Carbon* **31**(8), 1219 (1993).
6. S. Bourbigot, M. Le Bras, R. Delobel, P. Bréant and J. M. Trémillon, *Carbon* **33**(3), 283 (1995).
7. S. Bourbigot, PhD thesis, University of Lille (1993).
8. D. Scharf, R. Nalepa, R. Heflin and T. Wusu, *Fire Safety J.* **19**, 103 (1992).
9. A. P. Taylor and F. R. Sale, *Makromol. Chem., Macromol. Symp.* **74**, 85 (1993).
10. M. Le Bras and S. Bourbigot, *Fire and Materials* **20**, 39 (1996).
11. H. K. Beyer, G. Borbely, P. Miasnikov and P. Rozsa, *Zeolites as Catalysts, Sorbents and Detergent Builders*, ed. by H. G. Karge and J. Weitkamp, Elsevier, Amsterdam (1989), p. 635.
12. J. V. Smith, Origin and structure of zeolites, in *Zeolite Chemistry and Catalysis*, ed. by J. A. Rabo, Am. Chem. Soc. Monograph 171, Washington, DC (1976).
13. R. Lowenstein, *Am. Miner.* **39**, 92 (1954).
14. D. W. Breck, *Zeolites Molecular Sieves*, R. E. Krieger Pub., Malabar (Florida) (1974).
15. R. Van Mao, *Revue de l'IFP*, 35 (1984).
16. W. M. Maier, *Molecular Sieves*, Soc. Chem. Ind., London (1968).
17. Fr. 9307387 (1993) and EU. 94401316.8 (1994), Elf-Atochem SA., invs.: S. Bourbigot, P. Bréant, R. Delobel and M. Le Bras; Fr. 9307388 (1993) and EU. 94401317.8 (1994), Elf-Atochem SA., invs.: S. Bourbigot, P. Bréant, R. Delobel and P. Nathiez.
18. S. Bourbigot, M. Le Bras, P. Bréant, J. M. Trémillon and R. Delobel, in *Extended Abstr. of Eurofillers 95*, ed. by E. Papirer, Imp. Centrale (Mulhouse), Mulhouse (1995), pp. 445–49.
19. S. Bourbigot, M. Le Bras, R. Delobel, P. Bréant and J. M. Trémillon, in: *Fire Retardant Polymers — Fifth European Conference*, ed. by D. Price, Salford (1995); S. Bourbigot, M. Le Bras, R. Delobel, P. Bréant and J. M. Trémillon, *Polym. Deg. & Stab.*, in press (1996).
20. R. M. Barrer, *Zeolites Sciences and Technology*, M. Nijhoff, The Hague (1984).
21. V. B. Kagansky, *Structure and Reactivity of Modified Zeolites*, Elsevier, Amsterdam (1984).
22. D. Bartomeuf, in *Catalysis by Zeolites—Studies in Surface Science and Catalysis* (Volume 5), ed. by B. Imelik, C. Naccache, Y. Ben Taerit, J. C. Vedrine, G. Coudurier and H. Praliaud, Elsevier, Amsterdam, p. 55 (1980).
23. R. Beaumond and D. Bartomeuf, *J. Catal.* **27**, 45 (1972).
24. I. D. Micheikin, I. A. Abromin, G. M. Thidsmirou and V. B. Kezinsky, *Kinet. Katal.* **18**, 1580 (1977).
25. B. Umansky, *J. Catal.* **127**, 128 (1991).
26. S. E. Tong, *J. Catal.* **17**, 24 (1970).
27. G. Camino, L. Costa, L. Trossarelli, F. Costanzi and A. Pagliari, *Polym. Deg. & Stab.* **12**, 213 (1985).
28. G. Engelhart, U. Lohse, M. Mägi and E. Lippmaa, in *Structure and Reactivity of Modified Zeolites—Studies in Surface Science and Catalysis*, Vol. 18, ed. by P. A. Jacobs, N. I. Jaeger, P. Jiru, V. B. Kazansky and G. Schulz-Ekloff, Elsevier, Amsterdam (1984), p. 23.
29. M. Stöcker, in *Advanced Zeolite Science and Applications — Studies in Surface Science and Catalysis*, Vol. 85, ed. by J. C. Jansen, M. Stöcker, H. G. Karge and J. Weikamp, Elsevier, Amsterdam (1994), p. 427.
30. D. Müller, G. Berger, I. Grunze, G. Ladwig, E. Hallas and C. Haubenreisser, *Phys. Chem. Glasses* **24**(2), 37 (1983).
31. D. Müller, W. Gessner, H. S. Benrens and G. Sheler, *Chem. Phys. Lett.* **79**(1), 59, (1981).
32. D. Müller, D. Hoebbel and W. Gessner, *Chem. Phys. Lett.* **84**(1), 25 (1981).
33. R. Dupree and D. Holland, *Glasses and Glass-ceramics*, Chapman & Hall, London (1989).
34. T. L. Weeding, B. H. W. S. de Jong, W. S. Veeman and B. G. Aitken, *Nature* **318**, 352 (1985).
35. H. Makart, *Helv. Chim. Acta.* **50**, 399 (1967).
36. E. Tillmans, W. Gebert and W. H. J. Baur, *J. Solid. State Chem.* **7**, 65 (1973).
37. F. Leban, G. Bissert and N. Koppen, *Z. Anorg. Allg. Chem.* **359**, 131 (1968).

Synergistic effect of zeolite in an intumescence process: Study of the carbonaceous structures using solid-state NMR
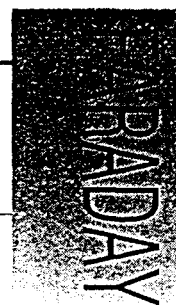
Serge Bourbigot,[a],* Michel Le Bras,[a] Rene Delobel,[a] Régis Decressain[b] and Jean-Paul Amoureux[b]

[a] Laboratoire de Physicochimie des Solides, E.N.S.C.L., Université des Sciences et Technologies de Lille, BP 108, F—59652 Villeneuve d'Ascq Cedex, France

[b] Laboratoire de Dynamique et Structure des Matériaux Moléculaires, URA—CNRS No. 801, Université des Sciences et Technologies de Lille, F—59650 Villeneuve d'Ascq, France

This work deals with the chemical effect of zeolite 4A added to the intumescent ammonium polyphosphate (APP)–pentaerythritol (PER) system [fire retardant (FR) polyethylene-based formulation]. The study of the thermal behaviour of the system using thermogravimetric (TG) analysis shows that the presence of the zeolite leads to an increase in the stability of the material at high temperature ($T > 500\,°C$). Chemical analysis and cross-polarisation dipolar-decoupled magic-angle spinning (CP–DD–MAS)^{13}C NMR reveals that the materials resulting from the thermal treatment of the APP–PER and APP–PER/4A systems are formed by carbonaceous and phosphocarbonaceous species and that the zeolite enhances the stability of the phosphocarbonaceous species. DD–MAS ^{31}P NMR indicates that this stability may be due to an absence of pyrophosphate species in the heat-treated APP–PER/4A system. Micro-Raman spectroscopy and ^{1}H NMR of the solid state provides information on the structure of the carbonaceous material. Thermal treatment led to the formation of a 'turbostatic carbon' with a local structure of this 'carbon species', with the zeolite permitting retention of the comparatively unorganised carbon species in the high-temperature range. Moreover, a low-resolution solid-state ^{1}H NMR study of the spin–lattice and spin–spin relaxations of the samples allows an evaluation of the size of the slow relaxation domains using the Goldman–Shen procedure. It is shown that the zeolite hinders the formation of small molecules in the polyaromatic network. Finally, the relationship between the formation of a coherent macromolecular network and the improved FR performance of the APP–PER/4A system is proposed.

Fire protection of flammable materials (in particular, paints, varnishes and cellulose-based materials) by an intumescence process has been known for several years.[1,2] Intumescent technology has more recently found a place in polymer science as a method of providing flame retardance to polymeric materials.[3,4] On heating, fire retardant intumescent materials form foamed cellular charred layers on their surface, which protects the underlying material from the action of the heat flux or flame. The proposed mechanism is based on the charred layer acting as a physical barrier, which slows down heat and mass transfer between the gas and the condensed phases (Fig. 1).

A mixture of an ammonium polyphosphate (APP) and pentaerythritol (PER) has been shown to be an efficient fire-retardant (FR) intumescent system for polyalkenic materials.[5,6] Previous studies[6,7] have proposed that the carbonisation leads to intumescence by means of a series of steps.

Moreover, we have demonstrated that dynamic properties of interest concerned with intumescent char can be explained in terms of the chemistry of the system (e.g. aromaticity, thermal polymerisation of aromatic molecules, aromatic molecules bridged by phosphate species).[8,9]

The APP–PER system provides good fire-proofing properties in FR polypropylene[5,6] and polyethylenic-based formulations.[10,11] A commercially available intumescent formulation often contains fillers, in addition to the active ingredients.[12–14] These fillers may act as synergistic agents in intumescent FR formulations.[12,14] Among the possible aluminosilicate fillers, Beyer et al.[15] have shown that the combination of zeolites and conventional heat-insulating materials ensures an enhancement of the protective effect.

We have investigated the intumescent FR APP–PER system in combination with zeolites,[11,16,17] in particular 4A zeolites, and have shown a high degree of improvement of the fire-proofing properties within different polymeric matrices[18] (Fig. 2).

The aim of this work is to study the chemical composition and the structural properties of the carbonaceous shield formed from the APP–PER and APP–PER/4A systems, in order to discuss the role which the zeolite plays in the formation and degradation of the intumescent shield. We hypothesize that this carbonaceous coating results only from the additives.

The materials were always examined in the solid state rather than via solvent extraction, as was the case in earlier studies which considered the APP–PER system.[5] Indeed, we consider that solvent extraction may modify the sample, e.g. the phosphate analysis of a carbonaceous structure may be affected by rapid hydrolysis when analysed in D_2O. Furthermore, it is impossible to render completely soluble an intumescent material which has a carbonaceous structure and therefore, any resulting analysis would not be representative of the material.
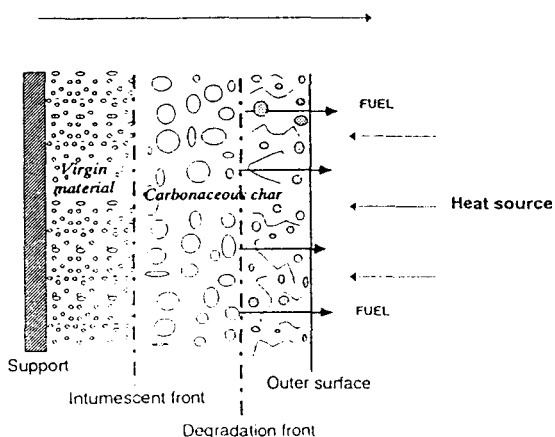

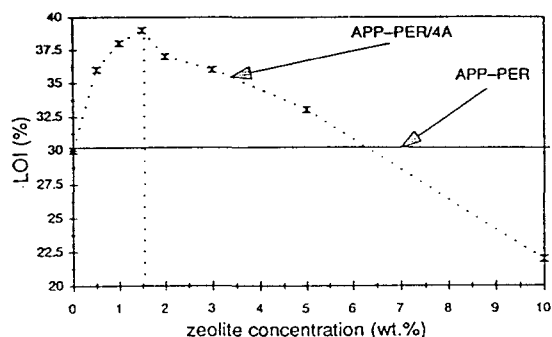Fig. 1 One-dimensional intumescence model

J. Chem. Soc., Faraday Trans., 1996, 92(1), 149–158   149

273

Fig. 2 Normalised fire testing values [limiting oxygen index (LOI)[19]] vs. zeolite concentration in a technical ethenic terpolymer (ethene–butylacrylate–maleic anhydride, Lotader P3200 from Elf-Atochem). The level of additives is kept at a constant 30 wt.% and the synergistic effect exhibits a maximum at the 1.5 wt.% zeolite 4A level.[16,17]

The thermal behaviour of the two systems was first studied by TG analysis to determine the temperature ranges which correspond to the development, stability and degradation of the intumescent materials. Materials resulting from each of these steps were characterised by chemical analysis, high-resolution ^{31}P and ^{13}C solid-state NMR and micro-Raman spectroscopies.

Additional structural information was obtained from low-resolution solid-state ^1H NMR. The shape of the free induction decay (FID) allows the measurement of the spin–spin relaxation times (T_2) after solid-echo sequences. Observation of the FID shows the presence of fast and slow components,[20] which may be assigned to rigid and amorphous domains, respectively.[11] On the basis of previous work by Cheung and Gerstein,[21] the domain-size measurement of the slow relaxation was then examined using, as a probe, the free precession of the protons present and the spin-diffusion phenomenon of the materials.

Experimental

Raw materials were zeolite 4A (Si/Al = 1, compensation cation: Na, as supplied by Ceca), PER (Aldrich, R.P. grade) and APP [$(NH_4PO_3)_n$, $n = 700$, Hoechst Exolit 422, soluble fraction in H_2O: <1 wt.%]. This study has been carried out using the APP–PER and APP–PER/4A mixtures for the ratios APP/PER = 3 (w/w) and (APP/PER)/4A = 19 (w/w), respectively. In the case of the polyethylenic materials, the fire-retardant properties are indeed a maximum for these ratios.[5,6,11,16,17] Initial mixtures were first prepared by ball-milling, after mechanical grinding and sifting (200 × 10^{-6} m) of the raw materials. They were then heat-treated, and characterised by four different highest temperatures of treatment ($T_{tr, max}$ = 280, 350, 430 and 560 °C, deduced from the TG analyses discussed in this text) during 12 h under an air flow (flow rate = 6 cm^3 s^{-1}).

The determination of the amounts of carbon and hydrogen was made by burning the sample in an excess of oxygen at 1050 °C. The quantity of the evolved CO_2 was then determined by coulometry and was proportional to the total quantity of carbon in the sample. The quantity of the evolved water condensed as liquid or ice at 0 ± 2 °C was determined by making a stoichiometric reaction between coal and water to form CO which was transformed to CO_2 on copper oxide at 1120 °C. The quantity of evolved CO_2 was then determined as above and was proportional to the total quantity of hydrogen in the sample.

The quantity of nitrogen was determined by burning the sample in He with 3% oxygen at 1050 °C. The evolved nitrogenated oxides were then reduced to molecular nitrogen, the

quantity of which was determined with a catharometer. The quantities of phosphorus, silicon, aluminium and sodium were determined by mineralisation in aqueous medium and the quantity of each element by plasma emission spectrometry.

TG analyses were carried out at a heating rate of 3 °C min^{-1} under synthetic air (flow rate = 5 × 10^{-7} m^3 s^{-1}; Air Liquide grade) using a Setaram MTB 10–8 microbalance. In each case, the mass of sample used was fixed at 15 mg. The precision in the temperature measurement was 1.5 °C over the whole temperature range.

High-resolution NMR spectroscopy of the solids was performed using a Brucker CXP100 weak-field spectrometer at a spinning speed of 3 kHz and using a Brucker probe head equipped with a 7 mm MAS assembly. The spectra were obtained with a simple 90° pulse acquisition programme with a pre-acquisition delay of 5 μs.

^{31}P NMR measurements were performed at 40.5 MHz using magic-angle spinning (MAS), with high-power ^1H dipolar decoupling (DD) and a repetition time of 2 s [the spin–lattice relaxation time (T_1) was always below 300 ms].[11] All spectra were acquired after 500 scans. H_3PO_4 in aqueous solution (85%) was used as reference.

^{13}C NMR measurements were performed at 25.2 MHz (2.35 T) with MAS, high-power ^1H decoupling and ^1H–^{13}C cross polarisation (CP). The Hartmann–Hahn matching condition was obtained by adjusting the power on the ^1H channel for a maximum ^{13}C FID signal of adamantane. All spectra were acquired with contact times of 1 ms (samples heat-treated at 280 and 350 °C) or 1.5 ms (samples heat-treated at 430 and 560 °C). It was shown that the intensities of the bands of the samples were maximised under these conditions. A repetition time of 10 s was used for all the samples because the spin–lattice relaxation time (T_1) remained below 2 s at all temperatures.[11] Typically, 10 000 scans were necessary to obtain spectra with a good signal to noise ratio. Tetramethylsilane was used as reference.

Raman microprobe examinations were performed with a Raman microspectrometer having a spectrographic dispersion and multichannel detection (Microdil 28-Dilor). An optical beam produced by a continuous-wave argon laser (laser beam wavelength, 514.5 μm; spectral slit width, 9 cm^{-1}) enters the microscope and is directed onto an objective lens that focuses it onto a 1 μm spot on the sample surface. To avoid sample heating, the power was kept below 4 mW.[9]

Electron paramagnetic resonance (EPR) spectra were recorded at 25 °C using a Varian 'E-line' spectrophotometer [$v = 9.5$ GHz (X-band); modulation 1 kHz; standard, 'Strong Pitch' Varian]. Every observed signal presents a near-Gaussian shape.[22] The concentrations of the paramagnetic species were computed using a trapeze method of integrating the signals (each point of the derivative curve is taken as the slope of the integral one).

Proton NMR studies were carried out using a Brucker CXP 100 spectrometer, operating at a proton frequency of 100.13 MHz and having a 7 mm solenoid probe. The method of inversion recovery [π–τ–$\pi/2$] was used to measure proton spin–lattice relaxation (T_1) times. The computation of T_2 was made using a solid-echo sequence [$(\pi/2)_x$–τ–$(\pi/2)_{-x}$].[23] Following the first 90° pulse, a second 90° pulse is applied to the system after an interval that is slightly longer than the dead time of the spectrometer (15 μs). This generates an echo which retains the shape of the free-induction decay (FID). We may consider that the FID lineshape after a solid-echo pulse is a reasonable approximation of the true FID.

In a heterogeneous material, it is possible to observe the effects of the spin diffusion with a Goldman–Shen pulse sequence [$(\pi/2)_x$–t_0–$(\pi/2)_{-x}$ – τ – $(\pi/2)_x$].[24] The magnetisation of each material shows a two-component free-induction decay with significantly different T_2. The fixed time, t_0, is chosen such that magnetisation M_z, which has a shorter

T_2, has decayed to zero while there is still sufficient magnetisation, M_1, remaining in the domain undergoing slow relaxation. Assuming that $t \ll T_1$, the recovery factor $R(t)$ may be formally written as:[21]

$$R(t) = \frac{M_2(t)}{M_2(t \to \infty)} \qquad (1)$$

The theoretical considerations of $R(t)$ have been previously presented by Cheung and Gerstein[21] and the principal conclusions of their work relevant to these studies are summarised here. From the spin-diffusion equation:

$$\frac{\partial m(r, t)}{\partial t} = D\nabla^2 m(r, t) \qquad (2)$$

where $m(r, t)$ is the local magnetisation density at site r and time t, and D the spin-diffusion coefficient[25] (which is assumed to be isotropic). With the appropriate initial conditions, the resolution of eqn. (2) and the development of Cheung and Gerstein lead to the following results, according to three different assumptions:

one-dimensional model:

$$\bar{b} = \bar{b}_x \ll \bar{b}_y \quad \text{and} \quad \bar{b}_z$$

$$R(t) = \frac{2}{\sqrt{\pi}} \left(\frac{Dt}{\overline{b^2}} \right)^{1/2} ; \qquad \text{if } t \ll \frac{\overline{b_2}}{D} \qquad (3)$$

$$R(t) = 1 - \frac{\overline{b_2}}{\pi D t} ; \qquad \text{if } t \gg \frac{\overline{b_2}}{D} \qquad (4)$$

two-dimensional model:

$$\bar{b} = \bar{b}_x = \bar{b}_y \ll \bar{b}_z$$

$$R(t) = \frac{4}{\sqrt{\pi}} \left(\frac{Dt}{\overline{b^2}} \right)^{1/2} ; \qquad \text{if } t \ll \frac{\overline{b^2}}{D} \qquad (5)$$

$$R(t) = 1 - \frac{\overline{b^2}}{\pi D t} ; \qquad \text{if } t \gg \frac{\overline{b^2}}{D} \qquad (6)$$

three-dimensional model:

$$\bar{b} = \bar{b}_x = \bar{b}_y = \bar{b}_z$$

$$R(t) = \frac{6}{\sqrt{\pi}} \left(\frac{Dt}{\overline{b^2}} \right)^{1/2} ; \qquad \text{if } t \ll \frac{\overline{b^2}}{D} \qquad (7)$$

$$R(t) = 1 - \left(\frac{\overline{b^2}}{\pi D t} \right)^{3/2} ; \qquad \text{if } t \gg \frac{\overline{b^2}}{D} \qquad (8)$$

where $\bar{b}$ is the mean width of the domain undergoing slow relaxation. The one-dimensional configuration is a good description for a layer-like domain in the statistical sense. In this statistical sense, we may also refer to the two-dimensional configuration as a rod-like domain shape and the three-dimensional model as a cubic or spherical domain shape.[21]

Results and Discussion

Chemical characterisation

TG analysis. The thermal behaviour of the APP–PER and APP–PER/4A systems was studied by TG analysis (Fig. 3). The APP–PER system presents an enhanced stability over the APP–PER/4A system up to 500 °C, over which it degrades rapidly (up to 600 °C) to form a stable residue (8 wt.%), whereas the APP–PER/4A system begins to degrade rapidly only from 550 °C and maintains a stable residue (30 wt.%) at temperatures beyond 600 °C. The zeolite leads, therefore, to the formation of a carbonaceous residue more stable at higher temperatures than is formed in the case of the APP–PER system. This may be explained either by the formation of a
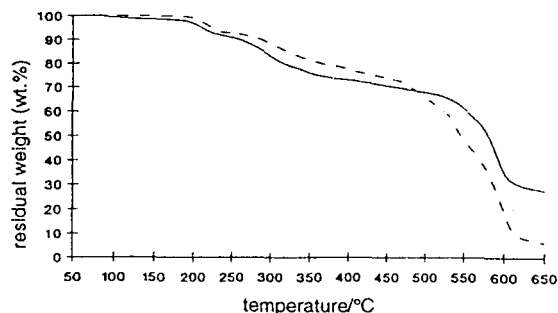

Fig. 3 TG curves of the APP–PER and APP–PER/4A systems

new carbonaceous species or by the formation of phosphorus compounds which are particularly stable at high temperatures.

APP and PER exhibit very different behaviours when separately thermally degraded.[6] Fig. 4 presents the curve of the weight difference computed on the basis of the difference between the experimental curve and the 'theoretical' curve (i.e. the curve calculated through a linear combination of the APP and PER weight losses). It demonstrates the strong interaction which is taking place between APP and PER to form an expanded carbonaceous shield.

The characteristic $T_{tr, max}$ chosen for the isothermal treatments are therefore 280 (corresponding to the formation of the intumescent material), 350 (the beginning of the degradation of the intumescent shield), 430 (the formation of a carbonaceous residue) and 560 °C (corresponding to the stable residue in the high-temperature range).

Chemical analysis. The composition of the materials obtained at different characteristic temperatures is given in Table 1.

The mechanism of intumescence which develops on heating the APP–PER mixture leads to the elimination of ammonia and water.[4,5] An assessment of the relative importance of the dehydration steps and the loss of ammonia is not possible since oxygen takes a part in the thermo-oxidative degradation of the intumescent carbonaceous material (any oxidised species may be created by reaction with oxygen of the air) and ammonia may react with carbonaceous species to form nitrogenated aromatic species. This last assumption has been previously verified by XPS[26] in the case of the APP–PER system and so needs to be verified only for the system with the zeolite.

Changes of the P/C ratios of the systems show that the zeolite stabilises the phosphorus and/or phosphocarbonaceous species. This stability may explain the thermal stability at the high temperature observed by TG of the APP–PER/4A system.
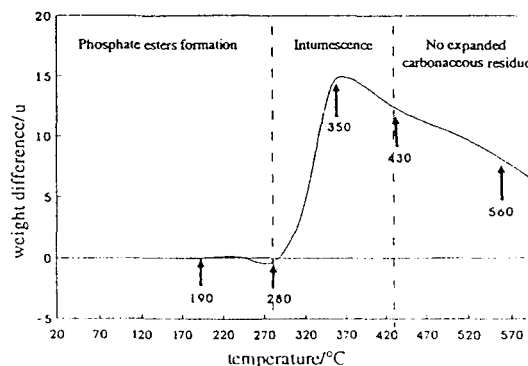

Fig. 4 Weight-difference curve of the APP–PER system

$T_{tr, max}/°C$	element/atom kg^{-1}							
	C	H	N	O	P	Si	Al	Na
APP–PER								
280	12	39	6	30	8	—	—	—
350	21	6	5	26	7	—	—	—
430	19	30	4	27	8	—	—	—
560	31	8	4	22	6	—	—	—
APP–PER/4A								
280	13	33	4	35	4	0.3	0.2	0.1
350	9	37	3	39	4	0.4	0.07	0.3
430	4	24	0.9	42	6	0.5	0.2	0.03
560	0.7	18	0.08	48	4	1.0	0.05	0.5

MAS–DD ^{31}P NMR. A previous study has shown that the APP–PER system forms a phosphocarbonaceous structure when the temperature is increased.[9,27] To examine and understand the role played by the zeolite in the development of the intumescent shield, ^{31}P NMR was found to be a powerful tool.

The spectrum of the pure APP (Fig. 5) shows a single band at about -22 ppm which may be assigned to the central groups of polyphosphates.[28,29] The terminal groups are not observed (band at about -10 ppm) owing to the length of the polyphosphate chains.

Comparison of the thermal behaviour of the systems (Fig. 6 and 7, Table 2) shows the disappearance of a band assigned to pyrophosphate groups above 430 °C (-7 ppm), of two bands assigned to pyrophosphate species and phosphorus oxides above 560 °C [-7 and $-(47–51)$ ppm, respectively] and the existence of polyphosphate chains at 350 °C (-23 ppm) in the case of the APP–PER/4A system. Moreover, the study shows the presence of phosphocarbonaceous structures in the systems at all temperatures studied.

These results lead to the assumption that the zeolite enhances the stability of the polyphosphate chain, hinders the stability of the pyrophosphate species and the formation of phosphorus oxides at high temperatures.

CP–MAS–DD ^{13}C NMR. The spectra are presented in Fig. 8 and 9 and their assignments shown in Table 3. Aliphatic carbons are observed only at 280 °C. At all temperatures, the spectra have a broad band between 100 and 160 ppm, implying several non-magnetically equivalent aromatic carbons in the materials.[30,31] As discussed previously,[9] this arises from the contribution of several aromatic and polyaromatic species.
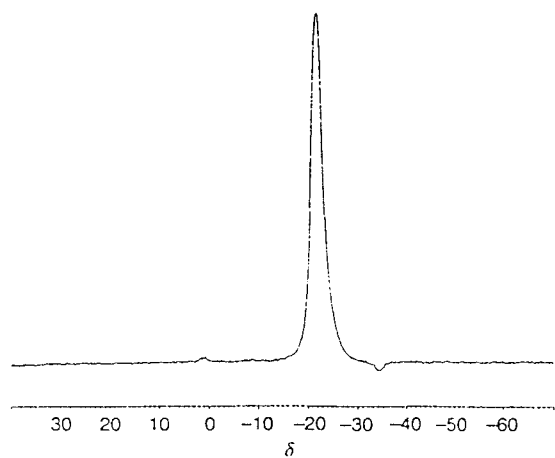
Note the disappearance of the broad band (assigned to aromatic species at 430 °C) for the system with the zeolite. This may be explained by the fact that aromatic carbons near free radicals 'trapped' in the structure of the material may escape detection. Indeed, the works of Ganapathy and Bryan[34] have shown that the reduction in the resolution of the ^{13}C signal was directly related to the anisotropy of the paramagnetic susceptibility of the aromatic compounds. This situation is strongly affected in the case of paramagnetic materials where the anisotropy of the magnetic susceptibility is large. An EPR study (the signal is assigned to free radicals 'trapped' in a polyaromatic structure[35]) confirms this assumption (Table 4). It is observed that the ratio of free radical carbons to the total number of carbon atoms is a maximum in the case of the intumescent shield obtained at 430 °C from the APP–PER/4A system. It shows, moreover, that the zeolite affects the carbonisation reactions of the APP–PER system differently, and leads to a more paramagnetic material with more stable radical species.

Micro-Raman spectroscopy. Micro-Raman spectroscopy complements the solid-state NMR used to characterise the carbonaceous species. Fig. 10 and 11 show the diffusion

30 20 10 0 −10 −20 −30 −40 −50 −60

δ

Fig. 5 MAS–DD ^{31}P NMR spectra of APP

280 °C
(x 6)

350 °C
(x 4)

430 °C
(x 1)

560 °C
(x 1)

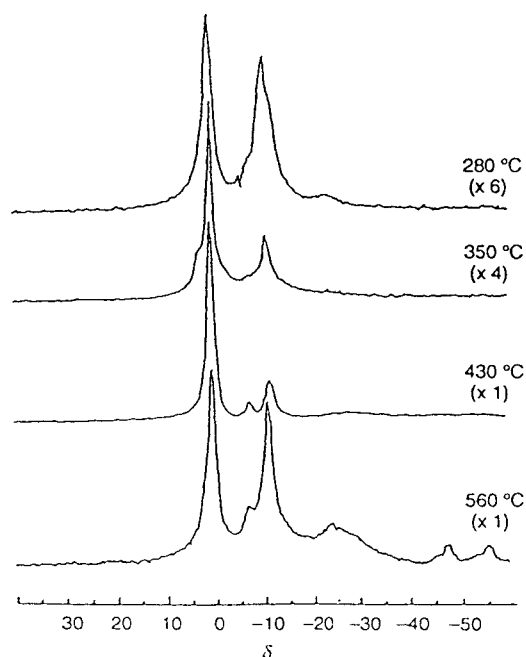30 20 10 0 −10 −20 −30 −40 −50

δ

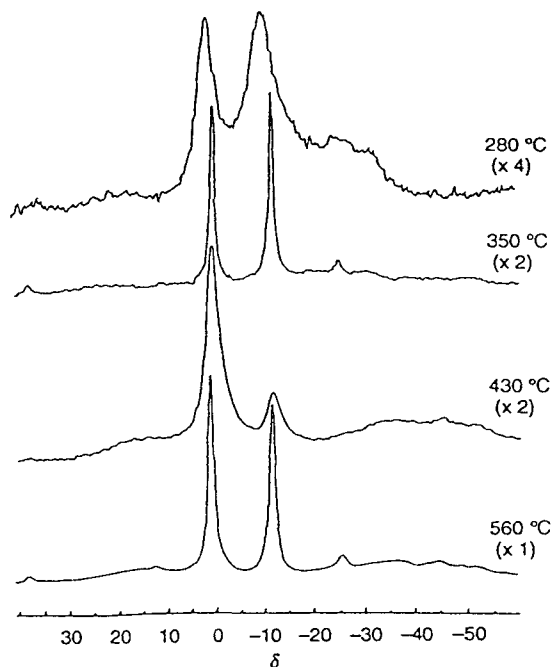Fig. 6 MAS–DD ^{31}P NMR spectra of the APP–PER system at the $T_{tr, max}$ indicated

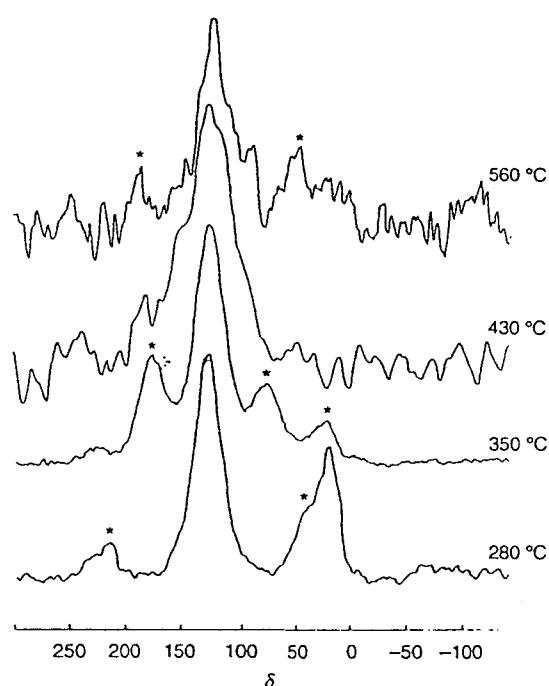Fig. 7 MAS-DD ^{31}P NMR spectra of the APP-PER/4A system at the $T_{tr, max}$ indicated

Fig. 8 CP-MAS-DD ^{13}C NMR spectra of the APP-PER system at the $T_{tr, max}$ indicated

spectra of the heat-treated samples. A continuous background signal arising from fluorescence emission is observed only for the system containing the zeolite at 280 °C, whereas in all other cases the spectra always exhibit two broad bands around 1580 and 1350 cm^{-1}. The first band may be assigned to the E_{2g} vibrational mode (C—C vibrations). The band at 1350 cm^{-1}, the so-called defect band,[36] is assigned to the A_{1g} vibrational mode, and may be related to the structural organisation of the carbonaceous matter (in particular, its shape and size of domain which present organisation of carbon in parallel layers).[37]

The spectra of the APP-PER systems (Fig. 10) show no significant evolution in the intensity and shape of the band at *ca.* 1350 cm^{-1} between 350 and 560 °C. An improved resolution of this band between 280 and 350 °C is observed. On the other hand, the evolution of this band for the APP-PER/4A system becomes significant between 350 and 560 °C, its resolution increases with increasing temperature. These changes, characteristic of the formation of the carbonaceous matter,[37,38] may be explained by an increase in the size of the domain, formed by stacks of polyaromatic species. In both cases, there is, therefore, formation of a 'turbostratic

Table 2 Assignments of the DD-MAS ^{31}P NMR spectra of the APP-PER and APP-PER/4A systems *vs.* $T_{tr, max}$.[9,28,29]

system	$T_{tr, max}/°C$	δ	assignment
APP-PER	280	−0.5	PO$_4$ in R$_2$HPO$_4$, RH$_2$PO$_4$ and/or H$_3$PO$_4$
		−10.5	PO$_4$ in Φ_2RPO$_4$ and/or Φ_2HPO$_4$ and/or polyphosphate chain (terminal group)
		−22	polyphosphate chain (central group)
	350	−0.5	PO$_4$ in R$_2$HPO$_4$, RH$_2$PO$_4$ and/or H$_3$PO$_4$
		−10.5	PO$_4$ in Φ_2RPO$_4$ and/or Φ_2HPO$_4$
	430	0.8	PO$_4$ in R$_2$HPO$_4$, RH$_2$PO$_4$ and/or H$_3$PO$_4$
		−7	pyrophosphate group
		−10.5	PO$_4$ in Φ_2RPO$_4$ and/or Φ_2HPO$_4$
	560	−0.5	PO$_4$ in R$_2$HPO$_4$, RH$_2$PO$_4$ and/or H$_3$PO$_4$
		−7	pyrophosphate group
		−10.5	PO$_4$ in Φ_2RPO$_4$ and/or Φ_2HPO$_4$ and/or polyphosphate chain (terminal group)
		−24	polyphosphate chain (central group)
		−47/−51	phosphorus oxides (P$_4$O$_{10}$ type)
APP-PER/4A	280	−0.5	PO$_4$ in R$_2$HPO$_4$, RH$_2$PO$_4$ and/or H$_3$PO$_4$
		−10.5	PO$_4$ in Φ_2RPO$_4$ and/or Φ_2HPO$_4$ and/or polyphosphate chain (terminal group)
		−23	polyphosphate chain (central group)
	350	−0.5	PO$_4$ in R$_2$HPO$_4$, RH$_2$PO$_4$ and/or H$_3$PO$_4$
		−10.5	PO$_4$ in Φ_2RPO$_4$ and/or Φ_2HPO$_4$ and/or polyphosphate chain (terminal group)
		−24	polyphosphate chain (central group)
	430	−0.5	PO$_4$ in R$_2$HPO$_4$, RH$_2$PO$_4$ and/or H$_3$PO$_4$
		−10.5	PO$_4$ in Φ_2RPO$_4$ and/or Φ_2HPO$_4$
	560	−0.5	PO$_4$ in R$_2$HPO$_4$, RH$_2$PO$_4$ and/or H$_3$PO$_4$
		−10.5	PO$_4$ in Φ_2RPO$_4$ and/or Φ_2HPO$_4$ and/or polyphosphate chain (terminal group)
		−25	polyphosphate chain (central group)

R = alkyl groups and Φ = aromatic or polyaromatic groups.

Table 3 Assignments of the CP and DD-MAS ^{13}C NMR spectra of the APP–PER and APP–PER/4A systems at different $T_{tr.\,max}$

system	$T_{tr.\,max}/°C$	δ	assignment	ref.
APP–PER	280	20	C_{CH2b}	30, 31
		129	C_{ar-H}, C_{ar-C}, C_{ar-O}, C_{ar-N}	30, 32, 33
		(broad band: 110–160)		
	350	129	C_{ar-H}, C_{ar-C}, C_{ar-O}, C_{ar-N}	30, 32, 33
		(broad band: 100–160)		
	430	124	C_{ar-H}, C_{ar-C}, C_{ar-O}, C_{ar-N}	30, 32, 33
		(broad band: 80–180)		
	560	119	C_{ar-H}, C_{ar-C}, C_{ar-O}, C_{ar-N}	30, 32, 33
		(broad band: 90–170)		
APP–PER/4A	280	18	C_{CH2b}	30
		139	C_{ar-H}, C_{ar-C}, C_{ar-O}, C_{ar-N}	30, 32, 33
		(broad band: 100–160)		
	350	128	C_{ar-H}, C_{ar-C}, C_{ar-O}, C_{ar-N}	30, 32, 33
		(broad band: 100–160)		
	430	110–130	C_{ar-H}, C_{ar-C}, C_{ar-O}, C_{ar-N}	30, 32, 33
		(very weak)		
	560	125	C_{ar-H}, C_{ar-C}, C_{ar-O}, C_{ar-N}	30, 32, 33
		(broad band: 120–150)		

C_{CH2b}, branched alkyl carbon; C_{ar-H}, protonated aromatic carbons; C_{ar-C}, non-protonated aromatic carbons; C_{ar-O}, oxygenated aromatic carbons; C_{ar-N}, nitrogenated aromatic carbons and/or nitrogenated carbons with conjugated bondings in heterocycles.
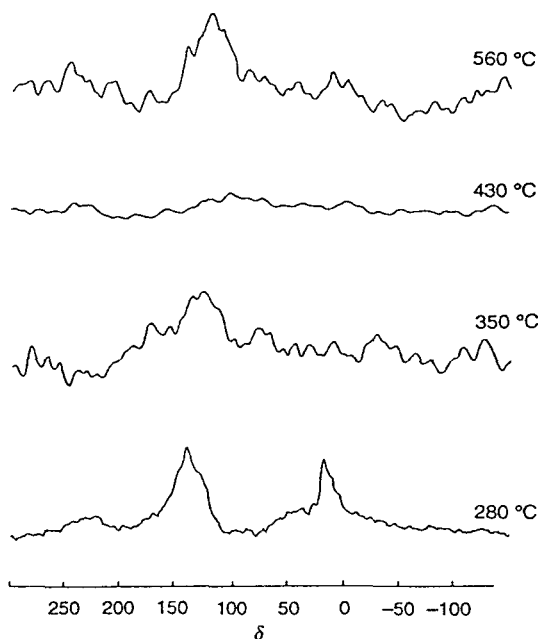
Fig. 9 CP-MAS-DD ^{13}C NMR spectra of the APP–PER/4A system at the $T_{tr.\,max}$ indicated

Table 4 Fraction of radical carbon atoms contained in the intumescent shields at different $T_{tr.\,max}$

system	$T_{tr.\,max}/°C$	$C^{\cdot}/C_{tot}$ [a]
APP–PER	280	1/7000
	350	1/6000
	430	1/7000
	560	1/5000
APP–PER/4A	280	1/4000
	350	1/3000
	430	1/1000
	560	1/5000

[a] Ratio of the radical carbons ($C^{\cdot}$) to the total numbers of carbons (C_{tot}).

carbon'[36] that is to say, a local structure of carbon species which is arranged in polyaromatic layers and which increases in size when the temperature increases.

Structural characterisation

The previously proposed correlation between the FR performances and the structural properties[9,39] prompts us to examine the structural characteristics of the intumescent materials. We have shown above that both systems form carbonaceous coatings which are strongly anisotropic materials

Fig. 10 Raman spectra of the APP–PER system at the $T_{tr.\,max}$ indicated

278

Fig. 11 Raman spectra of the APP–PER/4A system at the $T_{tr,\,max}$ indicated

(spectra labeled: 280 °C, 350 °C, 430 °C, 560 °C; wavenumber/cm^{-1} axes at 1600 1400 1200 and 1600 1400 1200 1000 800)

Fig. 12 T_1 values of the APP–PER and APP–PER/4A systems vs. $T_{tr,\,max}$

and which should, therefore, contain regions of differing mobility. A study of the molecular dynamics by low-resolution solid-state ^{1}H NMR may provide information on the heterogeneities within our materials.

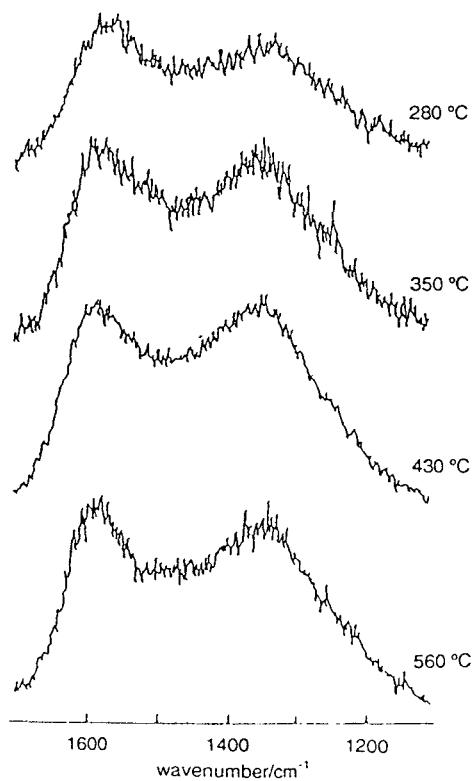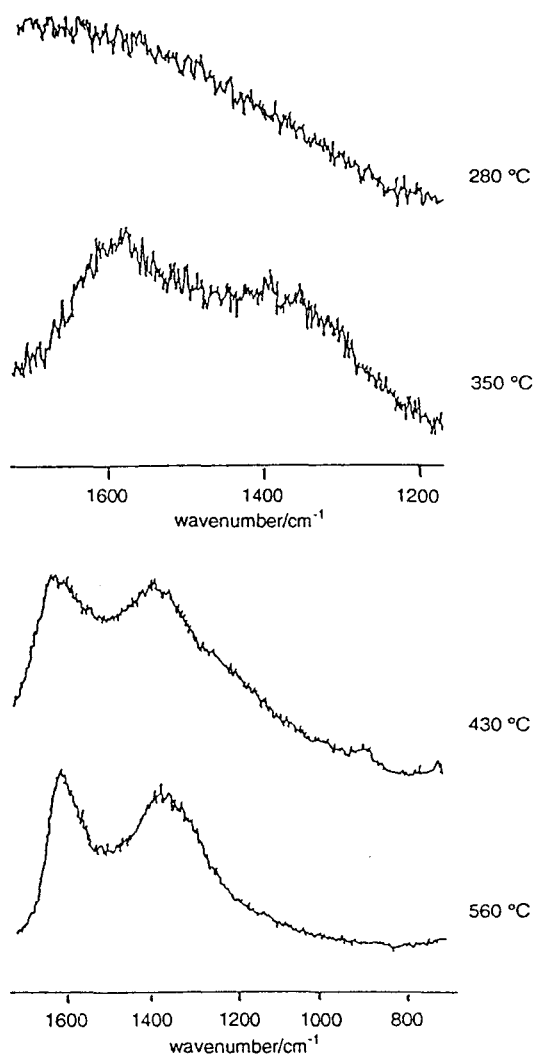**Spin–lattice relaxation.** Fig. 12 compares the T_1 values obtained after inversion-recovery sequences. Note that only one T_1 is observed at every $T_{tr,\,max}$ and it can therefore be expected that the size of the domain undergoing slow relaxation will be less than 10 nm.[25,40–42]
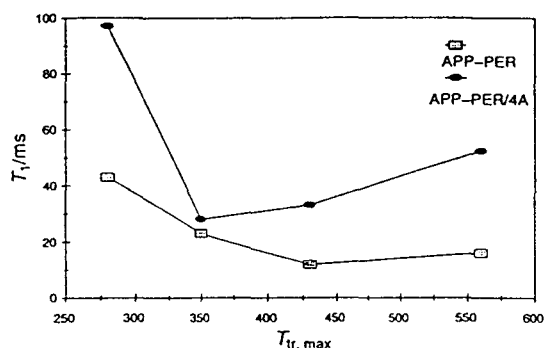
Comparison of the T_1 values of the two systems (Fig. 12) shows that their behaviour vs. $T_{tr,\,max}$ are different. At 280 °C, the T_1 value of the system with the zeolite is twice as large as that for the APP–PER system. It may be concluded that the materials formed at this temperature are structurally different. Indeed, a smaller T_1 means that molecular motions may be hindered and therefore that the structure may be more rigid. This hypothesis is confirmed by Raman spectroscopy, which has shown the formation of a structured carbon species in the case of the system without zeolite in the carbonaceous material and not in the case of the system containing zeolite.

Between 280 and 350 °C, the T_1 values decrease and become identical. As shown above by Raman spectroscopy, at 350 °C both systems are organised in stacks of polyaromatic species and it may be proposed that the two materials are structurally similar in an NMR sense. At higher temperatures, the T_1 values of the systems containing zeolite are always larger. It may be proposed that the structures of the two intumescent materials develop in different ways. The zeolite allows molecular motions and so the carbonaceous shields keep 'mobile' structures.

Spin–spin relaxation. The free precessions of the two systems have been recorded vs. $T_{tr,\,max}$ after the spin-echo sequence. In each case, they present complex shapes (superposition of several monoexponential decays). To a first approximation, we can distinguish two decays: one fast, up to approximately 50 μs, and the other slower (Table 5).

The fast decaying component is assumed to be Lorentzian and the slow decaying component is described by an intermediary shape between Lorentzian and Gaussian, represented by Weibullian functions. These latter functions have been proposed (initially by Kaufman and Bunger[43]) to be a better approximation of the FID than that obtained with a single mono-exponential relaxation. The transverse magnetisation $M(t)$ may therefore be written:

$$M(t) = M_{0c}\exp(-t/T_{2c}) + M_{0l}\exp\left(-t/T_{2l}\right)^\alpha \qquad (9)$$

Table 5 T_2 and values of amplitudes measured after solid-echo sequences (F: Fisher statistic, r: correlation coefficient)

system	$T_{tr,\,max}/°C$	parameter					fit statistic	
		$T_{2c}/\mu s$	$T_{2l}/\mu s$	M_{0c} (%)	M_{0l} (%)	α	r^2	F
APP–PER	280	19	364	82	19	1	0.991	5000
	350	17	270	82	18	1	0.993	4400
	430	20	296	41	62	2	0.996	66000
	560	20	400	78	23	1	0.992	2200
APP–PER/4A	280	16	330	51	49	1.7	0.998	13000
	350	14	335	46	54	1.8	0.997	12000
	430	15	297	34	68	2.4	0.999	98000
	560	14	330	11	91	2.1	0.999	18500

279

where t is the time, M_{0c} and M_{0l} are, respectively, the amplitudes of the fast and slow decaying components, T_{2c} and T_{2l} are, respectively, the spin–spin relaxation times of the fast and slow decaying components and α is the Weibullian coefficient ($1 < \alpha < 2$).

Two T_2 values are observed for each sample (Table 5) and the presence of two phases in the intumescent structure is thus demonstrated. On the basis of our above chemical characterisation, we may assign the fast decaying component to a macromolecular network consisting of stacks of polyaromatic species. The Lorentzian shape of the FID confirms this assumption, as previously discussed by Derbyshire et al.[44] in the case of coals. The slowly decaying component may be assigned to fast molecular motions of the protons in small free molecules not belonging to the molecular network, such as acidic phosphates and/or aromatic species.

It is worth noting that the Weibullian coefficient, α, is abnormally high in the case of the APP–PER/4A system heat-treated at $430\,^\circ\text{C}$. α is in this case higher than 2 although it is necessary for it to be in the range $1 \leqslant \alpha \leqslant 2$ in order to fit an FID.[43] As pointed out in our ^{13}C NMR and EPR analyses, this materials is strongly paramagnetic. Furthermore, it has been shown by Lynch et al.[45] in the case of coals having stable free radicals, that these radicals created dipolar interactions between the protons and the free electrons which distorted the FID signals. Therefore, it is proposed that the high α value is due to an FID distortion created by dipolar interactions between the protons and the free electrons of the polyaromatic carbons.

The computed T_{2c} for both systems are very close and there are no significant variations with $T_{\text{ir, max}}$. The T_{2l} values seem to vary with the temperature but we believe that it is due to the inhomogeneity of the applied radiofrequency field, which may create a signal distortion rather than a real variation.[46,47]

To conclude, the FID study of the carbonaceous materials has suggested two distinct structural phases in the intumescent shields and has confirmed the radical character of the intumescent shields containing the zeolite.

Size of the slow-relaxation domains. Experiments using the Goldman–Shen pulse sequence are carried out in order to obtain the size of the slow-relaxation domains. The interval, t_0, between the first pulses is selected such that $T_{2c} < t_0 < T_{2l}$. The times τ are always much shorter than T_1 and thus the assumption not to consider the spin–lattice relaxation term in the spin-diffusion equation [eqn. (2)] is verified.

Determination of the mean width, $\bar{b}$, of the domains undergoing slow relaxation requires a knowledge of the spin-diffusion coefficient, D. The value of this coefficient, assuming that the spin-diffusion mechanism is due to the dipolar interactions and considering that our systems have no perfect lattice, may be computed by eqn. (10):[48]

$$D \approx 0.13 \frac{\bar{a}^2}{T_{2c}} \qquad (10)$$

where $\bar{a}^2$ is the average of the square of distances between adjacent protons in the domain undergoing fast decay.[21] By considering the average of the square of the distances between two methylene protons on the same carbon and between two methylene protons on adjacent carbons in eclipse conformations, we assign $\bar{a}^2 \approx 0.0466 \text{ nm}^2$.

Eqn. (10) assumes that the mechanism of the spin diffusion is due to dipolar interactions. However, the magnetisation transfers are too fast for this mechanism. Indeed, the spin–spin relaxation time of the fast decaying component is too long ($300–400$ μs). We may therefore assume that the magnetisation recovery via spin diffusion is slow. If this is not the case, $R(t)$ becomes constant at approximately $\tau = 40$ μs and a spin-diffusion mechanism has to be considered rather than dipolar interactions. In the case of coals, which are a carbonaceous structure close to our materials, it has been proposed that the magnetisation transfer may be governed by a translational diffusion mechanism.[21]

The D value is one order of magnitude higher. Using this assumption, and knowing $\bar{a}^2$, we may estimate the $\bar{b}$ values of our materials (Table 6).

The one-dimensional model is a description for the layer-like domain in the statistical sense. From our Raman spectroscopy study, this model is not to be considered because the materials are not in a pre-graphitic state and are not in an arrangement with the polyaromatic species in parallel layers. This assumption is confirmed by measurements of spin–lattice relaxation times in the rotating frame $[T_{1\rho}(^1\text{H})]$ at $350\,^\circ\text{C}$ which have been found for the two components.[11] This result implies that the size of the slow relaxation is between 1 and 10 nm.[25,40–42]

The two- and three-dimensional models describe, respectively, in the statistical sense rod-like domain shapes and cubic or spherical domain shapes. The three-dimensional model is preferred because, considering our chemical characterisation, in disordered polyaromatic stacks containing the mobile phase, the spin diffusion takes place in three dimensions rather than in two. It is therefore demonstrated that the sizes of the amorphous domains of the materials containing the zeolite are always smaller than those without zeolite.

General discussion

The evolution of the carbonaceous coatings obtained from intumescent mixtures by isothermal treatment shows clearly the part played by the zeolite in the determination of the structures. The two systems develop a phosphocarbonaceous structure which is thermally stabilised by the presence of zeolite. In previous work,[11,16] it has been shown that the zeolite reacted with APP to form alumino- and silico-phosphates which may catalyse the synthesis of a protective carbon species by forming an 'alumino-silico-phospho-carbonaceous' thermally stable structure.

The intumescent materials containing the zeolite are strongly paramagnetic, particularly at $430\,^\circ\text{C}$, compared with the materials without zeolite (Fig. 13). This aspect seems very

Table 6   Estimation of the size of the slow relaxation domains of the systems vs. $T_{\text{ir, max}}$

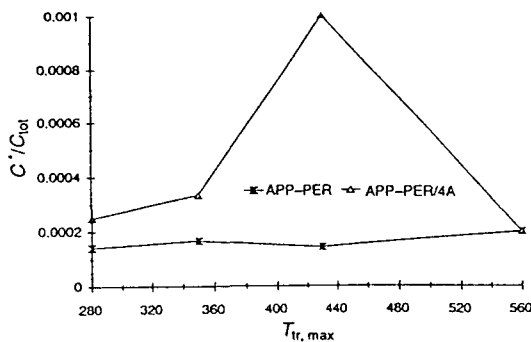| system	$T_{\text{ir, max}}/^\circ\text{C}$	$D/10^{-20} \text{ m}^2 \text{ ms}^{-1}$	$\bar{b}_{3D}/\text{nm}$	$\bar{b}_{2D}/\text{nm}$	$\bar{b}_{1D}/\text{nm}$
APP–PER	280	1.5	3.1(± 0.2)	2.1(± 0.2)	1.1(± 0.1)
	350	1.7	5.0(± 0.3)	3.4(± 0.2)	1.7(± 0.1)
	430	1.4	5.0(± 0.3)	3.4(± 0.2)	1.7(± 0.1)
APP–PER/4A	280	1.7	2.8(± 0.2)	1.9(± 0.2)	0.9(± 0.1)
	350	2.1	2.8(± 0.2)	1.9(± 0.2)	0.9(± 0.1)
	430	1.9	3.2(± 0.2)	2.1(± 0.2)	1.1(± 0.1)
	560	2.1	1.3(± 0.1)	0.8(± 0.1)	0.4(± 0.05)

Fig. 13 C°/C_{tot} [ratio of the radical carbons (C°) to the total number of carbons (C_{tot})] vs. $T_{tr, max}$

interesting because it suggests that if the intumescent shields become paramagnetic on treatment with a flame, the free radical formed in the structure may react with the degradation gases evolved and/or the radical species arising from the scission of the polymer chains (thermolysis of the polymer) and so, may, *via* radical reactions, trap polymer links into the carbonaceous structure.

The formation of the structure of the APP–PER/4A system is slower than that of the APP–PER system and is observed when the temperature increases. These results agree with previous work by us which has shown that the loss of the protective shield's efficiency was related to too large a degree of structure of the material (*i.e.* the development of a polyaromatic network in parallel layers).[8,27,36] It may thus be proposed that the zeolite has a controlling influence, permitting the retention of a 'poorly organised carbon species' to temperatures higher than those of the system without zeolite and, that this specific carbonisation is responsible for the FR performances of the intumescent material.

Moreover, the variations of the size of the domains undergoing slow relaxation *vs.* temperature (Fig. 14) suggest that the zeolite inhibits the increase of the size of the mobile phase and thus it allows the formation of a more coherent structure than is the case for the APP–PER system. It is also noted that the size increases with temperature up to 430 °C in the case of the system without zeolite, whereas the size remains constant in the case of the system containing the zeolite. It may be concluded that the zeolite orientates the structural properties of the material differently.

This study shows, therefore, that the zeolite acts on the chemical compositions and the structural properties of the intumescent shields in order to provide the properties of interest. We may propose that the formulation of a coherent phosphocarbonaceous macromolecular network stabilised by organic aluminosilicophosphate complexes and a small degree
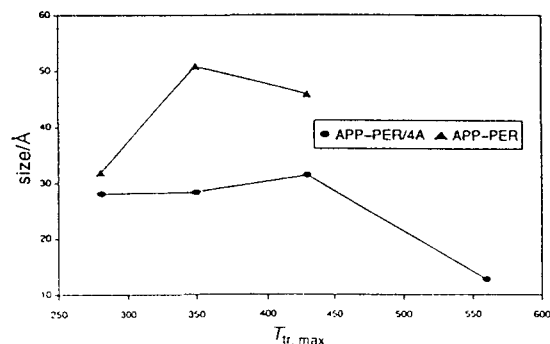

Fig. 14 Size of the slow relaxation domains of the intumescent systems vs. $T_{tr, max}$

of structure of the carbonaceous matter appear essential in order to provide the desired fire-proofing properties. Indeed the lack of cohesion and the too large a degree of structure in an intumescent coating provide a material which may not accommodate the stresses due to the temperature increase and so enhance the propagation of cracks in preferential directions in the structure. As a consequence, it may be proposed that the loss of the protective character is related to changes of the dynamic properties of the intumescent material.

Conclusion

In this work we have characterised chemically and structurally the carbonaceous materials arising from intumescence. These materials are formed by polyaromatic stacks and contain phosphocarbonaceous species. Furthermore, the presence of a zeolite in the formulation permits the existence of the phosphocarbonaceous species in the high-temperature range. We have shown that the addition of only 1% zeolite in an intumescent formulation leads to intumescent shields which exhibit large differences in the structure when compared with the shield arising from the system without zeolite. These differences may explain the improvement of fire-proofing properties in polymeric materials.

References

1 H. L. Tramm, *US Pat.*, 2, 106 938, 1938.
2 H. L. Vandersall, *J. Fire Flammability*, 1971, 2, 97.
3 G. Montaudo, E. Scamporino and D. Vitalini, *J. Polym. Sci., Polym. Chem.*, 1983, 21, 3361.
4 G. Camino, *Actes du 1er Colloque Francophone sur l'Ignifugation des Polymères*, ed. J. Martel, Saint-Denis, France, 1985, p. 36.
5 G. Camino, L. Costa and L. Trossarelli, *Polym. Degrad. Stab.*, 1985, 12, 213.
6 R. Delobel, M. Le Bras, N. Ouassou and F. Alistiqsa, *J. Fire Sci.*, 1990, 8, 85.
7 S. Bourbigot, M. Le Bras and R. Delobel, *J. Fire Sci.*, 1995, 13, 3.
8 R. Delobel, S. Bourbigot, M. Le Bras and J. M. Leroy, *Flame Retardancy of Polymeric Materials*, ed. V. Z. Janovic, Society of Plastic and Rubber Eng., Zagreb, 1990, p. 8/1.
9 S. Bourbigot, M. Le Bras and R. Delobel, *Carbon*, 1993, 31, 1219.
10 Y. Schmidt-Le Tallec, PhD Thesis, University of Lille, 1992.
11 S. Bourbigot, PhD Thesis, University of Lille, 1993.
12 D. Scharf, R. Nalepa, R. Heflin and T. Wusu, *Fire Saf. J.*, 1992, 19, 103.
13 A. P. Taylor and F. R. Sale, *Makromol. Chem., Macromol. Symp.*, 1993, 74, 85.
14 M. Le Bras and S. Bourbigot, *Fire and Materials*, submitted.
15 H. K. Beyer, G. Borbely, P. Miasnikov and P. Rozsa, *Zeolites as Catalysts, Sorbents and Detergent Builders*, ed. H. G. Karge and J. Weitkamp, Elsevier, Amsterdam, 1989, p. 635.
16 S. Bourbigot, M. Le Bras, R. Delobel, P. Bréant and J. M. Trémillon, in *Actes d'Eurofillers95*, Mulhouse, 1995; S. Bourbigot, M. Le Bras, R. Delobel, P. Bréant and J. M. Trémillon, *Macromol. Phys. Chem.*, 1995, submitted.
17 S. Bourbigot, P. Bréant, R. Delobel and M. Le Bras, *Fr. Demande*, 93 07387, 1993 and *EU Pat.*, 94 401 316.8, 1994 (Elf Atochem).
18 S. Bourbigot, M. Le Bras, R. Delobel, P. Bréant and J. M. Trémillon, *Polym. Degrad. Stab.*, 1995, submitted.
19 *Standard Test Method for Measuring the Minimum Oxygen Concentration to Support Candle-like Combustion of Plastics*, ASTM D2863/77, American Society for Testing Materials, Philadelphia, 1977.
20 D. W. McCall, D. C. Douglass and D. R. Falcone, *J. Phys. Chem.*, 1967, 71, 998.

281

21 T. T. P. Cheung and B. C. Gerstein, *J. Appl. Phys.*, 1981, 52, 5517.
22 M. Le Bras, R. Delobel, R. Descressain and J. M. Leroy, *Bull. Soc. Chim. Belg.*, 1989, 98, 735.
23 J. G. Powels and J. H. Strange, *Proc. Phys. Soc.*, 1963, 82, 6.
24 M. Golman and L. Shen, *Phys. Rev.*, 1966, 144, 321.
25 N. Bloembergen, *Physica*, 1949, 15, 386.
26 S. Bourbigot, M. Le Bras, L. Gengembre and R. Delobel, *Appl. Surf. Sci.*, 1994, 81, 299.
27 R. Delobel, M. Le Bras, Y. Schmidt and S. Bourbigot, *Actes du Moffis 91*, ed. J. C. Brosse, Groupement Français des Polymères (GFP), Le Mans, 1991, pp. 79–85.
28 J. R. Van Wazer, C. F. Callis, J. N. Shoolery and R. C. Jones, *J. Am. Chem. Soc.*, 1956, 78, 5715.
29 T. M. Duncan and D. C. Douglass, *J. Chem. Phys.*, 1984, 87, 339.
30 A. Grint, G. P. Proud, I. J. F. Poplett, K. D. Bartle, S. Wallace and R. S. Matthews, *Fuel*, 1989, 68, 1490.
31 G. E. Maciel, V. J. Bartuska and F. P. Miknis, *Fuel*, 1979, 58, 391.
32 W. L. Earl and D. L. Vanderhart, *J. Magn. Reson.*, 48, 35.
33 S. Supaluknari, I. Burgar and F. P. Larkins, *Org. Geochim.*, 1990, 15, 509.
34 S. Ganapathy and R. G. Bryan, *J. Magn. Reson.*, 1986, 70, 149.
35 L. S. Singer, I. C. Lewis and D. M. Rifle, *J. Chem. Phys.*, 1987, 91, 2408.
36 N. Nakazimo, R. Kammereck and P. L. Walker Jr., *Carbon*, 1974, 15, 259.

37 F. Tuinsta and J. L. Koenig, *J. Chem. Phys.*, 1970, 53, 1128.
38 N. Nakazimo, *Carbon*, 1991, 29, 757.
39 S. Bourbigot, M. Le Bras, R. Delobel, P. Bréant and J. M. Trémillon, *Carbon*, 1995, 33, 283.
40 A. Abragam and M. Goldman, *Nuclear Magnetism: Order and Disorder*, ed. A. Abragham, Oxford University Press, New York, 1982.
41 J. McBrierty and D. C. Douglass, *J. Polym. Sci., Macromol. Rev.*, 1981, 16, 295.
42 J. McBrierty and D. C. Douglass, *Phys. Rep.*, 1980, 63, 63.
43 S. Kaufman and D. J. Bunger, *J. Magn. Reson.*, 1970, 3, 218.
44 F. Derbyshire, A. Marzec, H. R. Schulten, M. A. Wilson, A. Davis, P. Tekely, J. J. Delpuech, A. Jurkiewicz, C. E. Bronnimann, R. A. Wind, G. E. Maciel, R. Narayan, K. Bartle and C. Snape, *Fuel*, 1989, 68, 1091.
45 L. J. Lynch, D. S. Webster, N. A. Bacon and W. A. Barton, *Magnetic Resonance. Introduction, Advanced Topics and Applications to Fossil Energy*, ed. L. Petrakis and J. P. Fraissard, Reidel Publishing, Dordrecht, 1984, p. 617.
46 S. Meiboom and D. Gill, *Rev. Sci. Instrum.*, 1958, 29, 688.
47 H. Tanaka and T. Nishi, *J. Chem. Phys.*, 1985, 82, 4326.
48 T. T. P. Cheung, *Phys. Rev. B*, 1981, 23, 1404.

Synergistic effect of zeolite in an intumescence process

Study of the interactions between the polymer and the additives

Serge Bourbigot,[a]* Michel Le Bras,[a] René Delobel[a] and Jean-Michel Trémillon[b]

[a] *Laboratoire de Physicochimie des Solides, E.N.S.C.L., Université des Sciences et Technologies de Lille, BP 108, F-59652 Villeneuve d'Ascq Cedex, France*

[b] *GRL (Elf-Atochem), BP 34, F-64170 Lacq, France*

The chemical effect of the zeolite 4A added to the intumescent ammonium polyphosphate (APP)–pentaerythritol (PER) system in a fire retardant (FR) ethylene–butyl acrylate–maleic anhydride terpolymer (LRAM3.5)-based formulation has been studied. Thermogravimetric (TG) analysis defines the different steps of the degradation of the formulation and shows that the presence of the zeolite leads to an increase in the stability of the material at high temperature ($T > 550\,^{\circ}C$). Spectroscopic characterisations, mainly ^{31}P, ^{13}C, ^{1}H and ^{27}Al NMR of the solid state, demonstrate that there are interactions between the polymer and the additives. In the case of the LRAM3.5–APP–PER formulation, the protection arises principally from the additives which make a thermal barrier between the flame and the material. When zeolite is present it plays an essential role, because it allows the formation of structures stabilising the polymer which can then participate in the formation of the intumescent protective shield and hence in its own protection. Moreover, we prove that the FR properties of the protective material obtained from the formulations depend on the 'quality' of the intumescent coating obtained from the additives. In particular, the presence of the zeolite decreases the size of the amorphous domains of the carbon.

In a previous paper,[1] we studied the chemical effect of a zeolite 4A (4A) added to the intumescent FR system APP–PER using, mainly, solid-state NMR spectroscopy. Zeolite acts as a synergistic agent in FR polyethylenic polymers with APP–PER based formulations, and leads to a marked improvement in the fire-proofing properties.[1–4] In the formulations, the protection of the polymeric matrix by the intumescent process, and hence the FR property, is obtained *via* the formation of an insulating foamed carbonaceous coating. The intumescent shield formed from the additives, consists of a phosphocarbonaceous structure with a local structuring of the 'carbon' ('turbostratic carbon'). The zeolite permits retention of this structure over a relatively high temperature range and hinders the formation of small molecules in the polyaromatic network. It was finally proposed that formation of a 'coherent' macromolecular network leads to the improved FR performance of the APP–PER–4A system.

The 'efficiency' of 4A depends strongly on the polymer and an important polymeric matrix effect has been previously reported.[2] As an example, the polyethylene-based formulations have limiting oxygen index (LOI, normalised fire testing value[5]) of 24% without zeolite and of 26% with zeolite whereas the LOI increases from 30% (without zeolite) to 39% (with zeolite) in LRAM3.5-based formulations. We have thus used the latter system to study the synergistic effect.

In our previous work, we hypothesised that the intumescent coating giving the fire-proofing properties results only from the additives. However, the polymer and/or its degradation products may play a part in the formation of the intumescent protective structure.[6,7] The aim of this study is to discuss the interactions between the polymer and the additives which occur during the carbonisation process (mechanisms leading to the formation of the intumescent protective shield) and the part played by 4A in increasing the FR performance of the coating.

Here, we study, first, the thermal behaviour of the two formulations LRAM3.5–APP–PER and LRAM3.5–APP–PER–4A by TG analysis to determine the temperature ranges which correspond to the development, the stability and the degradation of the intumescent materials, and to compare these with

the thermal behaviour of the additives and thus evidence interactions between the polymer and the additives. The materials are then characterised by chemical analysis, IR spectroscopy and high-resolution ^{31}P, ^{13}C, ^{1}H and ^{27}Al NMR in the solid state.

Additional structural information is obtained, as discussed previously,[1] from low-resolution ^{1}H NMR of the solid state by measuring the spin–spin relaxation times (T_2) after solid-echo sequences and size domain measurement of the slow relaxation, using as 'probe' the free precession of the protons present and the spin diffusion phenomenon in the materials.

Experimental

Materials used were 4A (Si/Al = 1, compensation cation: Na, as supplied by Ceca), PER (Aldrich R.P. grade), APP [$(NH_4PO_3)_n$, $n = 700$, Hoechst Exolit 422, soluble fraction in H_2O: <1 wt.%] and LRAM3.5 [terpolymer, ethylene (91.5 wt.%)–butyl acrylate (5 wt.%)–maleic anhydride (3.5 wt.%), as powdered Lotader P3200 supplied by Elf-Atochem]. The study was carried out using APP–PER and APP–PER–4A mixtures with APP/PER = 3 (by weight) and (APP/PER)/4A = 19 (by weight), respectively. With the polyethylenic materials, the FR properties are greatest for these ratios.[1–4] Initial mixtures [LRAM3.5/(additives) = 70/30 (by weight)] were first prepared by ballmilling, after mechanical grinding and sifting (200×10^{-6} m), of the raw materials. They were then heat treated, at four different maximum treatment temperatures (previously defined by TG analysis)[1] ($T_{tr.\,max}$: 280, 350, 430, 560 °C) for 12 h under air flow (flow rate = 6×10^{-6} $m^3\,s^{-1}$).

Methods for the determination of amounts of carbon, hydrogen, nitrogen, phosphorus, aluminium and silicon are described in ref. 1.

TG analyses were carried out at a heating rate of 5 °C min^{-1} under synthetic air (flow rate = 5×10^{-7} $m^3\,s^{-1}$; Air Liquide grade) using a Setaram MTB 10-8 microbalance. In each case the mass of sample used was fixed at 10 mg. The precision of the temperature measurement was 1.5 °C over the whole temperature range.

IR spectra were recorded using a Perkin-Elmer 683 spectrometer connected to a PE3600 data station. Samples were ground and mixed with KBr to form pellets.

High-resolution ^{31}P, ^{13}C and ^{1}H NMR spectra of the solids were obtained on a Brucker ASX100 spectrometer at a spinning speed of 5 kHz and using a Brucker probe head equipped with a 7 mm magic-angle spinning (MAS) assembly. The spectra were obtained with a simple 90° pulse acquire programme with a pre-acquisition delay of 10 μs. ^{31}P NMR measurements were performed at 40.5 MHz with MAS, high-power ^{1}H dipolar decoupling (DD) using a repetition time of 2 s. All spectra were acquired as a result of 1024 scans. The reference used was 85% H_3PO_4 in aqueous solution. ^{13}C NMR measurements were performed at 25.2 MHz (2.35 T) with MAS, high-power ^{1}H dipolar decoupling and $^{1}H-^{13}C$ cross polarisation (CP). The Hartmann–Hahn matching condition was obtained by adjusting the power on the ^{1}H channel to the maximum ^{13}C free induction decay (FID) signal of adamantane. All spectra were acquired with contact times of 1 ms. A repetition time of 10 s was used. Typically, 10 000 scans were necessary to obtain spectra with a good signal/noise ratio. The reference used was tetramethylsilane. ^{1}H NMR measurements were performed at 100.13 MHz with MAS using a repetition time of 2 s. All spectra were acquired as a result of 32 scans. The reference used was tetramethylsilane.

High-resolution ^{27}Al NMR spectra of were obtained on a Brucker MSL 300 spectrometer (7.05 T) and were recorded in a 4 mm Brucker probe, spinning at 10 kHz. The spectrometer frequency was 78.172 MHz. Typically 4000 scans for ^{27}Al were needed to obtain spectra with a convenient signal/noise ratio. The reference used was $Al(H_2O)_6^{3+}$. Note, that ^{29}Si NMR spectra have not been recorded because of the low natural isotopic abundance of silicon 29 (4.7%) and the very low amounts of zeolite in the formulations.

^{1}H NMR studies were carried out using a Brucker ASX 100 spectrometer, operating at a proton frequency of 100.13 MHz and with a 7 mm solenoid probe. The method of inversion recovery $[\pi-\tau-\pi/2]$ was used to measure proton spin–lattice relaxation (T_1) times. The computation of T_2 was made using a solid echo sequence $[(\pi/2)_x-\tau-(\pi/2)_{-x}]$.[9]

In a heterogeneous material, it is possible to observe the effects of spin diffusion with a Goldman–Shen pulse sequence $[(\pi/2)_x-t_0-(\pi/2)_{-x}-\tau-(\pi/2)_x]$.[10] The magnetisation of each material shows a two-component FID with significantly different T_2. The fixed time, t_0, was chosen such that M_2, which has a shorter T_2, has decayed to zero while there was still sufficient magnetisation M_1 remaining in the domain of slow relaxation. On the basis of the theoretical considerations of Cheung and Gerstein[11] recalled in ref. 1, we determined the mean width of the domain of the slow relaxation $(\bar{b})$.

Results and Discussion

Chemical characterisation

TG. The thermal behaviour of LRAM3.5, LRAM3.5–APP–PER and LRAM3.5–APP–PER–4A systems was studied by TG (Fig. 1). It was shown that the intumescent process leads to the protection of the polymeric matrix in the temperature range 250–450 °C and that the presence of the zeolite provides a residue stable at $T > 550$ °C.

On the basis of the observations of the materials obtained after the thermal treatment and our previous studies,[6,12] the different steps in the degradation processes can be assigned. In the 250–450 °C range an intumescent material is formed which degrades in the 450–550 °C range to provide a carbonaceous residue without any expanded character. This residue degrades at > 550 °C. With zeolite, the residue forms in the 450–500 °C range. Its comparatively high thermal stability at
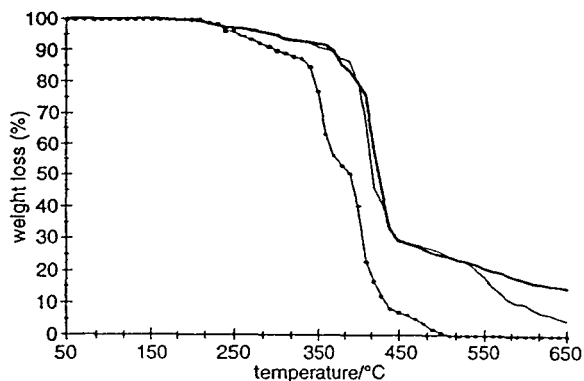
Fig. 1 TG curves for the LRAM3.5-based formulations: (—♦—) LRAM3.5, (——) LRAM 3.5–APP–PER, (——) LRAM3.5–APP–PER–4A

temperatures higher than 550 °C may be related to the formation of a stable carbonaceous material and to oxides arising from the degradation of 4A [the residue amounts (at 650 °C) are 15 and 5 wt.% in the systems with and without 4A, respectively].

Chemical analysis. The composition of the materials obtained at different $T_{tr, max}$ is given in Table 1.

The phosphorus amount remains constant in both materials, whatever the value of $T_{tr, max}$. At high temperature (560 °C) there is a comparatively high concentration of protons in the material with zeolite. The presence of these protons may be assigned to hydrocarbonaceous chains and/or phosphate acidic species.

In contrast to the single additives,[1] changes in the P/C and N/C ratios are different. This suggests that the polymer has an influence on the formation of the protective shield. As previously,[1] nitrogen is present at each temperature and it is assumed that the evolved ammonia (from the degradation of APP[13-14]) reacts with carbonaceous species to form nitrogenated species. This last assumption has already been demonstrated for APP–PER.[15]

The N/C ratios, in contrast to the case with additives alone,[1] exhibit different behaviour with $T_{tr, max}$ with more nitrogenated species than carbonated ones. This suggests that the polymer degrades to nitrogenated compounds; e.g. ammonia may react with the maleic anhydride part of the terpolymer to give amides.

IR spectroscopy. The spectra of the formulations are presented in Fig. 2 and 3 in the wavelength ranges 850–1350 and 2500–3700 cm^{-1}. The first spectral region corresponds to the absorption range of the P—O bonds[16] and allows us to characterize the phosphate species and to prove the formation of a phosphocarbonaceous structure (Table 2). The second spectral region corresponds to the absorption range of aliphatic groups which allows us to see the stability of the polymeric matrix in the intumescent coating.[16]

At every temperature, the spectra present broad bands between 1150 and 1300 cm^{-1} assigned, according to Mac Kee et al.,[17] to P—O—C bonds in 'phosphate–carbon' complexes. The additional broad bands about 1000 cm^{-1} may be assigned to symmetric vibration modes of PO_2 and PO_3 which are characteristic of phosphocarbonaceous complexes.[16-20] The spectra demonstrate, therefore, the formation of a phosphocarbonaceous structure from 280 °C which is maintained up to 560 °C whether in the presence of zeolite or not. Additionally, the change in these bands, decrease in intensity and broadening with temperature is explained by the formation of a phosphorus oxide such as P_4O_{10} from the thermal degradation of phosphate species.[18]

284

element	LRAM3.5–APP–PER				LRAM3.5–APP–PER–4A			
	$T_{tr, max}$				$T_{tr, max}$			
	280	350	430	560	280	350	430	560
C	47	30	10	1	51	33	12	9
H	106	51	43	19	107	47	30	34
N	1	1	0.2	0.5	1	1	1	1
O	14	25	38	39	11	24	38	37
P	2	4	6	7	2	4	5	7
Si	—	—	—	—	0.08	0.3	0.4	0.05
Al	—	—	—	—	0.07	0.1	0.1	0.01
Na	—	—	—		0.06	0.08	0.3	0.03

Note, that two bands are observed at ca. 950 and 1090 cm^{-1} and are assigned, respectively, to the asymmetric and symmetric vibration modes of a P—O bond in a chain P—O—P. The band at ca. 1090 cm^{-1} disappears above 350°C, which suggests the increasing asymmetry of the P—O—P bonds. Moreover, these condensed phosphate species are observed at every temperature.

The spectra exhibit two additional absorptions at 2920 and 2850 cm^{-1} which may be assigned to aliphatic groups —(—CH$_2$—)$_n$—.[16] The intensity of these bands decreases with increasing temperature and they are no longer observed at 560 °C in the case of the material without zeolite. These results suggest that the presence of the zeolite inhibits the degradation of the polymer by blocking polyethylenic links in the intumescent coating.
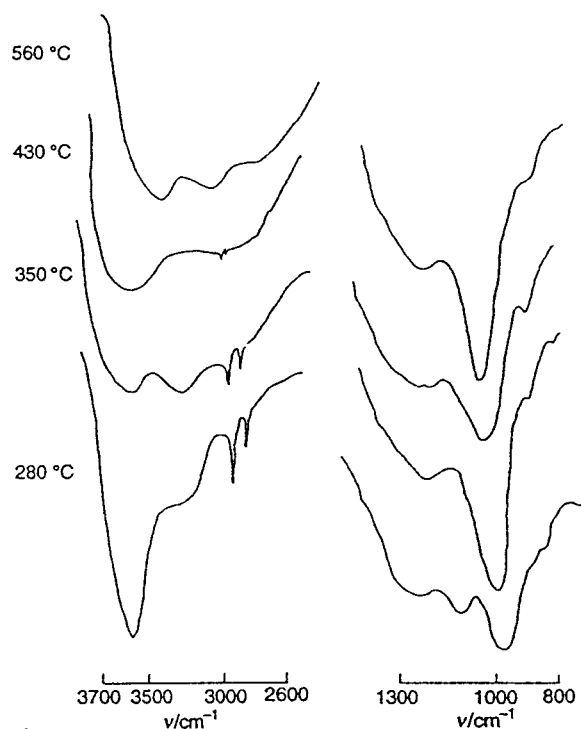

Fig. 2 IR spectra of LRAM3.5–APP–PER at different $T_{tr, max}$
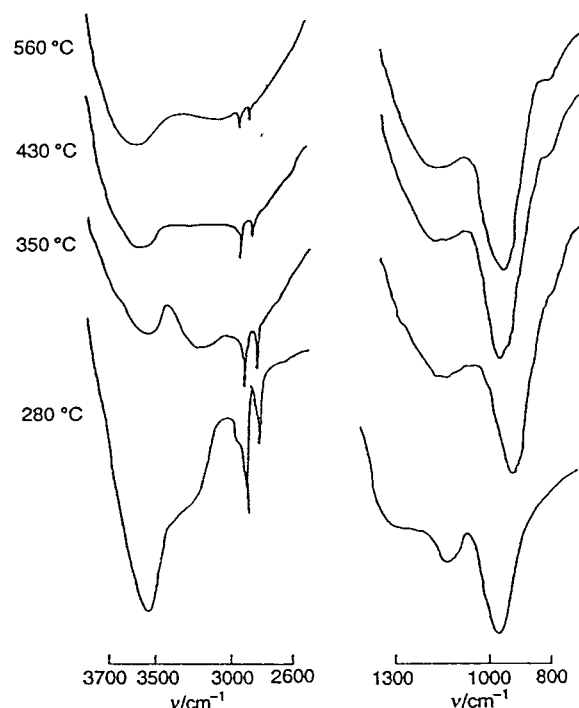
Fig. 3 IR spectra of LRAM3.5–APP–PER–4A at different $T_{tr, max}$

Table 2 IR absorptions of the heat-treated LRAM3.5–APP–PER and LRAM3.5–APP–PER–4A formulations

absorption bands/cm^{-1}	assignment	ref.
910–940	ν_{as} of P—O in P—O—P	18, 19
980–1020	ν_{sym} of PO$_2$ and PO$_3$ in complexes phosphate–carbon	17, 19, 20
1080–1100 (in overlap and up to 350 °C)	ν_{sym} of P—O in P—O—P	18, 19
1150–1300	stretching mode of P—O—C in complexes phosphate–carbon	17, 19, 20
1250–1260 (in overlap)	stretching mode in P=O	18, 19
2850	ν_{sym} of C—H in —(—CH$_2$—)$_n$—	
		16
2920	ν_{as} of C—H in —(—CH$_2$—)$_n$—	
3200–3600	valence vibration of O—H and/or N—H	16

MAS-DD ^{31}P NMR. The IR study has shown that the intumescent shield is partially composed of phosphocarbonaceous structures. To complete this study ^{31}P NMR was used.

Comparison of the thermal behaviour of the systems (Fig. 4 and 5, Table 3) shows that, above 280 °C the peak assigned to polyphosphate chains (−23 ppm) disappears and the intensity of the peaks around −11 ppm decreases relative to those around 1 ppm. This phenomenon may be explained by the
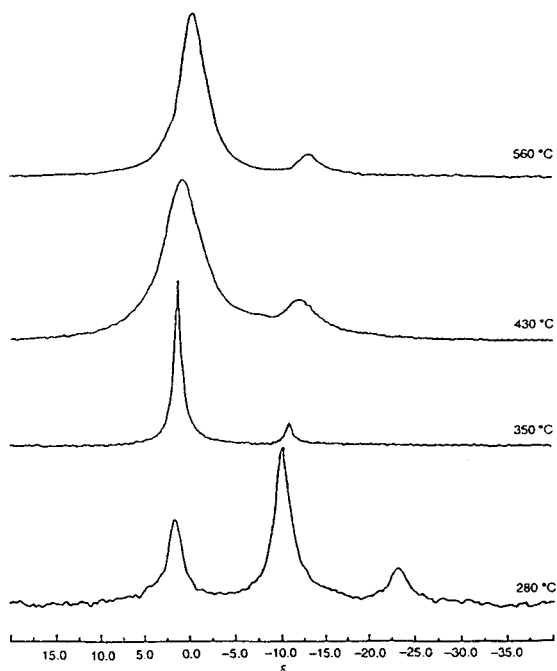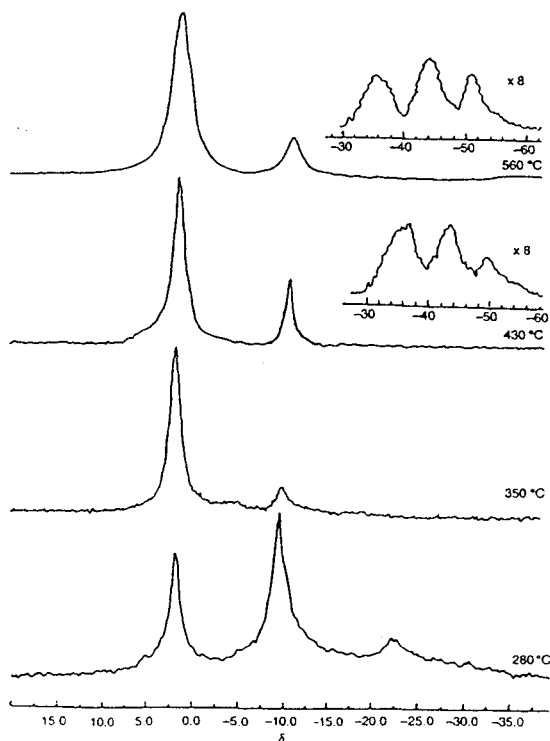
hydrolysis of P—O—P and/or P—O—C groups.[12] However, the spectra show that the presence of the zeolite hinders the hydrolysis and allows condensed phosphate species and/or the aromatic phosphocarbonaceous structure to exist at high temperature.

Phosphorus oxides are observed in the materials with the zeolite that are heat-treated at 430 and 560 °C in contrast to the results obtained on heating the additives alone.[1] This result may be explained by the different degradation modes of the polymer which may be stabilised in the carbonaceous structure in the material with zeolite. As a consequence, the evolution of water is reduced and hydrolysis is therefore slowed down.

These differences show the influence of the polymer on the degradation of the formulations and lead to the assumption that, by stabilising the polymer, the zeolite affects the carbonisation reactions to form the aromatic phosphocarbonaceous structure.

CP-MAS-DD ^{13}C NMR. The spectra are presented in Fig. 6 and 7 and their assignments in Table 4. At each temperature, an intense peak is observed at ca. 33 ppm which is assigned to —CH$_2$— groups in polyethylenic chains[23,24] arising probably from fragments of non-degraded polymer. This assumption may appear surprising because it is well known that the polyethylenic chains are degraded during isothermal treatment at ca. 200 °C. Nevertheless, this result has already been observed by several authors[25-29] for polymers (such as polypropylene, polyethylene or polystyrene) flame-retarded by phosphorus compounds. Moreover, this result is confirmed by the IR study and by the spectrum of the polymer alone (Fig. 8).

A peak of low intensity is observed at ca. 14 ppm at 280 and 350 °C for the two formulations. It may be assigned to —CH$_3$ groups belonging to the chain-end of the polymer.[23,24]

Fig. 4 DD-MAS ^{31}P NMR spectra of LRAM3.5–APP–PER at different $T_{tr, max}$

Fig. 5 DD-MAS ^{31}P NMR spectra of LRAM3.5–APP–PER–4A at different $T_{tr, max}$
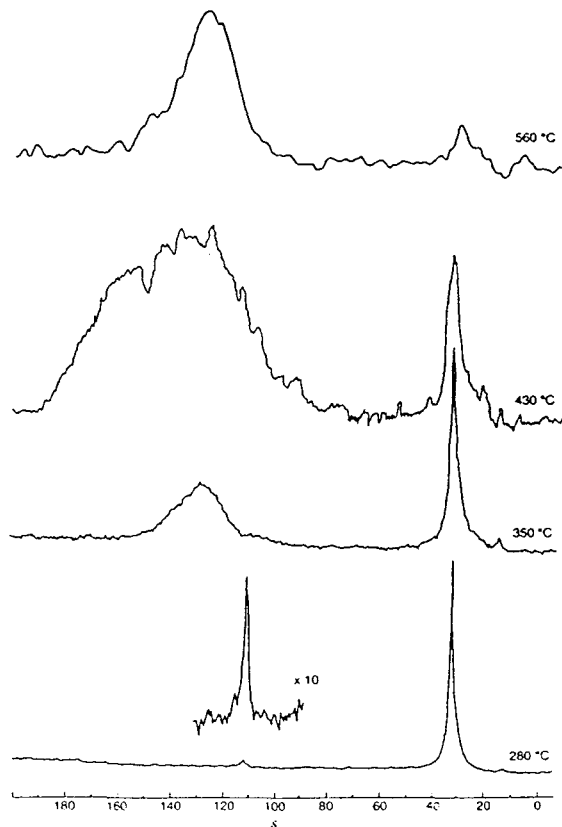

Fig. 6 CP-DD-MAS ^{13}C NMR spectra of LRAM3.5–APP–PER–4A at different $T_{tr, max}$

Table 3 Chemical shift assignments of the DD-MAS NMR ^{31}P spectra of the heat-treated LRAM3.5–APP–PER and LRAM3.5–APP–PER–4A formulations

system	$T_{tr,max}/(°C)$	chemical shift(ppm)	assignment	ref.
LRAM3.5–APP–PER	280	1.5	PO$_4$ units in R$_2$HPO$_4$, RH$_2$PO$_4$ and/or H$_3$PO$_4$.	1, 21, 22
		−10.2	PO$_4$ units in Φ$_2$RPO$_4$ and/or Φ$_2$HPO$_4$ and/or pyrophosphate group and/or polyphosphate chain (end-group).	
		−23	polyphosphate chain (central group).	
	350	1	PO$_4$ units in R$_2$HPO$_4$, RH$_2$PO$_4$ and/or H$_3$PO$_4$.	1, 21, 22
		−10.9	PO$_4$ units in Φ$_2$RPO$_4$ and/or Φ$_2$HPO$_4$ and/or pyrophosphate group.	
	430	0.8	PO$_4$ units in R$_2$HPO$_4$, RH$_2$PO$_4$ and/or H$_3$PO$_4$.	1, 21, 22
		−12	PO$_4$ units in Φ$_2$RPO$_4$ and/or Φ$_2$HPO$_4$ and/or pyrophosphate group.	
	560	−0.4	PO$_4$ units in R$_2$HPO$_4$, RH$_2$PO$_4$ and/or H$_3$PO$_4$.	1, 21, 22
		−12.6	PO$_4$ units in Φ$_2$RPO$_4$ and/or Φ$_2$HPO$_4$ and/or pyrophosphate group and/or polyphosphate chain (end-group).	
LRAM3.5–APP–PER–4A	280	1.6	PO$_4$ units in R$_2$HPO$_4$, RH$_2$PO$_4$ and/or H$_3$PO$_4$.	1, 21, 22
		−9.7	PO$_4$ units in Φ$_2$RPO$_4$ and/or Φ$_2$HPO$_4$ and/or pyrophosphate group and/or polyphosphate chain (end-group).	
		−23	polyphosphate chain (central group).	
	350	1.1	PO$_4$ units in R$_2$HPO$_4$, RH$_2$PO$_4$ and/or H$_3$PO$_4$.	1, 21, 22
		−10.5	PO$_4$ units in Φ$_2$RPO$_4$ and/or Φ$_2$HPO$_4$ and/or pyrophosphate group.	
	430	−0.8	PO$_4$ units in R$_2$HPO$_4$, RH$_2$PO$_4$ and/or H$_3$PO$_4$.	1, 21, 22
		−11.3	PO$_4$ units in Φ$_2$RPO$_4$ and/or Φ$_2$HPO$_4$ and/or pyrophosphate group.	
		−38/−44.7/−50	phosphorus oxides (P$_4$O$_{10}$ type).	
	560	−0.8	PO$_4$ units in R$_2$HPO$_4$, RH$_2$PO$_4$ and/or H$_3$PO$_4$.	1, 21, 22
		−11.3	PO$_4$ units in Φ$_2$RPO$_4$ and/or Φ$_2$HPO$_4$ and/or pyrophosphate group and/or polyphosphate chain (end-group).	
		−38/−44/−50.5	phosphorus oxides (P$_4$O$_{10}$ type).	

R = alkyl groups and Φ = aromatic or polyaromatic groups.

Table 4 Chemical shift assignments of the CP-DD-MAS NMR ^{13}C spectra of the LRAM3.5–APP–PER and LRAM3.5–APP–PER–4A systems vs. $T_{tr,max}$

system	$T_{tr,max}/°C$	chemical shift(ppm)	assignment	ref.
LRAM3.5–APP–PER	280	14.5	C_{CH_3}	23, 24
		33	C_{CH_2}	23, 24
		111	C_{ar-H}	30
	350	14.5	C_{CH_3}	23, 24
		33	C_{CH_2}	23, 24
		128	C_{ar-H}, C_{ar-C}, C_{ar-O}, C_{ar-N}	23, 31, 32
		(broad band: 115–160)		
	430	32	C_{CH_2}	23, 24
		140	C_{ar-H}, C_{ar-C}, C_{ar-O}, C_{ar-N}	23, 31, 32
		(broad band: 115–160)		
	560	32.6	C_{CH_2}	23, 24
		123	C_{ar-H}, C_{ar-C}, C_{ar-O}, C_{ar-N}	23, 31, 32
		(broad band: 100–160)		
LRAM3.5–APP–PER–4A	280	14.5	C_{CH_3}	23, 24
		32.7	C_{CH_2}	23, 24
		111	C_{ar-H}	30
	350	14.5	C_{CH_3}	23, 24
		32.7	C_{CH_2}	23, 24
		111	C_{ar-H}	30
		130	C_{ar-H}, C_{ar-C}, C_{ar-O}, C_{ar-N}	23, 31, 32
		(broad band: 120–150)		
	430	32.7	C_{CH_2}	23, 24
	560	33	C_{CH_2}	23, 24
		125	C_{ar-H}, C_{ar-C}, C_{ar-O}, C_{ar-N}	23, 31, 32
		(broad band: 120–150)		

C_{CH_3}: alkyl carbon, C_{CH_2}: alkyl carbon, C_{ar-H}: protonated aromatic carbon, C_{ar-C}: unprotonated aromatic carbon, C_{ar-O}: oxygenated aromatic carbon, C_{ar-N}: nitrogenated aromatic carbon and/or nitrogenated carbon with conjugated bonds in heterocycles.

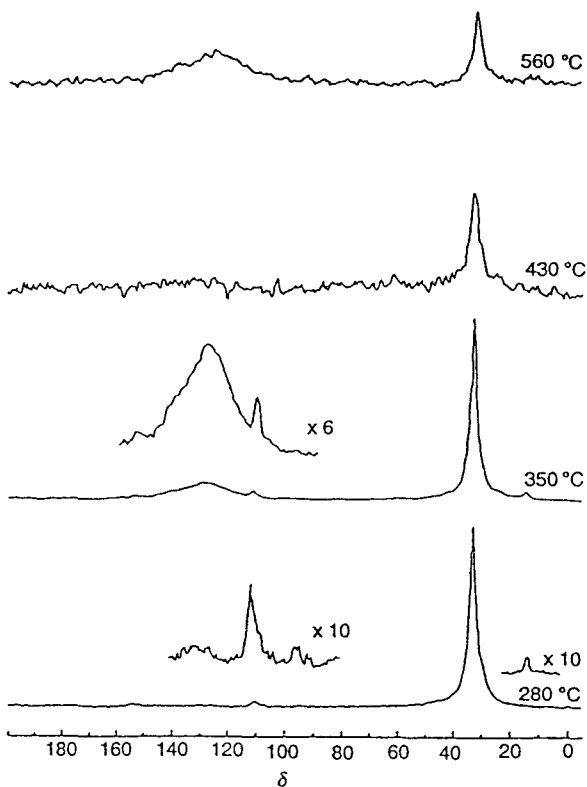*J. Chem. Soc., Faraday Trans.*, 1996, *Vol. 92* 3439

287

Fig. 7 CP-DD-MAS ^{13}C NMR spectra of LRAM3.5–APP–PER–4A at different $T_{tr, max}$

Nevertheless, to observe these end-groups, their ratio to the —CH_2— groups has to be sufficiently high. Therefore, a scission of the polyethylenic chains leading to the formation of shorter chains which are trapped in the intumescent coating and/or which are involved in its formation, must be assumed. The disappearance of the peak at *ca.* 14 ppm at 430 and 560 °C implies the oxidation of the —CH_3 end-groups. This oxidation leads, *via* a radical mechanism, to oxidised groups (carbonyl, hydroperoxides *etc.*) which react with phosphate acidic species[12] to form phosphocarbonaceous structures and/or aromatic species bridged by polyethylenic chains.

The spectra show, as in the case of the additives alone,[1] that the carbonisation process (characterised by the appearance of aromatic species) begins at 280 °C. The peaks about 111 ppm may be assigned, according to Hasan *et al.*,[30] to aromatic or polyaromatic species of small size (benzene, naphthalene, anthracene *etc.*). Above 350 °C, a broad peak between 110 and
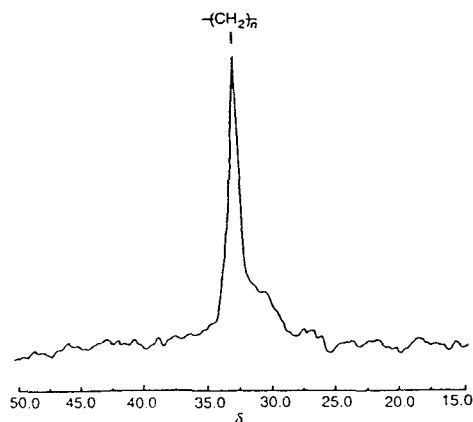

Fig. 8 CP-DD-MAS ^{13}C NMR spectrum of LRAM3.5

150 ppm is observed, which implies the presence of several non-magnetically equivalent carbons.[23] As discussed previously,[1] this peak may be assigned to several types of aromatic and polyaromatic species.[23,31,32]

Note, for the material without zeolite, the disappearance of the peak around −111 ppm above 350 °C. This suggests that the presence of the zeolite slows down the aromatisation process of the system. Comparison of the evolution of the peaks areas at 128 ppm and 33 ppm (between 350 and 560 °C) of the two formulations confirms this assumption.

The aromatic species are not detected in the spectrum at 430 °C for the formulation LRAM3.5–APP–PER–4A. This is, as in the case of the APP–PER–4A sample heat-treated at 430 °C, because of the paramagnetic character of the material,[1] with a large number of paramagnetic species which eliminate the NMR signal. Indeed, an EPR study of the additives has shown that the ratio of free radical carbons to the total number of carbons was a maximum in the case of the intumescent shield obtained at 430 °C from APP–PER–4A.[1]

MAS ^{1}H NMR. The MAS ^{1}H NMR study completes the results obtained by CP-DD-MAS ^{13}C NMR. The spectra are presented in Fig. 9 and 10 with the deconvolution of each spectrum assuming either Lorentzian or Gaussian signals. As in the case of the APP–PER system,[33] the spectra are relatively well defined and the combined rotation and multipulse spectroscopy (CRAMPS) technology is not absolutely necessary to discriminate between the peaks (Table 5).[34]

The results presented in Table 5 confirm that the carbonisation process begins at 280 °C. The peaks around 12, 9 and 7 ppm have already been observed and discussed in the case of the APP–PER system.[33] In the presence of the polymer, additional peaks appear. The peak around 1 ppm may be assigned, according to the ^{13}C NMR, to undegraded chain fragments —(—CH_2—)$_n$— of the polymer. The peaks at 0.2 and 0.6 ppm, observed, respectively, at 280 and 350 °C, may be assigned, according to the ^{13}C NMR study, to —CH_3 end-groups belonging to —(—CH_2—)$_n$— chains.

Two additional peaks (at 2.5 and 4.5 ppm) are observed in the case of the zeolite-absent materials at 430 and 560 °C. That around 2.5 ppm corresponds to aliphatic protons in —CH_3 groups linked to aromatic species and/or to —CH— groups.[35,36] These latter would stem from degradation and fragmentation of the polyethylenic chains, followed by recombination of these fragments with other chains and/or with the additives. The peak around 4.5 ppm may be assigned to aliphatic protons belonging to methylene groups bridging polyaromatic species.[35,36]

In the absence of zeolite, at temperatures from 350 °C, the ratio of aliphatic protons to aromatic and phosphate protons is small compared to the ratio with zeolite. This shows that the presence of zeolite inhibits the thermo-oxidative degradation of the polyethylenic chains which are stabilised in the intumescent coating over all the temperature range studied.

MAS ^{1}H NMR confirms the results obtained by IR and ^{13}C NMR studies *i.e.* that zeolite hinders the total degradation of the polymer chains by stabilising polyethylenic links in the intumescent shield.

MAS ^{27}Al NMR. The above studies have permitted us to characterise the role played by the zeolite in polymer degradation. However, the physicochemical role of the zeolite in these process is still to be explained. ^{27}Al NMR is a useful tool for this.

Fig. 11 presents the MAS ^{27}Al NMR spectra of the heat-treated LRAM3.5–APP–PER–4A formulation. The thermal treatment leads to the complete disappearance of the tetrahedral [AlO$_4$] unit of the zeolite (δ = 58 ppm)[37,38] and complete destruction of the zeolite framework.
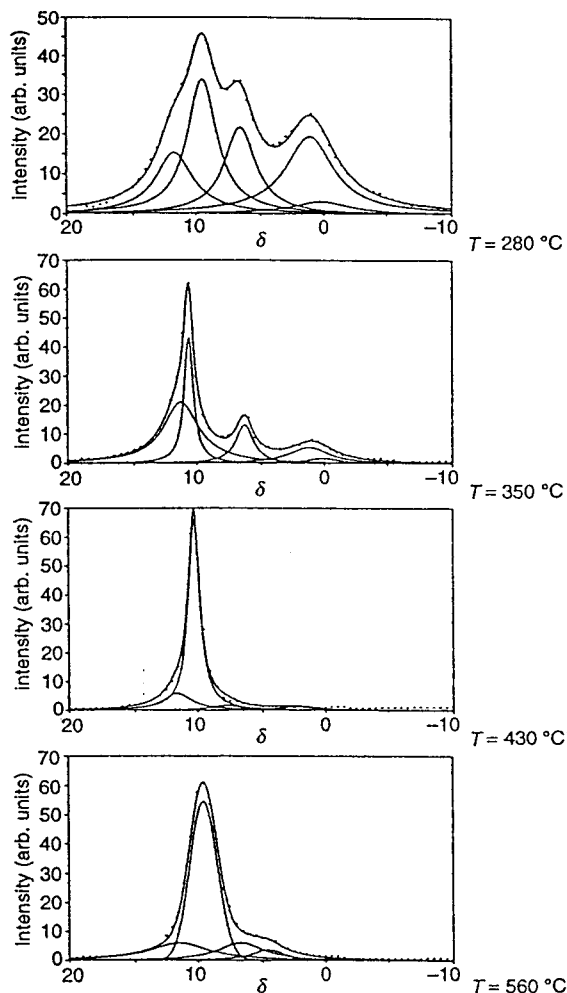
At each temperature, peaks around −20 ppm are observed

Fig. 9 MAS ^{1}H NMR spectra of LRAM3.5–APP–PER at different $T_{tr, max}$

Fig. 10 MAS ^{1}H NMR spectra of LRAM3.5–APP–PER–4A at different $T_{tr, max}$

which may be assigned to octahedral $[AlO_6]$ units.[39] The overlapping in the peaks observed at 350 and 430 °C may be assigned to $[AlO_6]$ units with different binding angles.[39] It is interesting to note that the peak position is shifted to higher fields. This is because of the presence of phosphorus, in particular, within the second sphere of coordination. This P has a marked effect upon the peak position of AlO_x units; e.g. from +10 for $Al[OAl]_6$ to −20 ppm for $Al[OP]_6$.[39–42] It is, therefore, demonstrated that the zeolite is destroyed to form aluminophosphates above 280 °C.

The reactivity in the solid state between the APP and the zeolite has been previously confirmed by heat treating an APP–4A mixture (1 : 1 w/w) at 280 °C.[3] The resulting MAS ^{27}Al NMR spectrum showed the partial destruction of the zeolite to give aluminophosphates.

These results are similar to those obtained with the APP–PER–4A system and thus the polymer does not modify the reaction between APP and the zeolite.

Structural characterisation

In our earlier study,[1] we have shown that the additives form carbonaceous coatings which are strongly anisotropic materials and which contain regions of different mobilities. In the case of the systems polymer–additives, a study of the molecular dynamics by low-resolution solid-state ^{1}H NMR may therefore provide information on heterogeneities in our materials and on the structural interactions between the polymer and the additives.
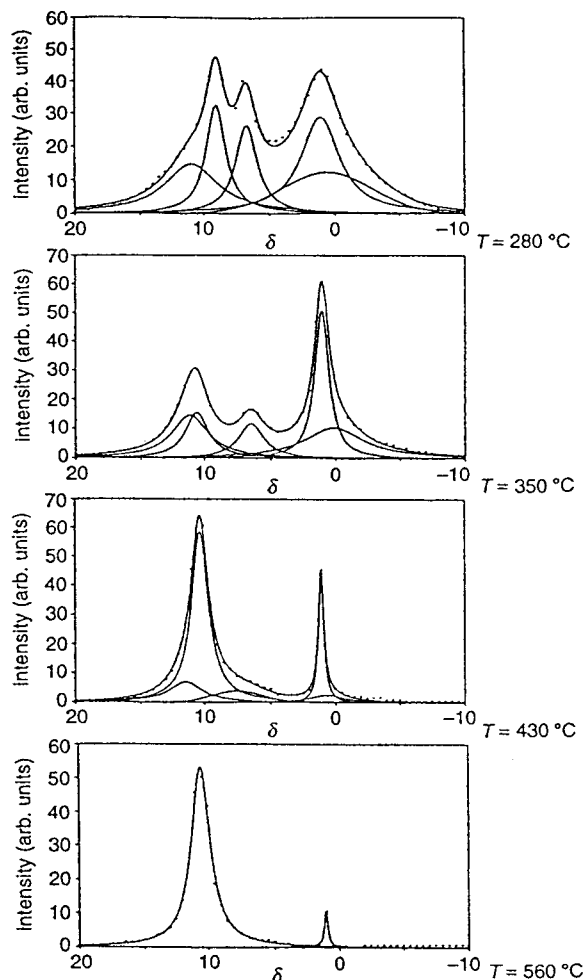
Spin–lattice relaxation. Fig. 12 compares the T_1 values obtained after inversion–recovery sequences. Note that, as in the case of the additives alone, only one T_1 is observed at every $T_{tr, max}$ and it can therefore be expected that the size of the domain undergoing slow relaxation will be <10 nm.[1,43–46]

Comparison of the T_1 values of the two formulations shows that their behaviours are indentical from 350 °C. However, at 280 °C, the T_1 values of the systems with zeolite are twice as large as without zeolite. It is concluded that the materials formed at this temperature are structurally different, a longer T_1 indicating that the molecular motions may be hindered and therefore that the structure may be more rigid.

Spin–spin relaxation. The free processions of the two formulations have been recorded vs. $T_{tr, max}$ after the spin–echo sequence. As in the case of the additive alone, they present complex shapes. To a first approximation, we can distinguish two decays: one fast, up to ca. 50 μs, and the other slower (Table 6). As presented in ref. 1, the fast-decaying component is assumed to be Lorentzian and the slow-decaying component is described by an intermediary shape between Lorentzian and Gaussian, represented by Weibullian functions.[47]

Two T_2 values are observed for each sample and the presence of two phases in the intumescent structure is demonstrated. On the basis of our above chemical characterisation and of the discussion of ref. 1, we may assign the fast-decaying component to a macromolecular network consisting of stacks of polyaromatic species and/or bridging polyethylenic chains.

Table 5 Chemical shift assignments of the MAS NMR ^1H spectra of the LRAM3.5–APP–PER and LRAM3.5–APP–PER–4A systems vs. $T_{tr, max}$

system	$T_{tr, max}/°C$	curve type	r^2	F	chemical shift(ppm)	assignment	ref.
			fit results				
LRAM3.5–APP–PER	280	Lorentzian			0.2	H—CH$_3$	35, 36
		Lorentzian			1.1	H—CH$_2$	35, 36
		Lorentzian	0.998	1800	6.7	H—POH	33
		Lorentzian			9.5	H—ar	35, 36
		Lorentzian			11.7	H—COOH	35, 36
	350	Lorentzian			0.2	H—CH$_3$	35, 36
		Lorentzian			1.2	H—CH$_2$	35, 36
		Lorentzian	0.999	2920	6.3	H—POH	33
		Lorentzian			10.5	H—ar	35, 36
		Lorentzian			11.7	H—COOH	35, 36
	430	Gaussian			2.5	H—ar—CH$_3$ and/or H—CH	35, 36
		Lorentzian	0.993	750	7.7	H—POH	33
		Lorentzian			10.3	H—ar	35, 36
		Lorentzian			11.6	H—COOH	35, 36
	560	Lorentzian			4.5	H—CH$_{2b}$	35, 36
		Lorentzian	0.998	2630	6.7	H—POH	33
		Gaussian			9.6	H—ar	35, 36
		Lorentzian			11.5	H—COOH	35, 36
LRAM3.5–APP–PER–4A	280	Gaussian			0.5	H—CH$_3$	35, 36
		Lorentzian			1.1	H—CH$_2$	35, 36
		Lorentzian	0.997	1010	6.8	H—POH	33
		Lorentzian			9	H—ar	35, 36
		Lorentzian			11	H—COOH	35, 36
	350	Lorentzian			0.2	H—CH$_3$	35, 36
		Lorentzian			1.1	H—CH$_2$	35, 36
		Lorentzian	0.998	1530	6.4	H—POH	33
		Lorentzian			10.4	H—ar	35, 36
		Lorentzian			11.2	H—COOH	35, 36
	430	Lorentzian			0.6	H—CH$_3$	35, 36
		Lorentzian			1.2	H—CH$_2$	35, 36
		Gaussian	0.991	450	6.5	H—POH	33
		Lorentzian			10.3	H—ar	35, 36
		Lorentzian			11.5	H—COOH	35, 36
	560	Lorentzian	0.992	1410	1.1	H—CH$_2$	35, 36
		Lorentzian			10.5	H—ar	35, 36

H—CH$_3$: —CH$_3$ protons, H—ar—CH$_3$: —CH$_3$ protons linked to aromatic species, H—CH: =CH— protons, H—CH$_2$: —CH$_2$— protons, H—CH$_{2b}$: —CH$_2$— bridging groups between aromatic species, H—POH: protons linked to a —P—OH acidic phosphate group, H—ar: protons linked to aromatic carbons, H—COOH: protons linked to a carboxylic group.

The slowly decaying component corresponds to fast molecular motions of the protons in small free molecules not belonging to the molecular network, such as acidic phosphates and/or aromatic species.

The variation in T_{2c} with $T_{tr, max}$ indicates the decrease in the molecular motions in the coatings. This suggests that the materials become more structured when the temperature increases. This result confirms the assumptions deduced from the T_1 study. By comparison with the T_{2c} values measured for the additives where the values remained approximatively constant, it can be seen that the presence of polymer leads to a more rigid macromolecular network.

Note that the presence of 4A leads to a comparatively high amount of protons in the rigid phase of the materials at each

Table 6 T_2 and values of amplitudes measured after solid echo sequences

system	$T_{tr, max}/°C$	T_{2c}/ms	T_{2l}/ms	M_{0c} (%)	M_{0l} (%)	α	r^2	F
		parameter					fit statistic	
LRAM3.5–APP–PER	280	17	240	77	23	1	0.999	9200
	350	12	260	44	62	1.5	0.999	51 000
	430	10	280	18	97	1.8	0.995	6000
	560	8	311	15	86	2.0	0.999	36 000
LRAM3.5–APP–PER–4A	280	19	250	88	24	1	0.999	41 000
	350	10	285	51	57	1	0.999	60 000
	430	10	251	41	63	1.9	0.999	35 000
	560	8	282	27	78	2	0.999	45 000

M_{0c} and M_{0l} are respectively the estimated amplitudes of the fast and slow decaying components (note that the curve fit may lead to a sum $M_{0c} + M_{0l}$ different from 100%). T_{2c} and T_{2l} are respectively the spin–spin relaxation times of the fast- and slow-decaying components, α is the Weibullian coefficient. F is the Fisher coefficient and r is the correlation coefficient.
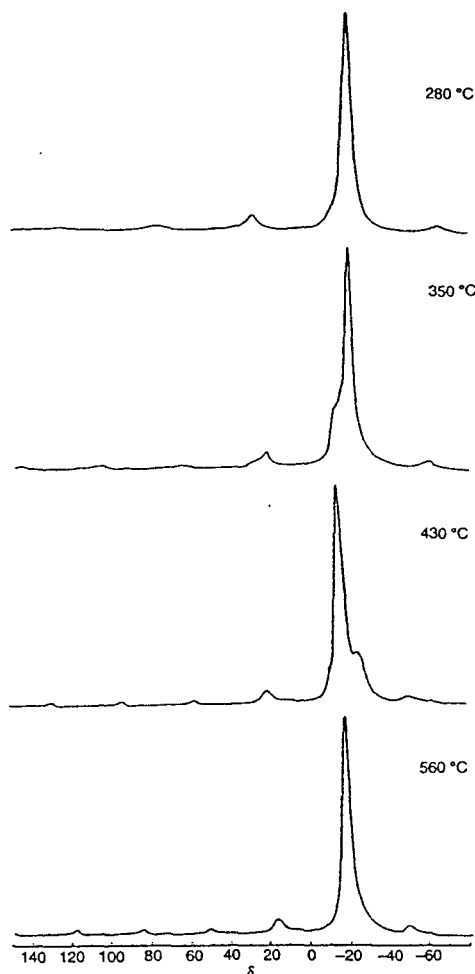
Fig. 11 MAS ^{27}Al NMR spectra of LRAM3.5–APP–PER–4A at different $T_{tr, max}$ (bands at ca. +30 and −65 ppm are spinning side bands)

temperature, most particularly at $T_{tr, max} = 430\,°C$. This result verifies unambiguously the presence of the —CH_2— group in the structured domains of the carbonaceous shields.

Size of the slow relaxation domains. Experiments using the Goldman–Shen pulse sequence were carried out in order to obtain the size of the domains undergoing slow relaxation using the same assumptions as in ref. 1. The values for the mean width of these domains, $\bar{b}$, are presented in Table 7. It is
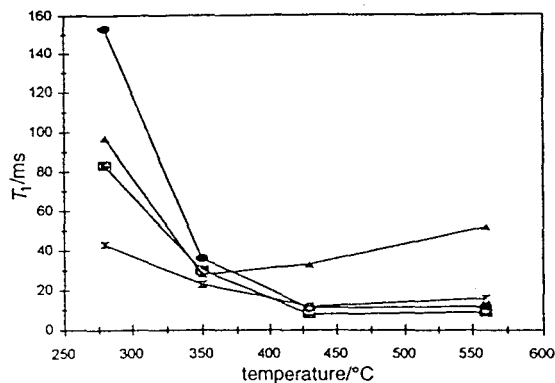
Table 7 Estimation of the size of the slow relaxation domains of the formulations vs. $T_{tr, max}$

system	$T_{tr, max}$/°C	$D/10^{-20} m^2\ ms^{-1}$	$\bar{b}$/nm
LRAM3.5–APP–PER	280	1.7	3.7
	350	2.5	5.7
	430	4.0	7.1
	560	4.8	8.6
LRAM3.5–APP–PER–4A	280	1.4	3.4
	350	2.8	4.8
	430	3.0	5.0
	560	3.7	6.1

seen that the amorphous domains of the materials containing the zeolite are always smaller than those without zeolite. However, the presence of the polymer increases the size of these domains showing that the presence of polymer leads to the formation of a more amorphous structure and/or to the retention of small molecules in the material.

General discussion

The intumescent coating synthesised from the formulation LRAM3.5–APP–PER–4A has fire-proofing properties very much greater than those of the system without zeolite. A study of the carbonaceous coatings obtained from intumescent formulations by isothermal treatment shows clearly the role played by the zeolite in the structures. The two systems develop a phosphocarbonaceous structure which is thermally stabilised by the zeolite. This structure blocks polyethylenic links under organic phosphates and/or aluminophosphates and limits the depolymerisation, i.e. the evolution of small flammable molecules able to feed the fire.

The variation in the size of the domains undergoing slow relaxation with temperature (Fig. 13) shows that the zeolite delays the increase in the size of the mobile phase and thus allows the formation of a more 'coherent' structure than in the case of the LRAM3.5–APP–PER formulation. Note, that the size increases continuously up to 560 °C in the case of the formulation without zeolite. In the case of the system with zeolite, the size first increases, then remains constant (350–430 °C) and finally increases. It may be concluded that the presence of zeolite and of polymer orientate differently the structural properties of the materials.

The formation of a 'coherent' macromolecular network and the participation of polyethylenic links seem therefore to be favourable for the required fire-proofing. Indeed, the development in the intumescent shield of a structure consisting of polyaromatic species creates a rigid material (LRAM3.5–APP–PER formulation). On the other hand, the stabilisation of polyethylenic links in the intumescent structure that are able to bridge polyaromatic species via alumino- and/or silicophosphate groups and/or, because of the paramagnetic character of the intumescent structure,[1] may provide the

Fig. 12 T_1 values for the APP–PER (✕) and APP–PER–4A (▲) systems and LRAM3.5–APP–PER (■) and LRAM3.5–APP–PER–4A (●) at different $T_{tr, max}$
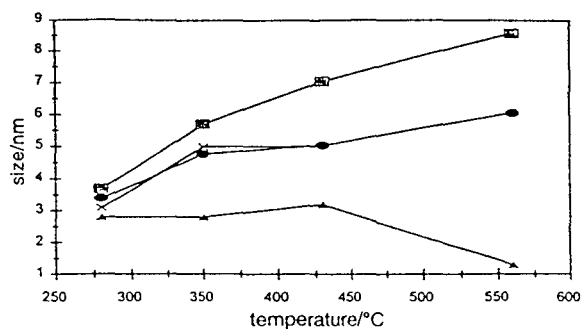

Fig. 13 Size of the slow relaxation domains of the intumescent formulations vs. $T_{tr, max}$; symbols as in Fig. 12

mechanical properties of interest for the intumescent coating. They give flexibility to the carbonaceous shield which in the conditions of a fire, retards the creation and propagation of cracks in which the air can diffuse to the polymeric matrix causing evolution of small molecules that can act as fuel for the fire.

To summarise, the conclusions deduced from the spectroscopic studies of the additives systems[1] and of the polymer–additives formulations, we can propose a reaction scheme for the carbonisation process. When the temperature increases, the intumescent structure develops. At 280 °C it consists of stacks of polyaromatic species linked principally by phosphohydrocarbonated bridges. These bridges provide the dynamic properties of interest to the structure which is then able to accomodate the stresses. At this time the structures developed from the formulations with and without zeolite are distinguished by the organisation of the carbon, the zeolite slowing down the organisation process.

Condensation of aromatic species and decrease in phosphocarbonated species, by scission of the P—O—C bonds, are observed when the temperature increases ($T_{tr, max} > 280$ °C). Consequently, the enlargement of the size of the polyaromatic stacks can increase drastically the viscosity of the material and thus lead to the loss of the FR properties of the coating. Addition of zeolite to the formulation keeps a large number of polyethylenic links in the structure stabilised by 'organic aluminosilicophosphate complexes', reduces the scission of the P—O—C bonds and therefore increases the size of the polyaromatic stacks. The fire-proofing properties are therefore maintained at high temperatures.

Conclusion

This work presents the chemical and structural characterisation of the carbonaceous materials arising from intumescent formulations. It demonstrates that interactions occur between the polymer and the additives. In the case of the classical APP–PER system, the protection arises principally from the additives which develop a thermal barrier between the flame and the material. The presence of zeolite allows the formation of structures that stabilise the polymer which forms the intumescent protective shield and therefore participates in its own protection. Moreover, we have shown that the properties of the protective material obtained from the formulations depend on the 'quality' of the intumescent coating obtained from the additives.

We explain the very large improvement in the fire-proofing properties in polymeric materials containing zeolite: the key to forming a very efficient intumescent shield is the ability of the additives to synthesise a structure which can trap the polymer in order to decrease first, the rate of feeding fuel to the flame and secondly to provide the dynamic properties of interest.

References

1 .S. Bourbigot, M. Le Bras, R. Delobel, R. Décressain and J. P. Amoureux, *J. Chem. Soc., Faraday Trans.,* 1996, **92**, 149.
2 S. Bourbigot, M. Le Bras, R. Delobel, P. Bréant and J. M. Trémillon, in *Fire Retardant Polymers—Fifth European Conference,* ed. D. Price, Salford University, 1995; S. Bourbigot, M. Le Bras, R. Delobel, P. Bréant and J. M. Trémillon, *Polym. Degrad. Stab.,* in the press.
3 S. Bourbigot, M. Le Bras, R. Delobel, P. Bréant and J. M. Trémillon, in *Actes d'Eurofillers95,* Mulhouse; S. Bourbigot, M. Le

Bras, R. Delobel, P. Bréant and J. M. Trémillon, *Fire Mater.,* in the press.
4 S. Bourbigot, P. Bréant, R. Delobel and M. Le Bras, *Fr. Demande* 9 307 387, 1993 and *EU Pat.* 94 401 316.8, 1994, (Elf Atochem).
5 *Standard Test Method for Measuring the Minimum Oxygen Concentration to Support Candle-like Combustion of Plastics,* ASTM D2863/77, Philadelphia.
6 K. Kishore and K. Mohandas, *Combust. Flame,* 1981, **43**, 145.
7 S. Bourbigot, M. Le Bras, R. Delobel, P. Bréant and J. M. Trémillon, *Carbon,* 1995, **33**, 283.
8 S. Bourbigot, Doctoral Dissertation, University of Lille, 1993.
9 J. G. Powles and J. H. Strange, *Proc. Phys. Soc.,* 1963, **82**, 6.
10 M. Golman and L. Shen, *Phys. Rev.,* 1966, **144**, 321.
11 T. T. P. Cheung and B. C. Gerstein, *J. Appl. Phys.,* 1981, **52**, 5517.
12 R. Delobel, M. Le Bras, N. Ouassou and F. Alistiqsa, *J. Fire Sci.,* 1991, **8**, 85.
13 G. Camino, in *Actes du 1er Colloque francophone sur l'Ignifugation des Polymères,* ed. J. Martel, Saint-Denis, France, 1985, p. 36.
14 G. Camino, L. Costa and L. Trossarelli, *Polym. Degrad. Stab.,* 1985, **12**, 213.
15 S. Bourbigot, M. Le Bras, L. Gengembre and R. Delobel, *Appl. Surf. Sci.,* 1994, **81**, 299.
16 *The Coblenz Society Desk Book of Infrared Spectra,* ed. C. D. Craver, Kirwood, 1980.
17 D. W. Mac Kee, C. L. Spiro and E. J. Lamby, *Carbon,* 1984, **22**, 285.
18 N. Ouassou, Doctoral Dissertation, University of Lille, 1991.
19 R. S. Brown, R. Anderson and L. J. Shannon, *Adv. Chem. Eng.,* 1968, **7**, 68.
20 R. A. Nyquist, *Appl. Spectrosc.,* 1957, **11**, 161.
21 J. R. Van Wazer, C. F. Callis, J. N. Shoolery and R. C. Jones, *J. Am. Chem. Soc.,* 1956, **78**, 5715.
22 T. M. Duncan and D. C. Douglass, *J. Chem. Phys.,* 1984, **87**, 339.
23 G. E. Maciel, V. J. Bartuska and F. P. Miknis, *Fuel,* 1979, **58**, 391.
24 G. E. Maciel, M. J. Sullivan, L. Petrakis and D. W. Grandy, *Fuel,* 1982, **61**, 411.
25 G. Camino, L. Costa, G. Clouet, A. Chiotis, J. Brossas, M. Bert and A. Guyot, *Polym. Degrad. Stab.,* 1984, **6**, 105.
26 Y. Schmidt-Le Tallec, Doctoral Dissertation, University of Lille, 1992.
27 S. K. Brauman, *J. Fire Retardant Chem.,* 1981, **8**, 8.
28 G. Montaudo, E. Scamporino and D. Vitalini, *J. Polym. Sci.,* 1983, **21**, 3361.
29 K. Kishore and K. Mohandas, *Combust. Flame,* 1981, **43**, 145.
30 M. U. Hasan, M. F. Ali and A. Bukhari, *Fuel,* 1983, **62**, 518.
31 W. L. Earl and D. L. Vanderhart, *J. Magn. Reson.,* 1982, **48**, 35.
32 S. Supaluknari, I. Burgar and F. P. Larkins, *Org. Geochim.,* 1990, **15**, 509.
33 S. Bourgibot, M. Le Bras and R. Delobel, *Carbon,* 1993, **31**, 1219.
34 S. F. Dec, C. E. Bronnimann, R. A. Wind and G. E. Maciel, *J. Magn. Reson.,* 1989, **82**, 454.
35 C. E. Bronnimann, B. L. Hawkins, M. Zhang and G. E. Maciel, *Anal. Chem.,* 1988, **60**, 1743.
36 L. M. Ryan, R. E. Taylor, A. J. Paff and B.C. Gerstein, *J. Phys. Chem.* 1980. **72**. 508.
37 G. Engelhart, U. Lohse, M. Mägi and E. Lippmaa, *Structure and Reactivity of Modified Zeolites,* in *Studies in Surface Science and Catalysis,* ed. P. A. Jacobs, N. I. Jaeger, P. Jiru, V. B. Kazansky and G. Schulz-Ekloff, Elsevier, Amsterdam, 1984, vol. 18, p. 23.
38 M. Stöcker, *Advanced Zeolite Science and Applications,* in *Studies in Surface Science and Catalysis,* ed. J. C. Jansen, M. Stöcker, H. G. Karge and J. Wiekamp, Elsevier Science, Amsterdam, 1994, vol. 85, p. 427.
39 D. Müller, G. Berger, I. Grunze, G. Ladwig, E. Hallas and C. Haubenreisser, *Phys. Chem. Glasses,* 1983, **24**, 37.
40 D. Müller, W. Gessner, H. S. Benrens and G. Sheler, *Chem. Phys. Lett.,* 1981, **79**, 59.
41 D. Müller, D. Hoebbel and W. Gessner, *Chem. Phys. Lett.,* 1981, **84**, 25.
42 R. Dupree and D. Holland, *Glasses and Glass-ceramics,* Chapman & Hall, London, 1989.
43 N. Bloembergen, *Physica,* 1949, **15**, 386.
44 A. Abragam and M. Goldman, *Nuclear Magnetism: order and disorder,* Oxford University Press, Oxford, 1982.
45 J. McBrierty and D. C. Douglass, *J. Polym. Sci., Macromol. Rev.,* 1981, **16**, 295.
46 J. McBrierty and D. C. Douglass, *Phys. Rep.,* 1980, **63**, 63.
47 S. Kaufman and D. J. Bunger, *J. Magn. Reson.,* 1970, **3**, 218.

Synergy in intumescence—application to β-cyclodextrin carbonisation agents in intumescent additives for fire retardant polyethylene formulations.

Michel Le Bras,[a]* Serge Bourbigot,[a] Yannick Le Tallec[a,b] & Jacky Laureyns[c]

[a]*Laboratoire de Physico-Chimie des Solides, E.N.S.C.L., Université des Sciences et Technologies de Lille, BP 108, F-59652 Villeneuve d'Ascq Cedex France*
[b]*Centre de Recherches et d'Etude sur les Procédés d'Ignifugation des Matériaux (CREPIM), Zone Initia, F-62 Bruay la Bussière France*
[c]*Laboratoire de Spectrochimie Infrarouge et Raman, UPR CNRS A-2631L, U.S.T.L., F-59 Villeneuve d'Ascq France*

(Received 8 May 1996; revised 28 July 1996; accepted ??)

The study first compares the FR performances of ammonium pyrophosphate (PY)–xylitol, PY–d-sorbitol and PY–β-cyclodextrin additives systems with the classical ammonium polyphosphate–pentaerythritol intumescent system in low density polyethylene(LDPE)-based formulations.

It shows that β-cyclodextrin, a starch derivative, whose thermal degradation leads to high amounts of carbonaceous residue, is not a carbon source of interest in intumescent FR additives for LDPE-based formulations. A comparative study using X-ray diffraction and Raman spectroscopy shows that the absence of the FR property may be connected both to the development of a free radical reaction in the additive system in the temperature range corresponding to processing reactions and to the presence of a crystalline phase in the carbonaceous materials formed from the additive.

Secondly, it is shown using the Sheffé procedure for experiments with mixtures that a synergistic effect exists in the ammonium pyrophosphate–d-sorbitol–β-cyclodextrin system. In particular, the method gives the corresponding composition of the additive mixture. The improved performance is explained by the formation of a large amount of carbonaceous residue when the formulation degrades. Moreover, the synergistic effect is discussed as a competition between antagonistic effects related to chemical characteristics of the char: amounts of free radical in carbon, structural organisation of the char and the presence of crystalline phases.

1 INTRODUCTION

Intumescent technology[1,2] has recently found a place in polymer science as a method of providing flame retardancy to polymeric materials.[3,4] On heating fire retardant (FR) intumescent materials form a foamed cellular charred layer on their surfaces, which protects the underlying materials from the action of heat flux and flame. The proposed mechanism is based on the charred layer acting as a physical barrier, which slows down heat and mass transfer between the gas and the condensed phase.[5,6]

Generally, intumescent formulations contain three ingredients: an acidic source (precursor of a carbonisation catalyst (CP)), a polyhydric compound (carbonisation agent (CA)) and a blowing agent. Ammonium orthophosphoric acid salts,[7] diammonium pyrophosphate (PY)[8] and ammonium polyphosphate (APP)[9,10] have been previously used as a CP in association with several CA (cellulose derivatives[11] or pentaerythritol (PER))[10] in carbonising and/or intumescent additive mixtures. The phosphoric

2

acids salts also act as blowing agents because their thermal degradation leads to evolution of water and ammonia.

Recently, we have developed new intumescent additive mixtures for FR polyolefins (polypropylene (PP) and polyethylene) which contain polyols produced by the agrochemical industry.[12] In particular, we reported that FR properties of interest are obtained using PY–xylitol (XOH) or PY–d-sorbitol (SOH) additive mixtures in PP-based formulations.[13]

XOH and SOH alone show the same thermal behaviour as PER, i.e. their thermo-oxidative degradations do not lead to the formation of large amounts of carbonaceous materials when the degradation temperature $T > 350°C$ (illustrative thermogravimetric (TG) curves reported in Fig. 1).

On the other hand, several dextrins (starch derivatives) and most particularly, β-cyclodextrin: cycloheptaamylose $((O-[C_5H_5(OH)_3O])_7$; BCOH) show thermal degradations which lead to the formation of comparatively large amounts of carbonaceous residues when $300 < T < 450°C$ (TG curve of BCOH reported in Fig. 1 (curve c)). A direct relation between FR properties (and most particularly, the limiting oxygen index (LOI))[14] and the carbonisation mode and/or the amount of stable carbonaceous material formed from FR formulations had been previously reported.[3,15] Thus, the use of BCOH as a carbonisation agent in FR additive systems seems to be promising.

This work compares the FR properties of the APP–PER, PY–XOH, PY–SOH and PY–BCOH binary additive systems in low density polyethylene (LDPE)-based formulations. The

observed differences between the FR performances is explained by the thermo-oxidative behaviour of the additive systems studied using thermogravimetric analysis (TG) and the structures of the carbonaceous residues formed during their degradation processes, studied using X-ray diffraction (XRD) and Raman spectroscopy which are methods developed for classical studies of synthetic carbons and fossil coals.

Moreover, eventual synergistic effects between two carbonisation agents (BCOH considered as a synergistic agent (SA)) were sought using the Scheffé procedure (simplex lattices) for experiments with mixtures and as a consequence, the use of BCOH as an active 'carbon' source will be evaluated. Chemical phenomena which occur during the intumescence process have been previously reported.[1,6,8–10,12,13] As a matter of fact, the study will discuss the observed FR effects using previously studied characteristics of the char and previously proposed relations between these characteristics and FR performances.

2 EXPERIMENTAL

2.1 Materials

2.1.1 Raw materials
The polymer was LDPE (LACTENE supplied as powder by Elf Atochem, melt index 20 g/10 min at 190°C).

The CP were APP $((NH_4PO_3)_n$, $n = 700$, Hoechst Exolit 422, soluble fraction in H_2O: < 1 wt %) and PY synthesised[12] using the procedure of Swanson *et al.*[16] (reaction of NH_3 with $H_4P_2O_7$ in ethanol at a temperature lower than 10°C). In fact, PY is a mixture of ammonium orthophosphate, pyrophosphate and polyphosphate with more than 50 wt. % of diammonium pyrophosphate).

The CA were PER (Aldrich R.P. grade), XOH (Aldrich, 98 wt. %), SOH (supplied by Aldrich, 97 wt. %) and BCOH (Roquette Frères (Lestrem - France)).

2.1.2 Formulations
Table 1 reports the compositions of the additive mixtures. Chosen [CP/CA] and [SA/(SA + CP + CA)] ratios correspond to the higher synergistic effect observed in the LOI curves or to compositions imposed by the experiments with mixtures.
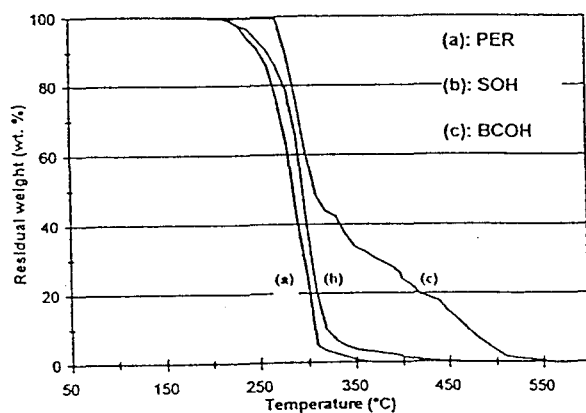

Fig. 1. TG curves of pentaerythritol, d-sorbitol and β-cyclodextrin under air flow.

Table 1. Composition of the additive mixtures

Mixture label	CP	CA	SA	CA/(CA + CP) (wt. %)	SA/(CP + CA + SA) (wt. %)
I	APP	PER	—	25	0
II	PY	XOH	—	33·33	0
III	PY	SOH	—	33·33	0
IV	PY	BCOH	—	66·66	0
V	APP	PER	BCOH	*	*
VI	PY	XOH	BCOH	*	*
VII	PY	SOH	BCOH	*	*

* 13 different mixtures which compositions imposed by the procedure for experiments with mixtures which compositions are reported in Table 3.

This study was carried out using the LDPE/(LDPE + additive) ratio: 70 wt. % which allows V0 rating and LOI > 30 % using the APP–PER system. Mixtures were first prepared by ball-milling after mechanical grinding and sieving (200×10^{-6} m) of the raw materials. The additives were then incorporated in LDPE. Sheets ($100 \times 100 \times 3$ mm^3) of each formulation were obtained after ball-milling, using a Darragon compression press at 200°C with a pressure of 3 MPa.

Before each spectroscopic analysis, isothermal treatments of the additive mixtures were carried out under air flow (10^{-5} m^{3}s^{-1}) at the characteristic highest temperatures of treatment (HTT) deduced from TG experiments (after Refs 12 and 13) during the time required to reach a stationary state, i.e. weight loss rates vs time became null. These HTT and materials resulting from the thermal treatment are presented in Table 2.

Corresponding reactions have been reported

previously (formulation I [Refs 4, 6 and 12]) or are presented as results (formulations II, III and IV) in this text.

2.1.3 Protocol for experiments with mixtures
The study was carried out assuming that the polymer acts only as an inert diluent and may be ignored in the analysis. So, the factor space in the mixture is a regular {3–1} dimensional simplex, i.e. a triangle (Fig. 2).

The FR property (in terms of the quantitative variable LOI) the so-called response is assumed to be a real-value function of the simplex. We studied this response using NEMROD (software commercialised by LPRAI (IUT G. Berger, Aix en Provence) which develops the Scheffé sequential procedure. The model used ({3–3} lattice, i.e. canonical reduced cubic model) needs seven experimental mixtures (circles in Fig. 2, numbers of the circles correspond to the numbers of the experiments in Table 3). Six additional

Table 2. Characteristics of materials resulting from the thermal treatment of the LDPE-based formulations

Additive mixtures	HTT (°C)	Treatment time (h)	Resulting material	Ref.
I	225	12	yellow polymer, esters formations from additive	8, 6
	350	12	intumescent material	12
	430	12	non-expanded 《carbon》 residue	12
	560	12	non-expanded 《carbon》 residue	12
II	230	12	brown polymer, esters formations from additive	12
	320	12	intumescent material	
	430	12	no expanded 《carbon》 residue	
	530	12	no expanded 《carbon》 residue	
III	230	12	brown polymer, esters formations from additive	12
	320	12	intumescent material	
	430	12	no expanded 《carbon》 residue	
	530	12	no expanded 《carbon》 residue	
IV	230	2d	black polymeric material	12
	320	24	carbonaceous glassy material	
	430	24	no expanded 《carbon》 residue	

4

Fig. 2. {3-3} lattice used for experiments with mixtures.

with x_1, x_2 and x_3 the respective concentrations of CP, CA and SA and with b_{ij} the computed effect coefficients (interaction terms with j the interaction order). These terms are limited by the procedure to first order terms (related to main effects and first order interactions effect) and to second and third order terms (corrective terms which representation in the effect decreases with the order).

A preliminary study in the whole of the possible mixture composition failed because the difference Δ between the computed and the experimental LOI values were higher than 1% (assumed higher confidence limit: 0·8 %). So, reduced coordinates (x_1, x_2 and x_3 in the upper triangle in Fig. 2) corresponding to comparatively low amounts of BCOH, were used. The relative concentrations of the components of the studied mixtures are presented in Table 3.

Higher order models may be used for more corrections, but they need higher numbers of experiments and tests. Calculated differences between experimental values of the LOI and computed corresponding values are low enough to consider that a third order model allows a good representation of the LOI changes vs an additive mixture composition.

experiments (squares in Fig. 2, squares 8 to 13 correspond respectively to tests 1 to 6 in Table 3) are needed to test the method.

The mathematical model associated with the chosen experiment matrix is

$$LOI = b_1 x_1 + b_2 x_2 + b_3 x_3 + b_{12} x_1 x_2 + b_{13} x_1 x_3$$
$$+ b_{23} x_2 x_3 + b_{123} x_1 x_2 x_3$$

Table 3. Composition of the three components systems used for experiments with mixtures

Mixture	Phosphate wt. %	Polyol wt. %	BCOH wt. %
experiment 1	83·3	16·7	0
experiment 2	50	50	0
experiment 3	50	16·7	33·3
experiment 4	66·7	33·3	0
experiment 5	66·7	16·6	16·6
experiment 6	50	33·3	16·7
experiment 7	61·1	27·8	11·1
test 1	61·1	38·9	0
test 2	72·2	27·2	0
test 3	61·1	16·7	22·2
test 4	72·2	16·7	11·1
test 5	50	27·8	22·2
test 6	50	38·9	11·1

2.2 Fire testing

LOI (Minimum Oxygen Concentration to Support Candle-like Combustion of Plastics) was measured using a Stanton Redcroft instrument on sheets ($120 \times 60 \times 3$ mm^3) according to the standard oxygen index test.[14] As an example, unmodified LDPE shows an LOI value of 17%.

UL-94 classification was obtained on sheets ($8 \times 60 \times 3$ mm^3) according to the conditions of the standard test[17] which provides only a qualitative classification of the samples (V0, V1, V2 and not classed (NC) labelled samples).

2.3 Thermogravimetric analyses

TG analyses were carried out at 7·5°C/min under synthetic air (flow rate $= 5 \cdot 10^{-7}$ m^3/s; Air Liquide grade) using experimental conditions previously described.[6] The curves of weight difference (Δ(T): difference between the experimental TG curves of the LDPE-based material and the TG curves corresponding to the combination of the weight loss of the HDPE alone and the weight loss of the considered two or three components

additive mixtures which contain the phosphate CP) were computed vs the temperature using a previously described procedure.[8] $\Delta(T)$ curves allow an eventual increase or decrease of the thermal stability of the polymeric formulations to be pointed out and to show the presence of stable products resulting from their thermo-oxidative degradations.

2.4 Spectroscopic study

2.4.1 X-ray diffraction
XRD spectra were recorded in the $10°-40°$ 2θ range using a 2 circles diffractometer (D5000 Siemens, 40 keV and 20 mA) using the $CuK_{\alpha 1,2}$ radiation and an Ni monochromator. Maxima of the diffraction line and full-widths at half-maximum. were measured using the Siemens DIFFRACT AT software. Sizes of crystalline carbonaceous structures were calculated using the simplified Debye–Sherrer relation.

2.4.2 Raman diffusion
Raman microprobe examinations were performed using a microspectrometer having spectrographic dispersion and multichannel detection (Microdil 28–Dilor). The optical beam produced by a continuous wave Ar laser entered in a microscope and was directed onto an objective that focused it to a one-micrometer spot on the sample surface. To avoid sample heating the power was kept below 4 mW. Subsequent visual examination of the surface was systematically made in order to check that no alteration had occurred around the focal point. In a typical experiment, the laser wavelength was 514·5 nm and the value of the spectral split width was $9\,cm^{-1}$.

3 RESULTS AND DISCUSSION

Table 4 reports the results of the fire retardancy tests depending on the additives used. It shows that all the formulations present an FR character

Table 4. Results of the fire retardancy tests of the binary formulations

Mixture label	I	II	III	IV
LOI (%)	30	26	23·5	21
UL-94	V0	V0	V0	NC

NC: not classed by the test

but that the (PY–BCOH) system does not admit an UL-94 rating because of both dripping and cumulative combustion time are higher than 70 s.

FR performances of intumescent formulations have to be explained using previous studies of our Laboratory: the effect results from several additional or antagonistic relations between effects assigned to chemical and/or physical characteristics of the char and the FR properties:

1. FR performance increases when the amount of acidic species in the char (phosphate species stable in the temperature range $28°-430°C$[8] or $280-560°C$[6,10,18] increases. The activity of these acidic species is explained, firstly, by the formation of esters resulting from the reactions of these species with oxidised products resulting from the thermo-oxidative degradation of the polymeric matrix and of the char. In another way, a further carbonisation process takes place[8,19] which leads to the formation of polyaromatic stacks. It is obvious that the formation of esters and of polyaromatic species in the condensed phase corresponds to a decrease of the mass transfer from the material to the flame,

2. the FR performance increases when the amount of 'active carbon' in the intumescent and the non-expanded materials increases.[20,21] 'Active carbon' corresponds to free radical polyaromatic species or free radicals trapped in polyaromatic stacks. This species decreases the mass transfer via termination reaction with radical gaseous products resulting from the degradation of the polymer or radical products resulting from the degradation of the protective materials in the condensed phase,

3. the FR performance increases when a coherent structure forms in the mobile (in an NMR sense) phase of the intumescent material.[22] This structural change directly affects the dynamic property of interest of the material,

4. the FR performance decreases when a part of the turbostratic carbon which constitutes the protective char transforms (structural change and/or coalescence) into mesophase or at least into precursor of mesophase.[23] The corresponding 'rigid' domain is proposed as an initiator for the formation of cracks in the coating. As a consequence,

6

'encapsulated' gases (products of the degradation of the polymer) evolve and contribute as 'fuels' to the flame,

5. finally, the FR performance decreases when the size of the crystalline phases in the protective material increases.[24] These phases may play the same part as the mesophase.

Moreover, recent results of this Group (Bourbigot, S. and Morice, L., unpublished results) show that other physical parameters, such as density, Cp and thermal conductivity have to be considered. These last parameters and amounts of acidic species (acidic phosphate species are observed using ^{31}P NMR of solids in every formulation) will not be considered in the further discussion.

To investigate the reactive character of the carbonaceous material, a thermogravimetric study of the additive mixtures is carried out. Fig. 3 presents typical TG curves.

PY–XOH and PY–SOH degradation curves are nearly the same, so the degradation of PY–SOH is only reported as an illustration in Fig. 6. These two additive systems present the same thermal behaviour as APP–PER. Three reaction steps are observed: formation of phosphate esters in the 170–290°C range,[8,12] formation of an expanded phosphocarbonaceous material relatively stable up to 470°C (APP–PER) or 530°C (PY–XOH and PY–SOH) and finally, formation of a stable 'high temperature' residue (residual weight: about 2 wt. % with the three additive systems) when T > 600°C.

On the other hand, the PY–BCOH system

presents a very different behaviour. The observed three reaction steps correspond respectively to a dehydration process (70 < T < 100°C), a carbonisation process with formation of a glassy carbonaceous material (130 < T < 550°C) and finally to the formation of a stable 'high temperature' residue (T > 600°C) in a comparatively high amount (about 8 wt).

The sequences

FR properties:	I > II > III ≫ IV,
amounts of carbonaceous material (300 < T < 550°C):	I > IV > II = III,
and amounts of 'high temperature' residue:	IV ≫ I = II = III

are not the same. So, a direct relation between the considered data may not be proposed. Different 'qualities' (activity or physical properties) of the materials which form via the thermal degradation of the additive systems have therefore to be assumed.

The spectroscopic study of materials corresponding to each step of the thermal degradation of the systems allows their characterisation. The signals of the APP–PER, PY–XOH and PY–SOH systems are quite similar[12] and therefore, the spectra of the PY–SOH system are only reported as illustrations.
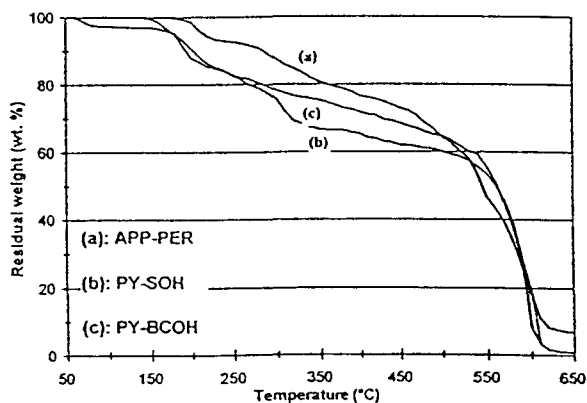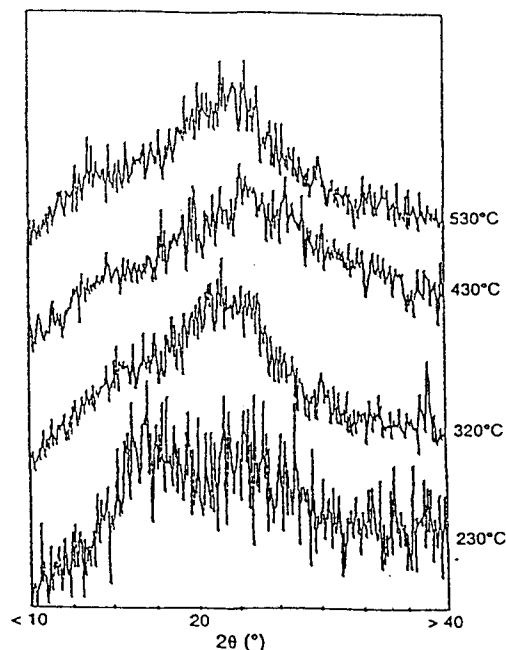
The XRD spectrum of the three FR systems

Fig. 3. Experimental TG curves of the ammonium polyphosphate–pentaerythritol (a), ammonium pyrophosphate–d-sorbitol (b) and ammonium pyrophosphate–β-cyclodextrin (c) additive systems.

Fig. 4. XRD spectra of the PY–SOH system treated at the HTT indicated.

(Fig. 4) presents, when HTT > 290°C, a single broad signal at 2θ about 23° which may be assigned to the conventional d_{002} diffraction of isotropic turbostratic carbon.[25] The size of the corresponding crystalline domains are approximately the same (about 4 nm) in the three intumescent materials.

The XRD spectra of the PY–BCOH system Fig. 5) present, when HTT < 180°C, diffraction peaks which may be assigned to polyphosphate species,[20] and when 255 < HTT < 350°C, well resolved peaks (assigned to new phosphorus-based crystalline species) in overlap with the broad signal of carbon observed when HTT > 320°C.

A comparison of the spectra sets shows that the whole of the crystalline phosphate species are destroyed probably via the esterification process which takes place at 190°C[8,12] in the APP–PER, PY–XOH and PY–SOH systems. On the other hand, the participation of PY in an esterification process when T < 350°C is not likely in the PY–BCOH system. The presence of crystalline or structurally organised phases in the last system explain as previously discussed, its poor FR performance.

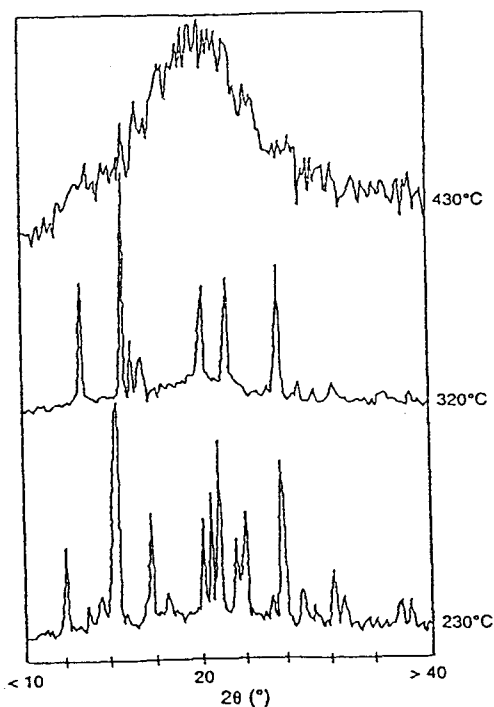Raman spectroscopy is a powerful tool for the characterisation of a carbonaceous material. The spectrum consists in the overlap of two diffusion bands at about 1580 cm^{-1} and 1360 cm^{-1} which are characteristic of pre-graphitic structures. The first one is assigned to the E_{2g} vibrational mode, when the second results from defects in the structure. Figure 6 presents the relative changes of the two bands vs the structural Organisation level of the 'carbon'.[26] These changes in frequency, relative intensity and widths of the bands have been observed by several authors and related to the graphitization degree.[27]

Figures 7 and 8 detect the beginning of the carbonisation process and compare the levels of organisation of the carbonaceous materials at each HTT. The signal of a 'carbon' material is discriminated from the intense ‑fluorescence background with HTT = 130°C and HTT = 230°C respectively with the PY–BCOH system and with the APP–PER, PY–XOH and PY–SOH systems.

The low temperature carbonisation process of PY–BCOH involves a low temperature free radical mechanism and so, the formation of a large amount of free radicals during the 200°C-high pressure processing of the polymeric material. These free radical species may be initiators for a free radical reaction in the polymer matrix which increases the amount of 'defects' (low molecular weight macromolecules resulting from the LDPE chain breaking, free radicals in the polymer chain which eventually react with absorbed molecular oxygen to form hydroperoxides and peroxides species which take a main part in the 'low temperature' degradation of the polymer). Resulting modifications of the chemical and physical properties may affect the
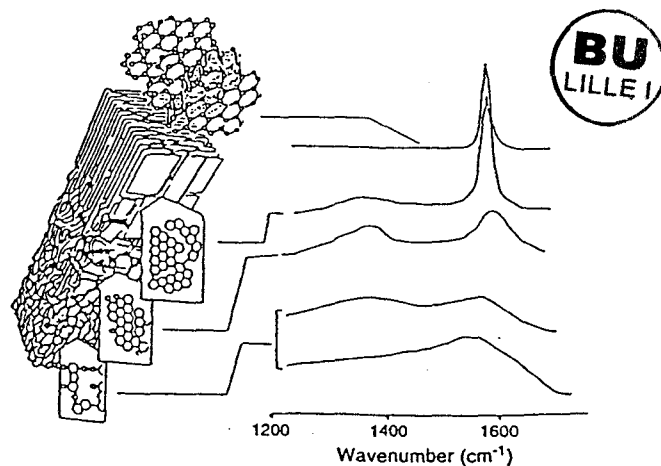

Fig. 5. XRD spectra of the PY–BCOH system treated at the HTT indicated.

Fig. 6. Raman spectra evolution from a carbonaceous material to graphite.[26]
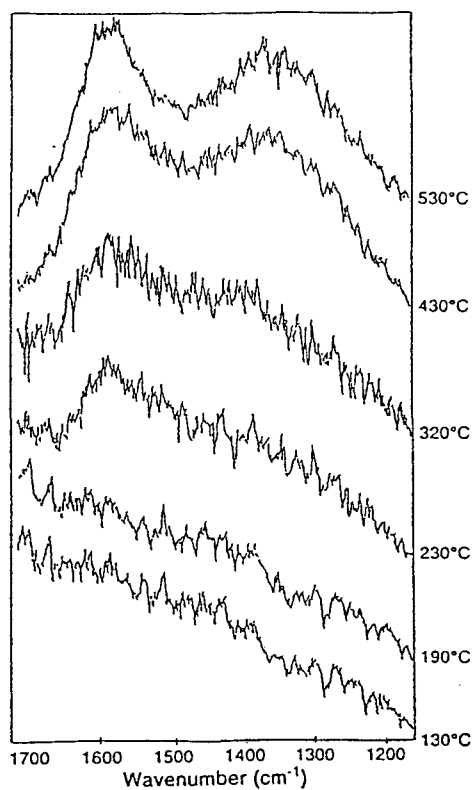
8

Fig. 7. Raman spectra of the PY–SOH system treated at the HTT indicated.
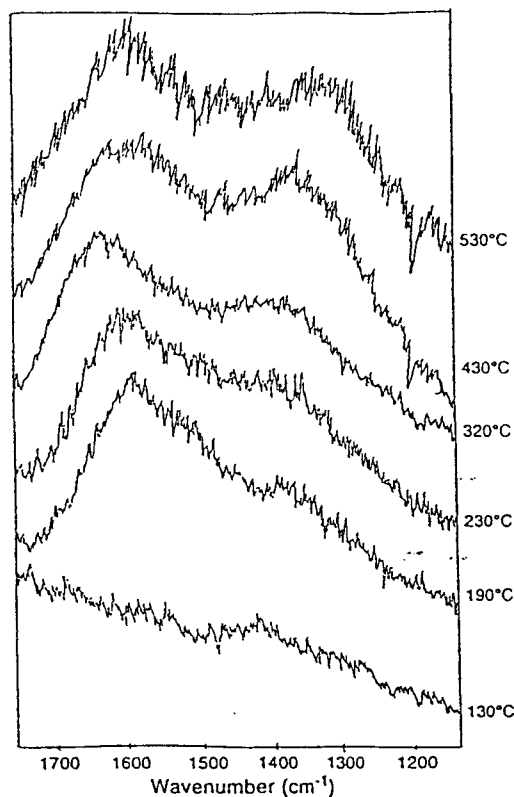

Fig. 8. Raman spectra of the PY–BCOH system treated at the HTT indicated.

dynamic properties of the polymeric matrix. This modification may so explain that the LDPE–PY–BCOH formulation does not admit an UL-94 classification (rating is directly related to the dynamic properties via melting and dripping).

Moreover, the Raman spectra of every formulation when HHT is equal or higher than 230°C, are quite similar. A same structural Organisation of the carbonaceous material may then be assumed depending on the conditions of the thermal treatment.

The LOI value is directly related to the regime of the upper flame. Heat transfer from the flame to the material affects the mass transfer from the material to the flame and as a consequence, the 'fuel' feeding of the flame. The structural organisations of the carbonaceous materials which compose the protective shields in the temperature range corresponding to the main degradation of the polymeric matrixes (300 < T < 400°C in the experimental conditions) do not then allow the explanation of the comparatively low FR performance of the formulation IV in term of LOI. This observation seems to confirm that the absence of FR property may be directly

assigned to the presence of crystalline phosphate species in the carbonaceous and/or phosphocarbonaceous material.

To summarise the first set of results, we propose that the FR properties are affected by the presence of a crystalline phase in the protective material and by the formation of a large amount of free radicals (about 10^{20} spins/kg in PY–BCOH heat treated at 190°C)[13] from the additives during the processing of the formulation. Moreover the study shows that BCOH in the additive system leads to the formation of a comparatively high amount of 'high temperature' carbonaceous residue

As a consequence the addition of BCOH to an intumescent phosphate-polyol formulation is assumed to increase the amount of 'high temperature' residue which acts as a protective thermal barrier during the FR process. Relatively low amounts of BCOH should be added to avoid the formation of a high amount of reactive free radicals during the processing of the polymeric formulations.

Crystalline phosphate species are not observed in the intumescent materials (their XRD spectra

300

only present the d_{002} reflection of carbon) because of ester formation via a reaction with PER, XOH and SOH

The Scheffé procedure gives three model equations

Formulation V

$$LOI = 23x_1 + 27x_2 + 22x_3 + 20x_1x_2 + 10x_1x_3$$
$$- 6x_2x_3 - 18x_1x_2x_3$$

Formulation VI

$$LOI = 22x_1 + 26x_2 + 23x_3 + 8x_1x_2 + 6x_1x_3$$
$$- 2x_2x_3 - 27x_1x_2x_3$$

Formulation VII

$$LOI = 23x_1 + 23x_2 + 23x_3 + 4x_1x_2 + 8x_1x_3$$
$$- 4x_2x_3 - 33x_1x_2x_3$$

Values of the inflation factors (F) are $1 < F < 1.8$ and check the validity of the model. Moreover the difference A between the computed and the experimental values of the LOI of each tested point (average $\Delta < 0.6\%$) remains close to the experimental error. Figures 9–11 present the LOI of LDPE formulations containing respectively the APP–PER–BCOH, PY–XOH–BCOH and PY–SOH–BCOH systems.

Testing the two first systems, the LOI values are almost a linear combination of the LOI values of the binary systems: addition of BCOH in the additive mixtures leads to the decrease of the FR performance.

On the other hand, LOI values in the last additive system show that a synergistic effect exists. A precise study in the LOI = 26% surface
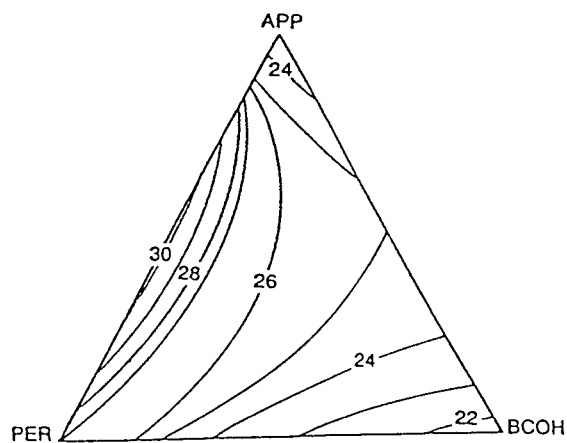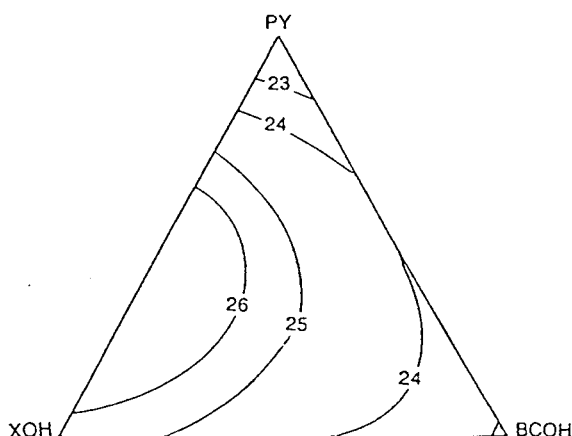

Fig. 10. LOI values of LDPE–PY–XOH–BCOH formulations in the (3–3) lattice used for experiments with the mixture.

confirms the increase of the performance, the optimised additive mixture (LOI 26.5 ± 0.5%, V0 rating) is composed of PY: 62 wt. %, SOH: 25.7 wt. % and BCOH: 12.3 wt.

Synergy in intumescent formulations has to be explained. We propose that it results from the reported additional or antagonistic effects. Figure 12 shows a representation of these effects. Presented relations are only arbitrarily schematic relations, effects 3 and 4 are linked in the same curve assigned to the part played by the structural Organisation of the 'carbon'. Addition of the effects allows us to plot a typical synergy curve.

The protective FR mechanism which occurs in formulations presenting the synergistic effect does not result from the proposed effects 4 and 5, indeed the spectroscopic study of the chars
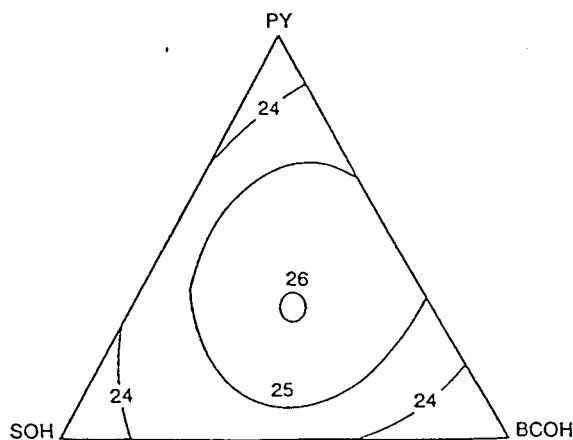

Fig. 9. LOI values of LDPE–APP–PER–BCOH formulations in the (3–3) lattice used for experiments with the mixture.

Fig. 11. LOI values of LDPE–PY–SOH–BCOH formulations in the (3-3) lattice used for experiments with the mixture.
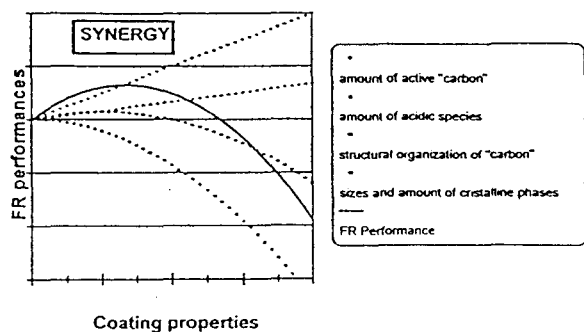
Fig. 12. Schematic assignments of the part played by chemical and physical properties of a carbonaceous intumescent coating on its FR performances.

Fig. 14. Weight difference curve of the LDPE–PY–BCOH formulation.

resulting from the thermal degradation of the optimal LDPE–PY–SOH–BCOH formulation does not show either the presence of a crystalline phase or any significant difference in the structural organisation between chars resulting from the degradations of the tested systems. The part played by BCOH in the increase of the performance may be deduced from a thermogravimetric study which compares the thermooxidative degradations of LDPE–PY–SOH, LDPE–PY–BCOH and the optimal LDPE–PY–SOH–BCOH formulation.

Weight difference curves (Figs 13–15) allow the calculation of the amounts of LDPE which are protected by the insulative shield arising from the additive mixture degradation and/or may participate in the protection of the formulation via links of its chains in the coating.[6,22] They show that that a part of the polymeric product (about 40 wt. % of LDPE–PY–SOH and LDPE–PY–SOH–BCOH and 25 wt. % with LDPE–PY–BCOH) is conserved in every carbonaceous material which forms during the intumescence or carbonisation processes which takes place in the 350–420°C range. This HDPE preservation explains the observed FR properties of the formulations.

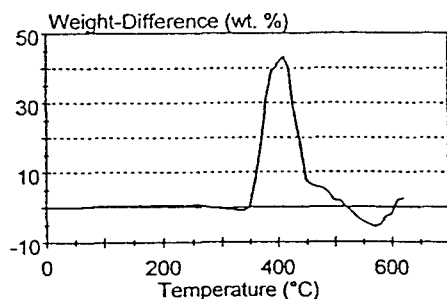The degradation of the carbonaceous material

in the 420–450°C range then leads to the formation of non-foamed carbonaceous residues which degrade in the 500–550°C range. The amount of residue formed from LDPE–PY–SOH–BCOH is twice as important as those formed from the LDPE–PY–SOH formulation. The increase of the FR performance may then be related to the presence of this residue. Moreover, TGA shows that the 'high temperature residue' formed from the optimised formulation is stable in a highest temperature range (T > 600°C).

The observed participation of LDPE in the formation of the residue may be discussed considering a free radical polymerisation process involving free radicals formation in the additive systems. The formation of these radicals has been previously studied: the concentrations of the trapped free radicals at 320 and 430°C are respectively $10^{22.3}$ and $10^{20.5}$ spins/kg in PY–SOH and $10^{20.9}$ and $10^{19.5}$ spins/kg in PY–BCOH.[13] Consequently, the chars resulting from PY–SOH–BCOH may be assumed reactants in polymerisation.

The increase of the FR property may be explained by the formation of the residue and the 'high temperature' residue involving LDPE degradation products. This formation lowers the evolution of flammable products during the degradation of the material and in addition,
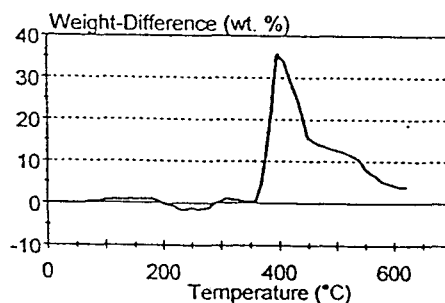

Fig. 13. Weight difference curve of the LDPE–PY–SOH formulation.

Fig. 15. Weight difference curve of the LDPE–PY–SOH–BCOH formulation.

the residue acts as an additional thermal protective material on the surface of the material.

The maximum of the FR performances obtained from a particulate formulation composition, i.e. the synergistic effect, then corresponds to a balance between the amount of the residues formed (related to the amount of eventually 'active' carbons) and the loss of the dynamic properties of interest related to the presence of crystalline phosphate species in the system when the initial concentration of BCOH is too high and as a consequence, the concentration of SOH too low to allow the reaction of all these species to form esters.

To conclude, increases of the FR property of intumescent polymer formulations are achieved using synergistic additive systems. These systems may be formulated considering the proposed antagonistic effects.

4 CONCLUSION

The study shows that β-cyclodextrin, a starch derivative, whose thermal degradation leads to high amounts of carbonaceous residue and so may be a typical carbon source for intumescence, is not a good carbon source in intumescent FR LDPE-based formulations, as compared to similar compounds (pentaerythritol, xylitol and d-sorbitol).

A comparative spectroscopic study reveals that the absence of UL-94 rating of PY–BCOH–LDPE formulations may be connected to the development of a free radical reaction in the additive system in the temperature range corresponding to processing. Moreover, it is proposed that the presence of a crystalline phase in the carbonaceous materials formed from PY–BCOH does not permit the protective property of interest to the intumescent materials and so explains the poor LOI value.

The Sheffé procedure for experiments with mixtures allows to point out a synergistic effect in the LDPE–PY–SOH–BCOH formulation and gives the optimised composition of the corresponding additive system.

Finally, the study proposes that synergy in FR intumescent material results from a competition between antagonistic effects resulting from the chemical properties of this char.

REFERENCES

1. Tramm, H. L., US Patent No. 2106938, 1996.
2. Vandersall, H. L., *J. Fire and Flammability*, 2 (1971) 97.
3. Montaudo, G., Scamporino, E. & Vitalini, D., *J. Polym. Sci., Polym. Chem.*, 21 (1983) 3361.
4. Camino, G., *Actes du Premier Colloque Francophone sur l'Ignifugation des Polymères*, ed. J. Martel, Saint denis, France, 1985 p. 36.
5. Bourbigot, S., Le Bras, M. & Delobel, R., *J. Fire Sci.*, 13(1-2 (1995) 3–22.
6. Bourbigot, S., Le Bras, M., Delobel, R., Decressain, R. & Amoureux, J.-P., *J. Chem. Soc., Faraday Trans.*, 921 (1996) 149–158.
7. Gay Lussac, J. L., *Ann. Chim.*, 182 (1821) 211.
8. Delobel, R., Le Bras, M., Ouassou, N. & Alistiqsa, F., *J. Fire Sci.*, 8 (1990) 85.
9. Camino, G., Costa, L. & Trossarelli, L., *Polym. Deg. and Stab.*, 12 (1985) 213.
10. Bourbigot, S., Le Bras, M. & Delobel, R., *Carbon*, 318 (1993) 1219–1230.
11. Leroy, J. M., Walrave, P., Delobel, R., Le Bras, M., Hennette, J.-F. & Le Maguer, D. in *Actes du Premier Colloque Francophone sur l'Ignifugation des Polymères*, ed. J. Martel, Saint Denis, France, 1985, pp. 87; Leroy, J.-M., Walrave, P., Delobel, R., Le Bras, M., Hennette, J.-F. and Le Maguer, D., *R.G.S.*, 1986, 56(8–9), 86.
12. Schmidt-Le Tallec, Y., Valorisation de Différents Polyols dans des Systèmes Retardants de Flamme: Application au Polyéthylène, Doctoral Dissertation, Lille, 1992.
13. Le Bras, M., Bourbigot, S, Delporte, C., Siat, C. and Le Tallec, Y., *Fire and Materials*, FAM 470, in press.
14. *Standard Test Method for Measuring the Minimum Oxygen Concentration to Support Candle-like Combustion of Plastics.* ASTM D2863/77, Philadelphia, 1977.
15. Van Krevelen, D. W., *Polymer*, 168 (1975) 615–620.
16. Swanson, C. & McCullough, F., *Inorg. Synth.*, 7 (1963) 65.
17. *Tests for flammability of Plastic Materials for Part in Devices and Appliances*, Underwriters Laboratories, Northbrook, ANSI/ASTM D635-77.
18. Le Bras, M. & Bourbigot, S., *Fire and Material*, 20 (1996) 39–49.
19. Bourbigot, S., Le Bras, M. & Delobel, R., *J. Fire Sci.*, 13 (1995) 3–22.
20. Le Bras, M., Bourbigot, S., Delporte, C., Siat, C. & Le Tallec, Y., *Fire and Materials*, FAM 577, in press.
21. Le Bras, M., Bourbigot, S., Delporte, C., Siat, C. and Leroy, J.-M., *Proceedings of the 11th Bratislava IUPAC/FECS Int. Conf. on Polymers—Thermal and Photo-induced Oxidation of Polymers and its Inhibition in the Upcoming 21th Century, Stara Lesna (Slovak Republic)*, June 24–28, 1996, ed. L. RICHLA, Slovak Academy of Sci., 1996, pp. 87–88.
22. Bourbigot, S., Le Bras, M., Delobel, R. & Tremillon, J.-M., *J. Chem. Soc., Faraday Trans.*, paper 6/01774 F/FAP, 92, in press.
23. Delobel, R., Bourbigot, S., Le Bras, M., Leroy, J.-M. and Kanovnik, B., *Polimerni Materijali Smanjene Gorivosti*, ed. Z. Janovic, Drustvo Plasticara i Gumaraca pub., Zagreb, 1990, pp. 08/01–08/04.
24. Delobel, R., Le Bras, M., Schmidt, Y. and Bourbigot, S., *Actes du MOFFIS 91—Mineral and Organic Functional Fillers in Polymers, Int. Symp., Le Mans.* 9–12 April 1991, pp. 79–85.
25. Benneth, D., Bradley, J. K. and Tatcher, K. J. F., *J. Appl. Chem.*, 1969, 19, 362; Menon, J.P. (assigned to Monsento Co.), Netherlands Patent No. 6409323, 1963.
26. Griffiths, J. A. and Marsh, H., Baden-Baden Carbon Conference, Baden-Baden, 1980, pp. 17–20.
27. Lespade, P., Al-Jishi, R. & Dresselhaus, M. S., *Carbon*, 205 (1982) 427–431.

III-2-b. Discussion synthétique

La synergie est observée lors de l'ajout d'un SA au mélange d'adjuvants. Pour une certaine teneur en SA, l'amélioration de la propriété n'est plus observée; un effet antagoniste peut, en plus, résulter d'un « excès » de SA.

L'augmentation quantitative de la propriété FR est souvent difficile à apprécier en considérant le classement, résultat d'un test ou d'un ensemble de tests différents. Selon son domaine d'application, le classement du matériau peut être bon, médiocre voire mauvais. A titre d'exemple, Le classement FR de PP/APP/PER résulte :

●de la valeur du LOI = 30.5 ± 0,5 % volumique,

●du classement UL-94 V0,

●du classement NF (P 92-501) M2,(ou M3, selon les conditions de sa transformation)

●du maximum du flux calorifique rhr $\leq$ 500 kW/m^2 (sous une irradiance de 50 kW/m^2, mesuré par calorimétrie de consommation d'oxygène [58]) qui correspond, après corrélation [191], à un matériau de classe A selon la norme suédoise STFI et SNTL (Statens Provingsanstalt),

●du temps d'ignition au calorimètre à cône [192] : t_i = 30 ± 5 s sous une irradiance de 50 kW/m^2,

●de la chaleur dégagée [69, 93, 102] t.h.e. $\leq$ 80000 kJ/m^2.

Cet ensemble de données permet par ailleurs de proposer la classification NBCC 4 du matériau [193].

Une augmentation de la propriété FR est proposée lorsque une ou plusieurs des valeurs des classements initiaux selon les 6 critères retenus sont améliorées sans perte des autres performances lors de l'addition d'un adjuvant à une formulation FR et sans augmentation de la charge en adjuvants.

Le temps d'accès au calorimètre à cône et le prix de revient des expériences obligent à limiter le nombre de mesures de t_i, du rhr et du t.h.e aux seules formulations « performantes ». Les mesures du LOI et le classement UL-94 restent

les outils de classement comparatif. Un effet de synergie dans une formulation FR correspond, dans ces conditions, à une augmentation des LOI lorsque le classement V0 est conservé.

Le kaolin de synthèse et l'argile T2847 sont les seuls SA du système PP/APP/PER/argile. L'incorporation des autres argiles dans la formulation conduit à un effet antagoniste. Néanmoins, l'étude comparative des formulations PP/APP/PER/argile montre l'influence de 18 paramètres chimiques (composition du matériau minéral, structure de ses composants, teneur en eau et stabilité thermique) et de 8 paramètres physiques (propriétés dynamiques et morphologie).

L'absence de liaison entre les variations du LOI et celles du résultat du test UL-94 est bien connue des chimistes et des techniciens des FR. En effet, une formulation de LOI = 26 ± 0,5 % volumique peut admettre un classement UL-94 V0 (NK, T2293 et T2815), V2 (T2371 et T2898) ou ne pas admettre de classement (T2086).

Le résultat du test LOI est fonction du régime de la flamme et doit pouvoir se calculer en considérant les limites supérieures et/ou inférieures des pressions partielles en hydrocarbures dans les mélanges combustibles (la variation de pression en O_2 pouvant, dans les conditions expérimentales, être négligée), présentées par les diagrammes P/T de changement de phase des combustibles solides et liquides [194-195]. Les valeurs faibles du LOI des formulations PP/APP/PER/argile, comparées à celle de PP/APP/PER, peuvent être expliquées par la présence de particules solides (de dimensions de l'ordre du micromètre) dans le revêtement intumescent qui entraîne la perte du caractère imperméable du matériau et la libération d'un flux de fuels suffisant pour alimenter la flamme.

Les variations des valeurs du LOI, selon les caractéristiques des argiles, sont expliquées par la capacité d'échange d'ions des argiles (désalumination et/ou insertion d'espèces phosphates dans le réseau cristallin de l'argile par substitution de Si). L'augmentation de l'indice limite est alors due (par analogie avec les résultat de l'étude des formulations PP/APP/PER/zéolithe) à la formation d'espèces catalytiques P - O - Al et P - O - Si actives. pour la réaction de carbonisation et pour la fixation des chaînes de polymère dans le matériau carboné.

Les valeurs élevées du LOI sont aussi mesurées lorsque les dimensions initiales des particules minérales sont importantes. Ces particules participent au cisaillement lors de l'opération initiale de mélange, conduite en utilisant un plastographe (mélangeur interne de laboratoire). La relation effet thermo-mécanique - ablation - LOI est, à nouveau, observée.

Les classements UL-94 prennent en compte les données de l'ignition : « facilité d'allumage », directement fonction de t_i, et hauteur de la flamme (classement NF), et les propriétés dynamiques du matériau fondu (chute de gouttes éventuellement enflammées). Ce test permet, en fait, une évaluation du caractère protecteur du revêtement intumescent en termes d'imperméabilité aux gaz, d'isolation thermique, mais en plus d'«encapsulation» de liquides dans un matériau solide alvéolaire.

L'étude ne dégage pas de relation entre la réactivité chimique des argiles et les résultats du test UL-94. Les classements sont mauvais pour des argiles dont la déshydratation conduit à l'agglomération des particules et/ou à un retrait à la cuisson. Les matériaux intumescents formés contiennent des particules d'argiles traitées à HTT = 190°C lors du mélange et de la mise en forme et à 280 < HTT < 350°C lors du développement de l'intumescence. L'exposition à la flamme (HTT estimée à 750°C) conduit à la perte d'eau résiduelle des argiles et à une modification des tailles des particules solides. Les contraintes résultantes induisent alors une fissuration ou des vides dans le matériau carboné solide qui, en conséquence, perd son caractère protecteur.

Les zéolithes, quels que soient leur groupe structural et leur composition, sont toutes des SA dans les formulations polyoléfine/APP/PER/zéolithe. L'augmentation des performances est observée pour des teneurs faibles en zéolithe. En illustration, les formulations PP/APP/PER/4A et PP/PY/PER/4A (teneur en APP/PER et PY/PER : 28,5 % pondéral, teneur en zéolithe 4A : 1,5 % pondéral) admettent respectivement les LOI : 43 et 51 % volumique (l'augmentation relative est respectivement de 43 et 70%) et conservent un classement V0 [46].

L'étude présentée, réalisée en commun avec Elf-Atochem (CERDATO, Serquigny), concerne des copolymères de l'éthylène et, plus particulièrement, le LRAM3,5 choisi comme matrice « hôte » modèle. Elle révèle qu'aux compositions qui correspondent à l'effet de synergie maximale (teneur en SA comprise entre 1,5 et 2 % pondéral) la zéolithe est totalement détruite lorsque l'intumescence se produit, par une réaction avec les espèces orthophosphates ou pyrophosphates du matériau phosphocarboné. La recherche de relations entre les propriétés topographiques, morphologiques et d'adsorbtion des matières premières minérales et l'effet de synergie est, de ce fait, impossible.

La perte de l'effet de synergie et la diminution de la propriété FR, observées pour des teneurs en SA supérieures à 2 % pondéral (13X) ou 8 % pondéral (mordénite ou Y), correspondent au maintien de particules cristallines résiduelles des minéraux dans le matériau intumescent.

Les zéolithes 4A et Y contribuent à une augmentation relative du LOI de l'ordre de 33 % dans la matrice LRAM3,5. La zéolithe 4A est retenue pour l'étude de compréhension de la synergie.

Une étude TG des formulations LRAM3,5/APP/PER/4A et LRAM3,5/APP/PER montre que leurs thermogrammes sont proches entre 200 et 530°C, mais avec une stabilité plus importante du premier système entre 400 et 450°C. La quantité plus importante de résidu du premier système, aux températures supérieures à 550°C, s'explique par la stabilité thermique des espèces aluminophosphates et silicophosphates formées. La présence de ces espèces est mise en évidence par MAS-RMN du ^{27}Al et du ^{29}Si des résidus de la dégradation thermo-oxydante de l'adjuvant APP/PER/4A aux HTT $\geq$ 280°C.

L'ATG comparative des adjuvants APP/PER/4A et APP/PER montre que le rendement de la carbonisation est plus faible entre 280 et 480°C en présence de la zéolithe 4A mais que, par contre, le matériau correspondant est plus stable aux températures supérieures. L'analyse chimique confirme la comparativement faible teneur en carbone du matériau intumescent issu de l'adjuvant avec la 4A (le rapport atomique C/P est 2,25, alors qu'il est 3 pour l'adjuvant APP/PER). L'ajout de zéolithe permet de conserver les produits organiques azotés dans le matériau (Le rapport atomique N/P est 0,75, au lieu de 0.72 avec APP/PER; une étude XPS [165, 167] caractérise des structures de type polypyrrole et pyridine [196, 197]) et n'affecte pas

la quantité d'ammoniac dégagé pendant la formation des esters des acides phosphoriques et leur dégradation pour donner le matériau phosphocarboné intumescent.

Nous avons proposé que le traitement thermique des adjuvants intumescents conduit à la formation d'un système catalytique constitué d'espèces orthophosphates et pyrophosphates acides supportées par un carbone en voie d'organisation. L'ajout de la zéolithe 4A modifie ce système en augmentant sa teneur en espèces phosphates et en permettant la formation des espèces aluminophosphates et silicophosphates, supposées actives dans des réactions catalytiques. L'étude RMN montre qu'il interdit, par ailleurs, la formation des espèces pyrophosphates et de l'oxyde P_4O_{10} . La stabilité thermique du système catalytique est plus élevée puisque l'élimination des espèces phosphorées, via la formation de l'oxyde et sa sublimation, est empêchée.

Le support constitué de carbone polyaromatique est lui aussi différent en présence de la zéolithe 4A. Son organisation en strates parallèles (pré-graphitisation) est moins avancée et il possède une caractère paramagnétique renforcé, suffisant pour interdire l'acquisition d'un spectre CP/DD-MAS RMN du ^{13}C bien résolu. Ces deux modifications du « carbone » contribuent à l'augmentation du caractère protecteur du revêtement intumescent.

Les valeurs des temps de relaxation spin - réseau, mesurées par RMN basse résolution du ^1H, permettent de présumer une agitation moléculaire moins importante dans le revêtement formé avec la zéolithe qui confirme une rigidité accrue du système. La mesure des temps de relaxation spin - spin montre que les matériaux intumescents, formés lors du traitement thermique des adjuvants avec et sans 4A, sont constitués d'une phase rigide « structures macromoléculaires polyaromatiques » et d'une phase mobile constituée de petites molécules (espèces phosphates et/ou aromatiques) sans liaison avec la structure rigide. L'ajout de la zéolithe 4A interdit une augmentation de la taille des domaines mobiles lorsque $280 \leq T \leq 430°C$. Cet ajout limite, en conséquence, une ségrégation des phases dans le revêtement susceptible de diminuer la viscosité apparente et/ou d'induire un cisaillement du matériau avec perte du pouvoir « encapsulant ».

L'étude comparative des formulations LRAM3,5/APP/PER et LRAM3,5/APP/PER/4A montre que le polymère est la source principale du carbone des revêtements intumescents et que les rapports atomiques C/P des matériaux intumescents (respectivement 7,5 et 8,25 à 350°C) ne semblent pas affectés par l'adjuvant 4A. Par contre, cet ajout conduit à une stabilité (relativement élevée à haute température) du matériau carboné; les rapports atomiques C/P à 560°C sont respectivement 0,14 et 1,3 avec LRAM3,5/APP/PER et LRAM3,5/APP/PER/4A. Il permet aussi une relative stabilité thermique des espèces contenant N (les rapports atomiques N/C à 430°C étant respectivement 0,02 et 0,4).

Le processus de carbonisation de LRAM3,5/APP/PER/4a est très différent de ceux de LRAM3,5/APP/PER et des autres formulations sans zéolithe (PP/APP/PER ou PE/APP/polyol présentées dans ce travail). En effet, il favorise la formation majoritaire de chaînes aliphatiques courtes pontées par des espèces phosphates ou aluminophosphates et celle d'espèces aromatiques ou polyaromatiques de petites tailles au détriment des structures polyaromatiques volumineuses.

La mesure des temps de relaxation met en évidence une « rigidité » moléculaire comparativement plus importante dans les matériaux carbonés ex-LRAM3,5/APP/PER/4A qui implique une organisation de ces matériaux assurée par de nombreux pontages inter-chaînes, organisation différente d'un arrangement structural puisque la teneur en amorphe dans les matériaux reste comparativement élevée.

Pour conclure, un SA qui modifie le système catalytique espèces acides supportées, doit participer à la fixation de motifs du polymère dans le matériau carboné intumescent sans favoriser la formation des édifices polyaromatiques organisés volumineux. Sa participation dans le mécanisme de protection est donc double : il réduit le flux de combustibles gazeux en phase gaz et assure les propriétés dynamiques optimales du matériau protecteur (cohésion assurée par de nombreux pontages et absence de contraintes internes expliquées par l'absence de structure cristalline).

Les systèmes intumescents APP/PER, PY/XOH et PY/SOH sont des adjuvants FR du PE. La performance obtenue avec l'adjuvant comprenant le SOH

est cependant médiocre et, plus particulièrement, la valeur du LOI inférieure à 25 % volumique risque d'interdire le développement de ses applications.

L'emploi de la β-cyclodextrine ne permet pas d'obtenir une propriété FR satisfaisante. La formulation PE/PY/BCOH placée dans les conditions d'un feu ne développe pas de bouclier carboné expansé mais un composé vitreux faiblement protecteur (LOI > 17,5 % volumique). L'étude montre que le traitement thermo-oxydant de PY/BCOH conduit à la carbonisation naturelle de la dextrine par un processus radicalaire, sans réaction avec le pyrophosphate dont la dégradation conduit à la formation d'espèces polyphosphates cristallines. L'absence de classement LOI est expliqué par les « défauts » de la chaîne du polymère résultant de la dégradation induite par les espèces radicalaires formées lors de la dégradation de BCOH dans les conditions de la mise en forme. La valeur faible du LOI provient, au moins en partie, de la présence d'espèces cristallisées dans le revêtement superficiel.

Le traitement thermique de BCOH seule conduit à un carbone, comparativement abondant, stable aux hautes températures (environ 9 % résiduel à 650°C), susceptible de participer à la protection des formulations intumescentes dans lesquelles les adjuvants ne permettent pas la synthèse du carbone stable.

L'effet protecteur n'est pas observé avec les adjuvants APP/PER/BCOH et PY/XOH/BCOH qui présentent une évolution des valeurs du LOI caractéristique d'un effet d'additivité.

La protection est notable avec la formulation intumescente PE/APP/SOH/BCOH, en particulier pour le mélange CP/CA de rapport pondéral: PY/(SOH + BCOH) = 1.6, avec des CA dans le rapport pondéral BCOH/SOH proche de ½, pour lequel la synergie est optimale. A ces concentrations relatives, la réaction d'estérification entre PY et SOH est suffisante pour assurer la stabilisation des espèces phosphates peu condensées et interdire la formation des espèces phosphates cristallines. L'effet de synergie est expliqué par la conservation d'un matériau carboné lors de la dégradation thermo-oxydante de PE/PY/SOH/BCOH. Abondant à HTT = 430°C, il se dégrade lentement aux HTT supérieures. La formation de ce résidu implique une réaction entre le polymère et/ou ses produits de dégradation avec le matériau carboné qui se forme à partir de PY/SOH et BCOH seul. Une réaction radicalaire en phase condensée est proposée.

En conclusion, les études montrent qu'une synergie est obtenue par l'ajout d'un adjuvant du type CP ou CA. Il est montré qu'un SA performant, membre d'une famille de matériau, n'implique pas nécessairement que tous les membres de sa famille soient des SA. Par ailleurs, un adjuvant, qui utilisé seul (argiles, zéolithes, homologues de la cellulose) ne permet pas d'obtenir la performance FR, est susceptible de participer à une synergie en association avec un autre adjuvant.

En outre, l'effet de synergie dépend de la nature du matériau polymère hôte. Cet « effet de matrice » est considéré dans le paragraphe suivant. La synergie dans un système intumescent est un effet complexe qui mérite une modélisation. Nous nous attacherons dans une discussion générale à proposer un telle modélisation.

III-2-c. Modélisation de l'effet de synergie

Le processus intumescent est toujours ablatif : la dégradation du matériau est initiée par les réactions entre adjuvants qui se produisent à une température inférieure à celle à laquelle la dégradation du polymère seul devient rapide. En effet, l'étude DSC des mélanges phosphates/polyol montre que les réactions d'estérification observées entre 150 et 310°C sont fortement exothermiques [39], la dégradation des esters avec formation du matériau observée entre 280 et 320°C étant endothermique. L'apport local de chaleur permet donc la dégradation des chaînes du polymère.

Un revêtement intumescent est très hétérogène. Il est constitué de gaz piégés et d'un matériau phosphocarboné alvéolaire (phase condensée), en fait un mélange de phases solides et liquides de type brais acides possédant des propriétés dynamiques globales qui permettent de « piéger » les produits gazeux et liquides de la décomposition du matériau polymère. Le matériau phosphocarboné est lui aussi un matériau complexe constitué d'édifices macromoléculaires polyaromatiques cristallins (plus ou moins organisés en strates parallèles) , de particules cristallines d'adjuvants et d'une phase amorphe qui enrobe les domaines cristallins. Cette phase amorphe est constituée de petites molécules polyaromatiques, d'espèces phosphates acides facilement hydrolysables, de chaînes alkyles formées lors de la

dégradation des esters des acides phosphoriques, et de fragments de la chaîne du polymère.

La phase amorphe conditionne le caractère protecteur du revêtement: elle doit être suffisamment volumineuse pour enrober parfaitement les domaines cristallins et posséder une rigidité adéquate pour fournir les propriétés dynamiques intéressantes au matériau. En particulier, sa viscosité apparente doit être suffisamment élevée, pour interdire l'écoulement ou la chute de gouttes, et suffisamment faible, pour accepter les contraintes induites par les phases cristallines enrobées et la pression relativement importante des gaz piégés par le matériau.

Le revêtement intumescent est une barrière pour les flux de chaleur externes vers les matériaux FR. En effet, il empêche l'augmentation brutale de la température de la résine, à la surface de laquelle il forme un bouclier, en conservant plusieurs zones isothermes en son sein (environ 350 et environ 550°C (Figure III-3)). Notre étude concerne plus particulièrement les paramètres chimiques et physico-chimiques des systèmes intumescents liés à l'effet de barrière thermique. L'étude, par notre Groupe, des paramètres physiques est en cours [51].
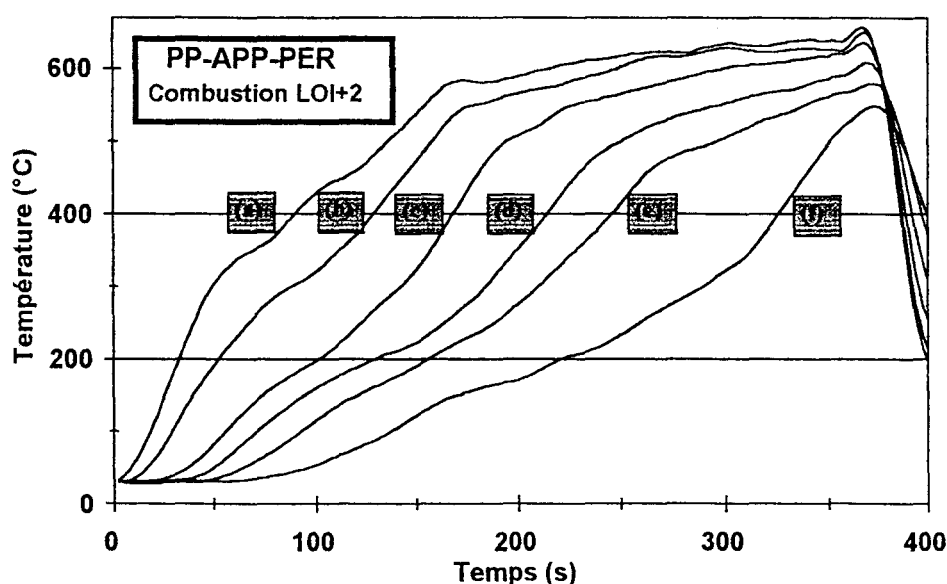

Figure III-3. Evolution de la température en fonction du temps au sein d'une formulation intumescente lors de son auto-combustion.
Formulation PP/APP/PER :
Conditions de l'auto-extinction (% volumique en O2 dans l'air de synthèse = LOI + 2),
Distances entre les capteurs et la surface de l'échantillon : (a) 1,5, (b) 4.5, (c) 7.5, (d) 10.5,
(e) 13.5 et (f) 16.5 mm.

Une relation entre les quantités de matériaux formés à chacune des étapes du processus de l'intumescence et la performance FR n'est jamais observée Un adjuvant, qui augmente le rendement de la carbonisation du système, ne conduit donc pas nécessairement à amélioration de cette performance. Il est donc nécessaire d'introduire la notion d'activité pour expliquer l'action d'un agent de synergie. Les matériaux intumescents présentent deux types de réactivités car:

• ils contiennent (supportent) des espèces catalytiques acides superficielles, actives pour la formation des aromatiques via la formation d'esters (réactions avec des produits oxydés qui résultent de la dégradation thermo-oxydante de la résine) et une réaction de type Diels Alder,

• ils contiennent des radicaux libres qui réagissent avec les espèces radicalaires crées lors de la pyrolyse de la résine.

Le matériau phosphocarboné est créé au sein de la formulation à 280°C, température où les processus de thermo-oxydation et de pyrolyse présentent des vitesses faibles. Les réactions adjuvant - résine prennent donc place, dans un premier temps, au sein de la résine où elles limitent le flux des produits oxydés gazeux et participent à des réactions de terminaison des chaînes radicalaires de la dégradation du matériau.

L'encapsulation des gaz, produits de la dégradation des esters (eau, ammoniac, aliphatiques) et de la résine (aldéhydes, cétones, monomère, autres aliphatiques, oxydes de carbone), permet le gonflement du matériau superficiel qui, parallèlement, se dégrade sous l'effet du flux de chaleur externe. Les deux types de réactions continuent à se produire dans les alvéoles du matériau et à la surface de la résine. Ces réactions assurent la régénération du matériau superficiel protecteur.

D'autres réactions chimiques à l'interface solide - gaz entraînent une modification de la composition et, éventuellement, des propriétés physiques du revêtement. Il s'agit, dans une première étape, de l'oxydation des espèces polyaromatiques et des chaînes alkyles avec formation de groupements acides carboxyliques, aldéhydes, cétones ou lactones. Ces groupements peuvent réagir ensuite avec l'ammoniac pour former des groupements amines, amides (via la décomposition thermique de sels d'ammonium des acides carboxyliques) et/ou pyrrole (via une synthèse de type Paal-Knorr).

Un agent de synergie doit donc accroître la réactivité du matériau superficiel, en fait participer à l'augmentation de la concentration en espèces acides actives et en espèces carbonées radicalaires (« carbone actif »). Par ailleurs, la réaction d'un SA avec des adjuvants peut former de **nouvelles espèces catalytiques acides stables**, dans la gamme des températures où les espèces catalytiques formées par réaction entre les adjuvants seuls sont détruites. La figure III-4 schématise ces effets, en considérant que la cinétique de formation des produits protecteurs correspond à une réaction d'ordre par rapport à ces espèces et est, ensuite, limitée par une concentration limite superficielle. L'influence éventuelle des modifications de la composition n'est pas prise en compte dans le modèle.

Propriétés du revêtement

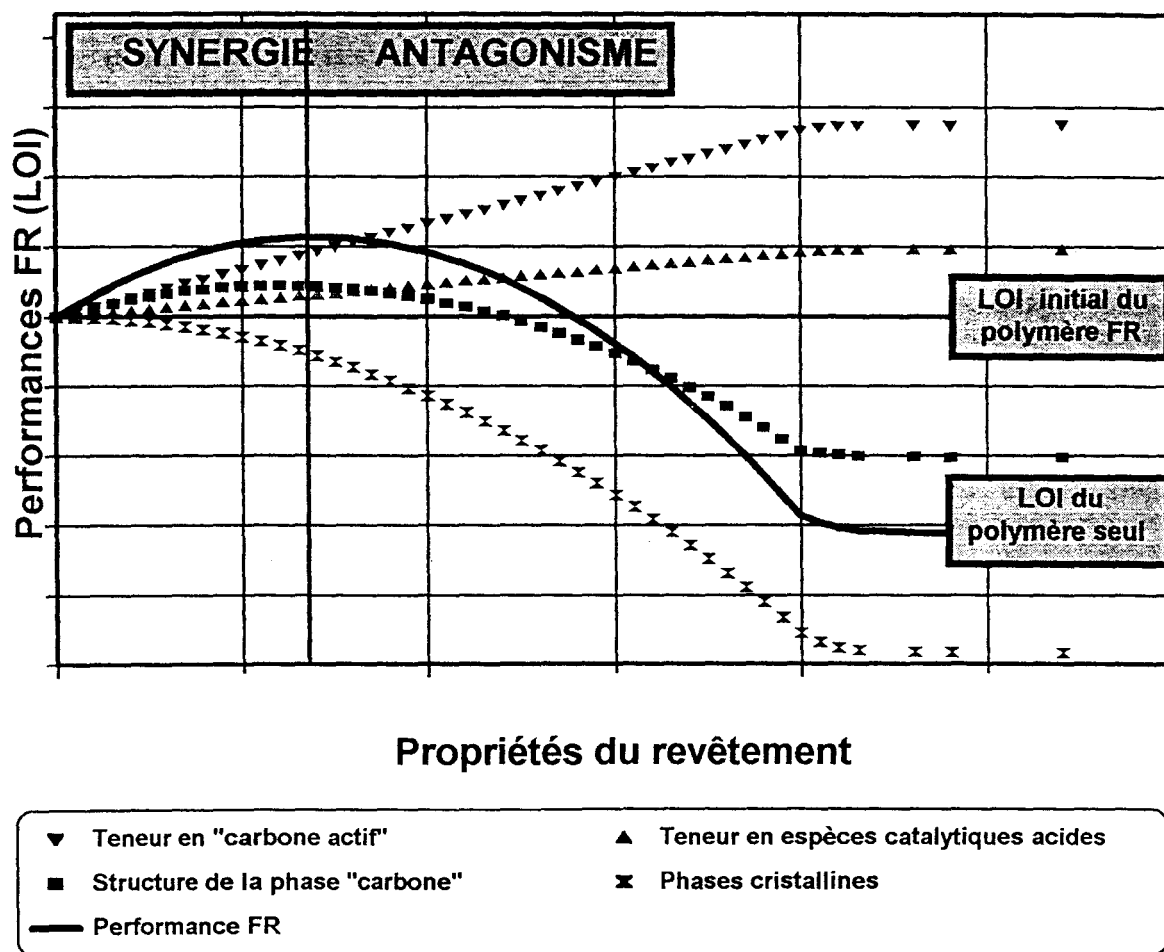| ▼	Teneur en "carbone actif"	▲	Teneur en espèces catalytiques acides
■	Structure de la phase "carbone"	✘	Phases cristallines
▬	Performance FR		

Figure III-4. Effet de synergie modélisé par addition des effets induits par la modification des propriétés du matériau intumescent, en fonction de la teneur en agent de synergie.

Il faut remarquer que la réactions des espèces phosphates acides avec le matériau carboné nécessite la présence de groupement oxydés dans le matériau. La

antagoniste qui s'explique par la formation de fissures, induites par les contraintes provenant de la présence des composés minéraux résiduels, et par les ponts thermiques créés par ces particules volumineuses dans le matériau carboné.

L'effet de synergie, obtenu par l'ajout d'un SA, se modélise donc par une somme des effets qui augmentent et limitent simultanément les propriétés du matériau intumescent, responsables de son caractère protecteur. Ces effets sont rapportés dans le Tableau III-1.

« Devoirs » du SA	Effets antagonistes éventuels induits
Haut rendement de carbonisation	
Augmentation de la teneur en espèces catalytiques acides	Ponts thermiques et contraintes induites par une phase cristalline résiduelle
Stabilité des espèces acides	
Augmentation de la teneur en espèces radicalaires	Décomposition du polymère
Augmentation de la teneur en amorphe	
Homogénéité de la fraction amorphe	Contraintes induites par le développement simultané d'une phase cristalline carbonée ou phosphocarbonée

Tableau III-1.   Devoirs et contraintes d'un agent de synergie dans une formulation intumescente.

III-3. *Cas particulier des copolymères fonctionnalisés - Discussion de la fonctionnalité des monomères constituants en tant que critère de choix du polymère d'une formulation intumescente*

Le choix d'un matériau FR doit répondre au plus près aux exigences du cahier des charges. Le choix débute par l'examen des polymères de grande consommation (PP, PE, PS) puis par celui des polymères techniques (ou de spécialité) de prix de revient supérieur [199].

Parmi les résines techniques, les copolymères de l'éthylène [200] ont éveillé notre intérêt par leurs propriétés mécaniques intéressantes qui permettent leur utilisation dans des applications électriques, en particulier en câblerie. Il sont, par

ailleurs, utilisés comme agents de compatibilité dans les mélanges techniques de polymères (blends).

Ces macromolécules présentent un enchaînement covalent de motifs monomères différents [201]. Le processus de leurs dégradations thermiques reste à ce jour peu connu. En effet, seul celui des copolymères éthylène - acétate de vinyle (EVA) a été extensivement étudié [202-204] : la première étape de la décomposition thermique de l'EVA affecte les motifs acétate de vinyle et conduit au dégagement d'acide acétique alors que la dernière correspond à la décomposition de la chaîne polyéthylène [205].

Le dégagement d'un acide lors de la dégradation de la matrice polymère est susceptible de favoriser le maintien/la stabilité des espèces catalytiques acides au sein des matériaux intumescent, espèces nécessaires pour assurer le caractère protecteur. Nous avons proposé que l'effet d'une zéolithe, agent de synergie dans les formulations intumescentes, concerne la stabilité des espèces acides du revêtement aux « hautes températures ». L'étude présentée dans ce paragraphe compare les performances FR des additifs (APP - PER) et (APP - PER- 4A) au sein de différentes matrices copolymères de l'éthylène.

Les copolymères étudiés peuvent être classés en quatre catégories selon la nature des produits de leur dégradation thermique :

• l'acide acétique, avec les copolymères ethylène-acétate de vinyle (EVA et LQVA)

• des acides carboxyliques à longues chaînes, avec les copolymères éthylène-acrylate de butyle (FEABu et LYABu)

• des acides carboxyliques et un anhydride d'acide carboxylique, avec le copolymères éthylène-acrylate de butyle-anhydride maléique (LRAM)

• absence d'acide carboxylique, avec le polyéthylène (LN) et le copolymère éthylène-acrylate de méthyle (LYAMe).

L'étude recherche les effets de synergie entre les additifs intumescents APP/PER et les comonomères fonctionnalisés et entre ces comonomères et la zéolithe 4A.

ELSEVIER   PII: S0141-3910(96)00055-5

4A zeolite synergistic agent in new flame retardant intumescent formulations of polyethylenic polymers—study of the effect of the constituent monomers

Serge Bourbigot,[a]* Michel Le Bras,[a] René Delobel,[a,d] Patrice Bréant[b] & Jean-Michel Tremillon[c]

[a]*Laboratoire de Physico-Chimie des Solides, E.N.S.C.L., Université des Sciences et Technologies de Lille, BP 108, F-59652, Villeneuve d'Ascq Cedex, France*
[b]*CERDATO (Elf-Atochem), F-27470, Serquigny, France*
[c]*GRL (Elf-Atochem), BP-34, F-64170, Lacq, France*
[d]*CREPIM, F-62160, Bully-les-Mines, France*

4A type zeolite adducted in the intumescent ammonium polyphosphate (APP)/pentaerythritol (PER) system, additives in fire retardant (FR) polyethylenic-based formulations (ethylenic co/terpolymers), leads to a synergistic FR effect. This study concerns ethylenic co- or terpolymers. It shows the part played by the polymeric matrix on the fire-proofing performances which depend on the chemical nature and amount of comonomer in the polymer. Further, the thermal analyses confirm the effect of the polymeric matrix and show the participation of oxygen in the formation of the intumescent coating. Measurement of the performances using the cone calorimeter puts forward that the zeolite causes different degradation of the intumescent materials and thus the formation in fire of a more thermally stable coating. © 1996 Elsevier Science Limited

1 INTRODUCTION

Polyethylenic polymers (PE and its copolymers, PP, their blends and alloys) are widely used in many applications, such as housing materials, transport and electrical engineering. These polymers are easily inflammable due to their chemical constitutions. To reduce their flammability, flame retardants (FR) are added. Intumescent technology has recently found a place in polymer science as a method of providing flame retardance to polymeric materials.[1,2] Fire retardant intumescent materials form on heating foamed cellular charred layers on the surface, which protects the underlying material from the action of the heat flux or a flame. The proposed mechanism is based on the charred layer acting as a physical barrier which slows down heat and mass transfer between gaseous and condensed phases.

The association of an ammonium polyphosphate (APP) and the pentaerythritol (PER) has been shown to be an efficient fire-retardant (FR) intumescent system for polyolefinic materials.[3,4] Nevertheless, the commercially available intumescent formulations could contain any of the following fillers: titanium dioxide,[5] resin binder and plasticizers,[6] and alumino-silicate (clay) materials.[7] These fillers may act as synergistic agents in intumescent FR formulations.[5,7] Among the possible alumino-silicate fillers, Beyer et al.[8] proposed that zeolites may present a potential application in FR material. The combination of zeolites and conventional heat insulating materials ensures an enhancement of the protective effect. In this laboratory, we have associated the intumescent FR APP/PER system (which gives a heat-insulating material in the conditions of fire) with zeolites[9-11] and shown the very large improvement in the fire-proofing properties of polymers such as polypropylene (PP), polyethylene (PE) and ethylenic copoly-

mers. Moreover, we have shown that enhanced fire retardant performances were obtained using a 4A type zeolite.

This work first compares the FR performances of formulations containing the 4A type zeolite with the classical polymer–APP/PER systems. The results presented deal with PE, ethylene–vinyl acetate, ethylene–methylacrylate and ethylene–butylacrylate–maleic anhydride-based formulations. In a second step, the results are discussed using TG analyses and cone calorimeter as the fire model.

2 EXPERIMENTAL

2.1 Materials

The polymers used (Table 1) are ethylene co/terpolymers in powder form supplied by Elf-Atochem.

The additives are 4A zeolite (Si/Al = 1, compensation cation: Na, supplied by Ceca), PER (Aldrich R.P. grade) and APP $((NH_4PO_3)_n$, $n = 700$, Hoechst Exolit 422, soluble fraction in H_2O: <1 wt%). The study has been carried out using the APP/PER mixture for the ratio APP/PER = 3 (wt/wt). In the case of the polyethylenic materials, the fire-retardant properties are maximum for this ratio.[3,4,9] The additives are always incorporated at 30% (wt/wt) in the polymer. Initial mixtures were first prepared after mechanical grinding and sifting (200 μm) of the raw materials. Sheets were then

obtained using a Darragon press at 160°C with a pressure of 30 bars.

2.2 Fire testing

2.2.1 Limiting Oxygen Index (LOI)
LOI was measured using a Stanton Redcroft instrument on sheets $(120 \times 60 \times 3)$ mm^3 according to the standard 'oxygen index' test (ASTM D2863/77).

2.2.2 UL-94 test
The test was measured on sheets $(127 \times 12.7 \times 3)$ mm^3 according to the American National Standard UL-94 (ANSI/ASTM D-635-77).

2.3 Thermal analyses

Thermogravimetric analyses were carried out at 3°C/min under synthetic air or nitrogen (flow rate = 5×10^{-7} m^3/s; Air Liquide grade) using a Setaram MTB 10-8 microbalance. In each case the mass of the sample used was fixed at 15 mg and the samples (powder mixtures) were positioned in open vitreous silica pans. The precision of the temperature measurement was 1.5°C over the whole range.

The curves of weight difference between the experimental and theoretical TG curves are computed as follows:

$M_{poly}(T)$: TG curve of the polymer,
$M_{add}(T)$: TG curve of the additives,
$M_{exp}(T)$: TG curve of the polymer + the additives,

Table 1. Polymers and their notations used in this work

Polymer composition	Commercial name	Melt index (g/10 min at 190°C)	Notation
Ethylene (100%)	Lotrène FB 3010 (PEBDr)	0.3	LN
Ethylene (95%)–butyl acrylate (5%)	Lotryl FE 2520	0.3	FEABu5
Ethylene (87%)–butyl acrylate (13%)	Lotryl 3400	2	FEABu13
Ethylene (70%)–butyl acrylate (30%)	Lotryl 3600	2	LYABu30
Ethylene (85%)–methyl acrylate (15%)	Lotryl FY 8560	0.5	LYAMe15
Ethylene (80%)–methyl acrylate (20%)	Lotryl FY 6140	0.3	LYAMe20
Ethylene (70%)–methyl acrylate (30%)	Lotryl 3610	5	LYAMe30
Ethylene (92.2%)–butyl acrylate (5%)–maleic anhydride (2.8%)	Lotader 2200	0.8	LRAM2.8
Ethylene (91.5%)–butyl acrylate (5%)–maleic anhydride (3.5%)	Lotader 3200	0.5	LRAM3.5
Ethylene (95%)–vinyl acetate (5%)	Lacqtène 1005 VN 3	0.3	LQVA5
Ethylene (85%)–vinyl acetate (15%)	Lacqtène 1005 VN 4	0.7	LQVA15
Ethylene (72%)–vinyl acetate (28%)	Evatane 2805	0.7	EVA28
	2825	25	EVA28–25
	28150	150	EVA28–150

$M_{th}(T)$: theoretical TG curve computed by linear combination between the TG curves of the polymer and the additives: $M_{th}(T) = 0.7M_{poly}(T) + 0.3M_{charge}(T)$,

$\Delta(T)$: curve of weight difference: $\Delta(T) = M_{exp}(T) - M_{th}(T)$.

The $\Delta(T)$ curves allow the observation of an eventual increase or decrease in the thermal stability of the polymer related to the presence of the additives.[4]

2.4 Cone calorimetry

Samples were exposed to a Stanton Redcroft Cone Calorimeter according to ASTM 1356-90 under a heat flux of 50 kW/m². This flux has been chosen because it corresponds to the heat evolved during a fire.[12] The rate of heat release data were computed using the oxygen consumption principle[12] using software provided by Polymer Laboratories.

3 RESULTS AND DISCUSSION

3.1 Synergistic FR effect

The 4A zeolite used in FR intumescent systems leads to a very important synergistic effect on the fire-proofing performances. As an illustrative example, the effect in LRAM3.5 terpolymer-based formulations is presented. The curve (Fig. 1) which presents the LOI values versus 4A zeolite' level (the additives' level APP/PER–4A remains constant at 30 wt%), shows that a synergistic effect is obtained at 1.5 wt% of 4A zeolite. For this level the LOI values are
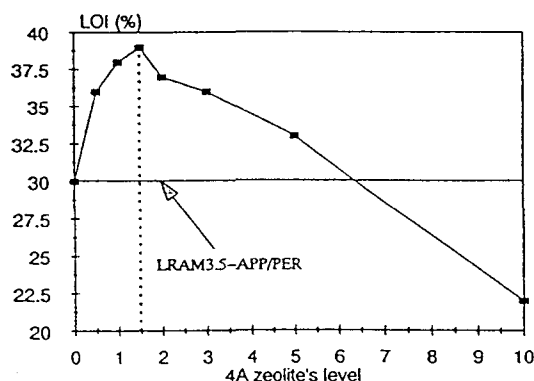

Fig. 1. Evolution of the LOI values versus zeolite's level in the terpolymer LRAM3.5

increased to 35% comparative to the classical APP/PER system. In the following work we will study, therefore, the effect of the polymeric matrix using an (APP/PER)/4A ratio equal to 19. It may be noted that high zeolite content (>5 wt%) leads to a drastic loss of the FR performances. It is also noted that the LRAM3.5–APP/PER and LRAM3.5–APP/PER–4A (1.5 wt% of 4A) are classed V-0 in the UL-94 test.

3.2 Effect of the polymeric matrix

The study on the effect of the polymeric matrix is led by the measurement of the LOI values for the three classes of ethylenic copolymers and for the class of ethylenic terpolymers (Table 1). For these four classes, the LOI values are plotted versus the comonomer level for both intumescent systems APP/PER and APP/PER–4A. Polyethylene is taken as a reference for the three first classes of copolymers and FEABu5 for the terpolymers. Figs 2–5 present the results obtained.

The curves show an increase in the LOI values with comonomer level, whatever the polymer class studied. A polymeric matrix effect is thus proposed. This effect leads to an important variation of the LOI values (from 25% to 37% for the APP/PER and from 27% to 40% for the APP/PER–4A systems). In order to compare the influence of the level of comonomer on the FR performance, the curves of the LOI values versus the mole content of the different comonomers for 100 g of polymer are plotted on the same graph for both systems (Figs 6 and 7).

For a given class of polymer, these curves show that the LOI values increase when the level of comonomer increases. Nevertheless the variation remains different for each constituent monomer. As an example, in the formulation LYAMe30–APP/PER–4A, the LOI value is 37% with a comonomer level equaling 0.35 mol/100 g whereas for LRAM3.5–APP/PER–4A this is 39% with a comonomer level equaling 0.075 mol/100 g. These results show, therefore, that the LOI values depend strongly on the chemical nature of the comonomer.

In previous works[4,13,14] dealing with the APP/PER system, the important part played by acid species in the development of the intumescence (creation of a spiro structure by an esterification reaction between APP and PER
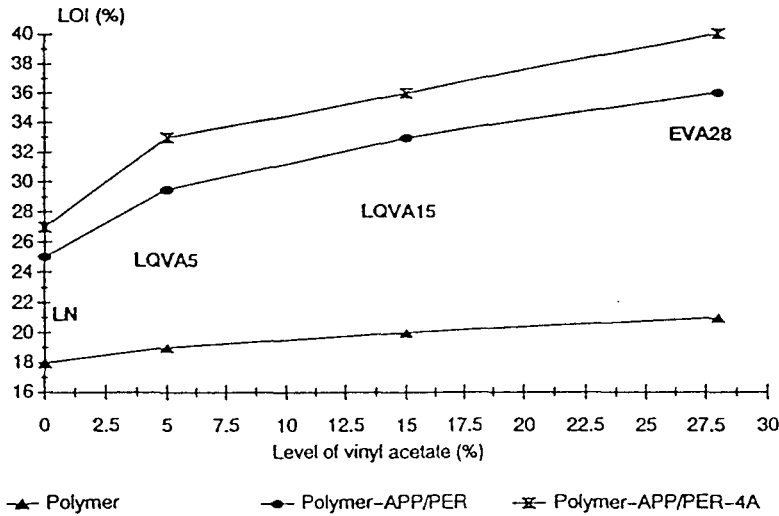
278

Fig. 2. Curve of the LOI values versus the level of vinyl acetate.

leading to the expanded carbonaceous structure which is thermally stable) has been shown. For the four classes of polymers studied, the comonomers in the polyethylenic chains can reinforce the acidity of the APP/PER and APP/PER–4A systems by the creation of acid functions during thermal degradation of the polymers. In this assumption, the different behaviours between the polymers ethylene–methyl acrylate and ethylene–butyl acrylate may be explained by taking into account the following two step scission mechanisms:[15,16]

—homolytic scission of the chain for both polymers:
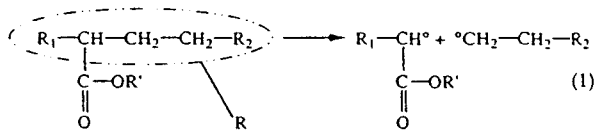
—six centres intermediate leading to a carboxylic acid:
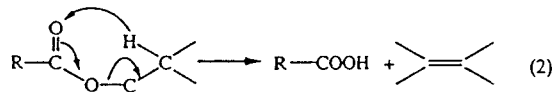
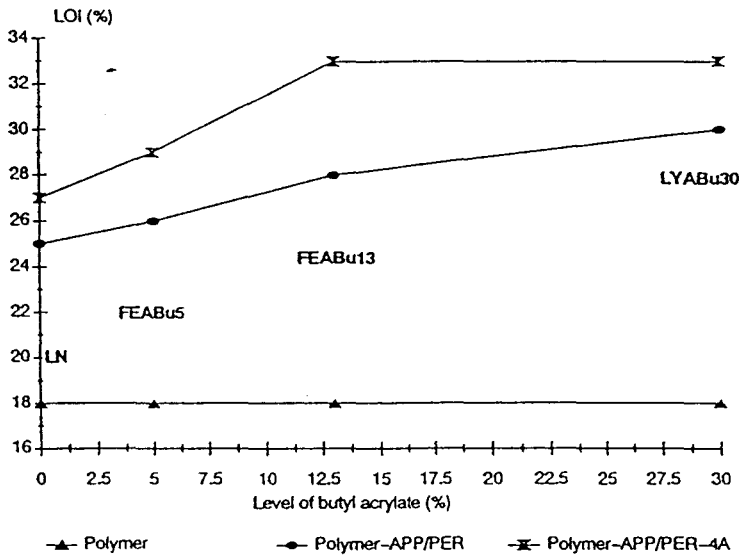The acid created by the last mechanism may thus reinforce the efficiency of the APP/PER and

Fig. 3. Curve of the LOI values versus the level of butyl acrylate.
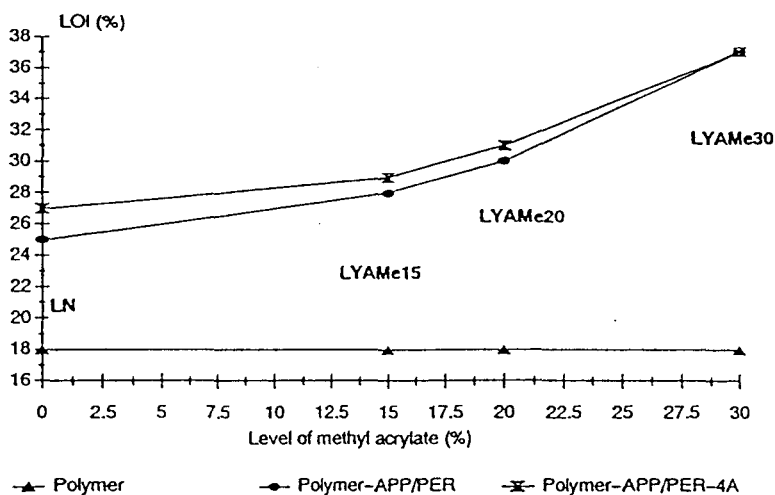
321

Fig. 4. Curve of the LOI values versus the level of methyl acrylate.

APP/PER–4A systems. The second step of the mechanism is only possible in the case of ethylene–methyl acrylate polymer.

The curves of Fig. 8 show the influence of the zeolite by plotting the 'fire-proofing power' (relative variation of the LOI values between the formulations polymer–APP/PER and polymer–APP/PER–4A, see eqn (1)) versus the comonomer level for the four polymer classes.

$$\frac{\Delta(\mathrm{LOI})}{\mathrm{LOI}} = \frac{(\mathrm{LOI})_{\mathrm{APP/PER-4A}} - (\mathrm{LOI})_{\mathrm{APP/PER}}}{(\mathrm{LOI})_{\mathrm{APP/PER}}} \quad (1)$$

with $(\mathrm{LOI})_{\mathrm{APP/PER-4A}}$ = LOI value for a formulation polymer–APP/PER–4A, and $(\mathrm{LOI})_{\mathrm{APP/PER}}$ = LOI value for a formulation polymer–APP/PER.

These curves show that the zeolite always improves the performance of the formulations but that the 'fire-proofing power' depends on the chemical nature of the comonomers. Three behaviours are observed:

—the 'fire-proofing power' increases with the terpolymers. This behaviour may be explained by the reinforcement of the acidity of the material during the degradation process which may reinforce the action of the zeolite. Indeed the butyl acrylate may lead to an acid and the anhydride function may hydrolyse to form a diacid which may react in the condensed phase;

—it remains approximately constant (copolymers vinyl acetate–ethylene and butyl acrylate–ethylene) versus the comonomer level. The
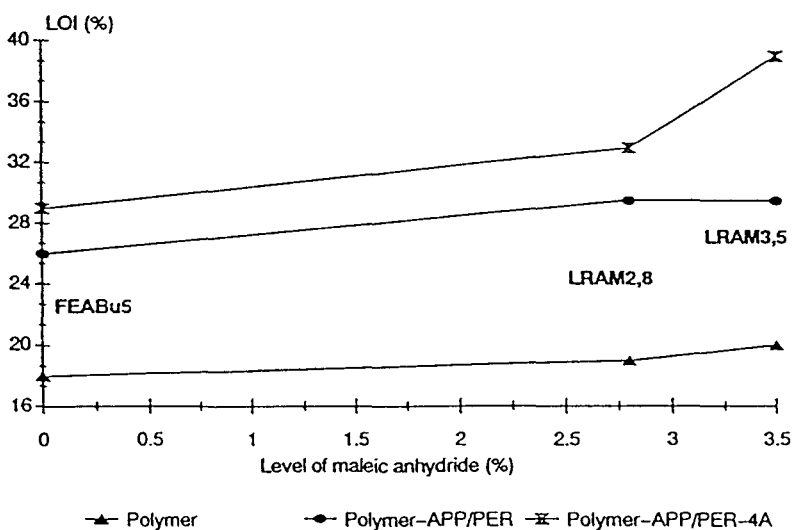

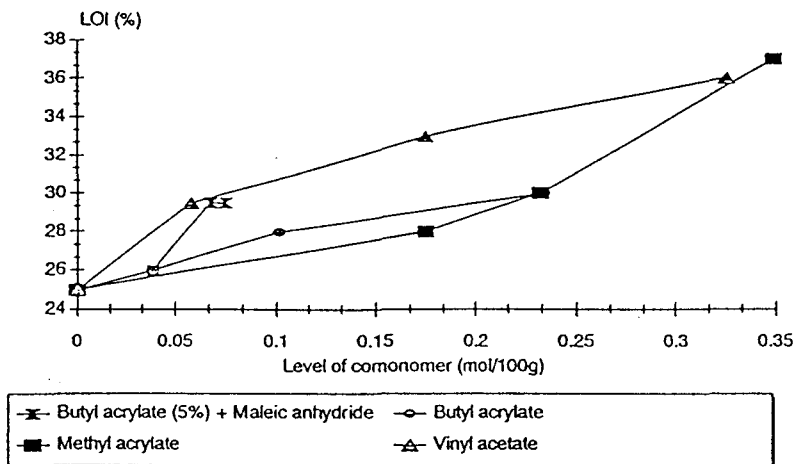**Fig. 5.** Curve of the LOI values versus the level of maleic anhydride.

Fig. 6. Curve of the LOI values versus the level of comonomer in the case of formulations polymer–APP/PER.

degradation mechanisms of the polymers leads in both cases to carboxylic acids: acetic acid (LQVA and EVA) and long chain carboxylic acids (FEABu and LYABu). It may be proposed that these resulting carboxylic acids do not act in the same way as the zeolite leading to the improvement of the FR character.

—it decreases (copolymers methyl acrylate–ethylene) versus the comonomer level. This third behaviour may be explained by the non-reinforcement of the acidity of the material because polymer degradation does not lead to the formation of a carboxylic acid.

Further it is of interest to note that the 'fire-proofing power' is maximum in the case of the terpolymers' class and in particular for the LRAM3.5. This last point will be studied in the following.

3.3 Thermogravimetric behaviour under air

The thermograms (Figs 9–12) show that, in the case of the systems containing a zeolite, the high temperature residue $(T > 550°C)$ is higher. It is suggested that the adduct of zeolite in intumescent formulations leads to the formation of a more thermally stable material than is created by classical intumescent systems.

The eventual interactions between the polymeric matrix and the additives are revealed by the curves of $\Delta(T)$ (Figs 13 and 14). The formation of stable materials in the temperature range 250–450°C is observed for the formulations polymer–APP/PER and polymer–APP/PER–4A. It has been proposed that these carbonaceous materials[17] form the surface protective coating of the FR formulations under fire
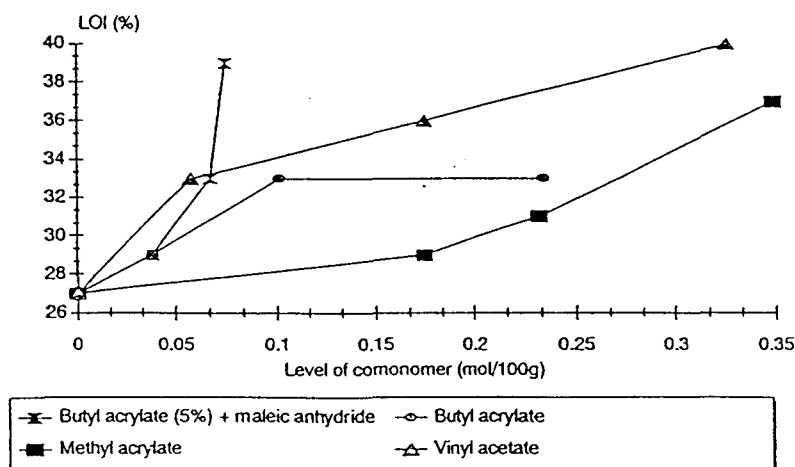

Fig. 7. Curve of the LOI values versus the level of comonomer in the case of formulations polymer–APP/PER–4A.
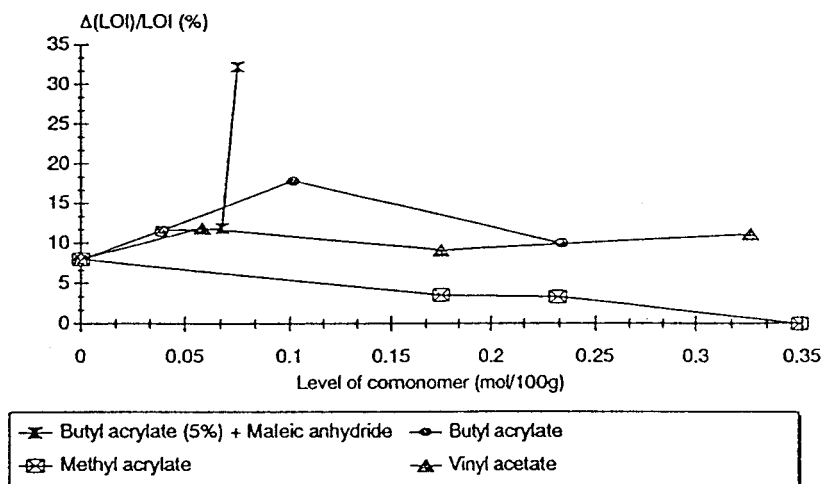
Δ(LOI)/LOI (%)

Level of comonomer (mol/100g)

-✖- Butyl acrylate (5%) + Maleic anhydride   -●- Butyl acrylate

-⊠- Methyl acrylate   -▲- Vinyl acetate

Fig. 8. Relative variation of the LOI values between the formulations polymer–APP/PER and polymer–APP/PER–4A.

conditions.[18] The differences observed between the theoretical and experimental curves confirm the previously proposed participation of the polymeric matrix[17] and/or of the oxygen in the formation of the protective intumescent shields.

In both cases (with and without zeolite) the systems with sole polyethylene show a more important difference in weight loss at 400°C. Nevertheless, it is important to note that the other systems develop a two step formation of the carbonaceous material. There is therefore no relation between the residual amount formed and the fire-proofing properties. As an example, the system LRAM2.8–APP/PER–4A has a LOI

value equaling 33% and a residue at 400°C equaling 24%, whereas the system LN–APP/PER only has a LOI value equaling 27% for a residue equaling 38%. To explain the difference in fire behaviour of the systems, it may be proposed that the protective coating in the case of the polyethylene develops at too high a temperature ($T > 340°C$) to be efficient. Inversely the systems with the co/terpolymers show two step formation of carbonaceous materials between 300 and 370°C and between 370 and 440°C. The additional process which begins at about 300°C may be assigned to the reactivity of the comonomers and so, these latter may ensure the
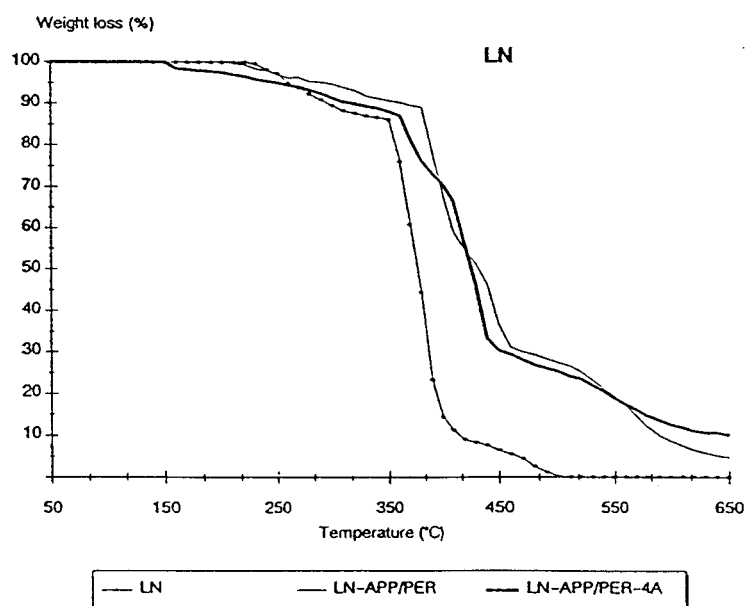
Weight loss (%)

Temperature (°C)

—— LN   —— LN-APP/PER   ▬▬ LN-APP/PER-4A

Fig. 9. TG curves under air of the formulations LN–APP/PER and LN–APP/PER–4A.
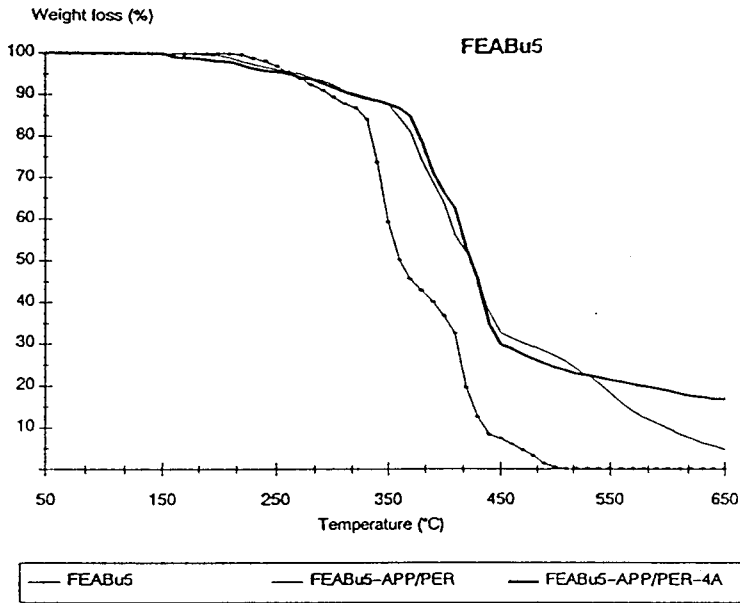
Fig. 10. TG curves under air of the formulations FEABu5-APP/PER and FEABu5-APP/PER-4A.

development of the protective coating at lower temperatures and would hinder the earlier degradation of the material. Finally, three important results have been shown:

- a relationship between the 'amount of residue' and 'fire-proofing properties' does not exist;
- the polyethylenic chains play a part in the formation of the protective shield;

- the reactivity of the comonomers can influence the fire behaviour.

3.4 Thermogravimetric behaviour under nitrogen

The curves of the weight difference (Figs 15–18) indicate the part played by oxygen in the formation of the intumescent shield. Under pyrolytic degradation conditions, the curves of

Fig. 11. TG curves under air of the formulations LRAM2.8-APP/PER and LRAM2.8-APP/PER-4A.

Weight loss (%)
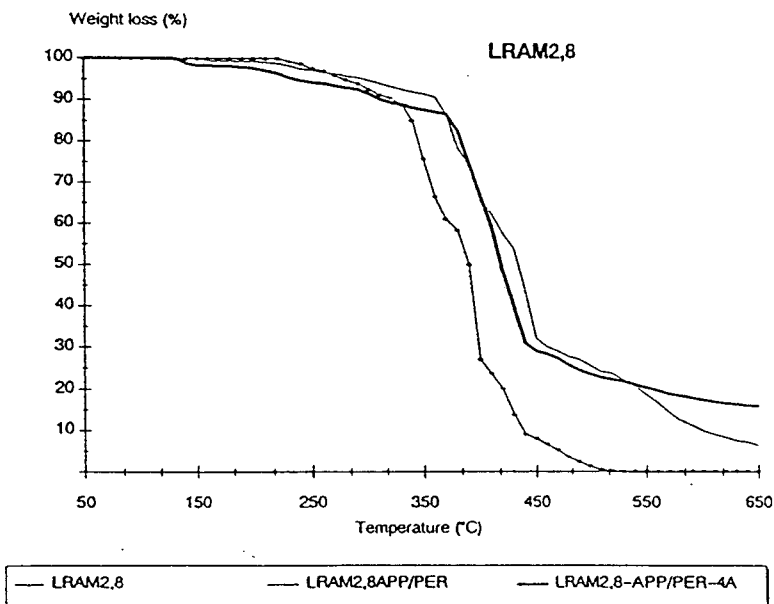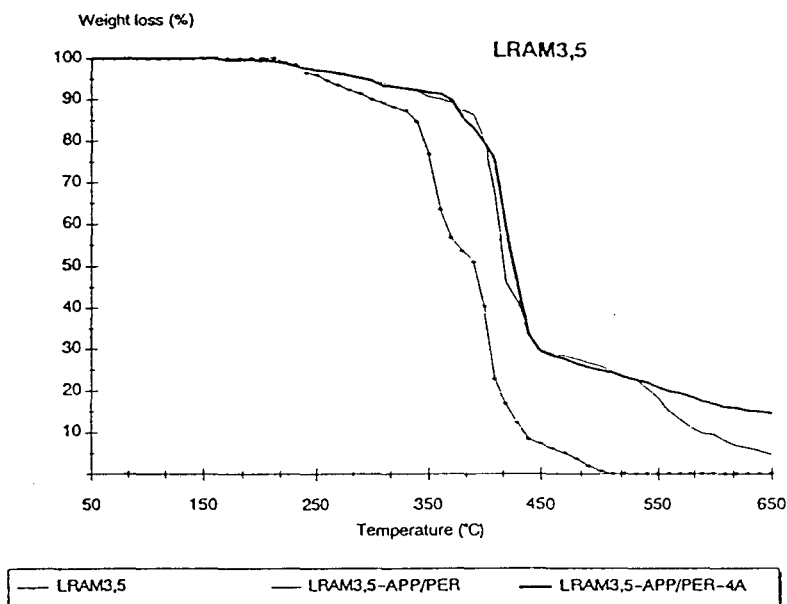

Fig. 12. TG curves under air of the formulations LRAM3.5–APP/PER and LRAM3.5–APP/PER–4A.

the formulations polymer–APP/PER always have lower weight loss differences than the same formulations with zeolite. This is because the zeolite allows the formation of a material which is thermally stable by reaction between the matrix and the additives without any oxygen.

3.5 Heat release in the conditions of a fire

The improvement of the FR properties of the system of additives by the adduct of 4A zeolite is

maximum in the terpolymer LRAM3.5. In order to identify the part played by the zeolite in the formation of the intumescent coating during the combustion process of the LRAM3.5-based formulations, the cone calorimeter fire model is a powerful tool.

Curves of the variations of the rate of heat release (rhr) versus time (Fig. 19) show a significant decrease of the rhr maximum values of the flame retardant polymers in comparison to the sole polymer. In the case of the intumescent
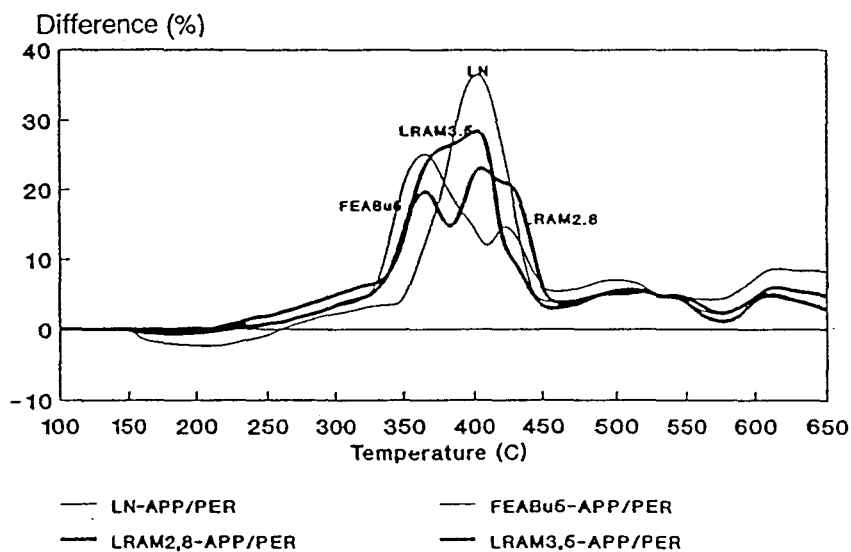
Difference (%)

Fig. 13. Curves of weight difference between the experimental and theoretical TG curves of the formulations polymer–APP/PER.
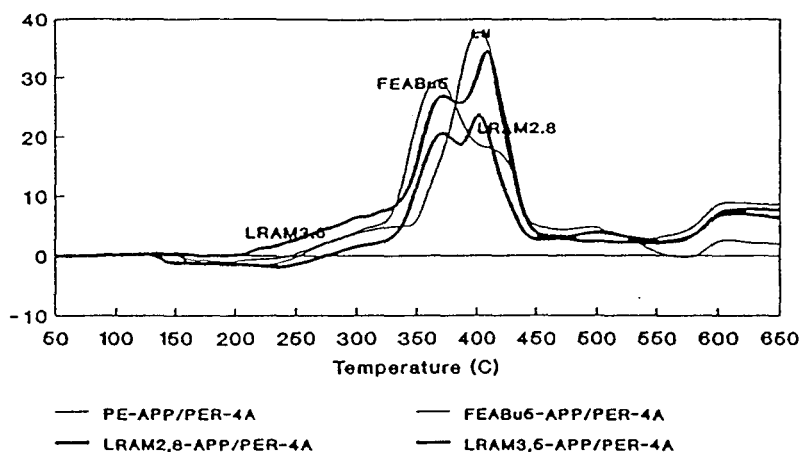
Fig. 14. Curves of weight difference between the experimental and theoretical TG curves of the formulations polymer–APP/PER–4A.
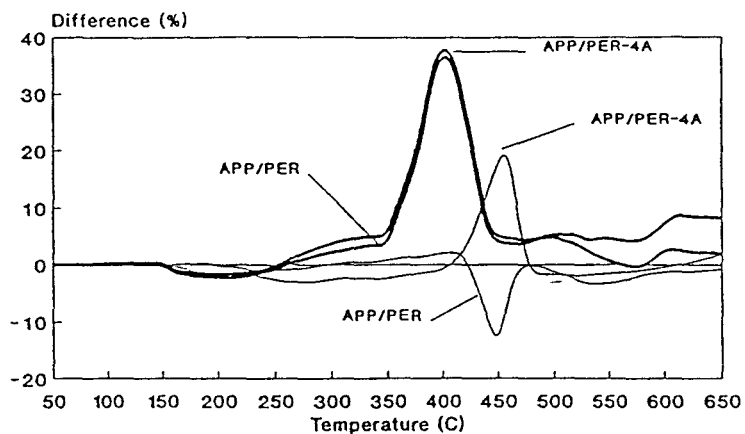
Fig. 15. Curves of weight difference between the experimental and theoretical TG curves under air (heavy line) and nitrogen (light line) of the formulations LN–APP/PER and LN–APP/PER–4A.
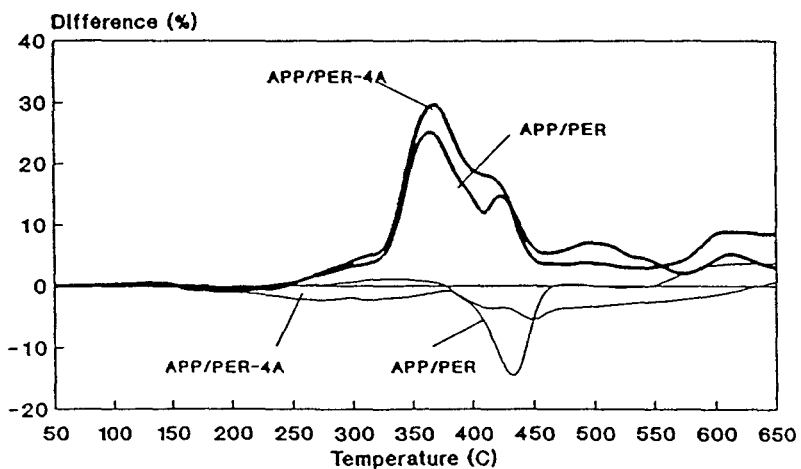
Fig. 16. Curves of weight difference between the experimental and theoretical TG curves under air (heavy line) and nitrogen (light line) of the formulations FEABu5–APP/PER and FEABu5–APP/PER–4A.
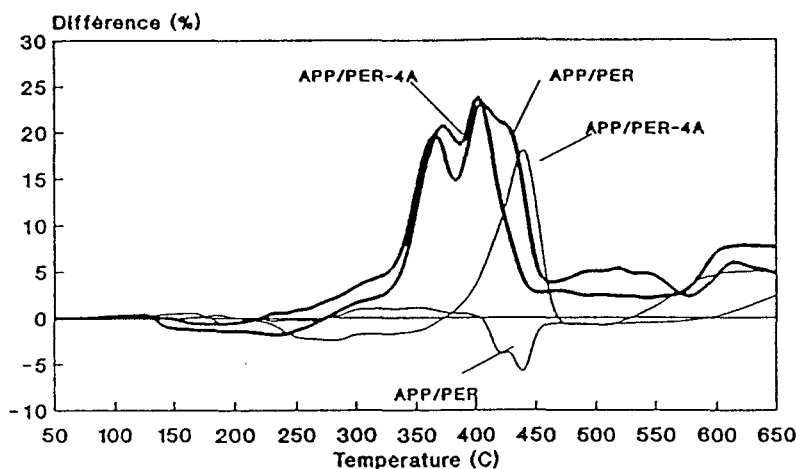
Fig. 17. Curves of weight difference between the experimental and theoretical TG curves under air (heavy line) and nitrogen (light line) of the formulations LRAM2.8-APP/PER and LRAM2.8-APP/PER–4A.

formulations, the rhr decreases strongly after the ignition. The three rhr maxima have been discussed elsewhere.[9]

It is important to note that the rhr behaviours of the flame retardant polymers are similar but that the rhr values are different. These differences become very significant for high time values which correspond to the highest temperature of the samples.[18] As an example, at $t = 600$ s, the rhr value is only 150 kW/m² for the system with zeolite whereas it is 300 kW/m² for the system without zeolite. These results imply that the characteristics of the protective coatings formed are very different and confirm that the zeolite alters the degradation of the formulations

in the high temperature range. It may be proposed that the presence of the zeolite leads to a lower evolution rate of the resulting fuel and/or to a different composition of this fuel.

To clarify these assumptions the total heat evolved (THE) values are plotted versus time (Fig. 20). The THE values of the flame retardant polymers never reach the THE values of the sole polymer. So, not only is the combustion retarded, but new thermally stable materials are created which do not take part in the combustion process. Further, these curves confirm that the zeolite alters the degradation of the formulations. Indeed it is observed that the THE values are the same up to $t = 300$ s but after that they differ
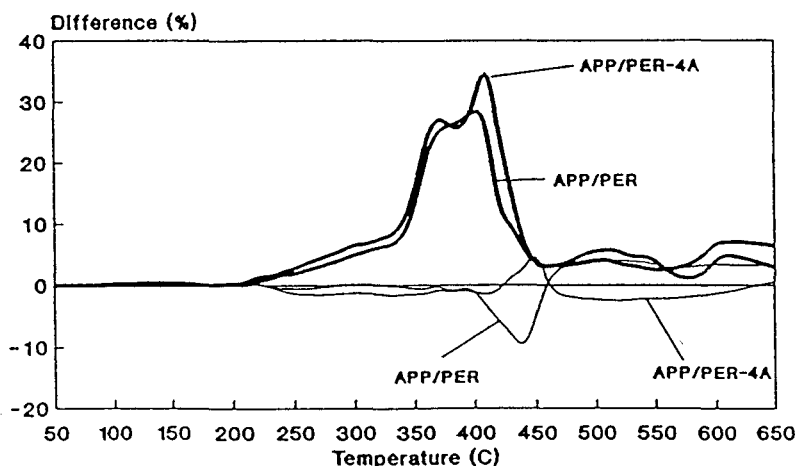
Fig. 18. Curves of weight difference between the experimental and theoretical TG curves under air (heavy line) and nitrogen (light line) of the formulations LRAM3.5-APP/PER and LRAM3.5-APP/PER–4A.

286
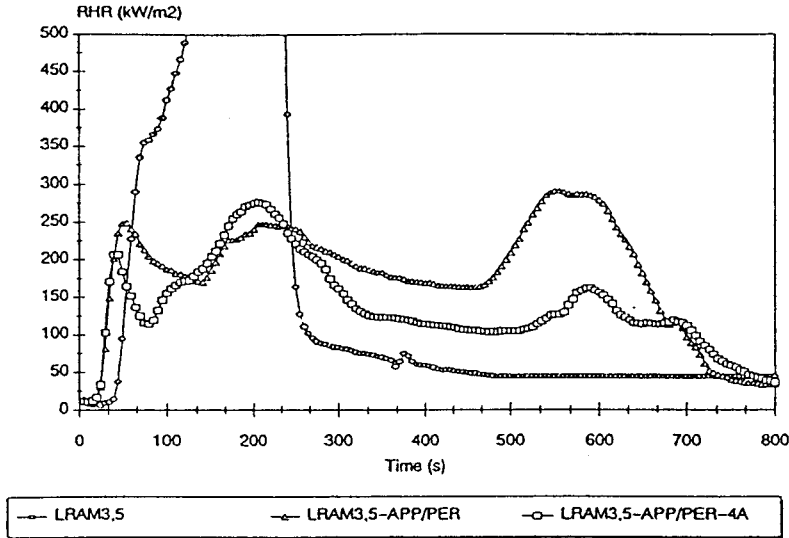
Fig. 19. rhr versus time of the systems LRAM3.5, LRAM3.5–APP/PER and LRAM3.5–APP/PER–4A.

distinctly. In the case of the system with zeolite, the THE values increase slowly between 300 and 800 s and the slope of the curve remains constant. In the case of the system without zeolite a change in the slope is observed between 450 and 600 s. It may be correlated to a change in the degradation mode of the system. These results show, therefore, that the zeolite allows the creation of a more stable material which may act as a 'relay system' for the protective material formed from the APP/PER system.

4 CONCLUSION

A study of the systems polymer–APP/PER–4A shows that the adduct of the 4A type zeolite improves considerably the fire-proofing properties of the materials. Nevertheless it is shown that the 'efficiency' of the zeolite depends on the polymer. The comparative study between different classes of ethylenic co/terpolymers proposes an important effect of the polymeric matrix. The influence of the chemical nature and
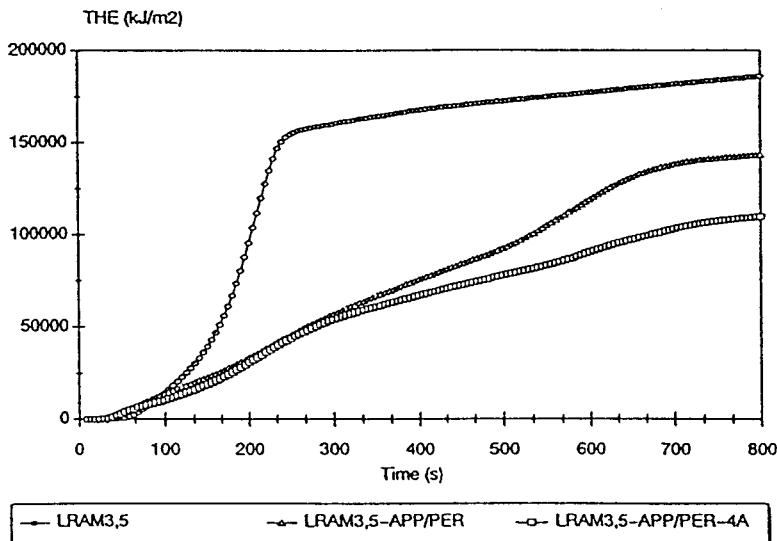
Fig. 20. THE versus time of the systems LRAM3.5, LRAM3.5–APP/PER and LRAM3.5–APP/PER–4A.

Taux de charge (%massique)	Agent Interfacial*	LOI (%)	Classement UL-94
30	-	22	V-0
	TEOS	26	V-0
40	-	24	V-0
	TEOS	30	V-0

Tableau III-1 : *LOI et classement au test UL-94 des formulations EVA8-APP et EVA8-(APP-TEOS).*

Conditionnement des espèces phosphates :
Le protocole concerne les polyphosphates $(PO_3NH_4)_n$, les formulations contenant du pyrophosphate diammonique, les orthophosphates d'ammonium et les différents mélanges de ces produits.

Des mélanges de tétraéthyle siloxane (TEOS) et d'eau (H_2O) de rapport molaire $H_2O/TEOS$ compris entre 2 et 8 en solution dans l'éthanol à raison de 40 à 60 g dans 100 ml d'éthanol sont mis en agitation mécanique à température ambiante. Les espèces phosphates à raison de 50 à 250 g sont ensuite dispersées dans la solution. L'agitation est maintenue jusqu'à l'obtention d'une pâte homogène. Le dit produit peut ensuite être introduit soit, directement, soit après réticulation en étuve puis broyage, dans des polymères thermoplastiques lors d'une transformation en plastographe ou en extrusiographe et dans les résines par mélanges avant réticulation.
A titre d'exemple, le conditionnement permet d'obtenir des formulations à base de copolymères d'éthylène possédant des propriétés « retard au feu » aptes au calandrage et pour lesquelles le phénomène d'apparition de voile n'est plus ou peu observé.

Le matériau se comporte dans les conditions du feu comme un matériau intumescent avec gonflement et formation de bulles superficielles. L'étude de compréhension, conduite depuis septembre 1996 (Siat C., Le Bras M. et Bourbigot S., résultats non publiés), permet de proposer le maintien des produits de dégradation du polymère (monomères et fragments courts de la chaîne du copolymère) via une réaction avec des espèces phosphates et silicophosphates superficielles.

En conclusion, l'étude comparative de plusieurs systèmes intumescents constitués, soit d'une matrice chargée en adjuvants associant agents de carbonisation, précurseurs d'espèces catalytiques et/ou agents de synergie différents, soit de différentes matrices contenant un même système d'adjuvants a permis de relier les modifications des performances « feu » aux propriétés physico-chimiques des matériaux polymères exposés à la chaleur ou à la flamme.

Il est montré que la synergie dans un système FR intumescent résulte de la somme des effets additifs ou supplémentaires (antagonistes ou d'amélioration) induits par l'augmentation de la teneur d'un des constituants du système. Ces effets ont été expliqués par la chimie des systèmes. Les propriétés physiques intéressantes en relation avec la synergie, actuellement étudiées par notre Groupe, ne sont pas rapportées dans ce Mémoire.

Le présent travail prouve :

•que les polyalcools et les dérivés de l'amidon sont des agents de carbonisation qui permettent d'obtenir la propriété FR. Leur emploi reste néanmoins limité par leur instabilité dans les formulations (rejet et exsudation). Leur substitution par un polymère ou un mélange de polymère susceptible de carboniser se révèle une solution prometteuse,

•que l'évaluation des précurseurs de catalyseur de carbonisation de type phosphates ou borate doit être poursuivie,

•que l'association de ces précurseurs avec des adjuvants contenant de la silice conduit à une synergie importante dans les systèmes présentant une carbonisation dans les conditions d'un incendie,

•que l'emploi de systèmes à base de phosphates et de silice ou de ses dérivés dans des polymères fonctionnalisés permet l'obtention des propriétés FR via un processus intumescent sans carbonisation.

CHAPITRE IV

FORMULATION DE NOUVEAUX MATERIAUX THERMOPLASTIQUES
RETARDATEURS DE FLAMME INTUMESCENTS.

PERPECTIVES
LES MELANGES DE POLYMERES

Les résultats présentés dans les paragraphes précédents concernent le PE, le PP, leurs mélanges (PER) et leurs copolymères. Les données de la Littérature concernant deux grandes familles de polymères de consommation : les polystyrènes et les polyamides, ne rapportent pas de systèmes où les performances FR sont obtenues via l'intumescence [207]. En particulier, l'obtention industrielle de polyamides FR intumescents par ajout direct de phosphates ou de mélanges d'additifs phosphates - CA n'a, à notre connaissance, pas été menée à bien à ce jour. Les difficultés rencontrées avec ces systèmes sont de deux ordres :

• une réaction du polymère et de l'additif se produit lors de la fusion du polymère et conduit à la perte des caractéristiques rhéologiques nécessaires pour la mise en forme par des procédés classiques (extrusion, injection - moulage ou calandrage) [Le Bras M. et Poutch F., étude débutée en septembre 1996],

• la solidification du matériau après l'opération de mélange en mélangeur interne s'accompagne du rejet presque total des espèces phosphates. En effet, le mélange de polyamides et de phosphates à l'état fondu donne, après trempe, un matériau hétérogène montrant la charge minérale à la surface du matériau polymère. De plus, le vieillissement de ces mélanges ou des formulations contenant ces mélanges conduisent à l'exsudation (apparition d'un voile) d'espèces phosphates par les matériaux. Un même phénomène est observé après les opérations unitaires de mise en forme ou de transformation desdits polymères [156].

Les résultats rapportés dans le chapitre précédant montre que l'association du polyamide-6 et des phosphates d'ammonium donne des adjuvants FR intumescents. Cette association est, dans ce chapitre, considérée dans des formulations retardatrices de flamme et dans des mélanges maîtres FR.

Les travaux de Levchik et al. [171] ont précisé l'interaction chimique entre le PA-6 et l'APP lors d'un traitement thermique. La réaction débute à environ 270°C avec, dans une première étape, attaque des liaisons alkyle - amide par l'acide phosphorique condensé (formé par élimination de l'ammoniac de l'APP). Cette attaque conduit à la rupture de la macromolécule avec formation d'esters de l'acide phosphorique et de groupements amides primaires en bout de chaîne. La décomposition thermique se poursuit, dans la seconde étape, par deux mécanismes parallèles : rupture des chaînes du polymère avec départ de caprolactame et des oligomères [179, 208] et formation d'un résidu carboné (char) dès 320°C [209].

Une étude récente de notre groupe [SIAT C., BOURBIGOT S. et LE BRAS M., résultats non publiés (1996-1997)] montre que le matériau intumescent, qui se forme dans les conditions de l'auto-inflammation de PA-6/APP, est constitué d'espèces polyaromatiques (signal RMN large entre 100 et 150 ppm, maximum à 130 ppm). Les teneurs relatives en chaînes aliphatiques (signal RMN à 25 et 50 ppm) et en espèces oxydées et ou en espèces aromatiques comprenant l'hétéroatome N (caractérisées par l'épaulement entre 150 et 180 ppm) décroissent dans le matériau intumescent lorsque les conditions de l'inflammation deviennent sévères (Figures IV-1 et IV-2).

Ces résultats préliminaires semblent impliquer un comportement au feu du système PA-6/APP similaire à celui des systèmes d'additifs intumescents préalablement présentés, le PA-6 étant l'agent carbonisant du système.

L'addition du mélange PA-6/APP dans un polymère peut être conduit selon deux modes différents :

• par une mise en forme du matériau directement à partir du mélange polymère/PA-6/APP par les techniques classiques de transformation (mélange en malaxeur, extrusion, calandrage ou injection - moulage) [SIAT C., étude en cours]

• ou par préparation initiale d'un mélange-maître PA-6/APP et ajout de ce mélange au polymère.
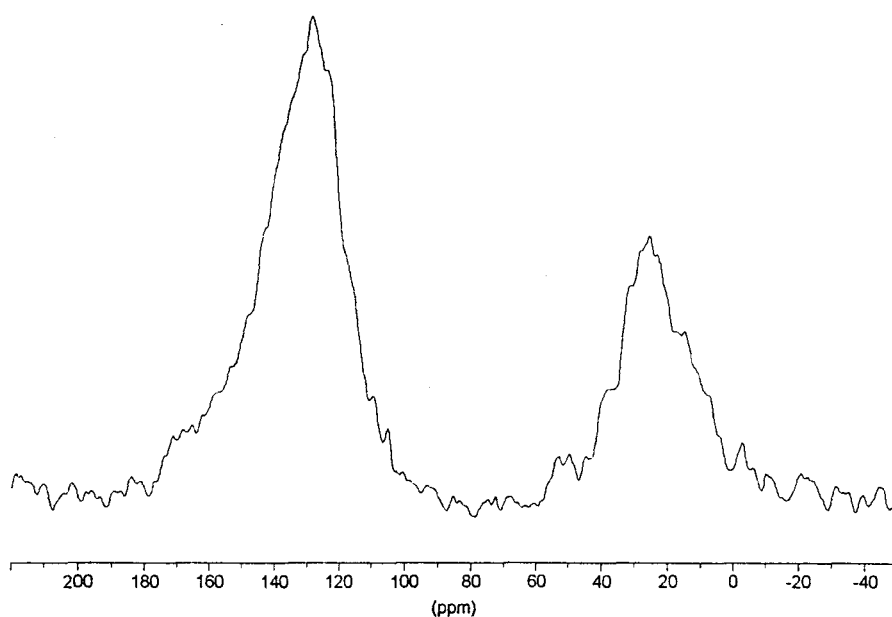
Figure IV-1. Spectre CP/DD MAS RMN du solide du mélange PA-6/APP après auto-inflammation sous air et sous une irradiance de 25 kW/m^2.
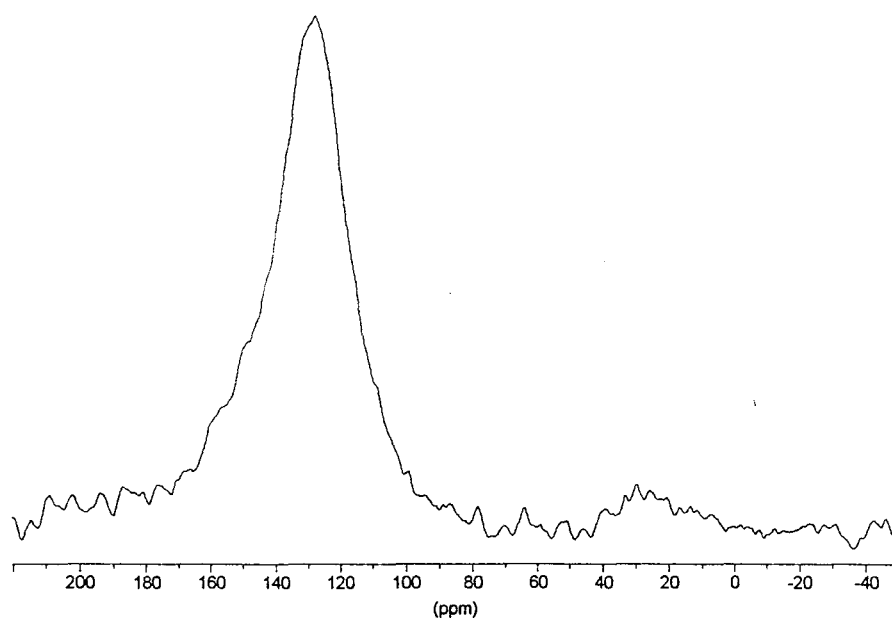
Figure IV-2. Spectre CP/DD MAS RMN du solide du mélange PA-6/APP après auto-inflammation sous air et sous une irradiance de 50 kW/m^2.

Le dernier mode d'addition fera l'objet des résultats présentés dans cette partie du Mémoire. L'obtention du mélange-maître nécessite une compatibilisation initiale du mélange. Nous faisons l'hypothèse que le polyphosphate d'ammonium se comporte lors du mélange comme un polymère et que le problème du rejet des

phases peut se traiter comme celui des migrations de phases dans un mélange
(« blend ») incompatible de deux polymères polaires. Dans ce cas, la compatibilité
est obtenue par addition d'une relativement faible quantité d'un copolymère
fonctionnalisé [210].

La compatibilisation du PA-6 dans des mélanges de polymères selon ce
principe a fait l'objet de nombreux travaux. A titre d'exemples, les copolymères
fonctionnalisés utilisés comme agents interfaciaux peuvent être les copolymères
propylène - acide acrylique [211, 212], (styrène - anhydride maléique) - (éthylène -
co - butylène) - styrène [213], éthylène - anhydride maléique [214], LDPE -
anhydride maléique - acrylate de butyle [215] ou un mélange commercial PP - PA-6
compabilisé (orgalloy) [216].

Nous avons testé comme agents interfaciaux [47, 48] les copolymères
fonctionnalisés participant à une synergie lorsqu'ils sont associés à l'APP dans un
mécanisme FR. Ces derniers ont fait l'objet de l'étude présentée dans le Paragraphe
III-3.

Dans une première partie, un exemple illustre la mise en forme d'un mélange-
maître PA-6/EVA/APP, ses performances feu ainsi que les techniques
spectroscopiques qui prouvent la compatibilité des constituants dans le mélange.
Dans une dernière partie, nous présenterons les performances FR de formulations
de plusieurs polymères et copolymères chargés avec des additifs mélanges-maîtres
du PA-6/APP.

IV-1. **Etude du mélange - maître PA-6/EVA8/APP**

Notre Groupe travaille à la formulation de polymères FR aptes à être utilisés
en câblerie électrique en tant que gaines des câbles « basse tension » et, tout
particulièrement, à celle des copolymères éthylène - acétate de vinyle. L'utilisation
de ces copolymères en tant qu'agents interfaciaux est, dans un premier temps,
testée. L'étude est une approche des phénomènes qui permettent la compatibilité
après mélange.

Structural Study of the Polymer Phases in intumescent PA6-EVA-FR Additive Blends.

Catherine SIAT[1,2], Serge Bourbigot[1] and Michel Le Bras[1]

[1] LCAPCS, *E.N.S.C.L. (U.S.T.L.), BP 108, F-59652 Villeneuve d'Ascq Cedex*
[2] *CREPIM, Zone Initia, F-62 Bruay la Bussière .*

Abstract

Polymers may be used as carbonization agent in FR intumescent additives master batches. In particular, polyamide - 6 is extensively used in polyethylenic FR formulations. The paper presents a typical master batch in which a blend of polyamide - 6 and a ethylene - vinyl acetate copolymer can solubilize the ammonium polyphosphate, i.e. the carbonization catalyst. It is shown that the additives system develops the same protective mechanism that a classical FR intumescent system. The problem of the migration of the phosphate throughout the polymeric matrix is discussed. ^{1}H NMR spectroscopy is presented as a tool to predict and explain the part played by a covering agent.

Introduction

Uses of polyolefins in electrical, building or transport applications are often limited because of their bad fire properties. A solution to limit the kinetics of the burning mechanism (thermal and thermooxidative decomposition via a radical chain mechanism with both direct and indirect branching, and combustion) consists in developing on the outer surface of the polymer a glassy or an expanded shield which may at least partially, limit the transfer of fuel to the gas phase, the transfer of heat from the gaseous phase to the condensed phase and eventually oxygen diffusion in the condensed phase. This Laboratory develops several fire retardant (FR) polyolefin-based formulations where the protection is carried out by the formation in the conditions of a fire of a surface intumescent material, i.e. the formation of an expanded carbonaceous structure on the flame front [1]. Intumescent additives formulations are generally mixtures of carbonization agents and carbonization catalysts (products which form stable acidic species when heated - salts of phosphoric acids and / or boric acid) and eventually, a spumific agent. Previous studies of this Laboratory have shown that the intumescent structure consists in carbonaceous and polyaromatic species which structure (carbon organisation characteristic of a pregraphitization stage) grows when the temperature increases [2].

Most recently, we have developed new additives mixtures using polymers as carbonisation agents. In particular, intumescent mixtures of the additives: ammonium polyphosphate (APP) and polyamide-6 (PA-6) has been developed for use in polypropylene, ethylene propylene rubber, ethylene - vinyl acetate copolymers and other polyethylenics. Unfortunately, the two additives are not compatible when mixed and then master batches of the additives mixtures may not be obtained. The solution consists in processing the mixture using a compatibilizing agent (ethylene - vinyl acetate copolymer, functionalized terpolymers of ethylene, siloxane or silane - based resins) which maximises the interfacial bonding and so prevents the reject of the mineral additive throughout the polymer matrix [3]. Among these agents, ethylene-vinyl acetate (8 %) (EVA8) has been selected because it is easily introduced in the mixtures using an internal mixer, it increases the « compatibility » of APP and PA-6 and more reveals to be a synergistic FR agent.

In a first part, this paper discusses the conditions of the master batch process. It reports then the FR performances of the APP/PA-6/EVA8 additives mixtures using Limiting Oxygen Index and UL-94 tests.

Additional structural information was finally obtained from low resolution ^{1}H NMR of the solid state. The shape of the free induction decay (FID) allows the measurement of the spin-spin relaxation times (T_2) after solid echo sequences. The observation of the FID shows the presence of a fast and slow component [4] which may be respectively assigned to rigid and amorphous domains [5]. On the basis of the previous work of Cheung and Gerstein [6], the size domain measurement of the slow relaxation was then examined using as « probe » the free precession of the protons present and the spin diffusion phenomenon in the materials.

Materials

The raw materials (PA-6 as pellets supplied by Nyltech, APP (Exolit 422) as supplied by Hoechst and EVA8 (powdered Lacqtène 1005VN3) as supplied by Elf Atochem) and the additives mixtures preparation had been previously reported [7]. The PA-6/EVA8 = 6 weight ratio was chosen because it corresponds to the higher ratio to obtain both the compatibilizing action and a marked enhancement of the FR performances. Mixtures were mixed using the Brabender Laboratory Mixer measuring head (type 350/EH, roller blades, checking of the mixing conditions using the data processing torque rheometer system Brabender Plasticorder PL2000) during the time requisite to obtain constant values of the torque in the processing conditions (constant shear rate: 50 s^{-1}). Approximate melt rheological properties of the polymeric mixture can be calculated directly from torque rheometer data (η = K M / s, where η is the viscosity, M the torque, s the spinning speed, and K the instrument constant [8]).
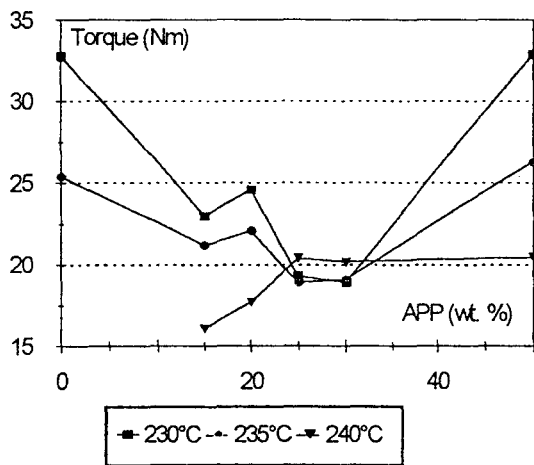
Figure 1. Rheological data of the mixing process vs. the temperature and the APP content.
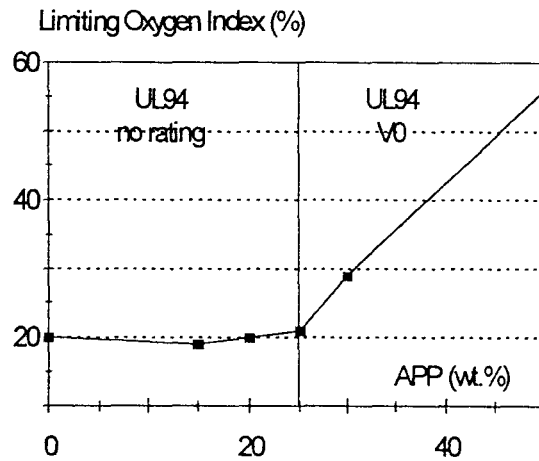
Figure 2. Fire performances of the APP/PA-6/EVA8 systems vs. the APP content.

Apparent values of the viscosity (Fig. 1) show that APP plays different parts versus the temperature and its content in the melts. With a content lower than 25 wt. %, it acts as a plasticizer at 230 and 235°C and as an hardener at 240°C. Moreover, it always acts as an hardener at 230 and 235°C when its contents are higher than 30 %. Two important results are deduced from the study:

- the apparent viscosity is nearly a constant at 240°C. This behavior may be explained by a carbonization process which takes place in the processing conditions,

- the polymer blend does not present the behavior of a thermoplastic resin ($\eta \neq \eta_0$ exp Eγ/RT) when 25 < APP < 32 wt. %. It suggests an important chemical and /or physical modification of the blend.

Fire Retardant Performances and thermal behaviour

The FR property of the APP/PA-6/EVA8 blend increases significantly with APP contents higher than 25 wt. % (Fig. 2). A master batch (APP/ (APP/PA-6/EVA8) = 30 wt. %) with a LOI of about 30 % has been added in several polyethylenic formulations and gives significant FR properties. As examples, addition of 30 wt. % of this additives mixtures in EPR and EVA8 leads respectively to LOI$_{EPR}$ = 28 % and LOI$_{EVA5}$ = 26 %. Additivity of the FR property is not observed; the synergistic effect may be then explained by a reaction between the carbonaceous materials (formed from the additives) and the polymer and/or its degradation products. Existence of a free radical mechanism has been in that case, previously discussed [7]. In all ethylenic formulations, the protection of the material is obtained via the formation of an expanded carbonaceous shield.

A study of the formation of the protective intumescent material from the additives mixture has been carried out using both thermogravimetry (TG) and NMR of the solid carbonaceous materials. The comparison between the curves of the APP-PA6 mixture and those of its sole components (Fig. 3) shows that the carbonization process begins at about 200°C (this reaction explains the loss of the thermoplastic property observed during the processing). It leads to the formation of an expanded carbonaceous material which degrades at about 390°C with a loss of the foamed character. The resulting carbonaceous material is relatively thermally stable in the temperature range 400 - 550°C.

The ^{31}P DD/MAS NMR spectrum of the intumescent material formed from APP/PA-6/EVA8 (Fig. 4) shows the existence of several P(V) species: acidic orthophosphate species (chemical shift $\delta \approx$ 0 ppm), end and middle groups of polyphosphate species (δ respectively -11 and about -25 ppm) and phosphorus oxides with different P-O-P bond angles (δ = -45 and -53 ppm [9]). The corresponding ^{13}C CP DD/MAS NMR spectrum (Fig. 5) shows a broad band (maximum at 127 ppm) assigned to polyaromatic species, a signal in overlap at about 160 ppm may be assigned to oxidized polyaromatic species [2 and Ref. therein]. This priliminary study proves that the thermal behaviour of the PA-6 based additive is quite the same than this of the previously studied APP/pentaerythritol intumescent system [10], it is formed of polyaromatic stacks which allow the existence of acidic phosphates in a relatively high temperature range [11].
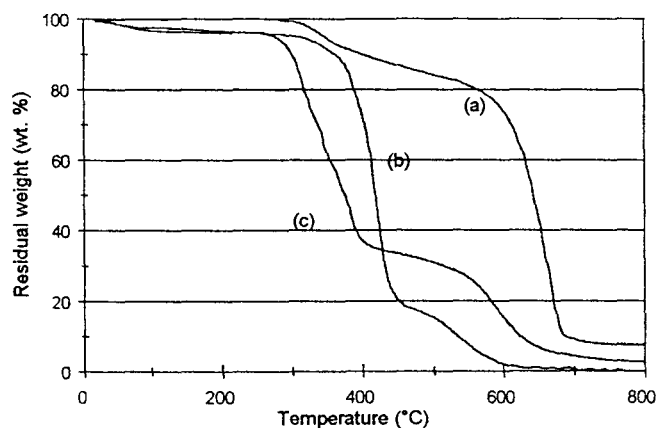
Figure 3. Experimental TG curves of APP (a), PA-6 (b) and the APP/PA-6 mixture (c) under air flow.
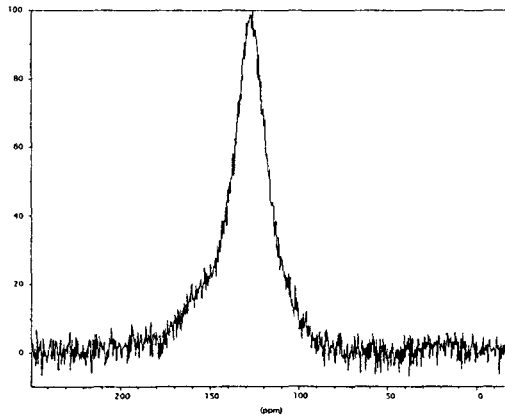
Figure 4. CP - MAS - DD ^{13}C NMR spectrum of the APP/PA-6/EVA8 system at 385°C.
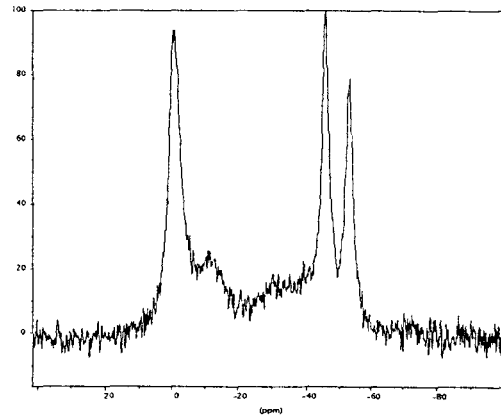
Figure 5. MAS - DD ^{31}P NMR spectrum of the APP/PA-6/EVA8 system at 385°C.

Structural Study   Compatibility of the components in the master batch

A preliminary 13C CP - DD/MAS NMR study of the polymeric master batches (processed at 235°C) shows that the spectra of the mixtures presents the unmodified signals of their components and as a consequence, that the polymer chains are not severely modified during the process.

Spin - lattice relaxation

Proton NMR studies allow, using the method of inversion recovery [π-τ–π/2], the measurement of proton spin - lattice relaxation (T_1) times. Only one T_1 value is observed for each formulation (Table 1). This result implies that the polymeric systems do not present any structural heterogeneity with a size higher than 10 nm.

Spin - spin relaxation

The free precessions of the systems have been recorded after the spin - echo sequence and after a complementary solid echo sequence [12]. In each case, they present complex shapes. In a first approximation, two decays may be distinguished: one fast and the second slower (table 2). The fast decaying component is assumed to be Lorentzian and the slow decaying component is described by functions 1 (combination of a Gaussian and a Weibullian), 2 (Gaussian) or 3 (combination of a Gaussian and a Lorentzian):

Sample	T_1 (ms)
PA-6	495
APP	1970
EVA5	278
PA-6/EVA5	348
APP /PA-6	586
APP/ EVA5	303
APP /PA-6/EVA5	520

Table 1. T1 values

1    $M = M_{0c}\exp(-(t/T_{2c})^{e}) + M_{0L}\exp(-(t/T_{2L})^{2})$

2    $M = M_{0}\exp(-(t/T_{2})^{2})$

3    $M = M_{0c}\exp(-(t/T_{2c})^{2}) + M_{0L}\exp(-t/T_{2L})$

where t is the time, M_{0c} and M_{0l} are, respectively, the magnetization amplitudes of the fast and slow decaying components, T_{2c} and T_{2l} are respectively, the spin - spin relaxation times of the fast and slow decaying components and e the Weibull coefficient ($1 < e < 2$).

Sample	Function	M_{0c} (%)	M_{0L} (%)	T_{2c} (µs)	T_{2L} (µs)	e
PA-6	1	86,4	11	9,2	55,3	1,6
APP	2	99		31,8		
EVA8	3	10,2	93,2	10,2	27,7	
PA-6/EVA8	1	74,9	23,4	10,04	51,7	1,5
PA-6/APP	1	69	29	10,4	29,8	1,7
APP/EVA8	3	5,6	96	10,3	24,6	
APP/PA-6/EVA8	1	70,9	27,8	10,7	37,4	1,5

Table 2. values of T_2 and magnetization amplitudes.

APP presents only one decay which is easily explained by its cristalline structure. Moreover, two T_2 values are observed from each polymeric sample and the presence of two phases in these materials is thus demonstrated. A previous XRD study has shown that the polymer(s) in the « blends » present(s) a semicristalline structure. So, the fast component may be assigned to the cristalline phase and the slowly decaying component to fast molecular motion of the protons in the amorphous phase. The decrease of the T_{2L} values after addition of APP in PA-6 proves the increase of the rigid character of the amorphous phase. On the other hand, the comparatively high value of T_{2L} shows that the rigid character of the amorphous phase is lower in APP/PA-6/EVA8 than in the APP/PA-6 system.

M_{0c} and M_{0l} values are directely related to the relative content in protons in respectively the cristalline and the amorphous phase. The FID study shows an increase of the protons content of the amorphous phase when APP is added in PA - 6, this increase may be explain either by the selective localisation of the phosphate in the amorphous phase [13] or by an increase of the size of this amorphous phase. Measurement of T_2 values brings information on compatibility of materials: T_2 of a mixture equale to T_2 of a virgin component shows incompatibility of the mixture components [14]. Compatible compounds gives mixtures with T_2 values between those of the virgin components.

The study compares the T_{2L} values because APP does not present a fast decaying component. It confirms that APP and PA-6 are not compatible and that addition of EVA8 in their mixture gives compatibilisation of the mineral - polymer compound.

Size of the slow relaxation domain

The variation of the size of the domains undergoing slow relaxation were computed from low resolution ^{1}H NMR spectra using Goldman - Shen sequences [15]

Formulations	D (cm^2/s)	a (nm)	$\overline{b}_{3D}$ (nm)
PA6	1,31 10^{-8}	0,9 59	1,9
PA6/APP	1,13 10^{-8}	0,9 51	2,3
PA6/EVA5/APP	1,10 10^{-8}	0,9 55	2,8

tableau 3. Spin - diffusion coefficient,average of the distance between two protons (deduced from XRD spectra) and size of the slow relaxation domain.

Table 3 shows that addition of APP in a polymeric matrix increases the size of the amorphous domain.

Discussion

The NMR study shows that addition of APP in the polymeric matrix does not lead to a chemical change of the polymer chains. The phosphate species location in the amorphous domains of the matrix explains the increase the increase of the size of the amorphous domains. More, the study shows that EVA8 in the blend allows the compatibility of APP in the polymeric matrix. It may be proposed that the amorphous character of EVA8 (initially 93 % of the protons belongs to its amorphous domains) allows the easy location of APP in the blend.

From Literature [16], formation of a blend of a semi-cristalline polymer and an amorphous polymer leads to the presence of two different phases in the blend, i.e. presence of both a mixture of the two amorphous phases and of a homogeneous mixture of the cristalline and a amorphous phase. The existence of these two phases in the blend is verified by the T_2 values. Moreover compatibility of an additive in a polymeric matrix may be achieve using a functionalized copolymer which acts as a covering agent. EVA8 located in the amorphous phase of PA-6, may

take this part. Particles formed by APP covered by EVA present a comparatively large size, and their formation explains the observed increase of the amorphous domains size.

Conclusion

Polyamide - 6 may be used as carbonization agent in FR intumescent additives master batches which are extensively used in polyethylenic FR formulations. A typical master batch is a blend of polyamide - 6 and a ethylene - vinyl acetate copolymer which can solubilize the ammonium polyphosphate, i.e. the carbonization catalyst. It is shown that the additives system develops the same protective mechanism that a classical FR intumescent system. The problem of the migration of the phosphate throughout the polymeric matrix is discussed. ^{1}H NMR spectroscopy is presented as a tool to predict and to explain the part played by EVA proposed the compatibilizing agent.

Bibliography

1 - DELOBEL, R., LE BRAS, M., OUASSOU, N., and ALISTIQSA, F., *J. Fire Sci.*, **8(2)** (1990) 85.

2 - BOURBIGOT, S., LE BRAS, M., DELOBEL, R., DESCRESSAIN, R., and AMOUREUX, J.-P., *J. Chem. Soc., Faraday Trans.*, **92(1)** (1996) 149.

3 - BOURBIGOT, S., SIAT, C., and LE BRAS, M., *« Matériaux Polymères et Procédés - Colloque Annuel du GFP »*, Nancy (21-23/11/1995), pp. 29.

4 - McCALL, D.W., DOUGLASS, D.C., and FALCONE, D.R., *J. Phys. Chem.*, **71** (1967) 998.

5 - BOURBIGOT, S., *Doctoral dissertation*, University of Lille, 1993.

6 - CHEUNG, T.T.P., and GERSTEIN, B.C., *J. Appl. Phys.*, **52** (1981) 5517.

7 - LE BRAS, M., BOURBIGOT, S., DELPORTE, C., SIAT, C., and LE TALLEC, Y., *Fire & Materials*, paper FAM/470 submitted for publication (1996).

8 - LEE, G.C.N., and PURDON, J.R., *Polym. Engineer. & Sci.*, **9(5)** (1969) 360.

9 - STERNBERG, U., PIETROWSKI, F., and PRIESS, W., *Z. Phys. Chem. Neue Folge*, **168** (1990) 115.

10 - BOURBIGOT, S., LE BRAS, M., and DELOBEL, R., *Carbon*, **31(8)** (1993) 1219.

11 - DELOBEL, R., LE BRAS, M., and OUASSOU, N., *Polym. Deg. & Stab.*, **30** (1990) 41.

12 - TANAKA, H., and NISHI, T., *J Chem. Phys.*, **82(9)** (1985) 4326.

13 - SCHLOTTER, N.E.,and FURLAN, P.Y., *Polymer*, **33(16)** (1992) 3323.

14 - KOSFELD, R.H., and ZUMKLEY, L., *« Polymer Compatibility and Incompatibility »* - *MMI Press Symp. Ser.*, 2 (1982) 2213.

15 - GOLDMAN, M., and SHEN, L., *Phys. Rev.*, 4 (1966) 321.

16 - STEWARD, M.E., *« Fundamentals of Polymer Blend Technology -Fire Retardant Blends, Alloys and Thermoplastic Elastomers »*, Spring Conf., Soc. of Plastics Engineers, PMAD Division and FR Chem. Association, (1991).

L'étude montre que la formulation des mélanges - maîtres est complexe. En effet, selon sa teneur, l'APP joue le rôle d'un agent plastifiant (teneur inférieure à 25 % pondéral) ou d'un agent épaississant (teneur supérieure à 30 % pondéral). Une teneur au moins égale à 30 % pondéral en APP est nécessaire pour obtenir le classement UL-94 V0. L'obtention du mélange - maître pose donc des problèmes liés aux variations brutales des propriétés rhéologiques en fonction de la composition du mélange et des conditions expérimentales de l'opération unitaire (température, cisaillement, balance entre énergie thermique et énergie mécanique fournie au système). L'optimisation des paramètres du mélange et de son obtention par extrusion est actuellement menée en couplant les mesures de viscosité dans un viscosimètre à cylindres, la DSC et diverses techniques spectroscopiques (RMN, IR, Diffraction des RX, microscopie électronique et fractographie).

Le comportement thermique sous air du matériau est similaire à celui du système APP/PER avec formation d'un bouclier intumescent, stable jusque environ 390°C, qui se dégrade au température supérieure pour former un résidu carboné « haute température ». L'étude spectroscopique vérifie que le matériau intumescent est formé d'espèces polyaromatiques et d'un mélange d'espèces phosphates contenant de l'acide orthophosphorique. Finalement, elle montre que la dégradation du matériau intumescent est accompagnée par la formation des oxydes de phosphore.

L'étude de la cinétique de la dégradation thermo-oxydante du PA-6 et du matériau issu du mélange maître, utilisant la méthode IKP et le calcul de la probabilité des lois de dégradation (Figures IV-3 et IV-4), complète les résultats présentés. Elle montre le comportement ablatif du matériau dans la gamme de température où le revêtement protecteur se forme [217]. En effet, si la vitesse initiale de sa décomposition est inférieure à celle du PA-6, elle est d'un ordre de magnitude plus élevée lorsque le degré de conversion atteint 30 % pondéral.

Finalement, une méthodologie pour l'étude de l'homogénéité d'un mélange de polymères et de la compatibilité des composants du mélange est présentée. Elle utilise les spectres RMN basse résolution du ^1H dans les solides obtenus en utilisant

la séquence présentée au paragraphe II-1-a. Cette méthode est systématiquement mise en œuvre lorsque des agents interfaciaux différents sont utilisés (terpolymères éthylène - acrylate de butyle - anhydride maléique (LRAM) , copolymères éthylène - acrylate de butyle (FEABu ou LYABu)).
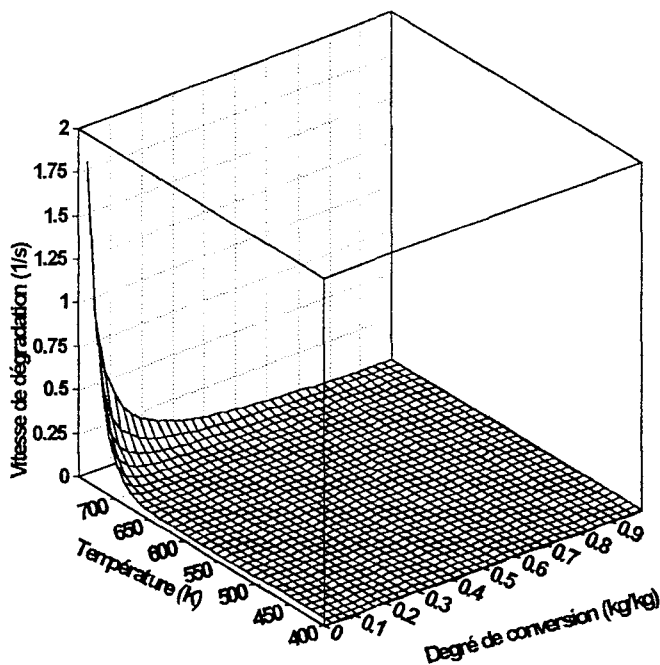

Figure IV-3. Vitesse de la dégradation thermo-oxydante du PA-6 fonction de la température et du degré d'avancement de la réaction.
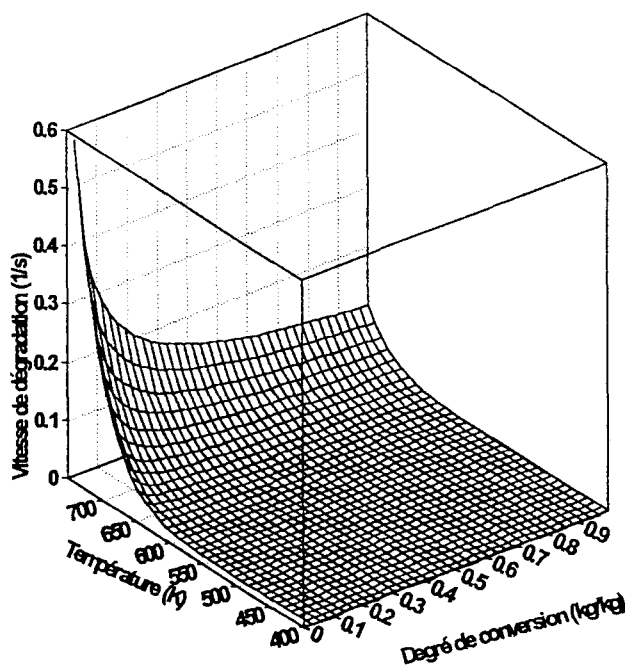
Figure IV-4. Vitesse de la dégradation thermo-oxydante du système PA-6/APP fonction de la température et du degré d'avancement de la réaction.

L'introduction de l'EVA-8 dans le mélange permet la compatibilité du PA-6 et de l'APP, entités macromoléculaires de nature chimique différente et, de ce fait, immiscibles. Son mode d'action reste à préciser (greffage sur la chaîne du polyphosphate par formation de groupements esters, formation de blocs qui minimisent les « hétérocontacts ». Il en résulte une perte d'entropie qui s'oppose à la macroséparation des phases [218] ou une interpénétration de phases qui donne un matériau apte à la formation de structures lenticulaires avec encapsulation des grains d'APP).

IV-2. Nouveaux polymères FR intumescents formulés par addition du système PA-6/APP

Les formulations rassemblées dans ce Paragraphe font l'objet de plusieurs revendications de propriétés industrielles [43, 44, 47, 48, 219]. De ce fait, nous limiterons notre présentation à une compilation de performances FR obtenues par ajout de l'additif dans différents polymères de commodité.

- Formulations du PA-6

APP (%pondéral)	Agent Interfacial (IA)	Teneur en IA (%pondéral)	LOI (%)	UL-94
28*	E-BuA-MA	12	36	V-2
28*	EVA(28%)	12	35	V-2
28*	EVA(5%)	12	32	V-2
28**	EVA(5%)	12	32	V-0

Glossaire : mise en forme *en plastographe, **en extrusiographe.
Tableau IV-1 : *LOI et classement au test UL-94 des formulations FR du PA-6 fonction de la nature de l'agent interfacial et de l'opération de mise en forme ;*

Les performances présentées dans le tableau IV-1 montrent qu'il est possible d'obtenir des formulations FR intumescentes du PA-6. Les performances FR dépendent alors de la nature du polymère agent de compatibilisation et des modalités de l'opération de mise en forme en accord avec les résultats présentés dans le paragraphe IV-1.

• Formulations du PP

Le tableau IV-2 présente les propriétés « retard au feu » du polypropylène isotactique chargé à 35 % pondéral par des mélanges de rapports pondéraux (E-BuA-MA)/PA-6+APP=1/6. Les propriétés optimales sont obtenues pour un rapport des additifs 0,5 <PA-6/APP < 0,3 kg/kg.

PA-6/APP kg/kg	Cisaillement (rpm^{-1})	LOI (%)	UL-94
2	$2,5\ 10^{-2}$	23	Non classé
1	$2,5\ 10^{-2}$	25	V-0
0,5	$2,5\ 10^{-2}$	29	V-0
0,33	$2,5\ 10^{-2}$	29	V-0
0,25	$2,5\ 10^{-2}$	27	V-0
0	$2,5\ 10^{-2}$	21	Non classé

Tableau IV-2 : *LOI et classement au test UL-94 des formulations FR du PP, fonction de la teneur en CP du mélange - maître, après mise en forme en plastographe.*

Le tableau IV-3 présente les propriétés « retard au feu » d'un polypropylène choc (PP choc : 20% massique de talc dans PP isotactique) chargé par les mélanges maîtres de la même série. L'addition de la charge de renfort (nécessaire pour obtenir les propriétés mécaniques du cahier des charges) n'interdit pas d'obtenir les propriétés FR mais oblige l'introduction d'une quantité du mélange maître plus importante.

Taux d'additifs FR (% pondéral)	PA-6/APP (kg/kg)	Agent Interfacial (5% pondéral)	LOI (%)	Classement UL-94
45	0.5	LRAM3.5	29	V-0
	0.33	LRAM3.5	29	V-0

Tableau IV-3 : *LOI et classement au test UL-94 des formulations FR du PP choc, fonction du rapport PA-6/APP du mélange - maître, après mise en forme par une séquence extrusion - thermomoulage.*

• Formulations du PS et d'un copolymère de styrène

Le tableau IV-4 présente les propriétés « retard au feu » d'un polystyrène standard (variété « cristal » : homopolymère, amorphe de structure atactique [220]) chargé à 30 % pondéral par le mélange - maître APP/PA6. Le LOI optimal est

obtenu pour 0.33 < PA-6/APP < 1, alors que les formulations ne répondent pas aux spécifications du test UL-94 quelque soit PA-6/APP.

PA-6/APP (% pondéral)	Cisaillement (rpm^{-1})	LOI (%)	UL-94
4	2,5 10^{-2}	19	non classé
2	2,5 10^{-2}	22	non classé
1	2,5 10^{-2}	25	non classé
0,5	2,5 10^{-2}	25	non classé
0,33	2,5 10^{-2}	26	non classé
0	2,5 10^{-2}	19	non classé

Tableau IV-4 : *LOI et classement au test UL-94 des formulations FR du PS standard, fonction de la composition du mélange - maître , après mise en forme en plastographe.*

Le tableau III-6 présente les propriétés « retard au feu » d'un polystyrène choc (« High Impact Polystyrene » (HIPS) : copolymère polybutadiène - styrène) chargé par des mélanges maîtres PA-6/APP. Le classement au test UL-94 est atteint lorsque le mélange - maître est ajouté à 50 % pondéral dans le copolymère. La substitution du mélange maître par des agents compatibilisants (copolymères fonctionnalisés) ou l'agent de synergie zéolithe 4A entraîne une perte des propriétés FR. La recherche de nouveaux agents doit donc être considérée afin de diminuer la teneur en adjuvants tout en maintenant des propriétés FR du HIPS similaires.

• Formulations de copolymères séquencés ethylène - propylène

Le tableau IV-6 présente les propriétés « retard au feu » d'un copolymère éthylène - propylène (EPR) chargé à 35 % pondéral par des mélanges maîtres PA-6/APP. Ces mélanges maîtres ont des rapports pondéraux APP/PA-6 = 3, APP/PA-11 = 2 et (agent compatibilisant/PA+APP)=1/6. Les performances FR optimales sont obtenues en associant le PA-6 et l'EVA(5%) dans le mélange-maître. Bien que n'admettant pas un classement UL-94, les trois formulations peuvent être utilisées comme matériaux d'un revêtement de sol avec un classement AFNOR M2 car elles sont aptes à un calandrage.

Taux de charge (% pondéral)	PA-6/APP (kg/kg)	Compatibilisant (%massique)	4A[(1)] (%massique)	LOI (%)	UL-94
40	1	-	-	29	N-C
	0,5	-	-	30	N-C
	0,33	-	-	32	N-C
	0,2	-	-	31	N-C
45	1	5% LRAM3.5[(2)]	-	28	N-C
	0,5	5% LRAM3.5[(2)]	-	28	N-C
	0,33	5% LRAM3.5[(2)]	-	29	N-C
	1	5% EVA8[(3)]	-	29	N-C
	0,5	5% EVA8[(3)]	-	32.5	N-C
	0,333	5% EVA8[(3)]	-	32	N-C
40-45	0,33	-	1	31	N-C
		-	3	34	N-C
		-	5	34	N-C
50	1	-	-	33	V-0
	0,5	-	-	42	V-0
	0,33	-	-	44	V-0

Glossaire : (1) : zéolithe sodique de type 4A - (2) Terpolymère de l'éthylène : éthylène - acrylate de butyle - anhydride maléique - (3) Copolymère de l'éthylène : éthylène - acétate de vinyle.

Tableau IV-5 : *LOI et classement au test UL-94 des formulations FR du « PS choc », fonction de la composition du mélange - maître et de l'addition de zéolithe 4A, après mise en forme en plastographe.*

Polyamide	Copolymère (AI)	LOI (%)	UL-94	AFNOR
PA-6	E-BuA-MA	24*	Non classé	M2
		24**	Non classé	M2
PA-6	E-VA(5%)	25**	Non classé	M2
PA-11	E-BuA-MA	23**	Non classé	M2

Glossaire : * : après calandrage, ** : en extrusiographe.

Tableau IV-6 : LOI et classement au test UL-94 des formulations FR de l'EPR, fonction de la composition du mélange - maître et des conditions de mise en forme.

- Formulations du copolymère éthylène - acétate de vinyle (8 %)

Le tableau IV-7 présente les propriétés FR du copolymère éthylène - acétate de vinyle (8%massique) : EVA8 chargé par des mélanges maîtres PA-6/APP.

Taux de charge (% pondéral)	PA-/6APP (kg/kg)	Agent d'enrobage	LOI (%)	Classement UL-94
30	1	-	22	N-C
	0,5	-	23	V-0
	0,33	-	23	V-0
	0,2	-	26	V-0
40	1	-	26	N-C
	0,5	-	27	V-2
	0,33	-	29	V-0
	0,2	-	31	V-0
30	0,5	TEOS	26	V-0
	0,33	TEOS	27	V-0
	0,2	TEOS	31	V-0
40	0,5	TEOS	29	V-0
	0,33	TEOS	29	V-0
	0,2	TEOS	34	V-0

Tableau IV-7 : LOI et classement au test UL-94 des formulations FR de EVA8, fonction de la teneur en additif, de la composition du mélange - maître et de la présence de l'agent d'enrobage, après mise en forme en plastographe.

Rappel : conditionnement des espèces phosphates :
Des mélanges de tétraéthylesiloxane (TEOS) et d'eau (H_2O), de rapport molaire H_2O/TEOS compris entre 2 et 8, en solution dans l'éthanol à raison de 40 à 60 g dans 100 ml d'éthanol sont mis en agitation mécanique à température ambiante. Les espèces phosphates à raison de 50 à 250 g sont ensuite dispersées dans la solution. L'agitation est maintenue jusqu'à l'obtention d'une pâte homogène.

> Le dit produit peut ensuite être introduit dans des polymères thermoplastiques après réticulation en étuve puis broyage, lors d'une transformation en plastographe ou en extrusiographe.

Les performances FR sont optimales avec les rapports pondéraux PA-6/APP < 0,33. La faible teneur en PA-6 nécessaire pour obtenir ces propriétés s'explique par l'interaction entre l'APP et le copolymère qui conduit au processus d'intumescence sans carbonisation (processus discuté dans le chapitre précédent). L'agent d'enrobage TEOS est un agent de synergie intéressant puisqu'il permet de diminuer la teneur en adjuvants de 10 % pondéral tout en conservant des performances FR satisfaisantes.

IV-3 **Approche du mécanisme d'action de l'additif intumescent PA-6/APP dans une formulation de l'EVA-8**

Le mécanisme d'action du système additif peut être, au moins partiellement, caractérisé par une étude de la cinétique de la dégradation du matériau. Nous limitons l'approche à l'étude d'une formulation EVA8 - PA-6/APP. La formulation étudiée est mise en forme par mélange à 230°C en plastographe. Sa composition est celle de la formulation optimale présentée dans le tableau IV-7 (PA-6/APP = 0,2, taux d'adjuvants : 40 % pondéral).

La comparaison des courbes TG de la dégradation thermo-oxydante du PA-6 et du mélange PA-6/APP (Figure IV-5) vérifie la formation à basse température (environ 80°C inférieure à celle du PA-6 seul dans les conditions expérimentales utilisées) du matériau intumescent protecteur stable jusque environ 550°C.

L'analyse thermogravimétrique (Figure IV-5) montre, par ailleurs, que le matériau carboné intumescent protecteur se forme à 350°C. Sa dégradation, à environ 450°C, conduit à un résidu carboné abondant stable jusqu'à 550°C, qui se dégrade en deux étapes successives (à environ 500 et 580°C) pour former un résidu « haute température » peu abondant (2 % pondéral au delà de 700°C). Le caractère expansé du matériau carboné, issu du système, est conservé jusque 580°C.

La courbe TG de la formulation EVA8/PA-6/APP vérifie la conservation de l'EVA dans le matériau intumescent. En effet, la masse résiduelle (environ 40 %

pondéral) est supérieure à celle déduite par addition des résidus ex-EVA8 et PA-6/APP (environ 15 % pondéral). Ce résultat confirme la participation de la matrice polymère à sa protection et explique la synergie préalablement observée entre les constituants de la formulation.
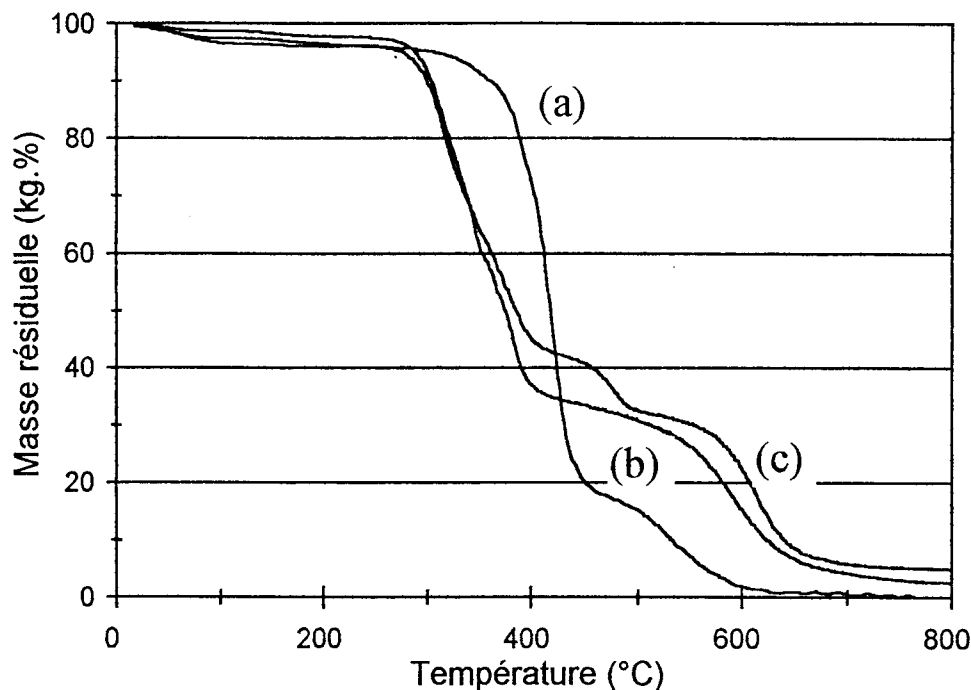

Figure IV-5. Courbes TG du PA-6 (courbe a), du mélange adjuvant PA-6/APP (courbe b) et de la formulation EVA8/PA-6/APP (courbe c) sous air [217].
débit d'air : 5 x 10^{-7} m^3/s, vitesse de chauffe : 7,5 °C/s

Le caractère ablatif de la dégradation thermo-oxydante de l'EVA8 en présence de l'APP est montré par la comparaison des vitesses de dégradation de l'EVA seul (Figure IV-6) avec celle du système EVA8/APP (Figure IV-7). La vitesse de dégradation du mélange, initialement comparativement très élevée, reste supérieure à celle du polymère seul, quels que soient la température et le degré d'avancement de la réaction. Cette vitesse implique une réaction entre l'additif et le polymère avec formation de produits volatils.
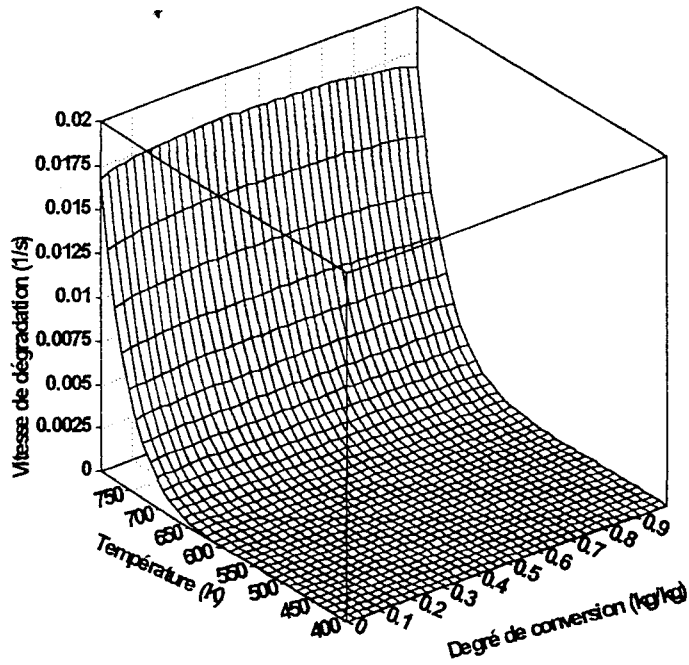
Figure IV-6. Vitesse de la dégradation thermo-oxydante de l'EVA8 fonction de la température et de l'avancement de la réaction.
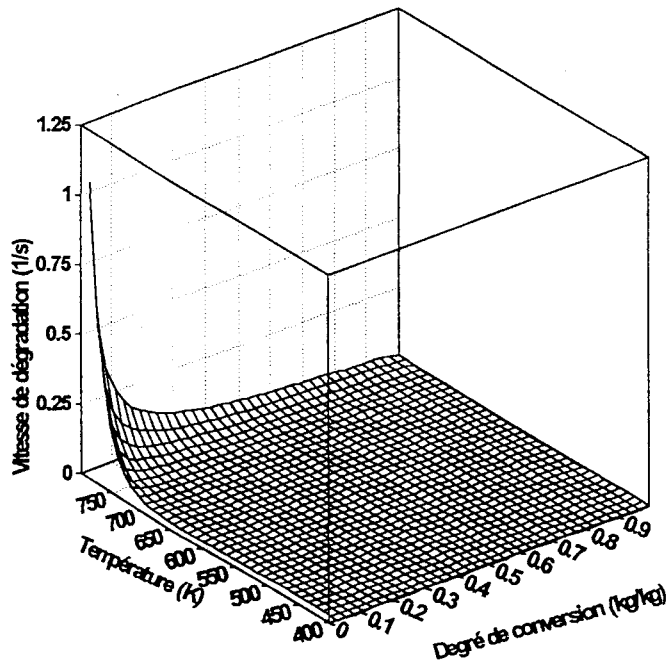

Figure IV-7. Vitesse de la dégradation thermo-oxydante du mélange EVA8/APP (teneur en APP : 28 %pondéral), fonction de la température et de l'avancement de la réaction.
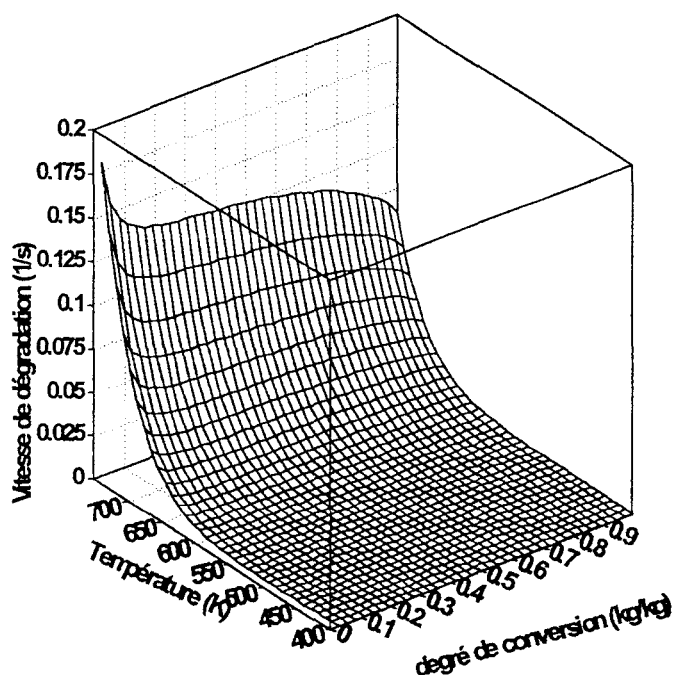
355

Figure IV-8. Vitesse de la dégradation thermo-oxydante du mélange EVA8/PA-6/APP (teneur en adjuvants : 28 %pondéral, PA-6/APP : 0,20 kg/kg), fonction de la température et de l'avancement de la réaction.

La vitesse de dégradation de la formulation EVA8/PA-6/APP (Figure IV-8) est très inférieure, à conversion nulle, à celles des mélanges PA-6/APP (Figure IV-4) et EVA8/APP. Elle est ensuite (α > 20 % pondéral) supérieure à celle de EVA8/APP et voisine de celle de PA-6/APP. La préservation du matériau résulte bien, dans ce cas, de la formation d'un matériau protecteur lors de la décomposition rapide de la formulation. Ce matériau protecteur est formé par réaction entre les trois constituants du matériau initial.

La protection au feu résulte bien, dans cet exemple, de l'ensemble des processus chimiques qui caractérise le processus d'intumescence et qui a fait l'objet de ce Mémoire.

L'approche, utilisant des matériaux préparés en plastographe, est en fait simplificatrice. En effet, les performances FR (figure IV-9) sont fonctions des conditions de la mise en forme des matériaux en extrusiographe. Elles sont classiquement optimales [221], quelle que soit la température du matériau, lorsque la vitesse de rotation des vis est rapide (environ 100 RPM), c'est à dire lorsque le cisaillement est important et, en conséquence, le temps de séjour en extrudeur court.

356
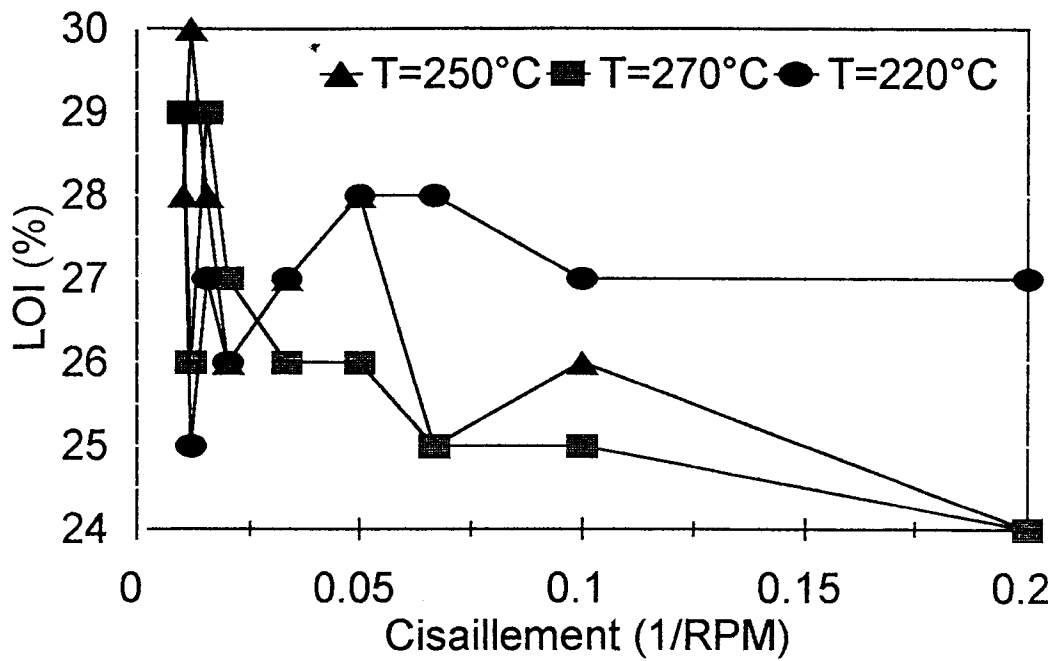
Figure IV-9. Valeurs du LOI de la formulation EVA8/PA-6/APP (teneur en PA-6/APP : 40 % pondéral, PA-6/APP : 0,20 kg/kg), fonction de la vitesse de rotation des vis lors de transformation de la formulation dans un ensemble d'extrusion à vis jumelles en contrarotation à différentes températures [Poutch F., Siat C. et Le Bras M., étude en cours (1996-1997)].
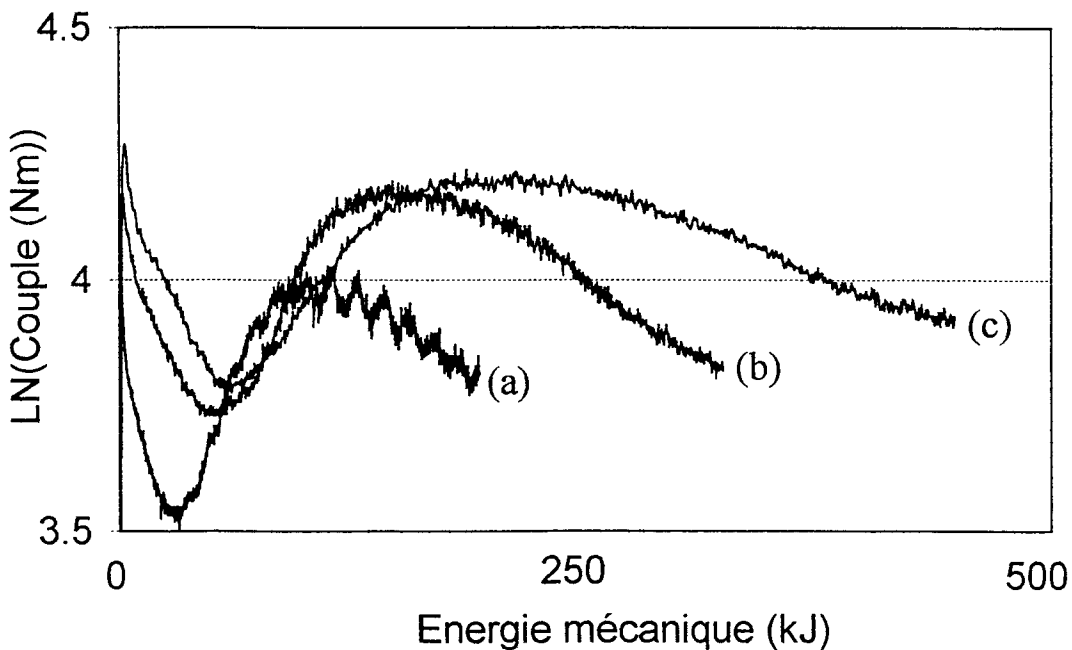
Figure IV-10. Valeurs du couple lors du traitement mécanique de l'EVA8 à 195°C en plastographe, fonction de l'énergie mécanique fournie à différents cisaillements ((a) : 15 RPM, (b) : 30 RPM et (c) : 50 RPM) [Poutch F et Le Bras M., étude en cours (1996-1997)].

Aux vitesses de rotation inférieures, la propriété FR décroît avec une augmentation du temps de séjour et/ou de la température. Il peut être proposé que le mécanisme thermo-mécanoradicalaire (scission de chaînes, départ de volatil, réticulation tridimensionnelle) et/ou la dissolution d'une(des) phase(s) par cisaillement [222] affecte alors la propriété FR en modifiant la composition (en conséquence, la dégradation thermique) et les propriétés dynamiques du matériau.

Cependant, le comportement classique n'est pas systématiquement observé puisque des performances FR intéressantes sont obtenues avec des températures de transformation relativement basses (T ≤ 250°C) lorsque la rotation des vis est de l'ordre de 20 RPM et que, en conséquence, le temps de séjour dans l'extrusiographe est élevé. La modification chimique du matériau polymère lors de sa transformation peut donc être une technique utile pour obtenir des formulations intéressantes.

L'étude en cours révèle que, dans la modélisation de la modification d'un tel matériau, les paramètres expérimentaux à considérer sont nombreux : nature et composition de l'additif, énergies mécanique et calorifique, température, cisaillement. En illustration, la modification chimique de l'EVA8 (dégraphage, avec départ d'acide acétique, et réticulation tridimensionnelle du polymère) en plastographe est rapportée. Elle est caractérisée par la modification de la viscosité à 195°C présentée dans la Figure IV-10. Les paramètres devant être considérés en interaction, leurs effets seront évalués en utilisant un plan d'expérimentation pour mélanges. [Poutch F., Siat C. et Le Bras M., étude en cours (1996-1997)].

Pour conclure, les mélanges des polymères se révèlent des opérations utiles pour obtenir des matériaux retardateurs de flamme intumescents. Notre pré-étude montre que cette approche peut concerner l'ensemble des matériaux thermoplastiques (polyamides et polystyrènes compris). Le sujet est vaste. En effet, outre la modélisation nécessaire des conditions de mélange et de mise en forme, il doit comprendre :

• la recherche de nouveaux polymères susceptibles d'intervenir comme agents de carbonisation ou comme agents de gonflement (polyamides de grades différents, polyalcool vinylique, polyuréthannes, polycarbonates)

- et la recherche et le développement de nouveaux systèmes catalytiques susceptibles de remplacer les systèmes à base de phosphore

En conclusion, la mise en œuvre des mélanges de polymères (« blends ») nous a permis de procurer la propriété FR, par développement de l'intumescence, à plusieurs familles de polymères thermoplastiques de commodité dont les polyamides et les polystyrènes et de développer de tels matériaux aptes au calandrage, au filage et/ou au thermosoudage. La conception de ces nouveaux matériaux mobilise actuellement une partie de notre Groupe.

Par ailleurs, les polymères fonctionnalisés, susceptibles de gonflement sans carbonisation en présence de systèmes catalytiques minéraux, méritent d'être plus particulièrement développés car ils présentent un intérêt certain comme matériaux pour applications électriques telles la câblerie. En effet, cette classe de polymères présente la propriété FR avec des systèmes d'adjuvants contenant de faible teneur en agents de carbonisation, susceptibles de développer une dégradation radicalaire lors de la transformation du matériau FR et, en conséquence, d'initier la dégradation de la formulation. Ces systèmes originaux nécessitent une charge minérale réduite de moitié par comparaison aux systèmes contenant des hydroxydes ($Mg(OH)_2$ [224] ou $Al(OH)_3$ [225]) et doivent, en conséquence, présenter des propriétés mécaniques comparativement intéressantes. Cette approche novatrice [226], parente de celle qui a permis d'obtenir des formulations intumescentes des thermoplastiques par ajout de silicone [227, 228] ou de dérivés de la silice [229], retient actuellement notre attention.

CONCLUSION GENERALE

Le présent travail présente une synthèse des différentes études effectuées au Laboratoire depuis 1978. Il traite de la formulation de matériaux polymères qui retardent leur inflammation via un processus de carbonisation de type ablatif. Le but du travail consiste à établir des modèles physico-chimiques permettant de d'expliquer les liaisons entre les performances au feu et la dégradation ablative des matériaux. Parmi les processus de carbonisation des résines considérés, l'intumescence est tout particulièrement étudiée car elle permet de réduire le dégagement de produits toxiques ou corrosifs lors de la mise en œuvre du processus FR.

La première partie (Tome 1) concerne deux matériaux modèles :

• des résines polyépoxydes développant, dans les conditions d'un incendie, un processus de carbonisation naturelle qui permet éventuellement une tenue au feu du matériau intéressante,

• un mélange d'adjuvants intumescents (polyphosphate d'ammonium - pentaérythritol), étudié plus particulièrement dans le polypropylène.

L'étude permet la caractérisation précise des matériaux « carbones » protecteurs en utilisant ou en développant des techniques analytiques utilisées classiquement pour l'étude des charbons fossiles ou des carbones de synthèse (diffraction des rayons X, diffusion Raman et XPS), celle des polymères (RMN du ^{13}C et du ^{1}H dans les solides et RPE, absorption dans l'infra-rouge) et celle des phosphates naturels et de synthèse (RMN du ^{31}P dans les solides).

Elle montre, en particulier qu'un revêtement intumescent protecteur est, en fait, un système catalytiques où les espèces acides minérales réactives sont supportées par une charpente carbonée constituée de domaines polyaromatiques pontés par des motifs polymères .

Les analyses thermogravimétriques classiques sont exploitées, dans cette partie, pour obtenir les paramètres cinétiques invariants des dégradations

thermiques et/ou thermo-oxydantes ainsi que des équations représentatives des fonctions de dégradation des formulations FR. Ces données sont utilisées dans l'exploitation des données cinétiques des matériaux placés dans les conditions quasi-réelles d'un incendie. Elles permettent de valider un modèle unidirectionnel représentatif des dégradations et finalement d'expliquer les comportements au feu des matériaux en terme de flux de chaleur.

La deuxième partie (tome 2) applique ces méthodes pour :

• expliquer les performances au feu de différents systèmes d'adjuvants FR, intumescents ou carbonisants, dans les polymères thermoplastiques, en considérant les comportements antagonistes ou en synergie des adjuvants en association et la composition de la matrice polymère,

• proposer des formulation d'adjuvants originales.

Elle met en évidence l'existence de liaisons entre les caractéristiques chimiques (acidité, teneur en radicaux libres) ou physico-chimiques (organisation de la phase amorphe, structure du « carbone », présence d'espèces cristallisées) du matériau intumescent et ses performances FR.

Finalement, l'étude présente des exemples de formulations en milieu rhéologiques complexes. Elle préconise l'association des adjuvants phosphates (ou borates) à des agents dérivés de la silice (ou aluminosilicates) qui optimise les performances des précurseurs d'espèces catalytiques acides. L'intérêt d'une « fonctionalisation » du polymère est ensuite montrée : les produits acides formés lors de l'inflammation assure la présence des espèces catalytiques aux « hautes températures ».

Notre travail conduit, en outre, à préconiser le remplacement des agents de carbonisation classiques (polyols) par des associations de polymères qui comprennent au moins une résine apte à la carbonisation. La réaction de cette résine avec des adjuvants acides conduit, alors, au matériau protecteur, support carboné des espèces catalytiques. Le mécanisme de la protection de ces nouvelles formulations met en œuvre un processus ablatif similaire à celui obtenu en utilisant les systèmes d'adjuvants intumescents classiques. L'étude montre que l'emploi de ces polymères en mélange permet d'éviter les phénomènes de rejet des adjuvants et

leur exsudation, qui interdisent l'addition des systèmes adjuvants classiques des peintures et vernis (sels des acides minéraux/polyols) dans les thermoplastiques.

Finalement, l'étude présente la formulation de nouveaux matériaux intumescents à base de polymères de consommation en cours de développement industriels (en particulier des formulations intumescentes des polyamides et du polystyrène), à des coûts égaux voire inférieurs à ceux des matériaux FR actuellement utilisés.

1- Fowell A.J., « *American Society for Testing and Materials - Fire and Flammability of Furnishings and Contents of Buildings* », ASTM STP 1233, Miami (USA) (Décembre 1992).

2- Gann R.G., « *Flame Retardants* » dans « *Kirk-Othmer Encyclopédia of Chemical Technology* » (4^{éme} édition), volume 10, John Wiley and Sons, New-York (1994) pp. 930-936.

3- Raufaste N.J., « *NIST Building and Fire Research Laboratory Projects Summaries, 1994* », NIST SP 838-5, Gaithersburg (USA) (,juin 1994).

4- Gay Lussac J.L., Annales. Chim., **18(2)** (1821) 211.

5- Rather L.O. et Russell C.K., « *The Market for Flame Retardants in the US - A Current Analysis* » dans « *Handbook of Flame Retardant Chemicals and Fire Testing Services* », Technomic Pub. Co., Lancaster (USA) (1988) pp.1-6.

6- « *Indices et Cotations* », l'Usine Nouvelle **2541** (1996) pp. 157-162.

7- Alakin M., Horrocks A.R. et Price D., J. Fire Sci, **6** (1988) 333.

8- Jin T. et Yamada T., J. Fire Sci., **8** (1990) 124.

9- Harland W.A. et Woolley W.D., « *Fire Fatality Study* » dans « *Building Research Establishment Information Paper* » **IP 18/79**, University of Glasgow (UK) (1979) ;
Woolley W.D., J. Macromol. Sci. A (Chemistry) **17(1)** (1982) 1.

10- Pal G. et Macskasy H., « *Studies in Polymer Science 6 - Plastics, their Behaviour in Fires* », Elsevier Sci. Pub. Co, New-York (USA) (1991) pp. 304-332 ;

11- Hommel G., « *Handbuch der Gefärlichen Güter* », Springer Verlag, Berlin (Allemagne) Volume I (1978), Volume II (1980), Volume III (1985).

12- Hilado C.J., « *Flammability Handbook for Plastics* », Technomic Pub. Co, Westport (USA) (1974).

13-   Camino G., « *Combustion and Fire Retardants* » dans le recueil des Cours de « *The Postdoctoral Course on Degradation and Stabilisation of Polymeric Materials* », Clermont-Ferrand (24-28 octobre 1994), CNEP et ENSCCF, Clermont - Ferrand (1994)

14-   5th Draft Status Report « *OCDE Worhshop on the Risk Reduction of Brominated Flame Retardant* », Neufchâtel (Suisse) (26 mai 1992, 22-25 février 1993), OECD - Direction de l'Environnement (Avril 1993).

15-   Preliminary 1st Draft report « *International Programme on Chemical Safety - Environmental Health Criteria for Brominated Diphenylethers* » (janvier 1993), 1st Draft report « *International Programme on Chemical Safety - Environmental Health Criteria for Tris(2,3-dibromopropyl) phosphate and Bis(2,3-dibromopropyl) phosphate* » (Janvier 1993), United Nations Environmental Programme, PCS/EHC/92.45, Rapports non édités.

16-   van Krevelen D.W., Polymer, **16** (1975) 615-620;

       Johnson P.R., J. Appl. Polym. Sci. **18** (1974) 491;

       Kourtides D.A., Polym. Plast. Technol. Eng. 11 (1978) 159.

17-   « *Standard Test Method for Measuring the Minimum Oxygen Concentration to Support Candle - like Combustion of Plastics* », ASTM D2863/77, Philadelphia (USA) (1977)

18-   Nyden M.R. et Brown J.E., Actes du « *Safety 12th Joint Panel Meeting* », Tsukuba (Japon) (27 octobre-2 novembre 1992), Building Research Institute, Ibaraki (Japon) (1994) pp. 257-266 ;

19-   Rose N., Costes B., Le Bras M. et Delobel R., Actes du Colloque « *Polymérisations: Mécanismes, Méthodes, Procédés* », Bordeaux (18-19-20 novembre 1991),.GFP (1991) *CA 27, p 73-74.*

20-   Bente, M.P., « *Réactivité à l'état fondu des systèmes époxy-cyanamide - dicyanamide-mélamine.* », Thèse, Pau (1993).

21-   Costes, B., « *Etude structurale du réticulat tétraglycidyle diaminodiphényle méthane - diaminodiphényle sulfone.* », Thèse, Le Mans (1989).

22-   Bourbigot S., Le Bras M., Delobel R. et Normand D., J. Chim. Phys.,**90** (1993) 1909.

23- Bourbigot S., « *Nouveaux agents de synergie dans les systèmes intumescents. Compréhension des mécanismes de protection du polyéthylène et de ses copolymères.* », Thèse, Lille (1993).

24- Butler K.M., Baum H.R. et Kashiwagi T., « *Three-dimensional Kinetic model for the swelling of intumescent materials* » dans « *Book of Abstracts - Annual Conference on Fire Research* », NIST, Gaithersburg (USA) (1994) pp. 109-110.

25- Kroenke W.J., J. Mater. Sci., **21** (1986) 1123-1173.

26- Levchik G.F., Levchik S.V., Sachok P.D., Selevich A.S., Lyakhov A.S. et Lesnikovich A.I., Thermochim. Acta, **257** (1995) 117-125.

27- Levchik G.F., Levchik S.V., Camino G., Costa L. et Lesnikovich A.I., Fire & Materials, **20(4)** (1996) 183-190.

28- Camino G., Costa L. et Trossarelli L., Polym. Deg. & Stab. **7** (1984) 25.

29- Olsen J.W. et Bechle C. W., Brevet US 2,442,706 (Anaconda Wire & Cable) (1948).

30- Tramm H.L., Brevet US, 2,106,938 (Ruhrchemie Aktiengesellschaft) (1938).

31- Murray T.M., Liberti F. et Allen A.O., dans « *Advances in Chemistry* (Volume 9) », ACS (1953).

32- Vandersall H.L., J. Fire & Flammability **2** (1971) 97.

33- Le Bras M., Bourbigot S., Delporte C., Siat C. et Le Tallec Y., Fire & Materials **20(4)** (1996) 191-203.

34- Lauring E.A., Brevet US 2,594,937 ((Minnesota and Ontario Paper Company) (1952).

35- Jones G., Brevet US 2,628,946 (Albi Manufacturing Company) (1953).

36- Le Bras M., Bourbigot S., Le Tallec Y. et Laureyns J., Polym. Deg. & Stab. (1996) soumis pour publication.

37- Kishore K. et Mohandas K., Combustion & Flame **43** (1981) 145-153.

38- Camino, G., dans les Actes du « *Premier Colloque Francophone sur l'Ignifugation des Polymères* », ed. Martel, J., Saint Denis (France) (1985) pp. 36.

39- Schmidt - Le Tallec, Y., « *Valorisation de Différents Polyols dans des Systèmes Retardants de Flamme : Application au Polyéthylène* », Thèse, Lille (1992).

40- Camino G., Costa L. et Martinasso, Polym. Deg. & Stab. **23** (1989) 359.

41- Zhu X., J. Fire Sci. (1996) soumis pour publication.

42- Le Bras M., Hermant M. et Leroy J.M., « *Recherche d'additifs du polypropylène apte au filage propre à conférer à ce polymère les propriétés d'ignifugation grâce à un phénomène d'intumescence* », Rapport de fin d'étude pour la Société SOMMER S.A. (1993).

43- Bourbigot S. et Le Bras M., « *Développement de formulations intumescentes pour polyoléfines* », Rapport de fin d'étude pour la Société TARAFLEX (1996).

44- Bourbigot S. et Le Bras M., « *Formulations du polypropylène retardateur de flamme apte au thermo-soudage* », Rapport de fin d'étude pour la C.E.A.C. (1996).

45- Le Bras M. et Leroy J.M., « *Optimisation de formulations du polypropylène aptes au filage et propres à conférer à ce polymère la propriété retard au feu grâce à un phénomène d'intumescence* », Enveloppe Soleau n° 67043 (04 juin 1992), titulaire SOMMER SA.

46- Bourbigot S., Bréant P., Delobel R. et Le Bras M., « *Compositions ignifugeantes pour résines synthétiques contenant une zéolithe et résines synthétiques renfermant les dites compositions* », Brevet français n° 93.07387 (18 juin 1993), Brevet européen n° 629677 A1 (21 décembre 1994), titulaire Elf-Atochem.

47- Bourbigot S. et Le Bras M., « *Association des polyamides et des phosphates d'ammonium dans des formulations ignifugeantes et des mélanges maîtres, additifs retardeurs de flamme utilisables dans des polymères et co-polymères de l'éthylène, du propylène et du styrène et dans des mélanges contenant les dits polymères* »,.Enveloppe Soleau n° 36972 (17 juillet 1995).

48- Le Bras M. et Bourbigot S., « *Formulations ignifugeantes et mélanges maîtres, additifs retardeurs de flamme utilisables dans des polymères et co-polymères de l'éthylène, du propylène et du styrène et dans des mélanges contenant lesdits polymères* », Enveloppe Soleau n° 59305 (30 mai 1996).

49- Le Bras M. et Bourbigot S., Fire & Materials **20** (1996) 39-49.

50-   Halpern Y., Mott D.M. et Niswander R.H., Ind Eng. Chem. Res. Dev. **23** (1984) 233.

51-   Morice L., « *Etude et Modélisation des Transferts Thermiques dans un Bouclier Intumescent - Application au Polypropylène " Retard au Feu " »* Rapport du Diplôme d'Etudes Approfondies « Génie des Procédés », Compiègne (septembre 1996).

52-   Beyler C., « *Thermal Decomposition of Polymers* » dans « *SFPE Handbook of Fire Protection* (Chapitre 1-12) », DiNenno P.J. ed., National Fire Protection Association pub., Quincy (USA) (Octobre 1992), pp. 165-178.

53-   Fenimore C.P. et Jones G.W., Combustion & Flame **10** (1966) 295-301.

54-   Lewis I.C. et Greinke R.A., J. Polym. Sci. **20** (1982) 1119-1132.

55-   Lesnikovich A.I. et Levchik S.V, J. Thermal Anal. **27** (1983) 89.

56-   Lesnikovich A.I., Levchik S.V. et Guslev V.G., Thermochimica Acta **77** (1984) 357.

57-   Babrauskas V., Fire & Materials **13(1-2)** (1984) 3.

58-   Babrauskas V., Lawson J.R., Walton W.D. et Twilley W.H., « *Unfoldered Furniture Heat Release Rates Measured with a Furniture Calorimeter.* » NBS-IR 82-2604 (1982)

59-   Rose N., Le Bras M., Delobel R. et Leroy J.-M., « *Etude de la Thermodégradation de Résines Organiques Aéronautiques - Amélioration des Propriétés Retard au Feu* », Rapport de fin d'étude, Aide MRT - GIS Ignifugation (1994), (Collaboration avec la Société Aérospatiale et Jouany J.-M., Laboratoire de Toxicologie de l'Université de Pharmacie (Rouen)).

60-   Wang X. et GillhamJ.K., J. Appl. Polym. Sci. **43** (1991) 2267-2277.

61-   Rose N., « *Etude de la Dégradation Thermique et du Comportement au Feu de Résines Epoxydes Utilisées dans l'Aéronautique* », Thèse, Lille (France), 1995.

62-   Draft Proposal ISO/DP 7111-1979, International Organization for Standardisation, Genève (Suisse) (1979).

63-   Alger R.S., « *Electron Paramagnetic Resonance : Techniques and Applications* », Interscience, New-York (1968) pp. 42-60.

64- Hyde J.S., *« Experimental Techniques in EPR »*, 6th Annual NMR-EPR Varian Workshop, Varian Associates Instrument Division, Palo Alto (1961).

65- Singer L.S. et Lewis I.C, Appl. Spectrosc. **36(1)** (1982) 52-57.

66- Thornton W., Philosophical Magazine & J. of Sci. **33(196)** (1917).

67- Hugget C., J. Fire & Flammability **12** (1980) ;
Hugget C., Fire & Materials **8(2)** (1980) 6.

68- Grayson S.J., *« Heat Release in Fire. »*, Elsevier, Oxford (GB) (1992).

69- FAR part 25, Amendment 25-61, Federal Aviation Administration, Atlantic City, NJ (USA) (1986).

70- Conley R.T. et Dante M.F., « Stability of Plastics » Tech. Conf. Soc. Plastics Eng., Washington, DC (juin 1964).

71- Ackhammer B.G., Tyron M. et Kline G.M., *« Chemische Struktur und Beständigkeit der Polymeren »* dans *« Int. Symp. on Macromolecules »*, IUPAC, Düsseldorf (Allemagne) (1959)

72- Lee J.H., J. Polym. Sci. A **3** (1965) 859.

73- Pal G. et Macskasy H., *« Studies in Polymer Science 6 - Plastics, their Behaviour in Fires »*, Elsevier Sci. Pub. Co, New-York (USA) (1991) pp. 63-70.

74- Park W.R.R. et Blount J., Ind. Eng. Chem., **49** (1957) 1897.

75- Bellenger V. et Verdu J., J. Appl. Polym. Sci. **30** (1985) 363.

76- Calcraft A.M. et Maries K., Plast. Polym. **42** (1974) 162.

77- Calcraft A.M. et Maries K., Plast. Polym. **42** (1974) 247.

78- Hidalo C.J., Chem. Tech. **24** (1972),232;
Hidalo J.C., J. Cell. Plast. **7** (1971) 181.

79- Delobel R., Bourbigot S., Le Bras M., Schmidt Y. et Leroy J. M., Makromol. Chem., Macromol. Symp., **74** (1993) 59-69.

80- Richard-Campisi L., Bourbigot S., Le Bras M. et Delobel R., Thermochimica Acta **275** (1996) 37-49.

81- Bourbigot S., Richard-Campisi L., Le Bras M. et Delobel R., J. Textile Institute, 1996, papier 5-96, sous presse,

82- Nikoalev A.V., Logvimenko V.A. et Gorberchev V.M., J. Thermal Anal. **6** (1974) 473.

83- Criado J.M. et Gonzalés M., Thermochimica Acta **46** (1981) 201.

84- Koga N. et Sestak J., J. Thermal Anal. **37** (1991) 1103.

85- Koga N., Sestak J. et Malek J., Thermochimica Acta **182** (1991) 333.

86- Koga N et Sestak J., Thermochimica Acta **182** (1991) 201.

87- Bishop B.P. et Smith D.A., Ind. Eng. Chem. **59(8)** (1967) 32.

88- Venger A.E., Fraiman Y.E. et Yurevich F.B., J. Thermal Anal. **27** (1983) 325.

89- Coquillaud X., Le Tallec Y., Le Bras M. et Delobel R., « *European Seminar on Vibration Spectroscopy in Materials Science* » Louvain-la-Neuve (Belgique) (21-22 Avril 1994).

90- Le Bras M., Coquillaux X., Le Tallec Y. et Delobel R., *Actes* des « *Journées Francophones des Jeunes Physico-chimistes* », Lille (16-18 juillet 1996), M. Martel et S. Obbade ed., U.S.T.Lille pub., Cession Posters P3 pp.43.

91- Mikroyannidis J.A. et Kourtides D.A., Polym. Mat. Sci. Eng. Proc. **49** (1983) 606.

92- Costes B., Henry Y., Buckingham M.R., Lindsay A.J., Stevenson D.E., Muller G., Morel E., Levchick S.V., Camino G., Luda, M.P., Costa L., Chambers P.L., Chambers C.M. et Kennedy A.C., « *Development of New Materials with Improved Fire Resistance, Reduced Smoke and Toxicity (Brite-Euram Progam 4412)* » dans « *Abstracts of Fire Retardant Polymers - 5th European Conference* », Salford (GB) (septembre 1995).

93- FAR part 25, Amendment 25-853 grade al. (« *Test OSU* »), Federal Aviation Administration, Atlantic City, NJ (USA) (1990).

94- Duncan T.M. et Douglass D.C., Chem. Phys. **87** (1984) 339.

95- Littré E., « *Dictionnaire de la Langue Française* », Gallimard et Hachette, Paris (1959).

96- Hugo V., dans « *L'homme qui rit* », Lacroix ed., Paris (1869) ; « *Victor Hugo - Romans* », les Editions du Seuil, Paris (1963).

97- Martel B., J. Appl. Polym. Sci. **35** (1988) 1213-1226 ;
Martel B., dans les « *Actes du $2^{ème}$ Colloque Francophone sur l'Ignifugation des Polymères* », Delfosse L. ed., USTL, Lille (1987) pp.13.

98- Tkac A., dans « *Developments in Polymer Stabilisation* (Volume 5) »,Scott G. ed., Applied Sci., Londres (1982) pp. 155.

99-   Camino G., Costa L., Trossarelli L., Costanzi F. et Pagliari A., Polym. Deg. & Stab. **12** (1985) 213.

100-   Delobel R., Le Bras M., Mouchel B. et Leroy J.-M., Annales des Composites, **1-2** (1990) 4-12.

101   Le Bras M., Delobel R., Descressain R. et Leroy J.-M., Bull. Soc. Chim. Belg., **98(9-10)** (1989) 735-740.

102-   « *Test for Flammability of Plastic Materials in Devices and Appliances* », Underwriters Laboratories, Northbrook (USA) (1977) ANSI/ASTM D635-77.

103-   Siat C., Bourbigot S. et Le Bras M., « *Recent Advances in FR of Polymeric Materials (Volume 7)* », Lewin M. ed., Business Communications Co Inc., Norwall (USA) (1996), sous presse,

104-   Alistiqsa F., « *Mise au Point de Nouvelles Formulations Intumescentes Polyphosphate d'ammonium - Pentaérythritol; Application à l'Ignifugation du Polypropylène.* », Thèse, Lille (1993).

105-   Delobel R., Le Bras M., Ouassou N. et Alistiqsa., J. Fire Sci., **8** (1990) 85-108.

106-   Bourbigot S., Le Bras M., Delobel R., Bréant P. et. Trémillon J.-M., Polym. Deg. & Stab. (1996) sous presse.

107-   Camino G., Costa L. et Trossarelli L., Polym. Deg. & Stab. **12** (1985) 203-211.

108-   Camino G., Martinasso G. et Costa L., Polym. Deg. & Stab. **27** (1990) 285-296.

109-   Ouassou N., « *Etude d'un nouveau système intumescent « retard au feu » :pyrophosphate diammonique - pentaerythritol - Application au polypropylène* », Thèse Lille (1991).

110-   Camino G., Costa L., Trossarelli L., Constanzi F. et Landoni G., Polym. Deg. & Stab. **8** (1984) 13.

111-   Camino G., Martinasso G., Costa L. et Gobetto R., Polym. Deg. & Stab. **28** (1990) 17-38.

112-   Delobel R., Le Bras M. et Ouassou N., Polym. Deg. & Stab. **30** (1990) 41-56.

113-   Lewis I.C., J. Chim. Phys. **81(11-12)** (1984) 751.

114-   Sternberg U., Prietrowski F. et Priess W., Z. Phys. Chem. **168** (1990) 115.

115- « *Studies in Inorganic Chemistry , Part 5 - Phosphorus, an Outline of ist Chemistry, Biochemistry and Technology* », Corbridge D.E.C. ed., Elsevier Sci., New-York (1985) pp. 157-221.

116- Sohma J., Colloid & Polym. Sci. **270** (1992) 1060-1065.

117- Butyagin P. et Abragjan G., Biophysics (traduction anglaise) **9** (1964) 161-171.

118- Sakaguchi M. et Sohma J., J. Polym. Sci. **13** (1975)1233-1245.

119- Sakaguchi M. et Sohma J., J. Appl. Polym. Sci. **22** (1978) 2915-2922.

120- Verdu J. dans les « *Proceedings of the 11th Bratislava IUPAC/FECS International Conference on Polymers - Thermal and Photo-induced Oxidation of Polymers and its Inhibition in the Upcoming 21th Century* », Stara Lesna (Slovaquie) (24-28 juin 1996) ML2 pp. 4-5.

121- Cullis C.F., Oxydation & Combustion Revs. **5** (1971) 83-133.

122- « *Chemical Kinetics of Degradation of Polymers* (Volume 14) », Bamford C.H. et Tipper C.F.H. ed., Elsevier Sci., New-York (1975) pp. 425-522.

123- Aseeva R.M. et Zaikov G.E. dans « *Combustion of Polymers Materials* », Nauka, Moscou (1981) pp. 280.

124- Mardorsky S.L. dans « *Thermal Degradation of Organic Polymers* », Interscience, New-York (1964).

125- Bourbigot S., Le Bras M., Delobel R., Revel B. et Trémillon J.-M. dans les « *Abstracts de la 6[éme] Réunion de Travail sur la Résonance Magnétique dans les Solides - Méthodologie RMN : de la Théorie à l'Application* », Eveux (23-26 octobre 1994).

126- « *First International Fire Prevention Congress - The Official Congress Report* », British Fire Prevention Comitee, londres (1903).

127- « *Federal Trade Commission Complaint on the flammability of Plastic Products* », File 732-3040 (31 mai 1973).

128- Marchal A., Delobel R., Le Bras M. et Leroy J.-M. dans les « *Actes du XXII[éme] Congrès National du GFP - Polymères et Civilisation* » Pau (22-24 novembre 1993), Grenier-Loustalot M.-F. ed., CNRS, Pau (1993), pp. 144-148.

129- Delobel R., Le Bras M., Schmidt Y. e-t Bourbigot S. dans les « *Actes du MOFFIS 91 - Mineral and Organic Functional Fillers in Polymers, International Symposium* », Le Mans (9-12 avril 1991) pp. 79-85.

130- Marchal A., Delobel R., Le Bras M. et Leroy J.-M., « *Gordon Research Conference on Analytical Pyrolysis and Oxidative Degradation of Materials* », Plymouth (USA) (13-18 juin 1993).

131- « *Test à l'épiradiateur* », AFNOR NF P 92-501 (1985).

132- Osawa T., Bull. Chem. Soc. Japn. **38(11)** (1965) 1881.

133- Flynn J.H., J. Thermal Anal. **27** (1983) 95.

134- Coats A.W. et Redfern J.P., Nature **201** (1964) 68.

135- Kotoyori T., Thermochimica Acta **5** (1972) 51-58.

136- Leroy-Paulay P., Marcellin V. et Van Den BOS V., « *Entreprise et Marchés - Matériaux* », l'Usine Nouvelle **2557** (11 juillet 1996) 20-21.

137- Nicco A dans les « *Actes du 2ème Colloque Francophone sur l'Ignifugation des Polymères* », Lille (septembre 1987), Delfosse L. ed., USTLFA (1987) pp. 13.

138- Gal E., Pal A., Rychly J. et Tarapcikova K. dans « *Flame Retardant 90* », British Plastics Federation, Elsevier, New-York (1990) pp. 134.

139- Kirschbaum G. dans « *Flame Retardant 90* », British Plastics Federation, Elsevier, New-York (1990) pp. 143.

140- Vogel H., « *Flammfestmachen von Kunstoffen* », Hüthig A. ed., Verlag, Heidelberg (1966).

141- Lyons J.W., « *The Chemistry and Uses of Fire Retardants* », Wiley Interscience, New-York (1970).

142- Bhatnagar V.M., « *Flame retardant Formulation Handbook* », Technomic Publishing Co., Westport (1972).

143- Howarth J.T., Lindstrom R.S., Sheth S.G. et Sidman K.R., Plastics World (Mars 1993) 65-73.

144- Trotignon J.-P., Verdu J., Pipéraud M et Dobraczynski A, « *Précis de Matières Plastiques - Structure - Propriétés, mise en œuvre et normalisation* », Quatremer R., Trotignon J.-P et AFNOR ed., Nathan, Paris (1988) pp. 20-22; Normes NF T 51-025/-105/-167/-770/-782/-783 et NF t 53-003.

145- Bieniek D., Bahadir M et Korte F., Heterocycles **28(2)** (1989) 719-722.

146- Pinkerton M.N., Kociba R.J., Petrella R.V., McAllister D.L., Willis M.L., Fulfs J.C., Thoma H. et Hutzinger O., Chemosphere **18(1-6)** (1989) 1243-1249.

147- Dumler R., Lenoir D., Thoma H. et Hutzinger O., Chemosphere **20(10-12)** (1990) 1867-1873.

148- Clausen E., Lahaniatis E.S., Bahadir M. et Bieniek D., Fresenius Z. Anal. Chem. **327** (1987) 297-300.

149- Montaudo G., Scamporrino E. et Vitalini D., J. Polym. Sci. Polym. Chem. Ed. **21** (1983) 3361.

150- « *Technical Literature No. CA-247. Preliminary Data, Fire Retardant XP-1668* », Fiche Produit de Borg-Warner Chemicals (1983).

151- Delobel R., Ouassou N., Le Bras M. et Leroy J.-M., Polym. Deg. & Stab. **23** (1989) 349-357.

152- Delporte Christelle, « *Etude du nouveau système intumescent retardateur de flamme pentaborate d'ammonium / pentaérythritol - Application au polypropylène* »,.Diplôme d'Etudes Approfondies « Spectroscopies », Lille (1995).

153- Le Bras M., Delobel R., Descressain R. et J.-M. Leroy, « *19ème Colloque National du GFP - Polymères de Spécialité.* », Namur (Belgique) (6-9 novembre 1989).

154- Schmidt Y., Bourbigot S., Marchal A., Le Bras M. et Delobel R. dans les « *Actes de SFC 91 - 4ème Congrès de la Société Française de Chimie* », Strasbourg (17-20 septembre 1991), SFC ed., Université de Strasbourg pub. (1991) AF. 010 pp.108.

155- Marchal A., Delobel R., Le Bras M. et Leroy J.-M., *Rapport de fin de Contrat MRT* n° 90.24/P/DEM en collaboration avec Alcatel-Alsthom Recherche (Janvier 1993).

156- Pouille Fabienne, « *Etude Spectroscopique de Formulations « Retard au Feu » à base de Polyamide.* », Diplôme d'Etudes Approfondies « Spectroscopies », Lille (1995).

157- Félix Emmanuelle, « *Etude structurale par RMN du Solide de Formulations ignifugeantes à base de PA6.* », Diplôme d'Etudes Approfondies « Spectroscopies », Lille (1995).

158- Bourbigot S., Siat C. et Le Bras M. dans les « *Actes du Colloque du GFP-Matériaux Polymères, Procédés* » Nancy (21-23 Novembre 1995), GFP (1995) pp. 29.

159- Bourbigot S., Siat C. et Le Bras M. dans les « *Proceedings of the 7th Annual BCC Conference on Flame Retardancy - Recent Advances in Flame Retardancy of Polymeric Materials* » Stamford (USA) (20-22 mai 1996).

160- Siat C., Le Bras M., Bourbigot S. et Pouille F. dans les « *Abstracts of the 11th Bratislava Conference on Polymers - Thermal- and Photo-induced Oxidation of Polymers and its Inhibition in the Upcoming 21th Century* », Stara Lesna (Slovaquie) (24-28 juin 1996), Richla ed., IUPAC/FECS, Bratislava (1996) pp.113-114.

161- Delporte C., Pouille F., Bourbigot S., Le Bras M. et Le Tallec Y., « *Journée de la Soc. Chim. de France* », Lille (1er juin 1995).

162- Bourbigot S., Le Bras M., Bréant P., Trémillon J.-M. et Delobel R. dans les « *Actes de Eurofillers 95* », Mulhouse (11-14 septembre 1995), Papirer E. ed., MOFFIS/FILPLAS, Mulhouse (1996) pp. 445-448.

163- Le Bras M., Bourbigot S. et Leroy J.-M. dans les « *Actes de Eurofillers 95* », Mulhouse (11-14 septembre 1995), Papirer E. ed., MOFFIS/FILPLAS, Mulhouse (1996) pp. 439-442.

164- Bourbigot S., Le Bras M., Delobel R., Bréant P. et Trémillon J.-M. dans les « *Abstracts of Fire Retardant Polymers - 5th European Conference* », Salford (GB) (4-7 septembre 1995), Price D. ed., SCI, Londres (1995).

165- Bourbigot S., Le Bras M., Delobel R., Revel B. et Trémillon J.M. dans les « *Proceedings of the 7th Annual BCC Conference on Flame Retardancy - Recent Advances in Flame Retardancy of Polymeric Materials* » Stamford (USA) (20-22 mai 1996).

166- Bourbigot S., Le Bras M., Delobel R., Revel B. et Trémillon J.M. dans les « *Abstracts of the 11th Bratislava Conference on Polymers - Thermal- and Photo-induced Oxidation of Polymers and its Inhibition in the Upcoming 21th Century* », Stara Lesna (Slovaquie) (24-28 juin 1996), Richla ed., IUPAC/FECS, Bratislava (1996) pp.30-31.

167- Bourbigot S., Le Bras M., Delobel R., Revel B. et Trémillon J.M., *« Recent Advances in FR of Polymeric Materials (Volume 7) »*, LEWIN M. ed., Business Communications Co Inc., Norwall (USA) (1996), sous presse.

168- *« Recommandations for Tests with Measuring Mixers »*, Fiche technique (*« Standard Methods »*)Brabender N° 2218 E, Brabender, Duisburg (Allemagne) (1986/88) ;

169- Myers R.E. et Licursi E, J. Fire Sci. **3(10-11)** (1985) 415-431.

170- Levchik S.V., Costa L. et Camino G., Polym. Deg. & Stab. **36** (1992) 31-39.

171- Levchik S.V., Costa L. et Camino G., Polym. Deg. & Stab. **36** (1992) 229-237.

172- Bellamy L.J., *« The Infrared Spectra of Complex Molecules* (Volume 1) *»*, Chapman and Hall, Londres (GB) (1975).

173- Colthup B., Daly H. et Wiberley E., *"Introduction to Infrared and Raman Spectroscopy"* Academic Press, New-York (1964).

174- Lehmann W.J., Onak T.P. et Shapiro J., J. Chem. Phys. **30** (1959) 1215.

175- Bradley, *Private Communication to JCPDS*, Powder Diffraction File 23-1034.

176- Senkovits et Hawley, *Private Communication to JCPDS*, Powder Diffraction File, 6-297.

177- Le Bras M. et Bourbigot S. dans les *« Actes des Journées sur les progrès récents et les applications de la RPE aux systèmes chimiques et biologiques »*, Paris (16-17 septembre 1996).

178- Scharf D., Nalepa R., Heflin R. et Wusu T., Fire Safety J. **19** (1992) 103.

179- Levchik S.V., Levchik G.F., Camino G. et Costa L., J. Fire Sci. **13** (1995) 23.

180- Beyer H.K., Boberly G., Miasnikov P. et Rosza P. dans *« Zeolites as Catalysts, Sorbents and Detergent builders »*, Karge H.G. et Weitkamp J. ed., Elsevier, Amsterdam (Pays Bas) (1989) pp. 635.

181- Taylor A.P., et Sale F.R., Makromol. Chem., Macromol. Symp. **74** (1993) 85.

182- Bulgakov V.K., Kodolov V.I. et Lipanov A.M. dans *« Modelling of Combustion of polymeric Materials »*, Khimiya, Moscou (Russie) (1990).

183- *« Catalysis by Zeolites - Studies in Surface Science and Catalysis* (Volume 5) *»*, ImeliK B., Coudurier G., Naccache C., Ben Taarit Y., Védrine J.-C. Praliaud H. ed., Elsevier, Amsterdam (1980).

184- Hermann E.F., Psych. **28** (1963) 161-172.

185- Delobel R., Bourbigot S., Le Bras M., Leroy J.-M. et Kanovnik B. dans « *Polimerni Materijali Smanjene Gorivosti* », Janovic Z. ed., Drustvo Plasticara i Gumaraca, Zagreb (Yougoslavie) (1990), pp. 08/01-08/04.

186- Goldman M. et Shen L., Phys. Rev. **144** (1966) 321.

187- Cheung T.T.P. et Gerstein B.C., J. Appl. Phys. **52** (1981) 5517.

188- Scheffé H., J. R. Stats. Soc. **20B** (1958) 344.

189- Antia F.K., Cullis C.F. et Hirschler M.M. , Eur. Polym. J. **18** (1982) 95-107.

190- Hirschler M.M., Polymer **25(3)** (1984) 405-411.

191- Sainrat A. dans « *Les Différentes Applications du Cône Calorimètre t son Utilisation sur le Plan International - Comparaison du Cône Calorimètre avec d'autres Essais de Réaction au Feu* », LNE, Trappes (France) (avril 1992). ISO TC 92, ISO DIS 5660, ISO DIS 9705, TR ISO 5658.

192- Babrauskas V. et Parker W.J., « *Ignability Measurements with the Cone Calorimeter* », Report N° NBSIR 86-3445, US National Bureau of Standards (NEL), Gaitherburg, MD (USA) (septembre 1986).

193- « *Classification System for Combustibility* », Florintek Canada Corp., CAN/ULC-S114, National Building Code of Canada, ASTM E 136.

194- Kanury A.M. dans « *Ignition of Liquid Fuels - SFPE Handbook of Fire Protection Engineering* (Section 1/Chapitre 20) », Beyler C.L. et DiNenno P.J. ed., NFPA et SFPE, Quincy, MA (USA) (1990) pp. (1-316)-(1-325).

195- Kanury A.M. dans « *Flaming Ignition of Solid Fuels - SFPE Handbook of Fire Protection Engineering* (Section 1/Chapitre 21) », Beyler C.L. et DiNenno P.J. ed., NFPA et SFPE, Quincy, MA (USA) (1990) pp. (1-326)-(1-340).

196- Pels J.R., Kapteijn F., Moulijn J.A., Zhu Q. et Thomas K.M., Carbon **33(11)** (1995) 1641.

197- Jansen R.J.J. et Van Bekkum H., Carbon 33(8) (1995) 1021.

198- Wilkie C.A. dans « *Improved Fire- and Smoke-Resistant Materials for Commercial Aircraft Interiors* », Publication NMAB-477-2, National Academy Press, Washington (USA) (1995) pp. 129.

199- Alger M.S.M. dans « Polymer Science Dictionary », Elsevier, Londres (1989).

200- Dominighaus H. dans « *Plastics for Engineers : Materials, Properties, Applications* », Hanser, Munich (1993).

201- Oudet C. dans « *Polymères - Structure et Propriétés, Introduction* », Masson, Paris (1993).

202- Dickens, J. Polym. Sci. Polym. Ed., **4** (1982) 1065.

203- Varma I.K. et Sadhir R.K., Angew. Makromol. Chem., **46** (1975) 1.

204- Barralès-Rienda J.M., Sanchez Chaves M. et Mazon Arechederra J.M., Polym. Deg. & Stab., **21** (1988) 55.

205- Nam J.-D. et Seferis J.C., J. Polym. Sci. Part B, Polym. Physica, **29** (1991) 601.

206- Mayot A ;, Le Maguer D., Lalart D., Ecuyer M. et Dhamelincourt P., « *Procédé de Greffage de Silice Amorphe sur un Substrat Ferreux* », Brevet Français 89 085 10 (27 juillet 1989) ; Mayot A., Le Maguer D., Dhamelincourt P. et Lalart D., Bull. Soc. Chim. Belges, 98(9-10) (1989) 788-793.

207- Bonin Y., (CLIPT, Saint Fons), Communication privée (1991-1993).

208- Levchik S.V., Costa L. et Camino G., Macromol. Chem., Macromol. Symp., **74** (1995) 95-99.

209- Levchik S.V., Levchik G.F., Camino G., Costa L. et Lesnikovich A.I., Fire & Materials, **20** (1996) 183-190.

210- Dépôt anonyme, Research Disclosure, disclosed 33012 (octobre 1991) 726-734.

211- Liang Z. et Williams H.L., J. Appl. Polym. Sci., **44** (1992) 699-717.

212- Chen C.C., Fontan E., Min K. et White J.L., Polym. Engineer. & Sci, **28(2)** (1988) 69-80.

213- Armat R. et Moet A., Polymer, **34(5)** (1993) 977-985.

214- Padwa A.R., Polym. Engineer. & Sci, **32(22)** (1992) 1703-1710.

215- Raval H., Singh Y.P., Mehta M.H. et Devi S., Polymer International, **26** (1991) 105-113.

216- Utraki L.A. et Sammut P., Plastics, Rubber & Composites Processing & Applications, **16** (1991) 221-229.

217- Siat C, Bourbigot S et Le Bras M., Polym. Deg & Stab., Papier PDS/NCB/404 (1996) soumis à publication.